[redacted]

E15-66

THIOKOL CHEMICAL CORPORATION
ELKTON DIVISION
ELKTON, MARYLAND

VOLUME I
FINAL REPORT

DESIGN STUDY OF HEAT STERILIZABLE SOLID ROCKET MOTORS FOR SPACE APPLICATION

PREPARED FOR:

JET PROPULSION LABORATORY
CALIFORNIA INSTITUTE OF TECHNOLOGY
PASADENA, CALIFORNIA

CONTRACT NO. 951405

JUNE 27, 1966

Jack Buchanan
for H. G. Jones
General Manager

This work was performed for the Jet Propulsion Laboratory, California Institute of Technology, pursuant to a subcontract issued under Prime Contract NAS 7-100 between the California Institute of Technology and the United States of American represented by the National Aeronautics and Space Administration.

FOREWORD

This report has been prepared by the Elkton Division of Thiokol Chemical Corporation for the Jet Propulsion Laboratory of the California Institute of Technology. Mr. W. Dowler was the JPL technical representative for the program.

The reported work was performed during the period from October 19, 1965, through January 9, 1966. Technical effort was performed by Messrs T. Kirschner[1] and W. G. Andrews[2] of our engineering staff, with the support of Mr. H. Schloss[3] of our research laboratory. Technical effort was supervised by Mr. John P. King. Mr. F. X. Cunningham was the Program Manager.

---

[1] Lead Rocket Engineer

[2] Senior Engineering Specialist

[3] Project Chemist

TABLE OF CONTENTS

TABLE OF CONTENTS (CONTINUED)

LIST OF FIGURES

LIST OF FIGURES (CONTINUED)

LIST OF FIGURES (CONTINUED)

ABSTRACT

This document contains the results of a design and analysis study of heat sterilizable solid propellant rocket motors for space application. Candidate designs and detailed performance summaries are presented. Problems associated with the design and subsequent dry heat sterilization of each motor system are identified.

SUMMARY

The results of a design and analysis study of heat-sterilizable solid propellant rocket motors for space applications are presented. The principal emphasis of the investigation was on the capability of candidate sterilizable designs to perform with 99.9% reliability after three dry-heat sterilization cycles. Four basic motor designs were considered: case-bonded spherical; case-bonded cylindrical; free-standing, internal burning; and free-standing, end burning. Propellant TP-H-3105 is the solid propellant upon which these studies are based. It was selected by agreement between Jet Propulsion Laboratory and Thiokol because of its ability to pass screening tests which imposed three 36-hour heat cycles.

Nineteen different motor designs were examined and subsequently rated for highest mass fraction, presence of stress concentrations, freedom from differential expansion, time to reach sterilization temperature, demonstrated reliability, design complexity, neutrality of motor thrust program, low temperature capability, total surface areas exposed, and effects of vibration and spinning on grain structure and ballistic performance.

This rating was used to reduce the number of candidate designs to five: two case-bonded and three free-standing types. Detailed layouts of these candidates were made and the five designs were again compared. The basis for comparison at this point included the parameters used for initial screening plus two additional items, sliver occurrence and adaptability to scale-up.

Based on this rating system the case-bonded designs are superior to the free-standing type, primarily because of their more rapid attainment of sterilization temperature and better adaptability to scale-up. The Circular Perforate Spherical Motor was the better of the two case-bonded candidates and the Internal-External Burning Motor was best of the free-standing designs.

The Case-Bonded Spherical Center Perforate Motor and the Internal-External Burning Free-Standing Grain Motor were subjected to thorough design analysis, including ballistic performance evaluation and structural integrity analyses. The effects of all pertinent motor life cycle loads on the structural reliability of each system were investigated. The results of these analyses indicate that both designs are capable of withstanding the environmental and operational loadings to which they will be exposed following sterilization.

The results of the study show that (within the design guidelines) the only significant problem in the design of a heat-sterilizable solid propellant motor is degradation of propellant-liner physical properties. The problems of differential expansion of propellant and case materials can be solved by judicious selection of materials and clearances.

It should be noted that this study is based on a type approval requirement of three 36-hour dry-heat cycles at 295°F. Recently, the Jet Propulsion Laboratory has considered a type-approval requirement for the Voyager Project which consists of six 53-hour dry-heat cycles at 275°F. The impact of such a requirement was not evaluated during this study; therefore, the results and conclusions reached must be utilized with caution.

I. INTRODUCTION

The two-month technical program reported in this document encompassed two general tasks:

a) A study of the design problems of heat-sterilizable solid propellant rocket motors, and

b) the design of two heat-sterilizable high performance solid propellant rocket motors which would meet certain design requirements:

1) The propellant shall be already developed and shall have demonstrated its capabilities for heat sterilization.

2) The propellant shall have the following characteristics:

a) A block of solid propellant 3" x 3" x 6" shall withstand three heat sterilization cycles of ambient to 295°F ± 2°F to ambient without visual evidence of gas evolution, interior degradation or mechanical failure.

b) The mechanical properties after three sterilization cycles shall be compatible with motor design requirements.

c) The propellant shall be able to undergo two years of earth storage and, after heat sterilization, one year of sealed space storage at 10^{-6} millimeters of mercury.

d) The propellant composition shall be such that only gaseous combustion products are ejected from the nozzle.

e) Its standard specific impulse shall be greater than 200 lbf-sec/lbm.

3) The liner, restrictor and bonding materials shall be compatible with other motor components and shall be able to withstand three heat sterilization cycles.

4) The propellant charge weight shall be 100 pounds plus or minus five pounds.

5) The motor mass ratio shall be greater than 0.85 for the case-bonded grain and 0.75 for the free standing grain. (These ratios are defined as the mass of loaded propellant divided by the initial motor mass.)

6) The motor chamber pressure is left to the discretion of the contractor designer, as is action time within the limits of five to 40 seconds.

7) A high strength metal is the preferred case material; however, filament wound fiberglass-plastic cases may be considered.

8) The ignition system shall perform in space vacuum. A "controlled flow" or "PYROGEN" igniter is preferred.

9) The nozzle shall have an expansion ratio of 30.

10)* The motor, excluding the nozzle, shall have a length to diameter ratio of less than three.

11) Motor life cycle: the motor design shall be such that the complete motor assembly is capable of firing within the design specifications with a reliability of 99.9 percent at a 90 percent confidence level after withstanding the following:

   a) Normal earth transportation and handling loads.

   b) Earth storage at 40 ± 80°F for two years.

*This criterion was modified to a target figure of 1.5 during the course of this study.

c) Three independent, hot oven, heat sterilization cycles over a period of three months. Sterilization conditions of 295° F ± 2° F for 36 hours shall be determined inside the motor where temperature lag is the greatest.

d) After sterilization, no inspection by disassembly shall be permitted.

e) Spacecraft static acceleration of 15 g's axial and 7.5 g's lateral. Spacecraft dynamic loads which can be simulated by a three-g RMS axial and a two-g RMS lateral vibration input to flight configuration on a hard mount using a sine sweep of one minute/octave from two to 100 cycles per second.

f) Motor storage and firing temperature in space of 40 ± 80° F.

g) Space storage for up to one year at 10^{-6} millimeters of mercury.

h) Motor firing during spinning at 100 revolutions per minute.

Because the rocket motors are ultimately intended for use as on-board interplanetary propulsion systems, an important design requirement is that the motors have a high probability of successful operation after three dry-heat sterilization cycles. For this program a single sterilization cycle was defined as: elevation of the conditioning temperature from ambient to 295° F and return to ambient, with a 36-hour dwell at 295° F.

When one considers solid propellant for use in an application involving thermal sterilization as a prerequisite, it is important to recognize the impact of this prerequisite on propellant structural capacity. Because of sterilization, and the temperature- and rate-dependent response of propellant to loads, sterilized propellant is a different viscoelastic material from what it was prior to sterilization. Therefore, mechanical properties must be characterized after final sterilization as well as after manufacture. This phenomen has been recognized and used in this study as a means of screening candidate grain designs, elastomeric insulations, boots, and liners.

Degradation of the physical properties of organic materials used in solid propellant rocket motors can be illustrated by the effect of heat sterilization on propellant structural capacity (see Figure 1).

In addition to problems of degradation in the mechanical properties of materials, dry heat sterilization raises problems of dimensional change of motor components due to differential thermal expansion.

This latter problem was approached through the technique of judicious material selection, stress-relieving mechanisms, and careful design of clearances.

As would be expected, the requirement of heat-sterilization capability had a major impact on the technical program. The candidate design propellant used in this study, TP-H-3105 (a PBAA/imine cured/ammonium perchlorate composite), was selected because of its ability to pass screening tests which imposed three 36-hour 295° F heat cycles. In conducting the program it was necessary to become thoroughly familiar with the problems involved in designing a motor to withstand the sterilization environment. Following this, a variety of different grain designs incorporating standard as well as novel features were studied and compared against specific rating criteria. The best designs were identified, finalized, and subjected to a thorough analysis to determine their ability to meet the environmental and operational requirements for interplanetary propulsion.

With the intent of presenting information to the reader in a logical and succinct manner, the main text of this report proceeds rapidly through candidate design screening and evaluation to a detailed presentation of the two final candidate designs. Much of the supporting information has been collected into Appendixes, which are referenced throughout the main text. Classified information on propellant TP-H-3105 will be found in Volume II (Confidential).

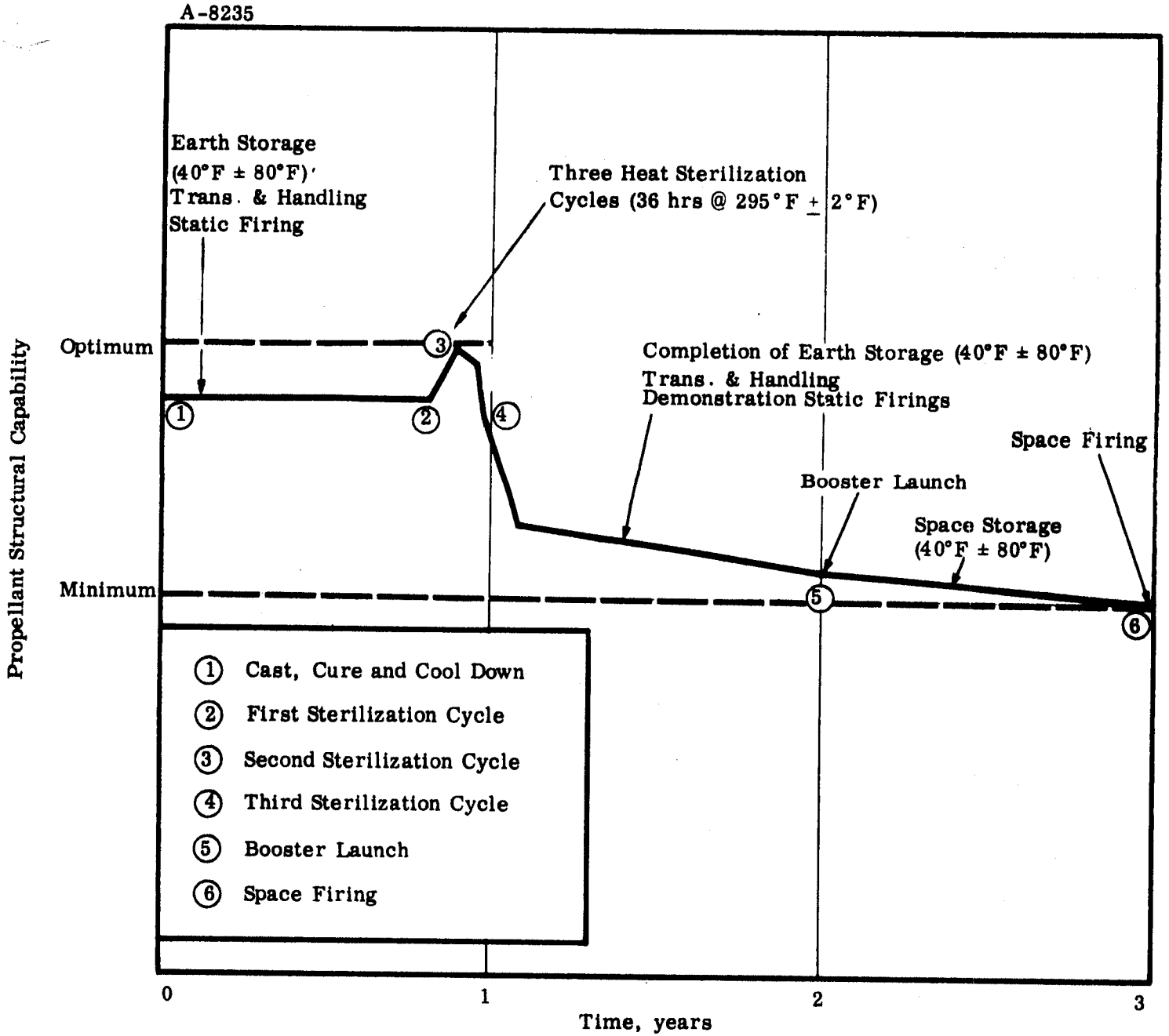

FIGURE 1. HEAT STERILIZABLE PROPELLANT CAPABILITY HISTORY

II. TECHNICAL PROGRAM

The objective of this study was to design two solid propellant rocket motors that would have a very high probability of successful operation after three dry heat sterilization cycles. One motor was case-bonded; the other, free-standing.

In order to achieve this objective, the study was broken down into three phases. The first phase was a thorough study of the problems involved in designing a motor to withstand the sterilization environment. The second included selecting a large number of different grain designs, studying them carefully, and selecting one case-bonded and one free-standing design. The final phase consisted of conducting a thorough analysis of the two selected designs.

A brief commentary is presented in this section on the procedure and the results of the work conducted under the first two phases; main emphasis here will be placed on the two designs selected for detailed analysis. The reader is referred to the appendixes for full details of the work conducted in the first two phases.

A. PROBLEM ANALYSIS

The problems caused by heat sterilization fall into two types: a) degradation of the physical and mechanical properties of materials, and b) dimensional changes; i.e., thermal expansion of motor components during sterilization.

During sterilization, two general types of chemical reactions involving the propellant binder can be expected to dominate: a) oxidative crosslinking of polymer chains, and b) polymer chain scission. The crosslinking reaction results in increased modulus, decreased elongation and hardening or embrittlement of the propellant. Chain scission causes loss of tensile strength and propellant softening. Both reactions are dependent on the presence of oxygen, and typically occur simultaneously. The overall effect of these reactions on the propellant binder, of course, is determined by whichever reaction is dominant. This, in turn, is determined by several variables including environmental temperature, the presence or absence of moisture, temperature, and polymer type.

Since oxygen is an important factor in these reactions, the effect of thermal sterilization on physical properties can be repressed by excluding oxygen from the sterilization environment. This can be done by using an inert gas such as nitrogen for the sterilization atmosphere. It has been shown (Appendix I) that with a polybutadiene acrylic acid-imine cured-ammonium perchlorate propellant (TP-H-3105) sterilization under nitrogen results in much less change in propellant physical properties than does sterilization under air.

All studies in this program have assumed that sterilization is conducted under nitrogen. The capabilities of TP-H-3105 to withstand foreseeable thermal sterilization requirements has been demonstrated by both JPL[14] and Thiokol[15]. These data are presented in Volume II, Appendix I. Although sterilization does cause change in the physical properties of TP-H-3105, the change, as demonstrated in this study, is not serious enough to indicate that a problem exists in this area.

The problem of change in mechanical dimensions is primarily one of differing thermal expansion coefficients of materials in the motor. A study of the magnitude of this problem was conducted early in the design effort. It was determined that judicious selection of materials and the use of proper clearances in the motor case would significantly reduce if not completely alleviate this problem. These thermal expansion effects are fully discussed in Section E of Appendix A, General Design Guidelines.

B. CANDIDATE DESIGN SCREENING

The second phase consisted of the detailed analysis and rating of 19 grain designs. These designs fall into the general categories of case-bonded spherical, case-bonded cylindrical free-standing cylindrical or free-standing end burning. The reader is referred to Appendix C for individual design descriptions.

All designs were rated as follows:

1) The maximum mass fraction of each motor was calculated from empirical equations which are used in the design of high mass-fraction motors. The cylindrical motors studied had length-to-diameter (L/D) ratios of 3:1, except for the end-burning designs which had 2:1 ratios.

2) Freedom from areas causing stress concentrations was rated on the basis of the presence of star points, irregular boundary conditions, and similar items.

3) Freedom from differing thermal expansion coefficients was rated by using engineering judgment. Items considered in the rating included presence of stress relief boots and types of support structure.

4) The time to reach sterilization temperatures was calculated for each design using heat transfer equations for transient heat flow into center-perforated cylinders. The designs were then rated on total time of exposure to sterilization temperature. This criterion, as well as 5) below, are indicative of the impact of a specific design on propellant surface degradation resulting from sterilization.

5) The exposed propellant surface area (i.e., the burning surface area) was calculated for each design and used as a rating on the basis that maximum propellant degradation will occur at interfaces between the propellant and the atmosphere, i.e., that degradation will be a function of exposed propellant surface area.

6) The design experience rating was based on industry state-of-the-art knowledge of the design.

7) Design complexity was based on an examination of manufacturing difficulties which could influence reliability during development and qualification.

8) Each design was also rated on the basis of freedom from slump, the effects of vibration, resonance and spin.

9) Grain neutrality was calculated and rated.

10) Each design was rated on its ability to operate at low temperatures, keeping in mind the possible stress and strain problems and the propellant properties after sterilization.

11) The feasibility of decreasing the L/D ratio to 1.5.

All 19 designs were rated from 1 to 4 on the items listed above. These were then multiplied by a weighting factor. The five designs having the highest total were selected. A complete discussion of the calculation methods, equations, rating criteria used, and the results obtained are discussed in Appendix C, Design Evaluation and Rating — Initial 19 Designs.

C. ANALYSIS OF FIVE DESIGNS

The five designs chosen for further analysis were:

Case Bonded

1) Case-Bonded, Spherical, Circular Perforate Motor

2) Circular Perforate Cylindrical Motor

Free-Standing

3) Internal-External Burning, Free-Standing Motor.

4) Externally Relieved, End-Burning Motor.

5) Rod and Tube Motor.

Description and detailed discussion of each of these designs is given in Appendix D.

Detailed layouts of these motors were analyzed. The analysis was conducted in essentially the same manner as that previously discussed except that sliver occurrence and adaptability to scale-up were considered, and the feasibility of decreasing the L/D ratio was not considered. However, much more detailed calculations were performed for each design.

The results of this analysis are presented in Appendix D. As is evident from Table D-1 of Appendix D, the case-bonded designs are superior to the free standing type primarily because of their more rapid attainment of sterilization temperature, more neutral surface area and less sliver, and better adaptability to scale-up. The most reliable of the case-bonded design types is the Case Bonded, Spherical Circular Perforate Motor; the most reliable of the free-standing design types is the Internal-External Burning, Free-Standing Motor. These motor designs are shown on Drawings E18605 and E18609, respectively, and they are the designs selected as the final candidates in this study.

D. FINAL DESIGNS

Having selected the Case Bonded Spherical Center Perforate and the Internal-External Burning Free Standing motors from among the original 19 candidate designs, it is necessary to assess more critically the ability of each to withstand operational and environmental loads. Phenomena such as slump, propellant-liner separation, cracking, and the so-called "Tormey's disease" (failure due to thermo-mechanical cyclic loadings) are some of the more widely observed deleterious effects that imposed loads can precipitate in composite propellant systems. For the most part, these arise from the observed fact that the internal structure and macroscopic integrity of highly filled polymers is markedly influenced by gravitational forces, changes in temperature, humidity and certain physico-chemical reactions.

Problems associated with predetermining the structural response of present solid propellant rocket motors are difficult to resolve. The mechanisms which govern the response of composite solid propellants to braod spectrum loadings are inherently complex. While many engineering materials can be treated (at least macroscopically) as elastic systems, present propellants cannot. They are members of a wide class of highly filled polymeric rubbers whose structural characteristics are typified by both instantaneous elastic and time dependent viscous responses when subjected to given tensile, shear or compressive forces. The problem is further complicated by the fact that the physical response and temperature dependence (and, hence, the load and strain capacity) of these materials do not, in general, remain the same throughout their life history. Thus, one is faced with the problem of ascertaining the reliability of a structure, the major component of which is continuously changing in its response to environmental and operational design loads. These considerations are of particular importance to this study since the repeated exposure of the motor charge to sterilization temperatures significantly alters the structural characteristics of the propellant-liner system.

The mission hypothesized for the selected sterilizable designs dictated a particular set of motor life cycle loads. These are summarized below:

STERILIZABLE MOTOR DESIGN LIFE CYCLE LOADS

Cure Shrinkage and Cooldown	T_c = 150°F
Motor Storage and Firing Temperature Range	(-40°F, 120°F)
Three Dry Heat Sterilization Cycles	(295°F, 36 hours per cycle)
Axial Acceleration	15 g's
Lateral Acceleration	7.5 g's
Motor Firing During Spinning	100 rpm

While probably not all units will be subjected to the extreme conditions, it must be assumed, for purposes of obtaining a valid reliability assessment, that some will; that is, a certain percentage of all production units will be exposed to ambient storage conditions as well as to low temperature space storage and firing, maximum acceleration levels and three dry heat sterilization cycles. These, together with occasional vibratory loads during transportation and handling, are the conditions upon which all conclusions concerning the structural soundness of the sterilizable designs must be based.

1. Method of Structural Analysis

The two final candidate motor designs underwent structural analysis using, for the most part, an axisymmetric, two-dimensional, stress analysis computer program (Thiokol Program Number E-43113). This program is based upon a finite element stiffness formulation and is capable of considering loadings due to propellant curing and cooldown, thermal shrinkage and expansion, acceleration and internal pressurization.

The method of superposition was used in determining the total stress and strain (deformation) requirements of the selected designs. Safety factors were computed for each design by comparing these deformation requirements with the tensile-temperature response of TP-H-3105. In Thiokol's experience, a preliminary design structural analysis can be made through further simplifications of structure based upon the theory of maximum principal strain (stress) structural failure and cumulative damage. The principal assumptions required for this analysis are:

1) The propellant is incompressible or, at most, exhibits a constant bulk modulus, and

2) The stress-strain capacity of the propellant at very low strain rates (temperature cycling) and moderate strain rates (pressurization and acceleration) can be, determined within engineering accuracy, from uniaxial tensile tests by means of the temperature shift factor, a_T.

Although there is some question of the validity of relating the contribution of pressurization strains to failure of the propellant in systems having metal motor cases, a structural analysis based upon the assumption that pressurization and shrinkage strains are of equal importance should result in a highly reliable design whose actual safety factor is greater than the computed safety factor. The uncertainty in considering these strains as additive is due to the fact that they are imposed upon the motor charge at widely different rates, whereas the ultimate properties of the propellant are actually very dependent on loading rates.

2. Effect of Sterilization on the Propellant-Liner System

a. Propellant (TP-H-3105)

Between 1963 and 1965 Thiokol studied a number of binder systems in different propellant compositions to define the best candidate for heat sterilization. A PBAA polymer cured with MAPO and sterilized under nitrogen was the most

promising binder system. Four test motors, containing propellant TP-H-3105 (PBAA/MAPO (ammonium perchlorate) which had been stored under nitrogen at 294°F for varied time periods operated successfully during subsequent ballistic test. Ballistic properties after the heating cycles were no different from those before heating. Data from these early tests under air and nitrogen are summarized in Appendix I of Volume II, which is classified.

During the summer of 1965, bulk samples of TP-H-3105 were subjected to three dry heat sterilizations in a nitrogen atmosphere. This sterilized propellant was subsequently cut into JANAF tensile dumbbells from which ultimate tensile properties were obtained as a function of temperature. The tests were run at a crosshead speed of 2 in./min. on an Instron tensile tester. Triplicate tensile tests were run at eight different temperatures between -65°F and 200°F. The results of these experiments are presented graphically in Figures 2 to 5.

It is readily apparent from examining these physical property data and the ballistic results in Appendix I that, while variations in ballistic performance are not observable, the structural characteristics are significantly altered. This observation is most apparent in Figures 4 and 5 where the effects on strain at maximum force ($\epsilon_{\sigma\ max}$) are shown. The difference in response of ultimate strain to temperature between unaged and sterilized propellant serves to enforce the conclusion that sterilization alters the structural material. The corresponding effect on load and strain capacity in combination is shown in Figure 6, which is a construction of uniaxial failure boundaries for sterilized and unsterilized TP-H-3105. The areas to the right of each boundary in Figure 6 represent load-strain requirements which are beyond the capacity of TP-H-3105 and would thus result in failure.

Where applicable, these effects were accounted for in the structural analysis of the selected motor designs.

b. Liner (TL-H-305) and Adhesive (Epon 912)

The reader is referred to Appendix H, Material Selection, for the results of tests of TL-H-3105 following sterilization. These tests show that when sterilized specimens are tested in shear at either 78°F or 295°F, the strength of the liner or adhesive exceeds that of the propellant. However, when tested at -40°F, liner failure occurs. But, in any case, the strength of both liner and adhesive exceeds 70 psi. When this figure (70 psi) is employed as representative of the ultimate capacity of the propellant-liner system a conservative margin of safety is demonstrated for both of the Final Candidate designs (cf. sections E.10.f and F.5.f - Margins of Safety).

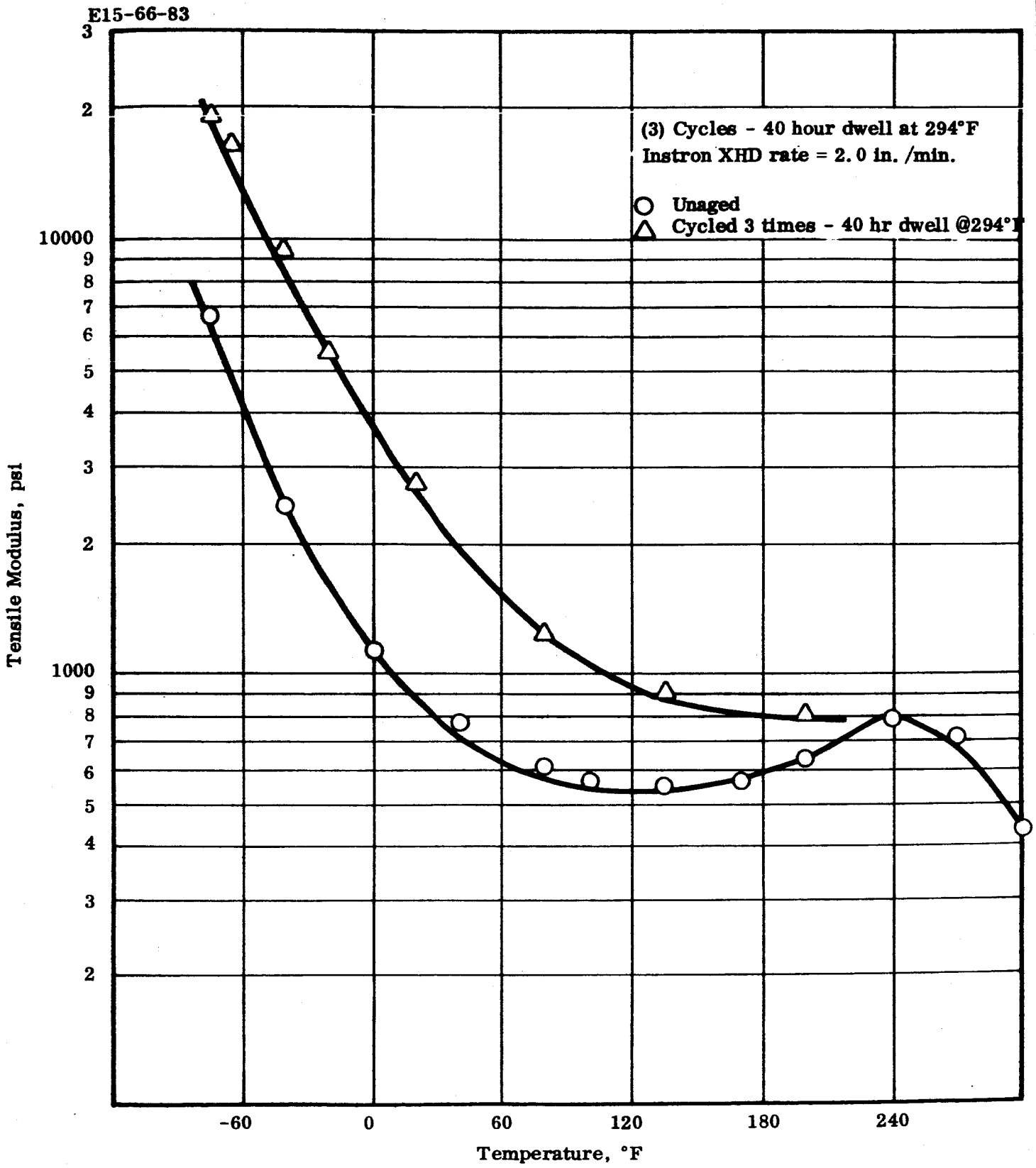

FIGURE 2. TP-H-3105 INSTRON JANAF PROFILE OF TENSILE MODULUS VERSUS TEMPERATURE AFTER THREE HEAT CYCLES

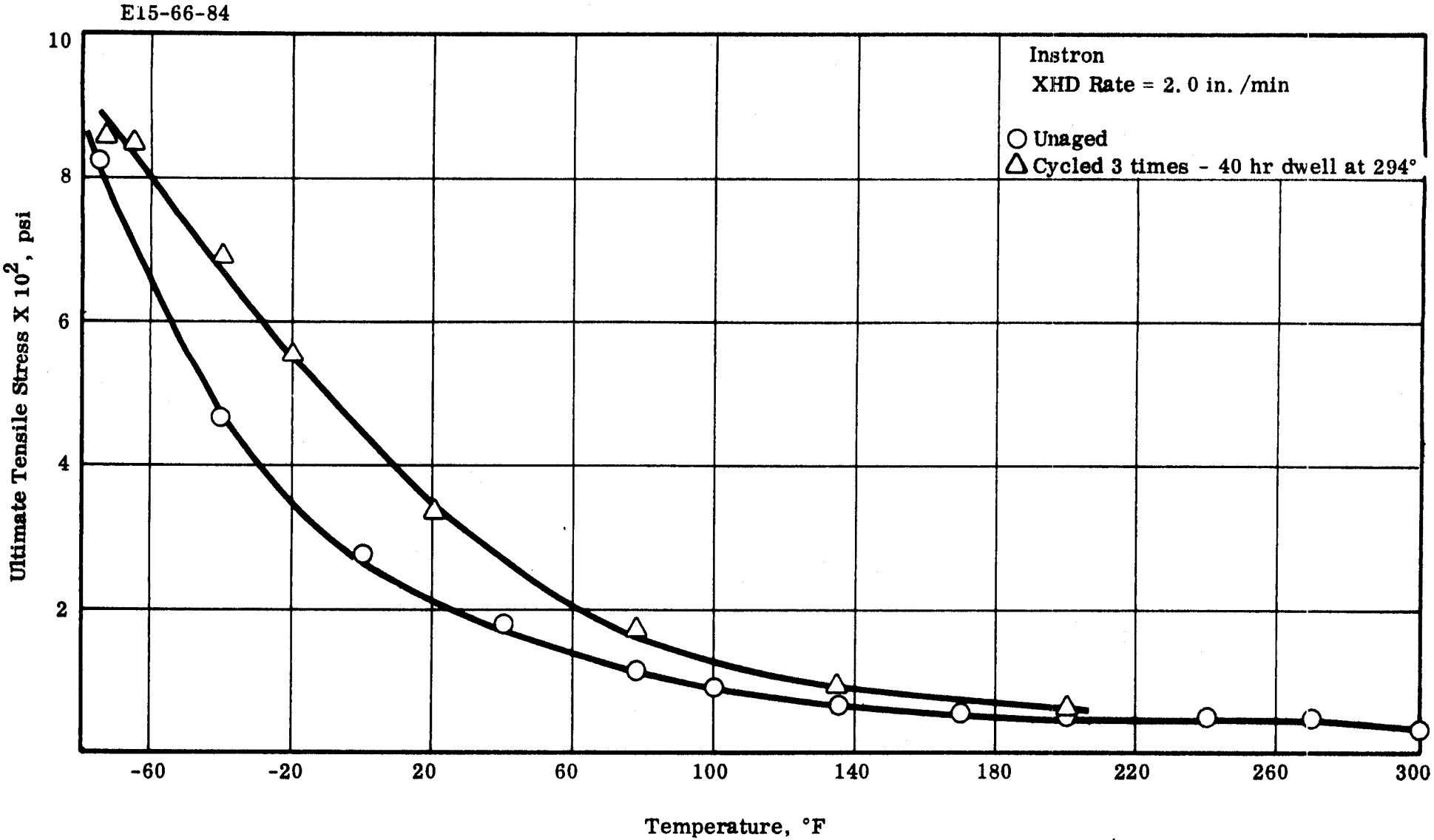

FIGURE 3. TP-H-3105 INSTRON JANAF PROFILE OF ULTIMATE TENSILE STRESS VERSUS TEMPERATURE AFTER THREE HEAT CYCLES

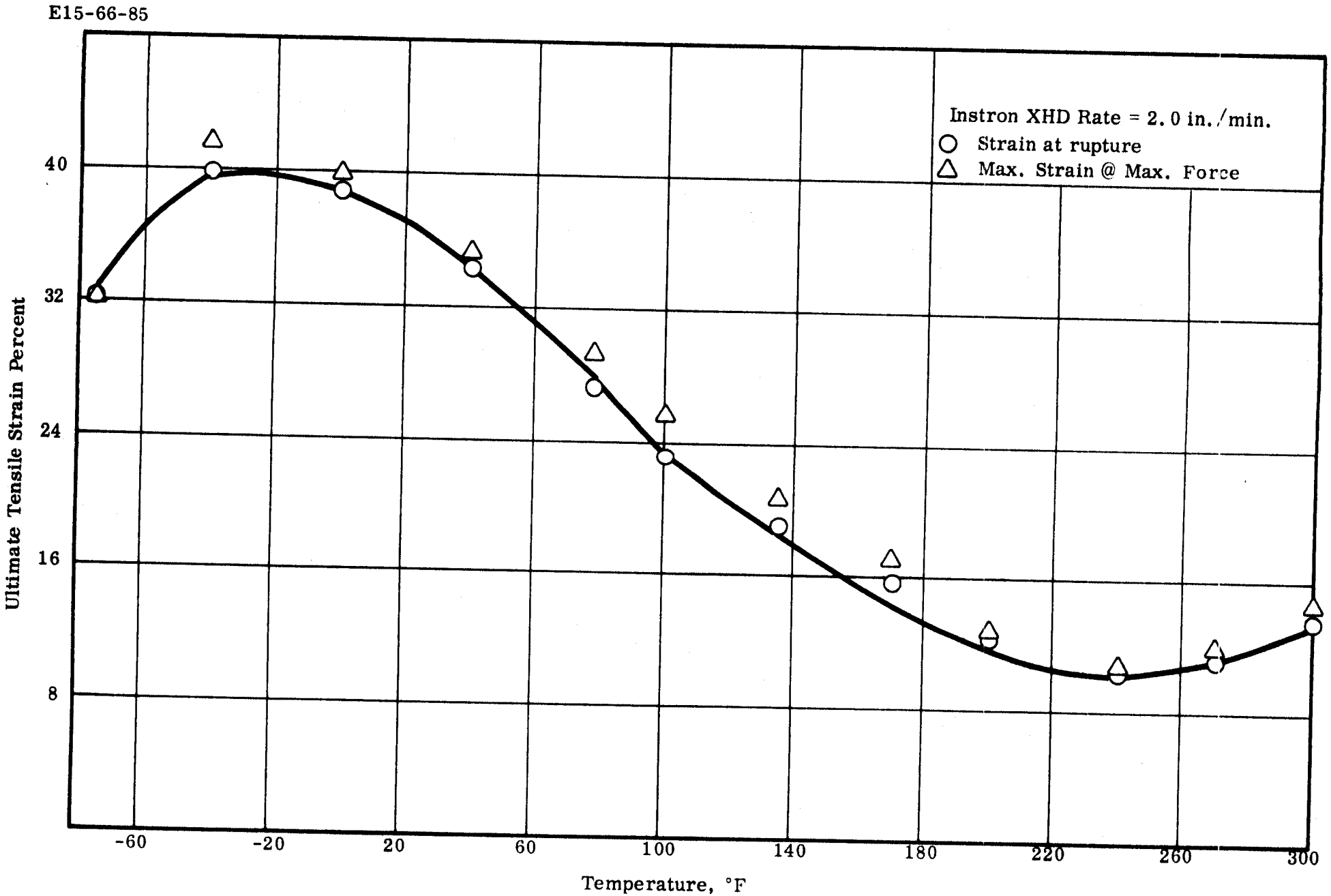

FIGURE 4. TP-H-3105 INSTRON JANAF PROFILE OF ULTIMATE TENSILE STRENGTH VERSUS TEMPERATURE AFTER THREE HEAT CYCLES

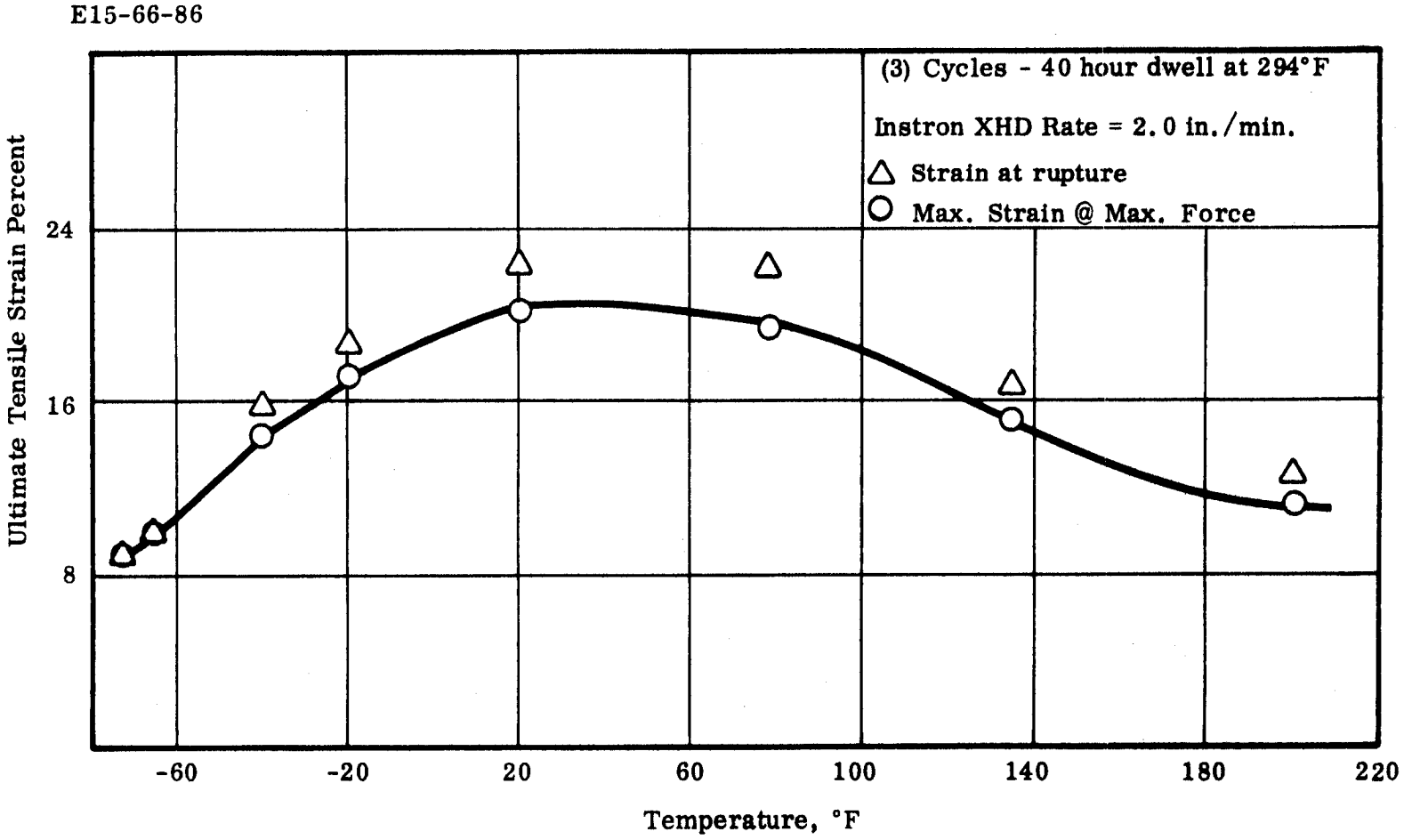

FIGURE 5. TP-H-3105 INSTRON JANAF PROFILE OF ULTIMATE TENSILE STRAIN VERSUS TEMPERATURE AFTER THREE HEAT CYCLES

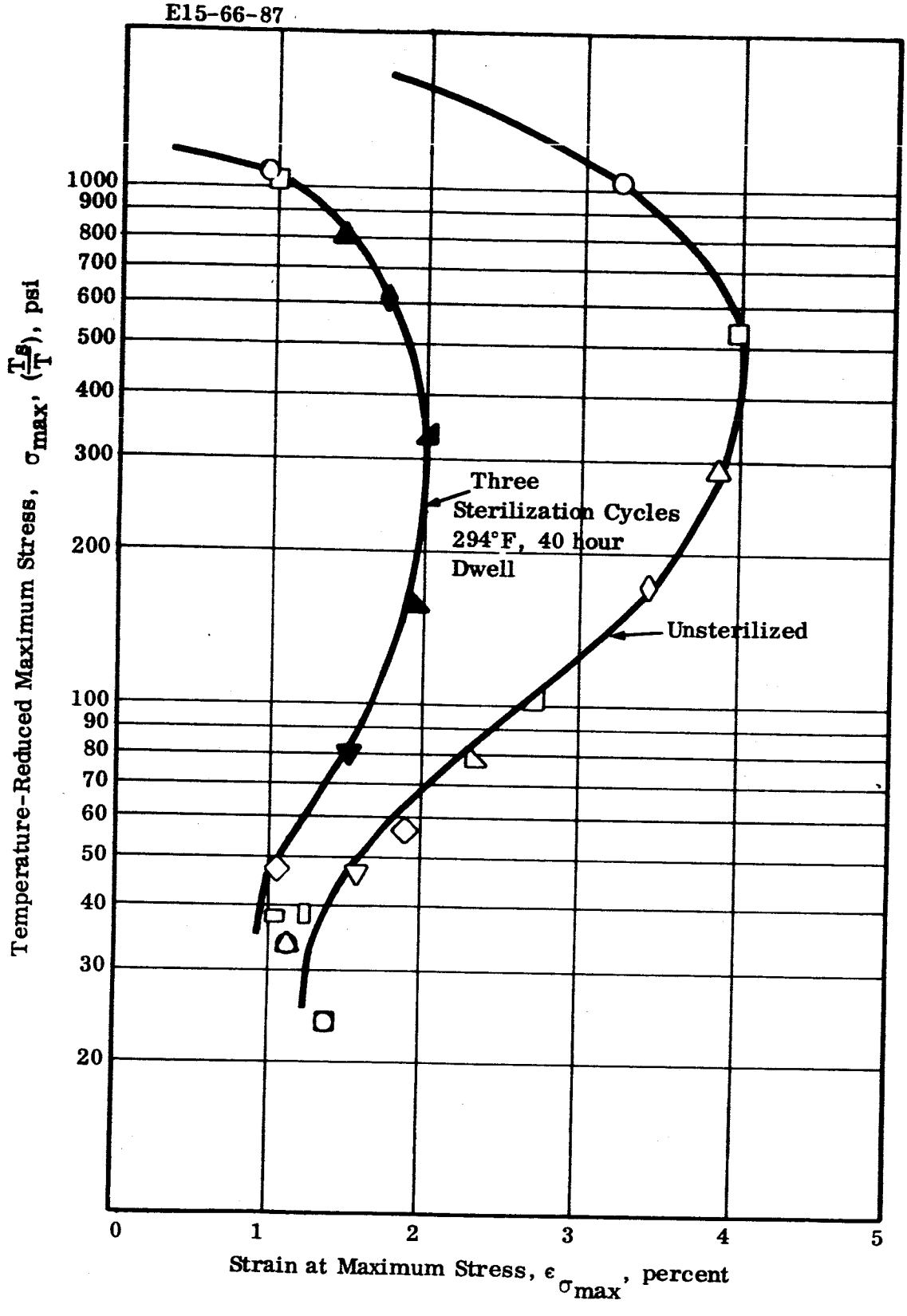

FIGURE 6. EFFECT OF STERILIZATION ON TP-H-3105 PROPELLANT FAILURE BOUNDARY

3. Designs Chosen

The two designs selected for detailed analysis and evaluation, Case-Bonded Spherical Circular Perforate and Internal-External Burning Free-Standing, will now be presented. A discussion of tne design will be given, followed by a performance summary, propellant and motor parameters, heating time, weight breakdown and discussion of component selection and design.

E. CASE BONDED SPHERICAL CIRCULAR PERFORATE MOTOR DESIGN

The case-bonded design selected for final study is the circular perforate spherical system having an O.D. of 16.23 inches. On the basis of the criteria selected, this design is superior to the other case-bonded designs; its rating on the Final Weighting Chart (Table D-I) is 108.5. The design is shown in Drawing E18605. This rocket motor has a grain of hydrocarbon propellant (TP-H-3015). The propellant grain is cast and cured in a spherical motor case of 6 Al 4V titanium alloy. The motor has a submerged conical nozzle and a PYROGEN ignition system. It has a total loaded weight of 113.9 pounds, 100 pounds of which is propellant. The time required to heat the entire motor from 70° F to 295° F is 40 hours. The design uses proven concepts and materials throughout and is similar to many other Thiokol-produced spherical motors, including the TE-M-442 (26-inch diameter, Sandia Upper Stage Motor), the TE-M-385 (12.7-inch diameter Gemini Retro motor), the TE-M-345 (13.5-inch diameter Titan Vernier), and the TE-M-364 (37-inch diameter Surveyor Main Retro motor).

1. Performance Summary

The motor performance characteristics are summarized below for temperatures of -40° F, +40° F and +120° F.

BALLISTIC PERFORMANCE AT VACUUM

Temperature, °F	-40	+40	+120
Maximum Thrust, lbf	1134	1258	1395
Average Thrust, lbf	943	1043	1160
Maximum Pressure, psia	514	570	632
Average Pressure, psia	427	474	525
Burning Time, sec	26.85	24.30	21.98

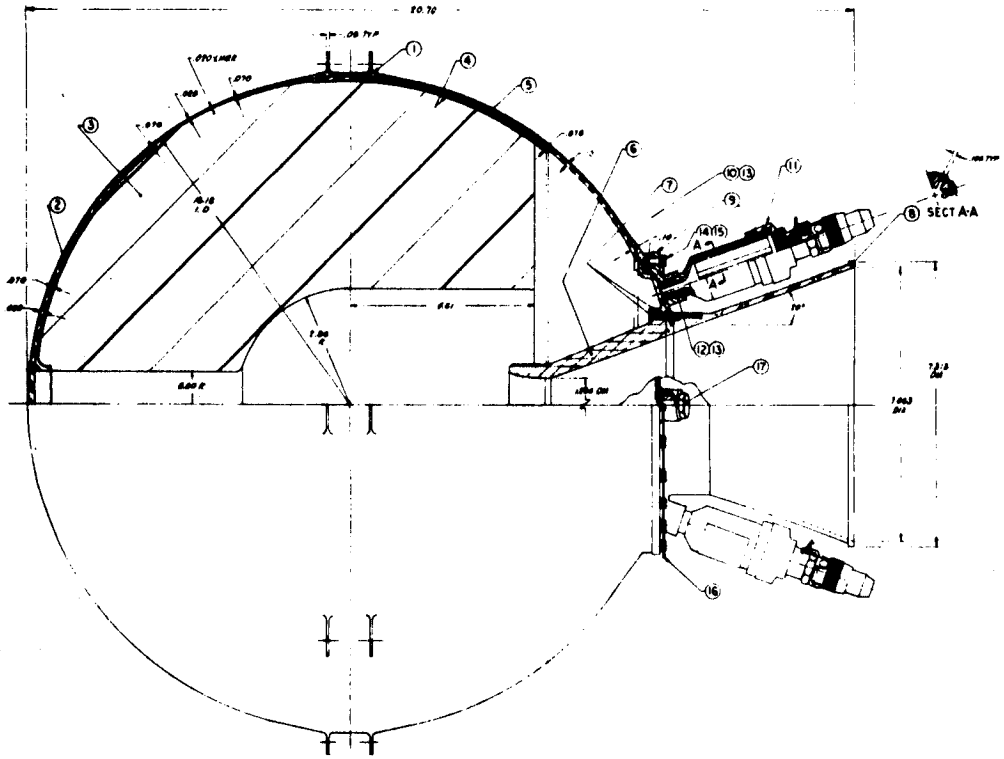
SECT A-A

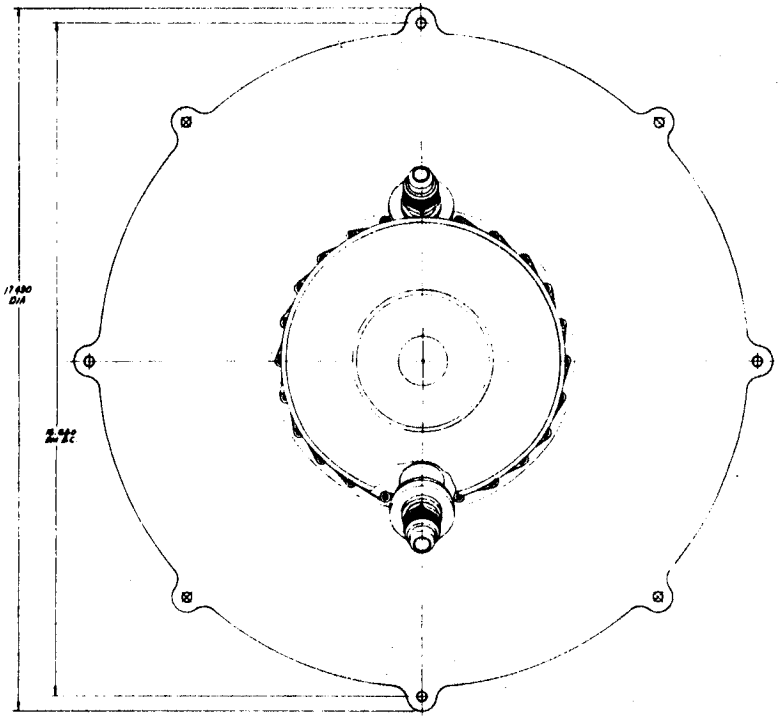

NOTES:

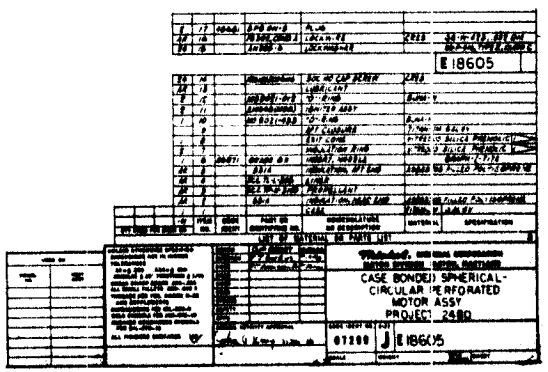
E18605
CASE BONDED SPHERICAL-
CIRCULAR PERFORATED
MOTOR ASSY
PROJECT 2480
01200
E18605

BALLISTIC PERFORMANCE AT VACUUM (CONTINUED)

Temperature, °F	-40	+40	+120
Total Impulse, lbf-sec	25,340	25,440	25,530
Propellant Specific Impulse, lbf-sec/lbm	253	254	255

Thrust and chamber pressure versus time curves at three temperatures are shown in Figures 7 and 8.

These performance values were calculated using Thiokol Computer Program No. 40243, "Internal Ballistic Performance Analysis." The following propellant and motor parameters were used. (Appendix E. Final Candidate Designs, contains a detailed listing of the motor performance parameters at -40, 0, +40, +80, and +120°F.)

PROPELLANT PARAMETERS

Burning Rate (r) at 70°F and 1,000 psi, in./sec.	0.28
Burn Rate Exponent (n)	0.32
Temperature Sensitivity of Equilibrium Pressure at Constant K_n (π_k), %/°F	0.13
Characteristic Exhaust Velocity (C*) at 1,000 psi and 70°F, ft/sec.	4848.0
Density (ρ), lb/in.^{3}	0.0595

MOTOR PARAMETERS

Nozzle Throat Area, in.^{2}	1.306
Expansion Ratio	30.0
Discharge Coefficient	0.96
Nozzle Half Angle, degrees	20

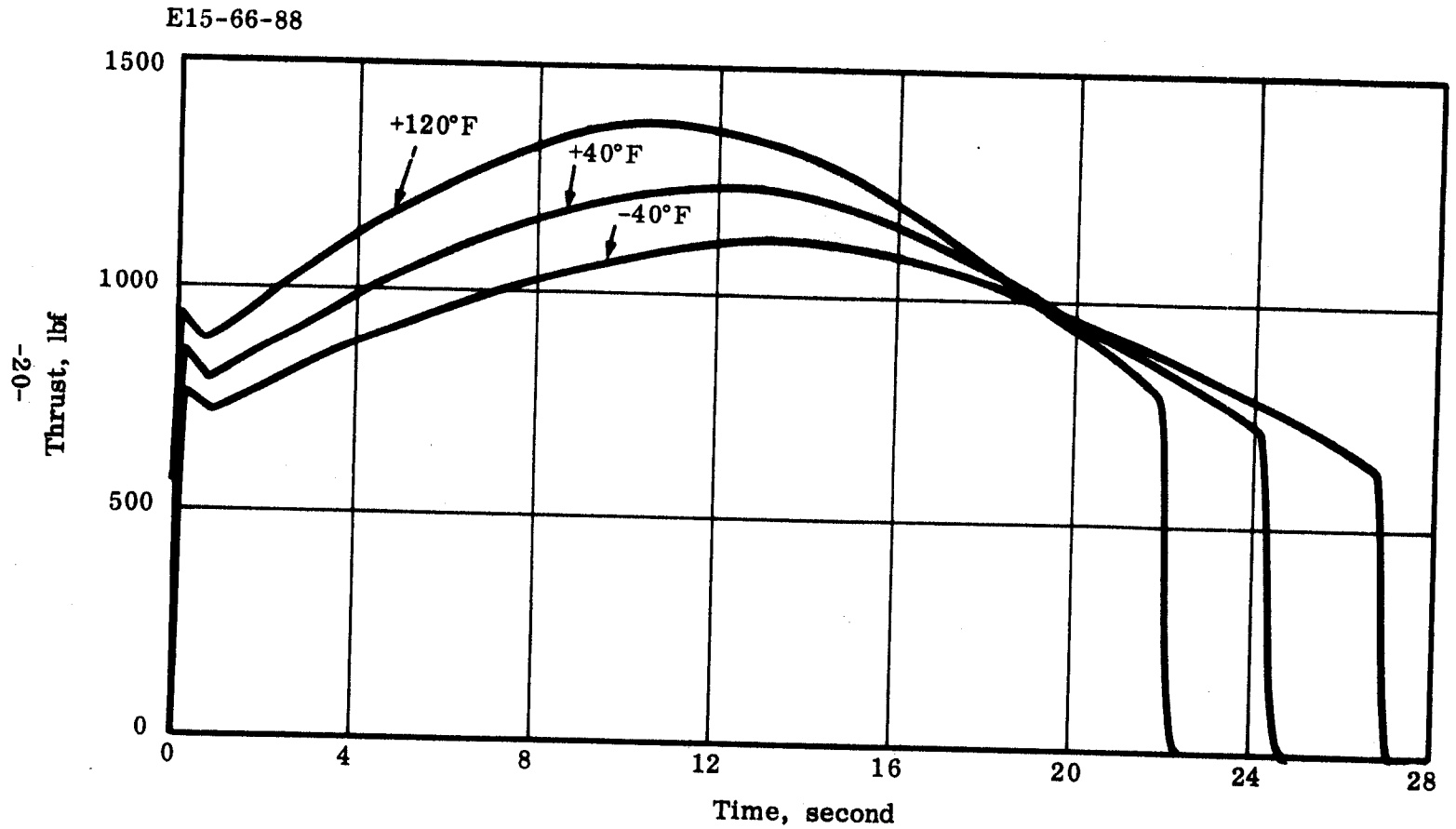

FIGURE 7. CASE-BONDED SPHERICAL CIRCULAR PERFORATE MOTOR DESIGN THRUST VERSUS TIME*

*Nominal Calculated at Vacuum, Expansion Ratio = 30, Discharge Coefficient = 0.96

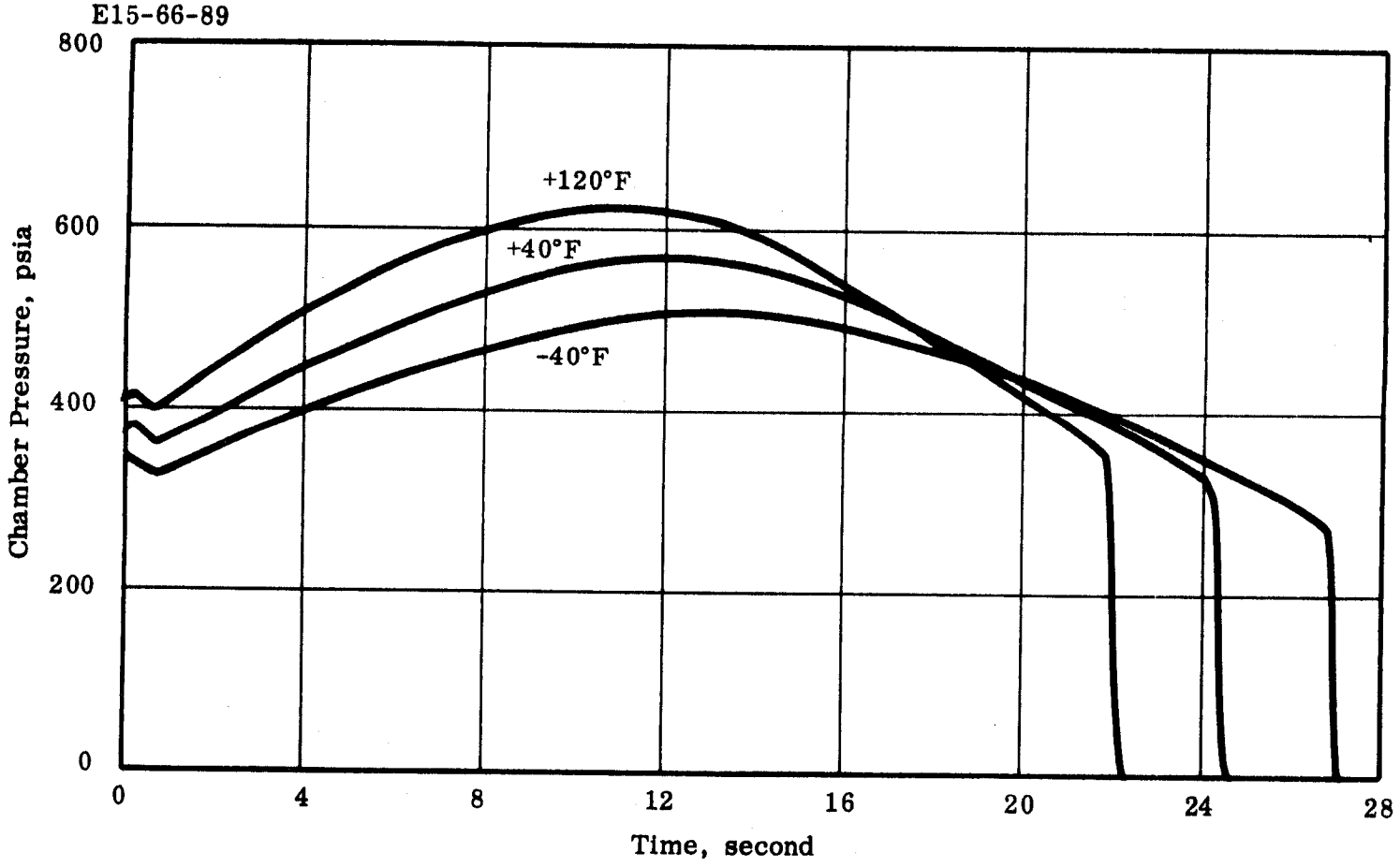

FIGURE 8. CASE-BONDED SPHERICAL CIRCULAR PERFORATE MOTOR DESIGN CHAMBER PRESSURE VERSUS TIME

2. Heating Time

The time required to heat this motor from 70°F to an equilibrium temperature of 293°F was calculated to be 40 hours for the point of greatest thermal lag which occurs on the internal surface of the propellant. Thiokol Computer Program No. 40702A "Arbitrary Node Thermal Computer Program" was used to perform the analysis, assuming a heat flux input to the external surface of the grain only. The analysis used external heat transfer coefficients based on forced convection. The results of this calculation are presented in Figure 9 for various nodal locations throughout the grain. Appendix F, Heating Time Calculations, presents the complete thermal analysis.

3. Weight Breakdown

The detailed weight breakdown of this motor is shown in the following table. Supporting calculations are given in Appendix G, Weight Analysis.

Component	Weight, lbs
Case	5.0
Insulation, Forward Case	0.8
Insulation, Aft Case	3.0
Liner and Adhesive	1.0
Exit Cone	0.9
Aft Closure	1.0
Insulation, Aft Closure	0.1
Insulation, Inert	0.1
Insert	0.9
Igniters (2)	0.7
Hardware	0.1
Unloaded Motor	13.6
Propellant	100.3
Loaded Motor	113.9
Mass Fraction	0.88

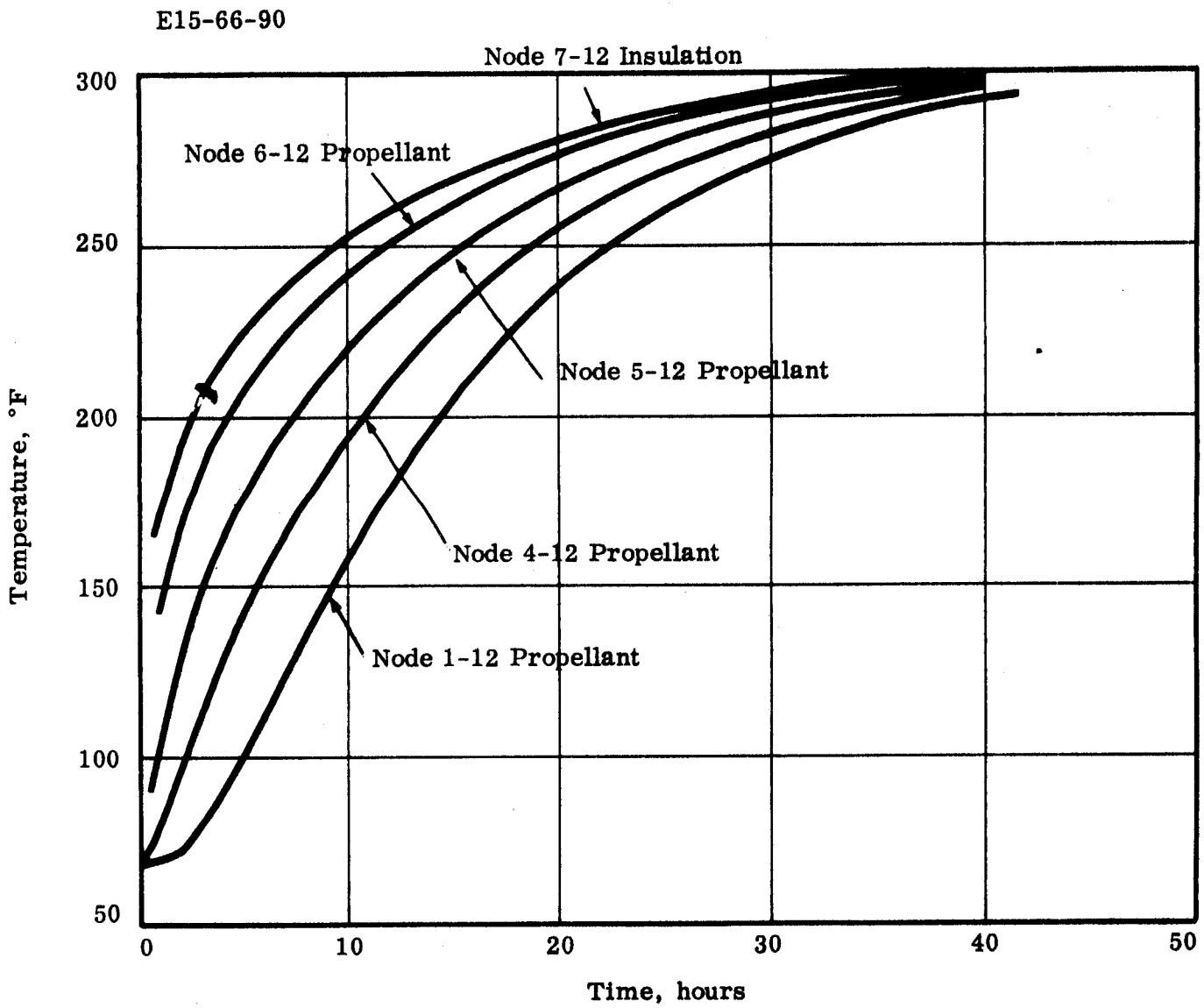

FIGURE 9. CASE-BONDED SPHERICAL CIRCULAR PERFORATE MOTOR DESIGN TEMPERATURE VERSUS TIME FOR HEATING BY FORCED CONVECTION

4. Case Design

The rocket motor chamber is a spherical pressure vessel comprised of two 6 Al 4V titanium hemispheres with a nominal thickness of 0.025 inch. The maximum chamber pressure at +120°F is 632 psia and occurs approximately 50 percent of the way through burning. The case design safety factor is 1.3, yield to P_{max}.

Eight equatorial attachments located 45 degrees apart are provided to attach the payload and thrust vector control system (if required)* to the motor case. These mounting attachments are typical of many that could be provided. The final design will depend upon the desired mating structure and the type and location of the thrust vector control system required. These attachment fittings will probably be machined from the hemispherical forging. The case wall at the attachment area is thickened to 0.070 inch.

A discussion of the selected material and the method of case manufacture is contained in Appendix H, Material Selection.

5. Case Insulation Design

That section of the case which will be exposed to hot gases before web burnout must be insulated to prevent case failure. Using a split or delamination in this insulation provides a means for relieving deformation and stress in the grain over the temperature range of -40°F to +295°F.

This successful insulating technique is used in the TE-M-364 (Surveyor Main Retro), the TE-M-385 (Gemini Retro), and other spherical motors, and is termed a "split boot". A split boot is comprised of two layers of insulation which are joined at one end and allowed to move at the other. One section of the insulation is bonded to the case; the other section is bonded to the grain. During thermal cycling, a portion of the grain is free to move, providing stress relief. Without a split boot, a bond failure could occur and cause either premature exposure of the case wall to flame temperature or a sudden increase in propellant burning surface, both of which lead to catastropic failure. In the case-bonded design originally selected, a split boot was provided at both ends of the grain. The boot in the aft end extended all the way from the equator to the motor aft end. In the stress analysis a conservative approach was used by assuming no stress relief except at the forward end of the case.

*TVC is allowed for as requested by the JPL Project Monitor. However, the mode of TVC, whether by jet vanes, nitrogen jets, or other has not been specified.

Since this analysis predicted acceptable stress levels, the extensive stress-relief boot in the aft end was eliminated. A stress-relief flap is still provided in the aft end (for purposes of cure shrinkage) but it is very short. This improves the design because the more fully case-bonded grain is better able to withstand vibration. The case insulation configuration selected was obtained directly from successful Thiokol experience with other spherical motors, including the TE-M-364 (Surveyor), TE-M-385 (Gemini), and the TE-M-442 (Sandia) spherical motors.

The split boot in the forward end of the case consists of two sections; one is bonded to the chamber wall and tapers from a thickness of 0.08 inch where the head end grain perforation joins the case to 0.070 inch at the outside of the insulation (See Drawing E18605). The other tapers from 0.070 inch near the head-end center perforation of the propellant to 0.050 inch where the section is bonded to the outer insulation. The boot is split for a distance of 1.4 inches axially from the head end of the case.

The aft insulation cap extends from 2.9 inches forward of the motor case equator at a thickness of 0.07 inch to the aft end of the grain where it is 0.10-inch thick. It continues at this thickness to the opening boss. Another layer of insulation is bonded to the first at the equator, where it is 0.05-inch thick. This increases to a total thickness of 0.070 inch at the aft grain surface. This insulation section can be used to provide stress relief if necessary. Since stress analysis indicates that a relief boot is not needed, it could be removed completely, thus saving some weight.

A discussion of the selection of asbestos-filled polyisoprene rubber (Thiokol Specification NE-1018) as the insulation material is contained in Appendix H, Material Selection.

6. Propellant Grain

a. Design

The grain design studied was a circular-perforate, case-bonded spherical design with a charge of TP-H-3105 propellant. The grain has a maximum outside diameter of 16.14 inches (excluding liner). The overall length of the grain, excluding inhibitor and stress-relief boots, is 12.45 inches. It has an uninhibited head-end perforation 1.6 inches in diameter. The aft section has a cylindrical perforation 5.72 inches in diameter. Forward of the equator, this cylinder blends into a hemisphere. This design greatly reduces the severity of the stress concentrations and slivers associated with star designs. Except that it has no star points, the design is virtually identical to that used in the TE-M-442 (Sandia) motor, and the TE-M-364 (Surveyor Main Retro).

This motor can be manufactured using the "pull out" core technique which lends itself to high quality and ease of manufacture.

No problems are anticipated from thermal loads imposed over the -40°F to +120°F operating range, or during sterilization. The separation boots described in the previous section, case internal insulation, will permit grain expansion during sterilization and shrinkage during any subsequent temperature cycling. The 100 rpm rotation during flight will have no measurable effect upon either structural or ballistic performance. The similar TE-M-442 (26-inch spherical) performed successfully at a 400 rpm spin rate. The acceleration and vibration loads are not expected to affect the structural or ballistic reliability of the motor system.

b. Manufacture

Tooling preparation, insulating the case, case cleaning, lining, curing the liner, casting, curing, disassembling the tooling, and finishings are the steps followed in the manufacture of the grain. This process is virtually identical to that used in assembling other case-bonded spherical motors.

7. Nozzle Design

The nozzle design is based on concepts demonstrated in the TE-M-385 (Gemini Retro motor), TE-M-364 (Surveyor Retro motor), and others. A monolithic graphite submerged section containing the nozzle throat is supported by an insulated aft closure ring as shown in motor assembly drawing E18605. The external exit cone, a one-piece, high pressure molding of vitreous silica phenolic, is threaded into the aft closure ring. The titanium aft closure ring includes a shear lip with a nominal 0.003-inch gap that prevents the submerged nozzle section from imparting structural loads to the exit cone section. The titanium is insulated from the nozzle graphite by two silica phenolic rings bonded to the metal. It is insulated from the motor chamber by a layer of asbestos-filled polyisoprene elastomeric insulation.

a. Nozzle Throat Insert

The nozzle insert (submerged section) will be fabricated from a high density graphite, Graph-I-Tite GX.* This material is presently used in the TU-122 (Minuteman First Stage), the TE-M-364 (Surveyor Main Retro), and the TE-M-442 (Sandia Upper Stage) motors. This material has superior physical properties and greater erosion resistance than other, currently available high density graphites.

*Graph-I-Tite is a tradename of the Basic Carbon Company and is used in identifying high density extruded graphite.

A numerical comparison of the physical properties of Graph-I-Tite GX, ATJ and CGW graphite is presented in Appendix H, Material Selection. Any of these materials would perform satisfactorily in this motor. However, in order to provide the highest assurance of integrity under the most stringent conditions, we have selected Graph-I-Tite GX. Indicative of Graph-I-Tite GX's excellent performance is its use in the TE-M-364 (Surveyor Main Retro), which has a 40-second burn time. In the TE-M-364, this high density graphite has repeatedly withstood extreme thermal shocks, vibration loads, and the erosive products in the exhaust of highly aluminized propellant.

The nozzle insert will be manufactured by simply machining the final contour from an extruded rod of a standard diameter.

The nozzle insert incorporates circumferential slots at the aft closure interface. During the assembly of the insert and the insulated closure, Epon VIII adhesive in the slots and at the aft graphite-phenolic interface forms a bond joint. The graphite is also restrained by being a press fit into the insulated aft closure ring.

b. Nozzle Exit Cone

The nozzle exit cone will be molded under high pressure from a phenolic resin reinforced with chopped vitreous silica cloth. Portions of the exit cone, such as the threads and mating surfaces, will be machined after molding. The material used in this exit cone is defined by Thiokol specification NE-1009; the molding will be made to Thiokol specification P-17001. Typical minimum average values for this material, when molded at 2000 psi, are:

Specific gravity, average	1.79
Compressive strength, psi	30,000
Tensile strength, psi	8,500
Flexural strength, psi	14,000
Shear strength, psi	14,500
Thermal conductivity, $\frac{\text{BTU-in.}}{\text{ft}^2\text{-hr-}^\circ\text{F}}$	2.37 @ 300°F
Specific heat, $\frac{\text{BTU}}{\text{lb-}^\circ\text{F}}$	0.22 @ 150°F

This material has been employed successfully in many Thiokol programs. It is used in exit cones for the TE-M-345, TE-M-375, TE-M-385, TE-M-442, and numerous other motors. Analyses of the erosion and charring of the silica-phenolic exit cone indicate that the thickness of the cone should be based on the pressure and acceleration loads rather than on the erosion of the material. The exit cone is threaded into the titanium aft closure-nozzle ring. The threaded area will be coated with an epoxy adhesive during assembly.

8. Ignition System

The ignition system consists of two PYROGEN igniters. The design of these igniters is based on the TE-P-386 (Gemini) PYROGEN. The PYROGEN case and cap material are titanium to minimize magnetic effects. The propellant charge is TP-H-3105 in an eight-point star configuration. This configuration provides a completely regressive burning PYROGEN, with a high initial weight flow rate of combustion gases which ensures rapid yet soft ignition of the main motor grain. The regressive character of the PYROGEN produces a gradual blend into the main motor pressure curve.

The pellet charge will be boron-potassium nitrate pellets conforming to Thiokol Specification ESRM-13. Detailed PYROGEN design was not made; however, all items considered in the design of the main motor, such as differential expansion and the use of heat sterilizable materials, have been allowed for.

The initiator would probably be based on the existing standard initiator (SO1-266-8) but modified to allow it to be sterilized by heat. This is one of the critical design problem areas; it is fully discussed in Appendix A, Design Guidelines.

9. Nozzle Closure

This is a critical design area which has not been resolved. Refer to Appendix A, General Design Guidelines, for discussion.

10. Grain Structural Analysis

The case-bonded spherical design was subjected to an extensive structural study. The effects of grain geometry (web thickness, cross-sectional perforation and boot reliefs), propellant-liner-insulation interfacing, and sterilization were considered.

The method of superposition was used to determine the stress and deformation requirements of the motor. Consideration was given to shrinkage due to cure, thermal shrinkage and expansion, pressurization, acceleration and interface bonding. Where possible, the temperature-rate dependence of TP-H-3105 was accounted for.

The results of these analyses indicate that this candidate sterilizable design is capable of withstanding the environmental and operational loadings to which it will be exposed following sterilization.

The longitudinal cross-section shown in Figure 10 formed the geometrical basis for all analyses with the exception of the split booting. As discussed earlier (Section E.5) it was assumed that the grain was bonded over the entire aft section of the spherical dome.

The structural response of this design was determined by means of a Thiokol digital computer program (E43113) which is based upon finite element stiffness theory. The cross section of this motor, as modeled for grain structural analysis, is shown in Figures 11 and 12. Figure 11 illustrates the element modeling and specifies nodal numbers; Figure 12 gives the element numbers. The computer program calculates stresses for each element and displacements for each node corresponding to specified loads and material properties. The results of these analyses have been presented in the form of deformation profiles, interface and bore stresses.

a. Thermal Expansion Due to Sterilization

(1) Deformations

The resultant deformation profiles due to sterilization are shown in Figures 13, 14 and 15. For this analysis it was assumed that the zero strain temperature (the temperature above cure temperature at which the internal profile of the grain corresponds to the external profile of the core) was 23°F above the cure temperature (150°F) of TP-H-3105 because of propellant shrinkage during cure. It was further assumed that, due to the low thermal conductivity of propellant and the consequent low thermal strain rate, the propellant would exhibit an equilibrium modulus of 200 psi during expansion. Deformations were obtained for a temperature rise of 122°F and for Poisson's ratio (ν) of 0.40 and 0.49. Figure 15 illustrates the effect that Poisson's ratio has on the internally deformed profile.

(2) Interface and Bore Stresses

The interface bond stresses and port hoop stresses corresponding to the deformations cited above are shown in Figures 16-19. The end boundary conditions are specified on each graph as being the boot termination and propellant-case juncture. The propellant was constrained to remain within the case boundary by allowing only deformations into the igniter port.

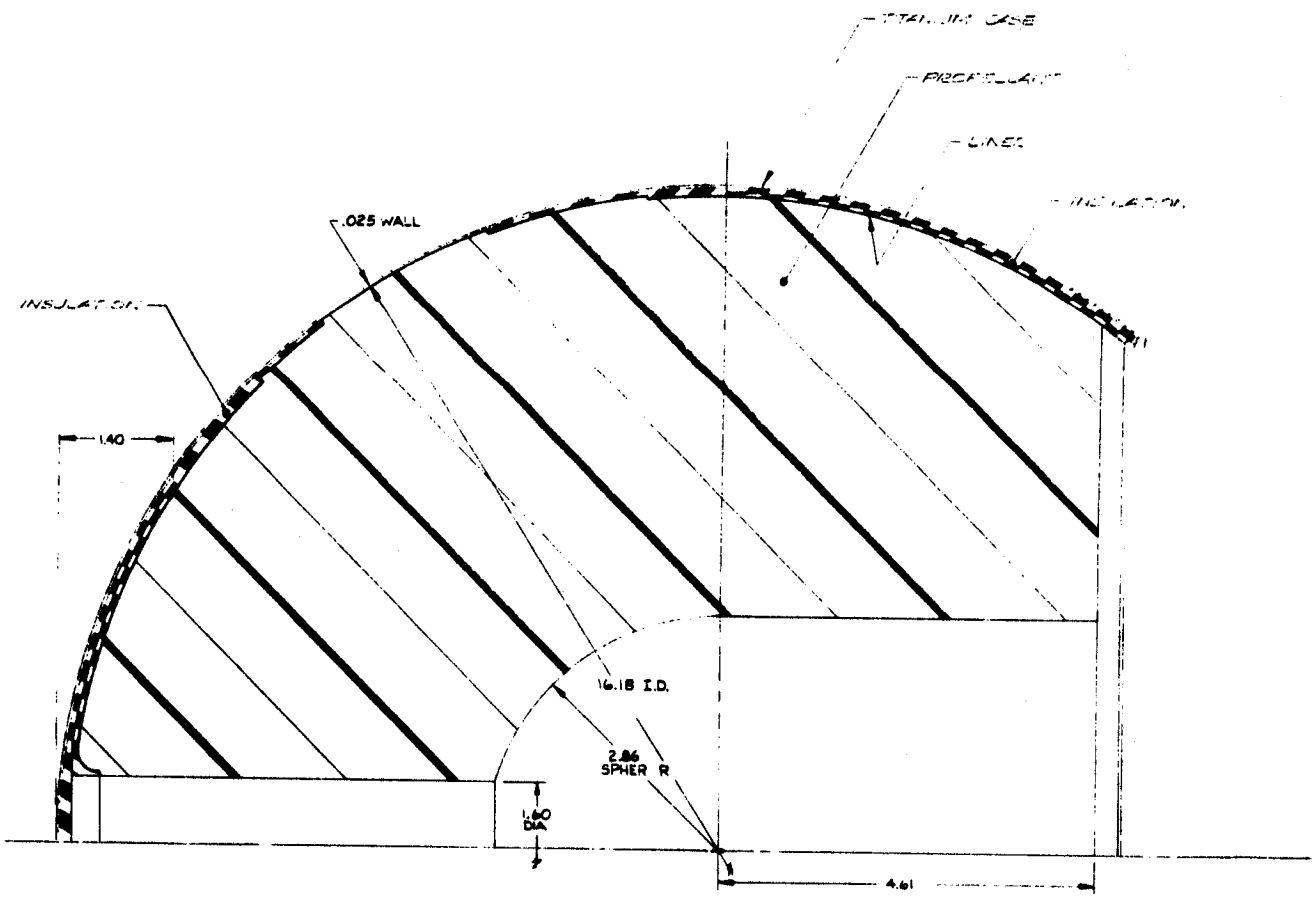

FIGURE 10. CASE BONDED SPHERICAL CIRCULAR PERFORATE MOTOR DESIGN

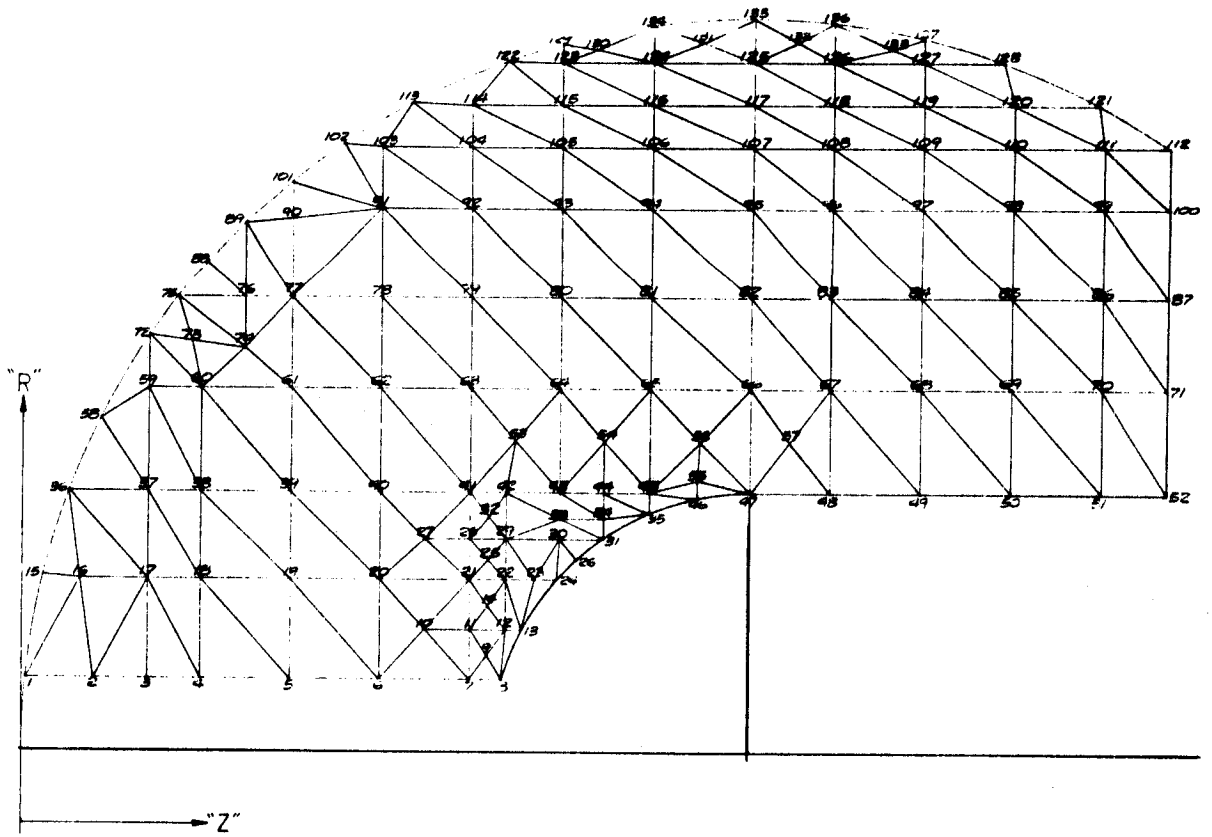

FIGURE 11. CASE BONDED SPHERICAL CIRCULAR PERFORATE MOTOR DESIGN. NODAL POINT NUMBERS

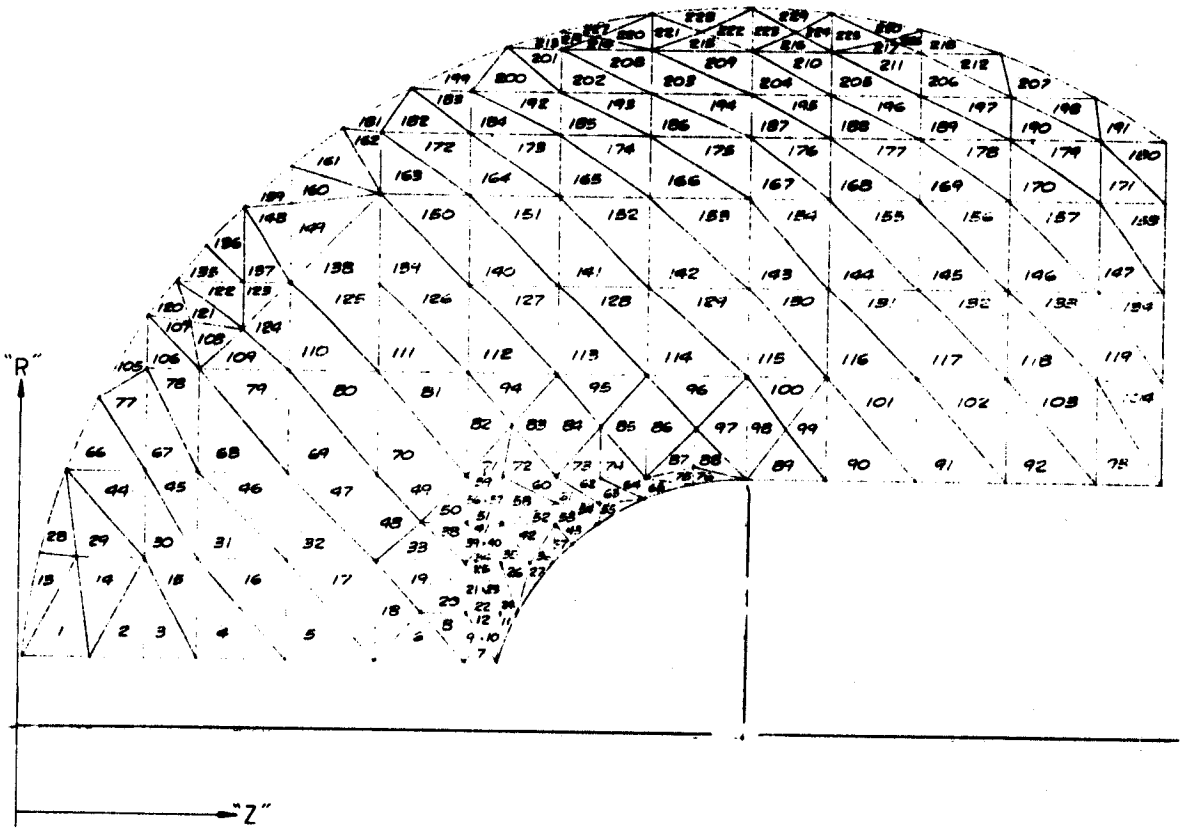

FIGURE 12. CASE BONDED SPHERICAL CIRCULAR PERFORATE MOTOR DESIGN ELEMENT NUMBERS

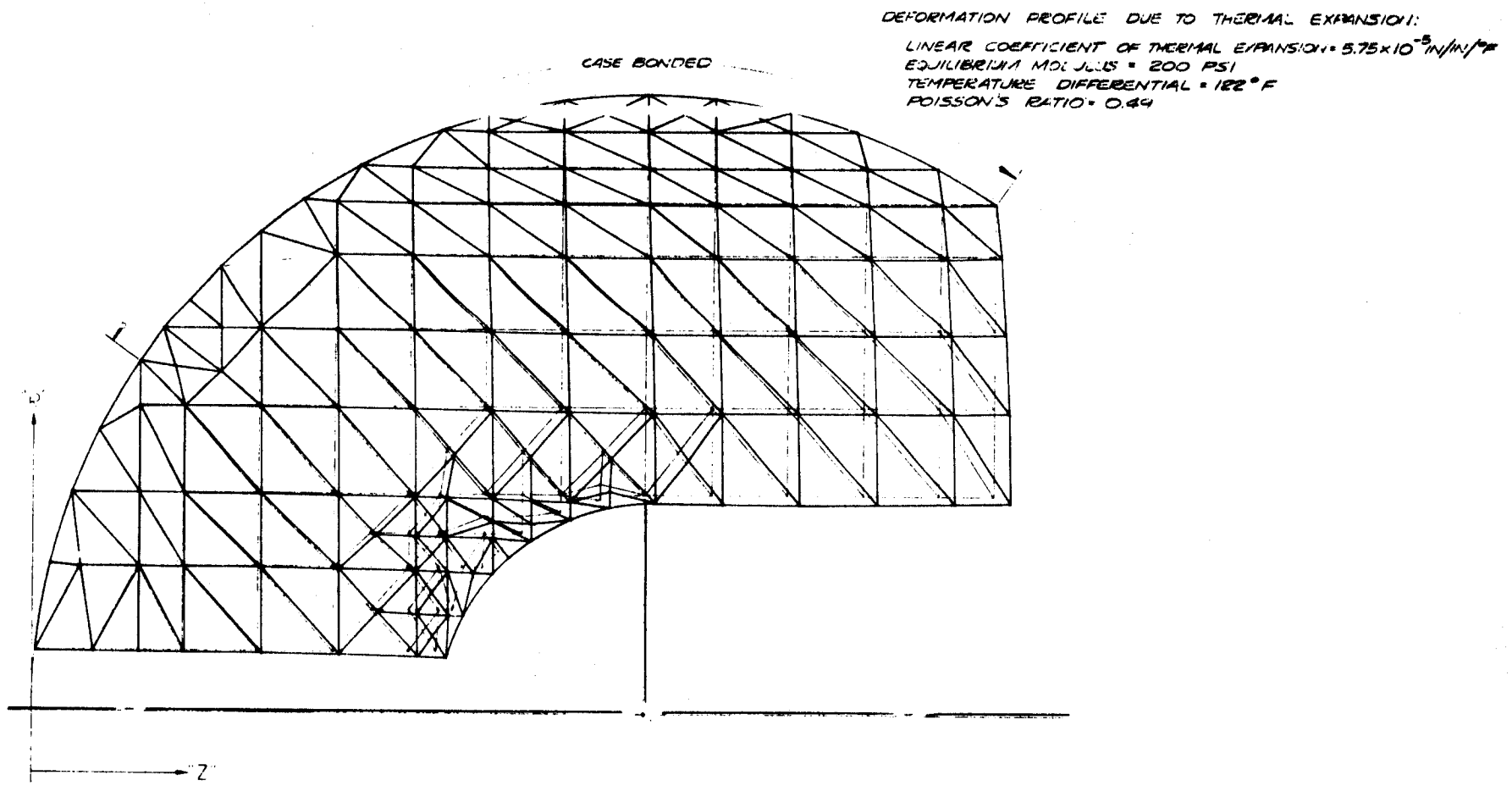

FIGURE 13. CASE BONDED SPHERICAL CIRCULAR PERFORATE MOTOR DESIGN

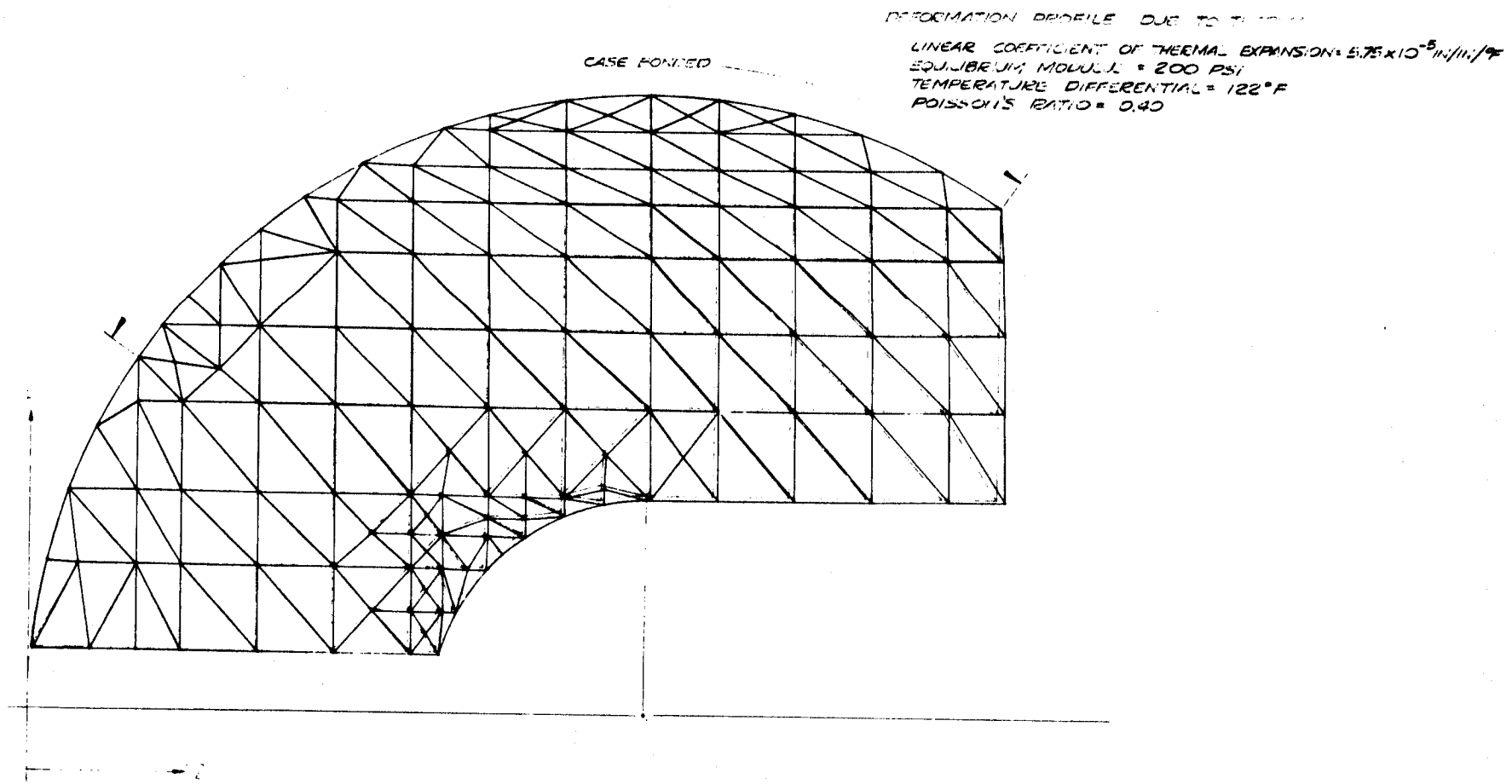

FIGURE 14. CASE BONDED SPHERICAL CIRCULAR PERFORATE MOTOR DESIGN

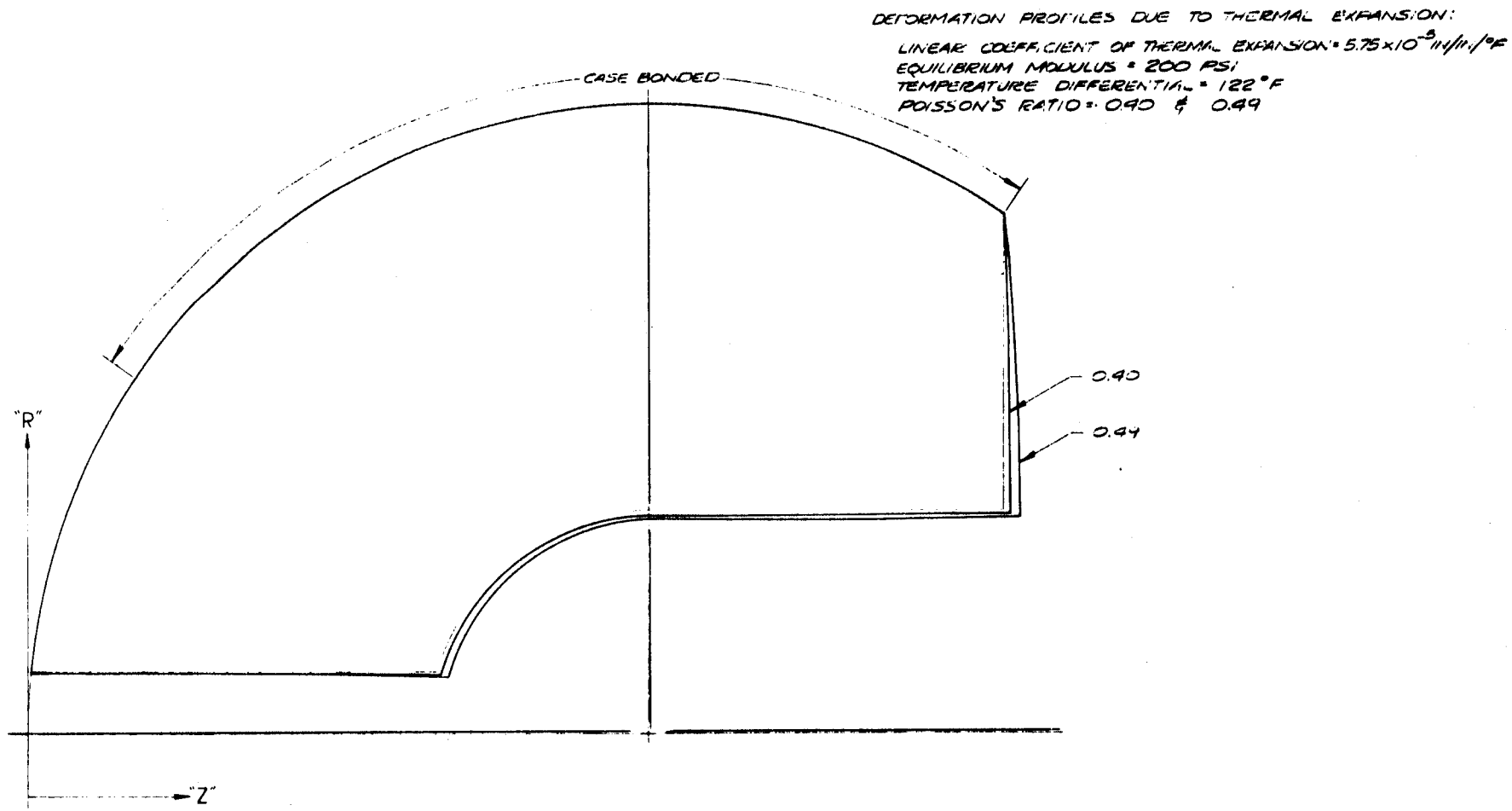

FIGURE 15. CASE BONDED SPHERICAL CIRCULAR PERFORATE MOTOR DESIGN

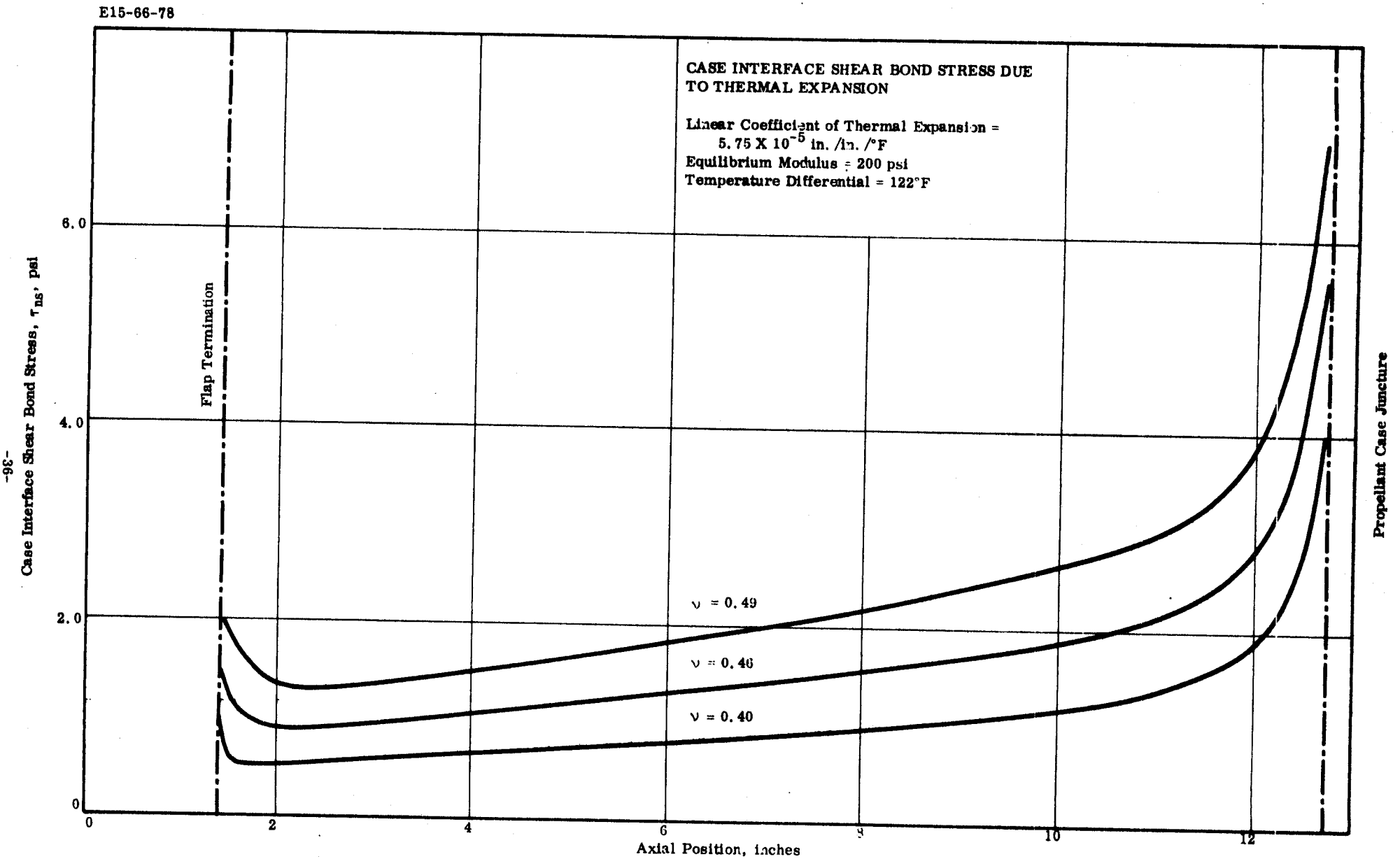

FIGURE 16. CASE BONDED SPHERICAL CIRCULAR PERFORATE MOTOR DESIGN

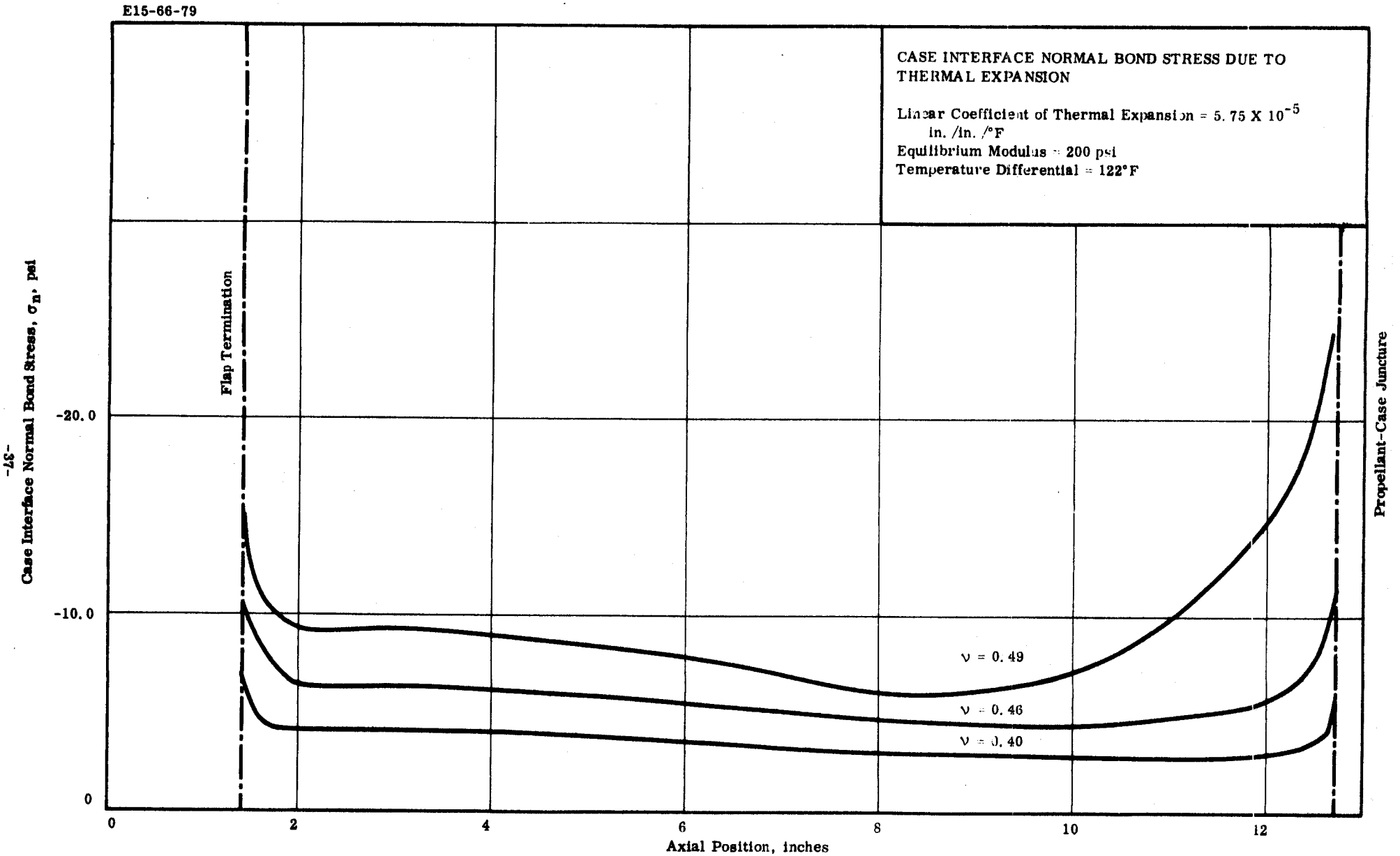

FIGURE 17. CASE BONDED SPHERICAL CIRCULAR PERFORATE MOTOR DESIGN

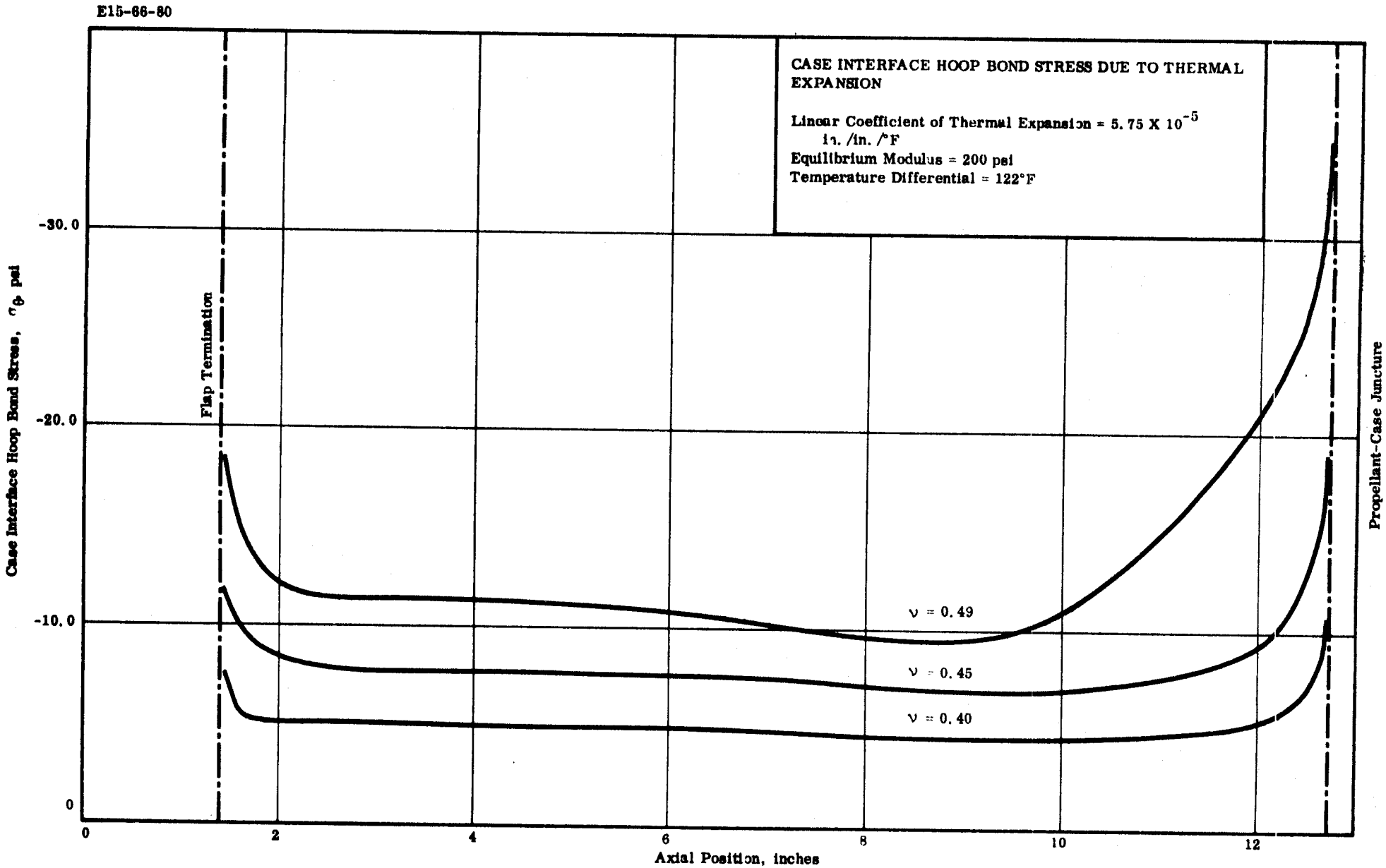

FIGURE 18. CASE BONDED SPHERICAL CIRCULAR PERFORATE MOTOR DESIGN

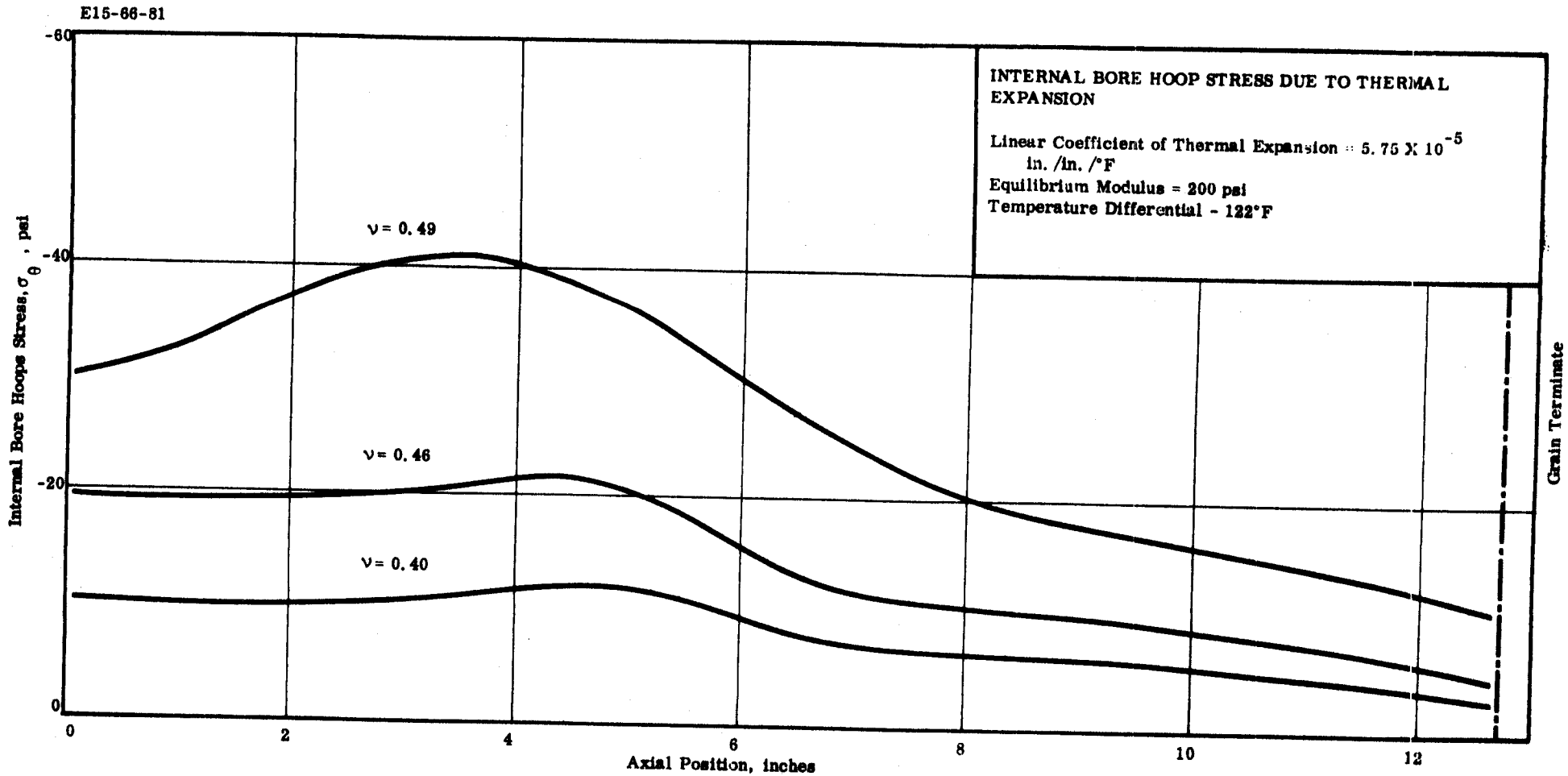

FIGURE 19. CASE BONDED SPHERICAL CIRCULAR PERFORATE MOTOR DESIGN

b. Thermal Shrinkage Due to Low Temperature Space Storage

(1) Deformations

The deformation profiles resulting from a drop to -40°F in space are shown in Figures 20, 21 and 22. Again, due to the low thermal conductivity of propellant, an equilibrium modulus of 200 psi was used, and results were obtained for Poisson's ratios of 0.40 and 0.49. The zero strain temperature, based upon the propellant linear coefficient of thermal expansion, was assumed to be 173°F, this is a temperature differential of 213°F at -40°F.

(2) Interface and Bore Stresses

The interface bond stresses and port hoop stress corresponding to the deformations cited above are shown in Figures 23 to 26. For these problems the igniter port split boot in the head end was provided for stress and deformation relief during shrinkage.

c. Internal Pressurization

(1) Deformations

It was assumed that the motor would be fired at -40°F in a space environment. A maximum ignition pressure of 325 psi was used to determine the profiles shown in Figure 27. Due to the low temperature and the rate of loading, an elastic modulus of 10,000 psi was employed. This corresponds approximately to the glassy modulus one would expect to observe in high rate - low temperature testing of sterilized TP-H-3105. Results in Figure 27 correspond to two values of Poissons ratio.

(2) Stresses

Since the relation of the compressive pressurization stress field to the structural integrity of the grain is yet an unknown quantity, no results are included. In point of fact, there is little information concerning the response of propellant to combined tensile-compression stress fields.

d. Axial Acceleration

(1) Deformations

The response of the motor to an axial setback force corresponding to a boost launch of 15 g's is given in Figure 28. A modulus of 200 psi and Poisson's ratios of 0.40 and 0.49 were used.

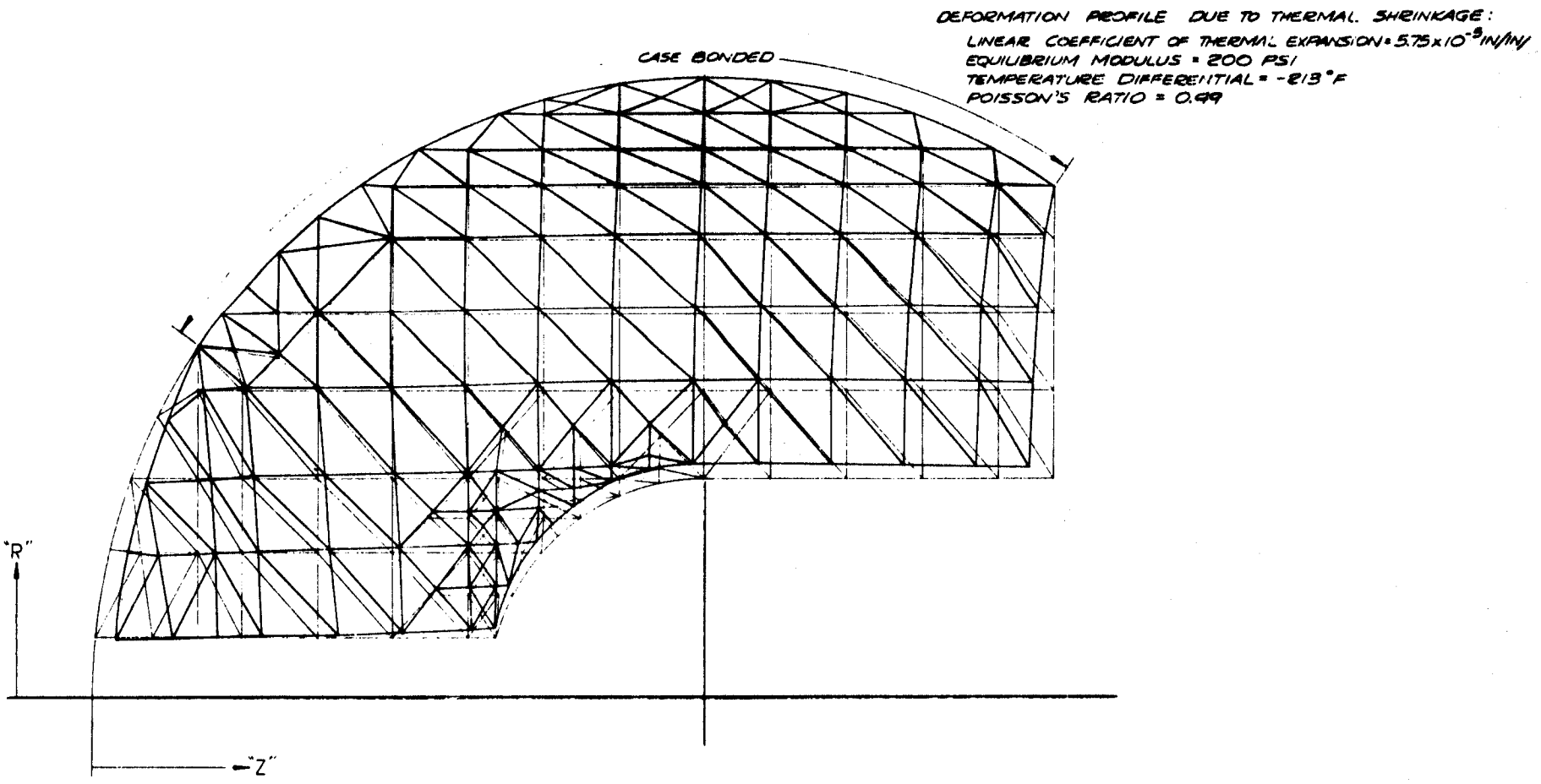

FIGURE 20. CASE BONDED SPHERICAL CIRCULAR PERFORATE MOTOR DESIGN

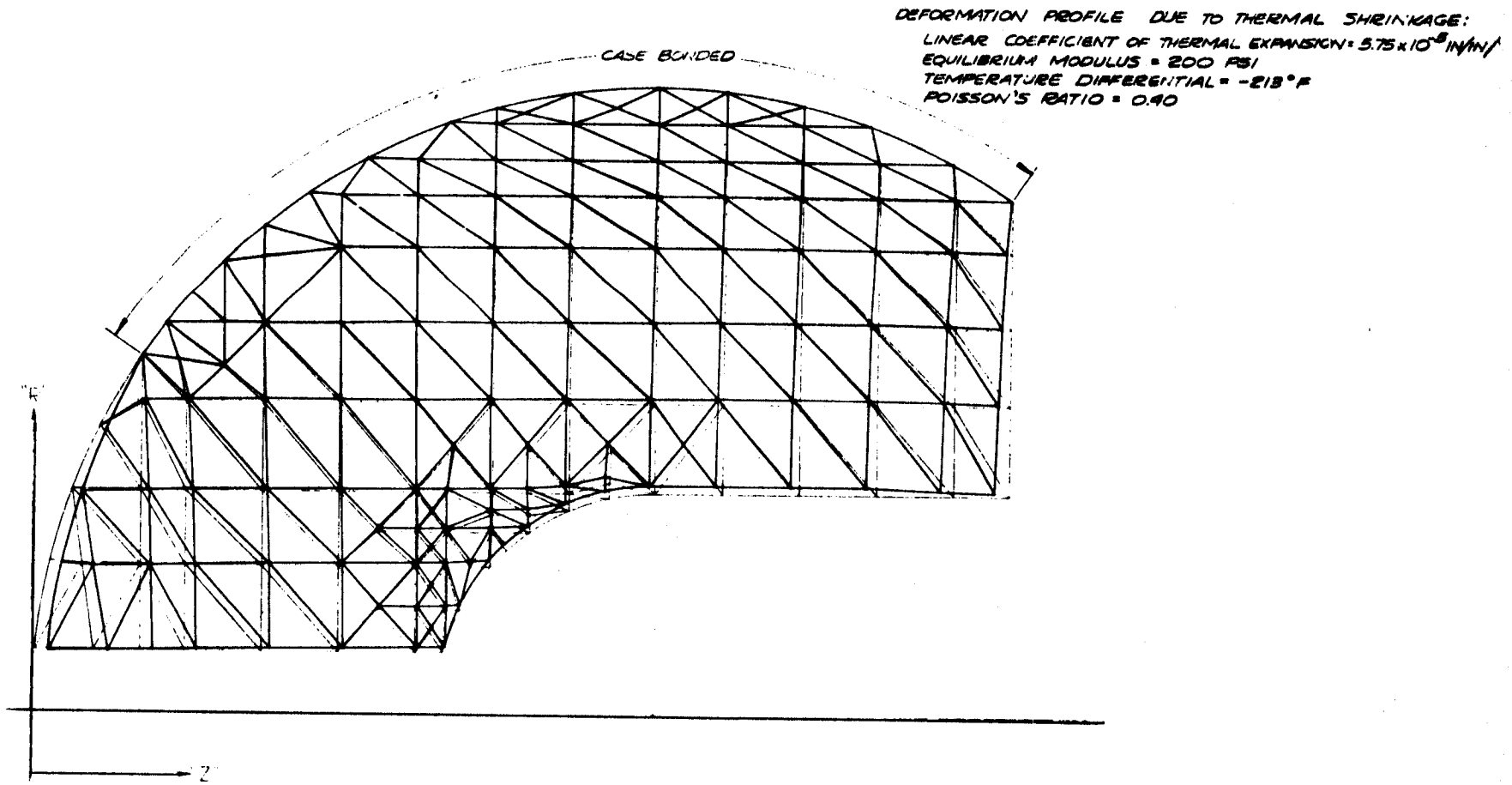

FIGURE 21. CASE BONDED SPHERICAL CIRCULAR PERFORATE MOTOR DESIGN

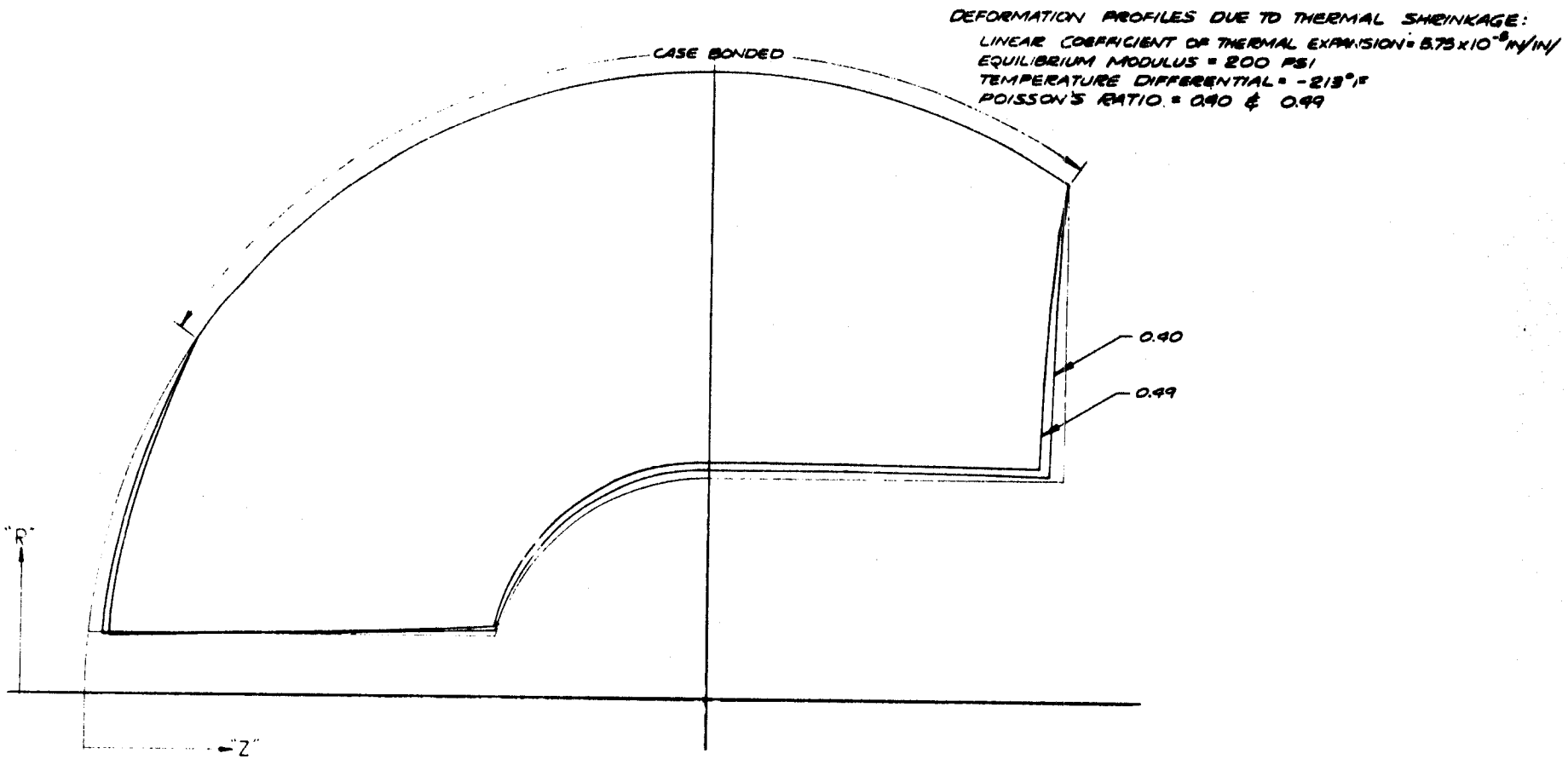

FIGURE 22. CASE BONDED SPHERICAL CIRCULAR PERFORATE MOTOR DESIGN

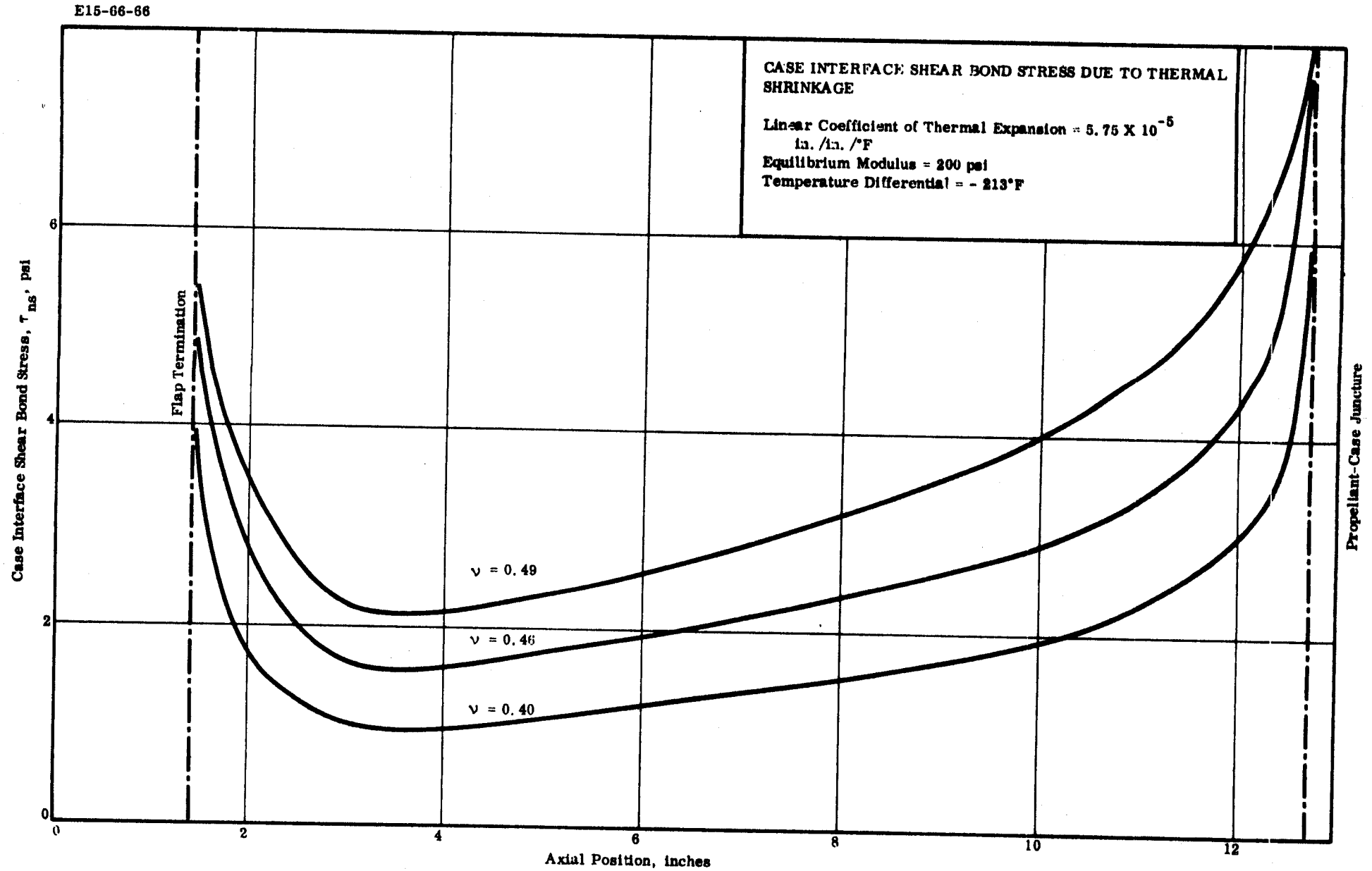

FIGURE 23. CASE BONDED SPHERICAL CIRCULAR PERFORATE MOTOR DESIGN

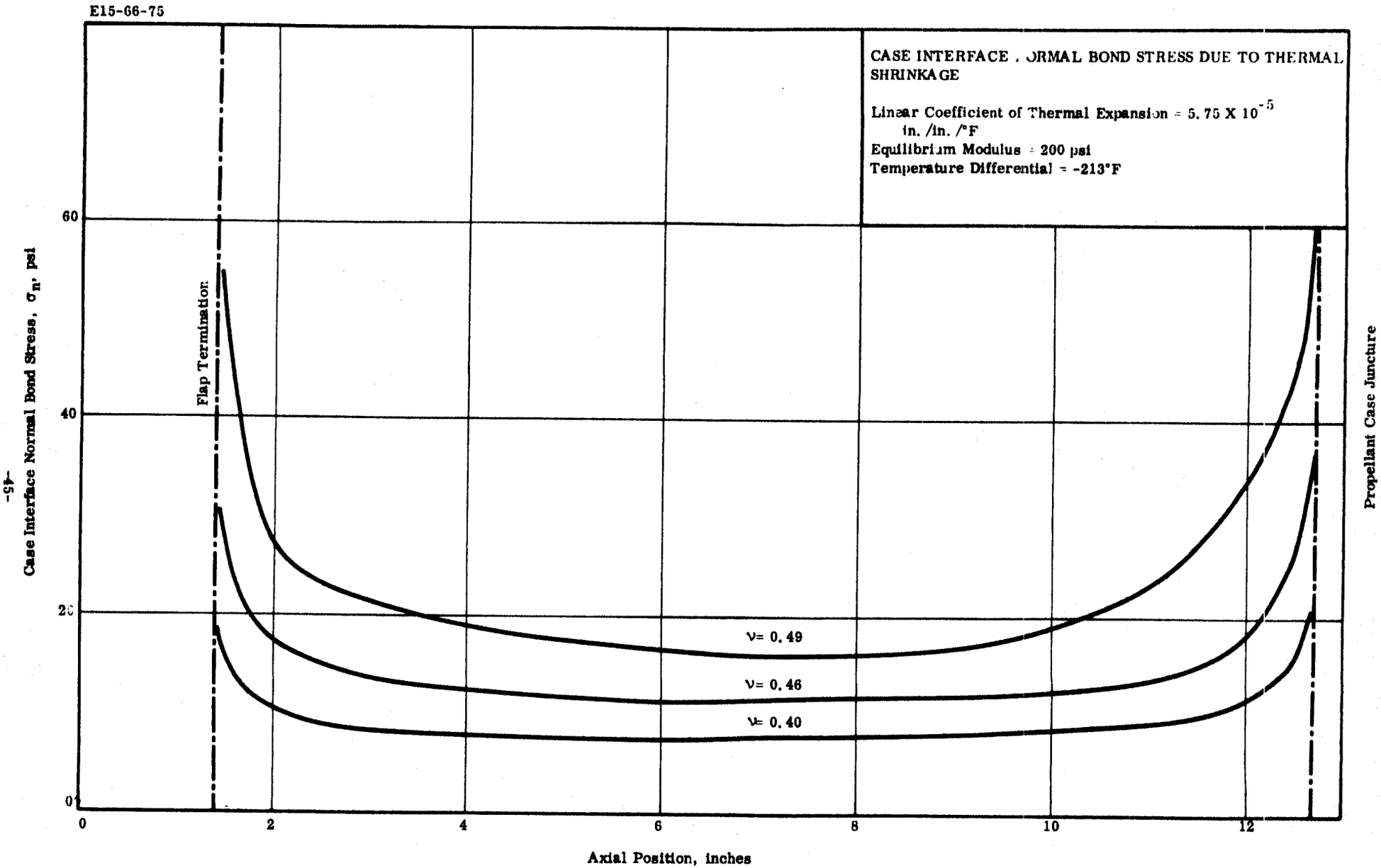

FIGURE 24. CASE BONDED SPHERICAL CIRCULAR PERFORATE MOTOR DESIGN

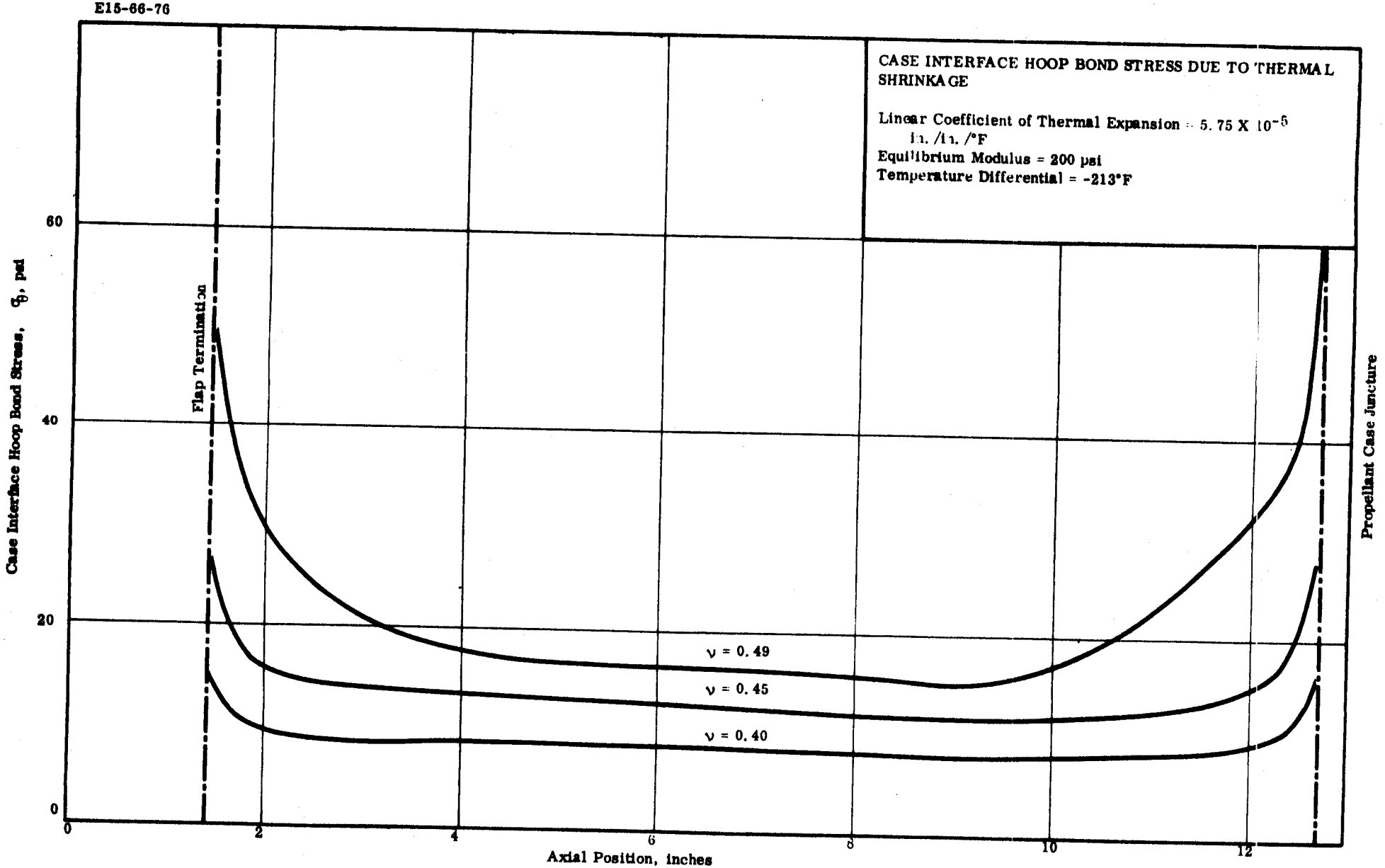

FIGURE 25. CASE BONDED SPHERICAL CIRCULAR PERFORATE MOTOR DESIGN

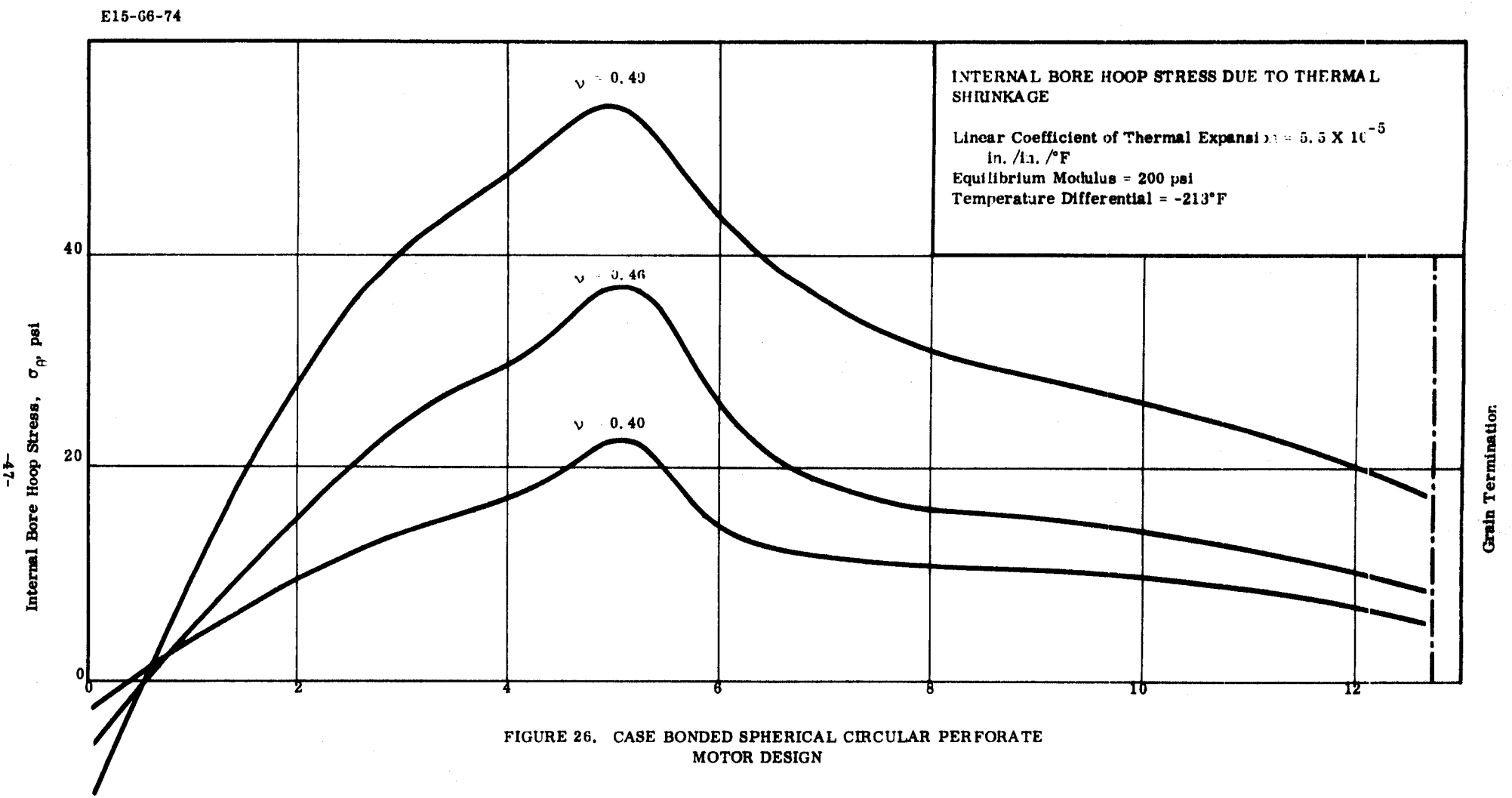

FIGURE 26. CASE BONDED SPHERICAL CIRCULAR PERFORATE MOTOR DESIGN

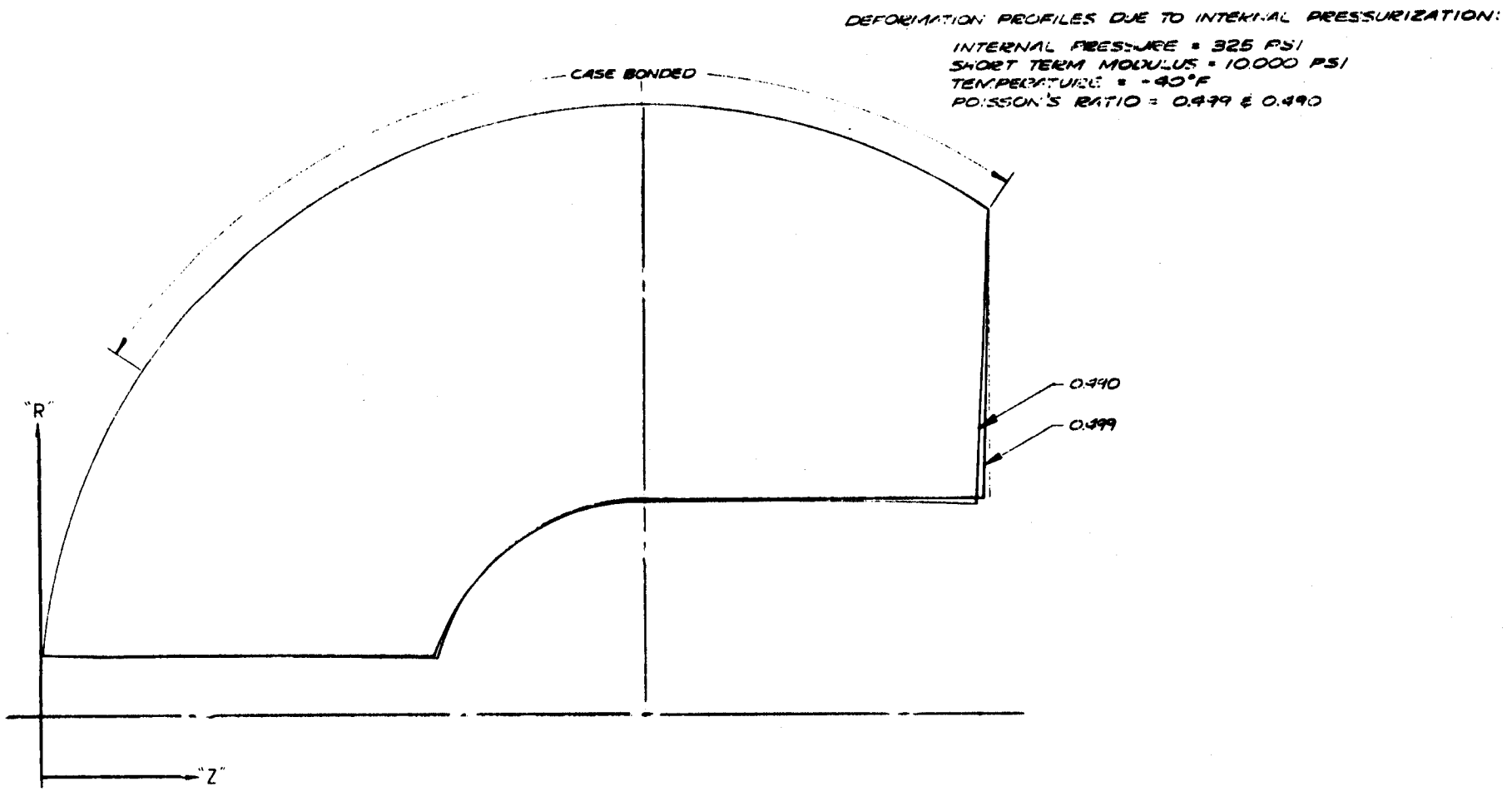

FIGURE 27. CASE BONDED SPHERICAL CIRCULAR PERFORATE MOTOR DESIGN

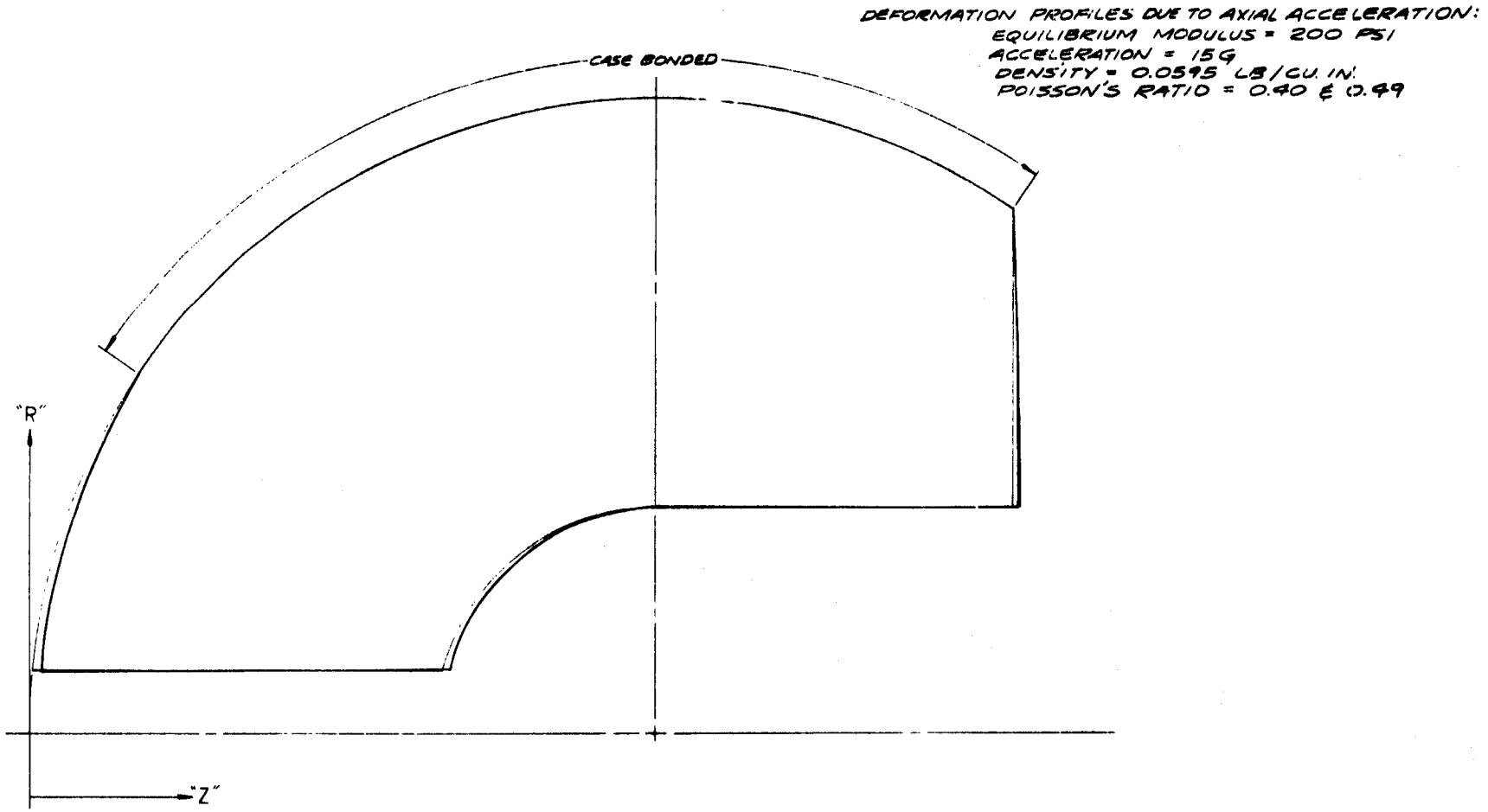

FIGURE 28. CASE BONDED SPHERICAL CIRCULAR PERFORATE MOTOR DESIGN

(2) Interface Bond Stresses

Stresses at the case - propellant interface due to an axial acceleration of 15 g's are presented in Figures 29, 30 and 31. Again, the igniter-port split boot was allowed to relieve the stresses.

e. Cumulative Effects

(1) Thermal Shrinkage and Internal Pressurization

The cumulative effect of superimposing the deformations due to internal pressurization on those due to thermal shrinkage is shown in Figure 32. The results were obtained by assuming that the most stringent structural requirement for this cumulative load would be imparted by a -40°F firing in space at an ignition maximum pressure of 325 psi.

(2) Thermal Shrinkage and Axial Acceleration

The cumulative effect of deformations due to thermal shrinkage and axial acceleration should not affect the reliability of the propellant-liner system because

a) Booster launch will take place at moderate temperatures (50°F to 100°F) so that deformations from thermal shrinkage will be low, and

b) The axial setback force during launch is rather small (15 g's) and results in deformations which tend to cancel each other.

f. Margins of Safety

The method of superposition was used to determine the total induced stresses and strains in the Case-Bonded Spherical Circular Perforate Motor design. Safety factors were computed based upon the theory of maximum principal strain (stress) structural failure and cumulative damage. The tensile-temperature profile of sterilized TP-H-3105, and the adhesive bond strengths of sterilized TL-H-3105 and Epon 912 were used as representative of the ultimate structural capacity of the propellant-liner system.

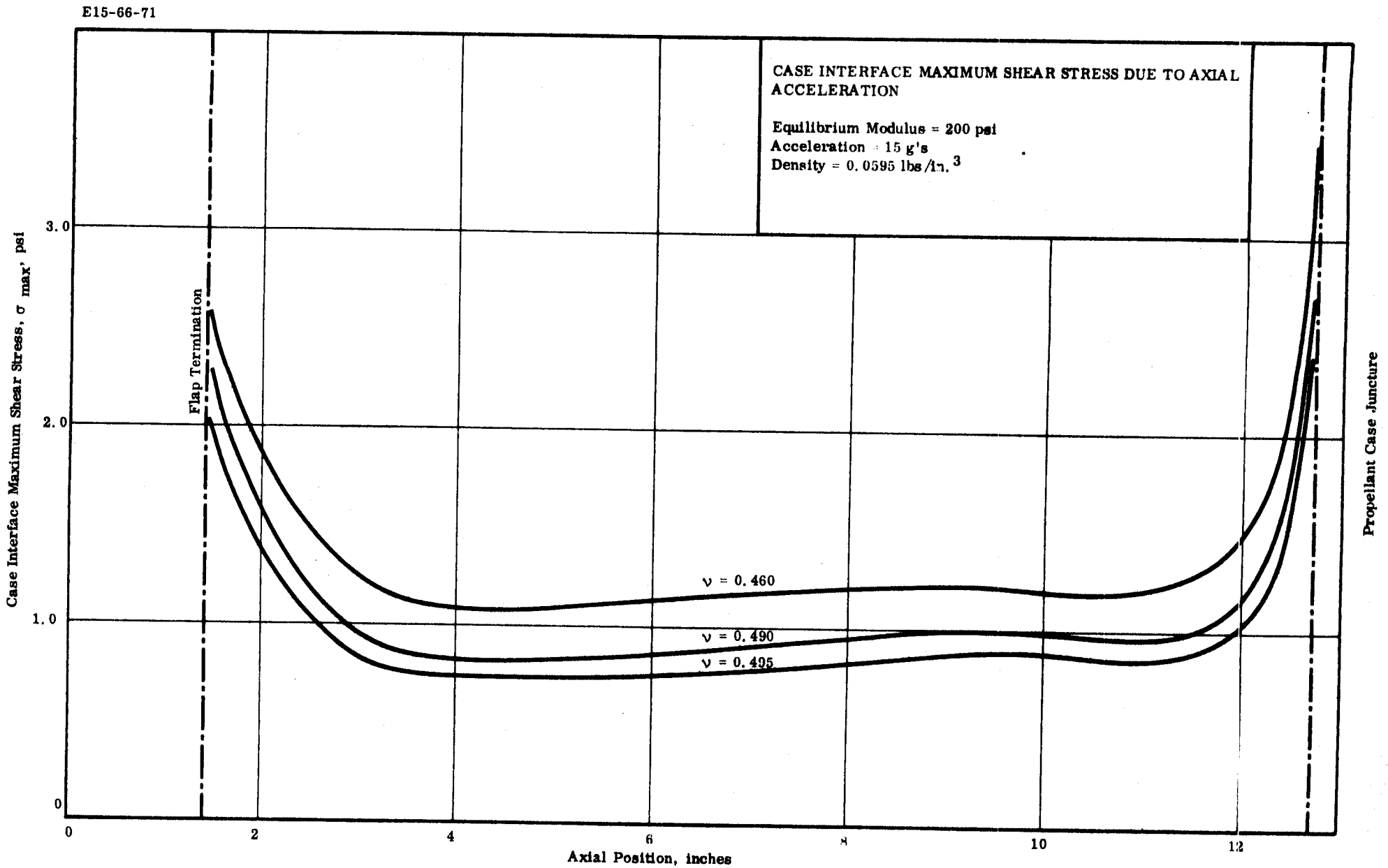

FIGURE 29. CASE BONDED SPHERICAL CIRCULAR PERFORATE MOTOR DESIGN

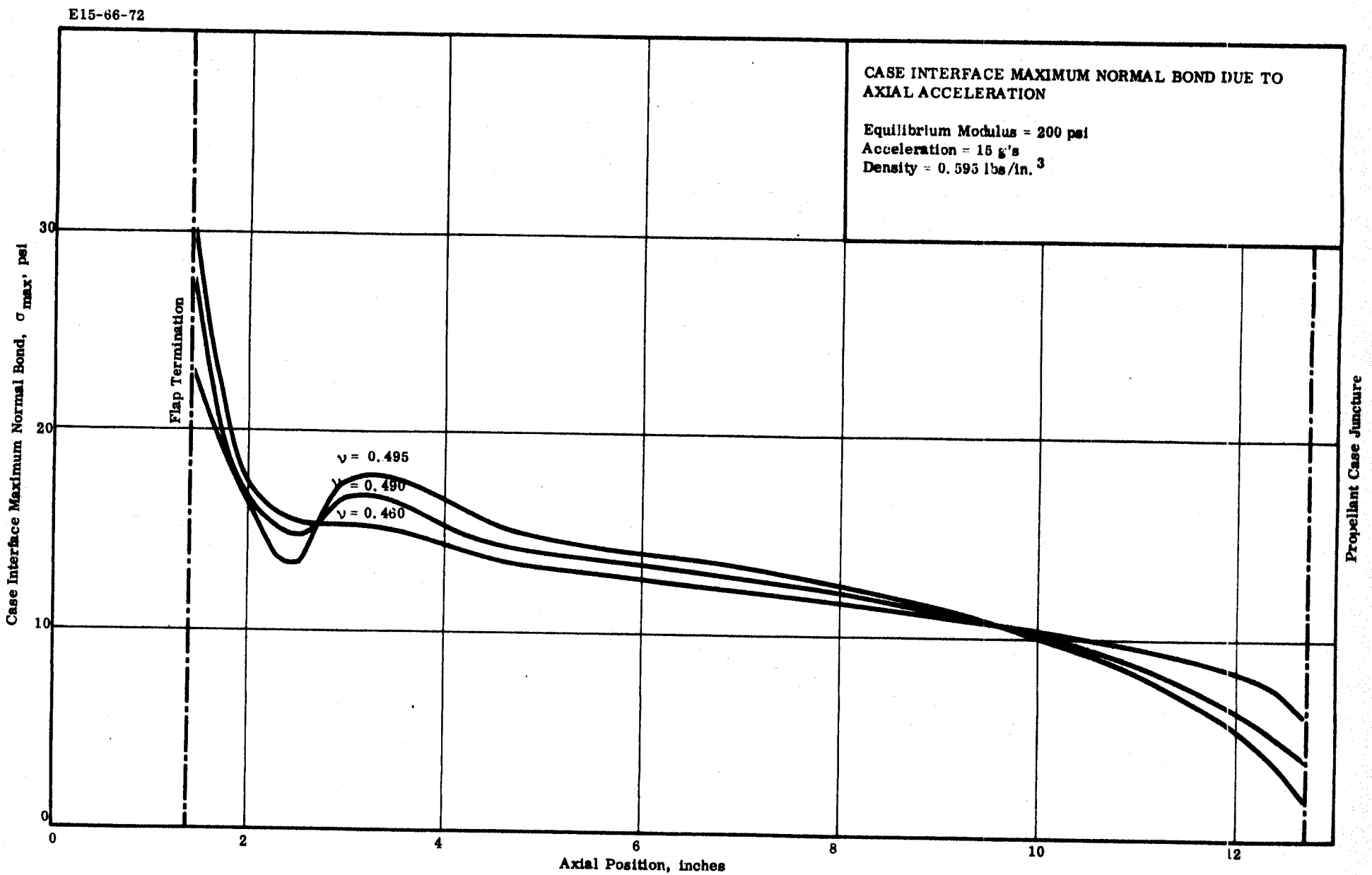

FIGURE 30. CASE BONDED SPHERICAL CIRCULAR PERFORATE MOTOR DESIGN

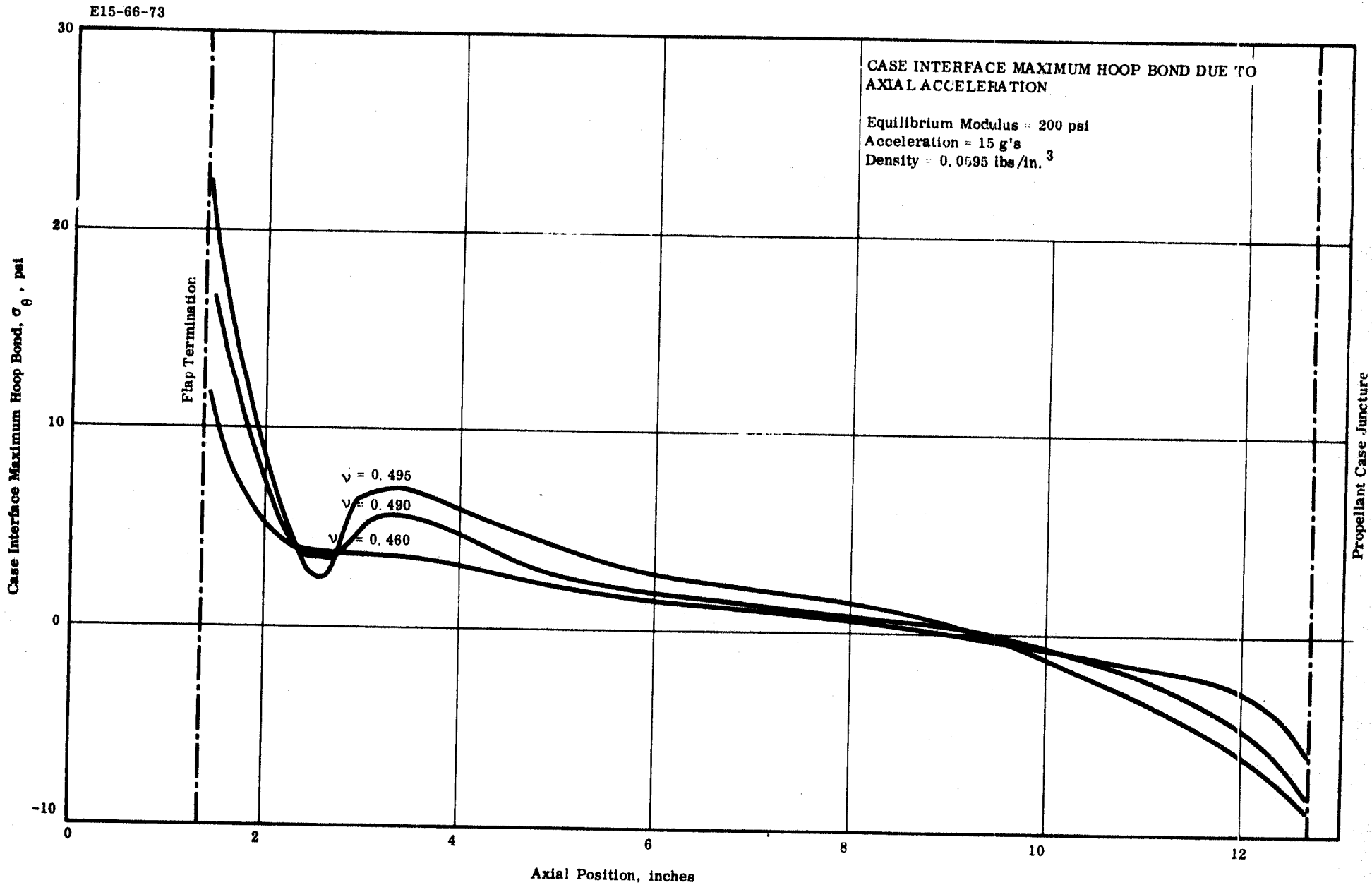

FIGURE 31. CASE BONDED SPHERICAL CIRCULAR PERFORATE MOTOR DESIGN

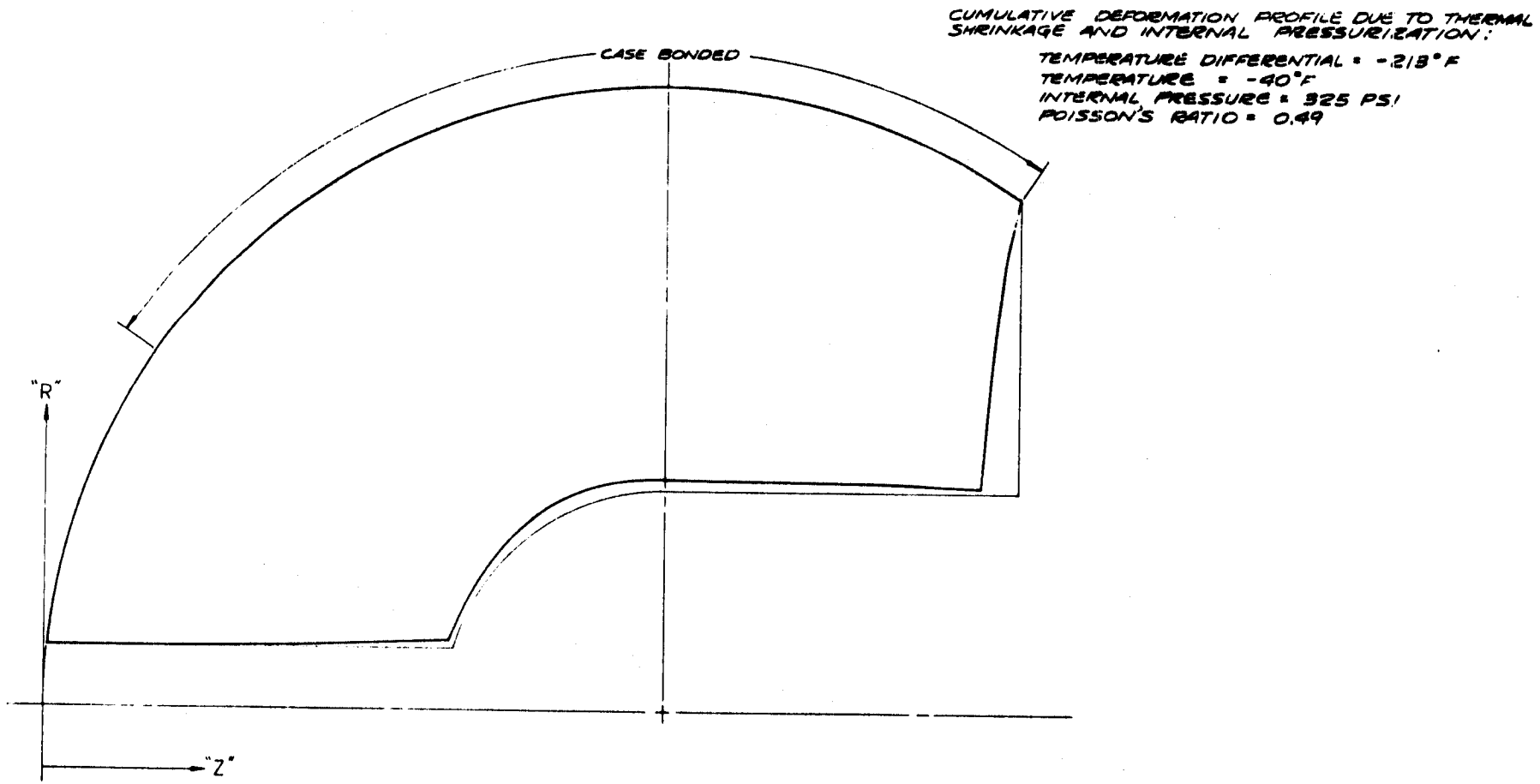

FIGURE 32. CASE BONDED SPHERICAL CIRCULAR PERFORATE MOTOR DESIGN

As shown below, accounting for variability in strength due to temperature but neglecting the effects of rate of imposed load, leads to a conservative estimate of the margins of safety. The factors of safety for a particular loading may be calculated from the respective relations:

$$(S.F.)_P = \frac{\text{Structural Capacity}}{\text{Structural Requirement}} \tag{1.1}$$

$$\frac{1}{(S.F.)_C} = \sum_{i=1}^{n} \frac{\text{Structural Requirements}}{\text{Structural Capacities}} \tag{1.2}$$

where:

$(S.F.)_P$ = Calculated safety factor due to a particular loading.

$(S.F.)_C$ = Calculated safety factor due to n cumulative loads.

The calculated safety factors for the loadings discussed above are:

Cure and Thermal Shrinkage (-40°F)

Interface Normal Bond Stress

$$(S.F.) = \frac{70 \text{ psi}}{40 \text{ psi}} = 1.75$$

Bore Stress

$$(S.F.) = \frac{70 \text{ psi}}{55 \text{ psi}} = 1.27$$

Bore Strain

$$(S.F.) = \frac{0.15 \text{ in./in.}}{0.13 \text{ in./in.}} = 1.15$$

Thermal Shrinkage and Axial Acceleration (-40°F, 15 g's)

Interface Normal Bond Stress

$$\frac{1}{(S.F.)} = \frac{40 \text{ psi}}{70 \text{ psi}} + \frac{7 \text{ psi}}{70 \text{ psi}}; \quad (S.F.) = 1.49$$

Thermal Shrinkage and Internal Pressurization (-40°F, 325 psi)

Bore Strain

$$\frac{1}{(S.F.)} = \frac{0.13 \text{ in./in.}}{0.15 \text{ in./in.}} - \frac{0.02 \text{ in./in.}}{0.15 \text{ in./in.}} \; ; \; (S.F.) = 1.36$$

These are the safety factors which are significant in the mission of the candidate design. The values listed are conservative; the rates of loading (mean thermal and mean pressurization strain rates) were assumed to be 0.77 in./in./min. This rate is obtained directly from ultimate strength tensile tests run at a crosshead speed of 2.0 in./min. In fact, the mean thermal strain rate is of the order, 1×10^{-4} in./in. min, whereas the mean pressurization strain rate is of the order, 1.0 in./in./min. Since the magnitude of the imposed stresses and strains is largely determined by those induced due to the temperature differential, the calculations are conservative.

F. INTERNAL-EXTERNAL BURNING, FREE-STANDING MOTOR DESIGN

The free-standing design selected for final analysis is the internal-external burning design with an internal support. The design is shown in Drawing E18609. This design is superior to the other free-standing designs (See Final Weighting Chart, Table D-1 - Appendix D.) The grain is internally supported by a carbon fiber reinforced - phenolic tube which provides support for the grain, reduces the effects of vibration, minimizes slump and spin imbalance, and allows expansion in the longitudinal direction.

The rocket motor has a cartridge-loaded grain of TP-H-3105 propellant that is free to burn on both internal and external surfaces. The grain is cast in a mold external to the motor case; during this operation, or shortly thereafter, the carbon fiber-phenolic support tube is inserted in the mold. This tube supports the grain during assembly and motor operation. The grain is loaded into a cylindrical motor case of 6 Al 4V titanium alloy and held in place by an aft support and a forward circumferential slot. The motor has a submerged conical nozzle and a PYROGEN ignition system. The total loaded weight of the motor assembly is 134.5 pounds, of which 100 pounds is propellant. The required time to heat the entire motor from 70°F to 295°F is 70 hours. The design uses proven concepts and materials throughout.

1. Performance Summary

The motor performance characteristics for this design are summarized as follows.

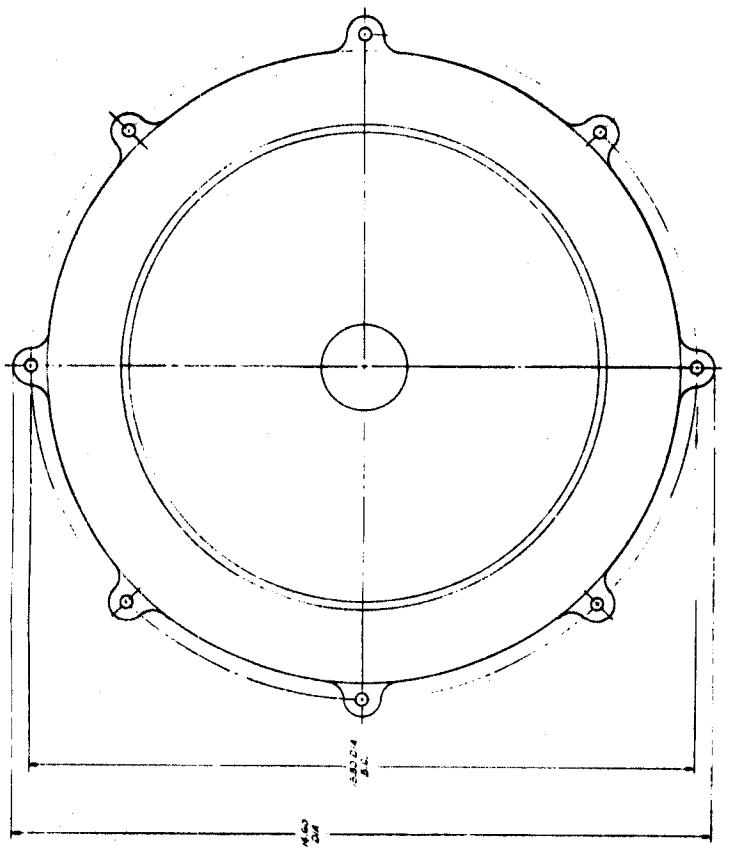

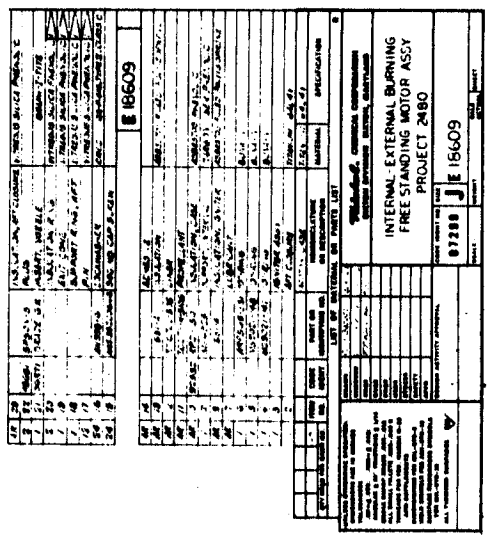

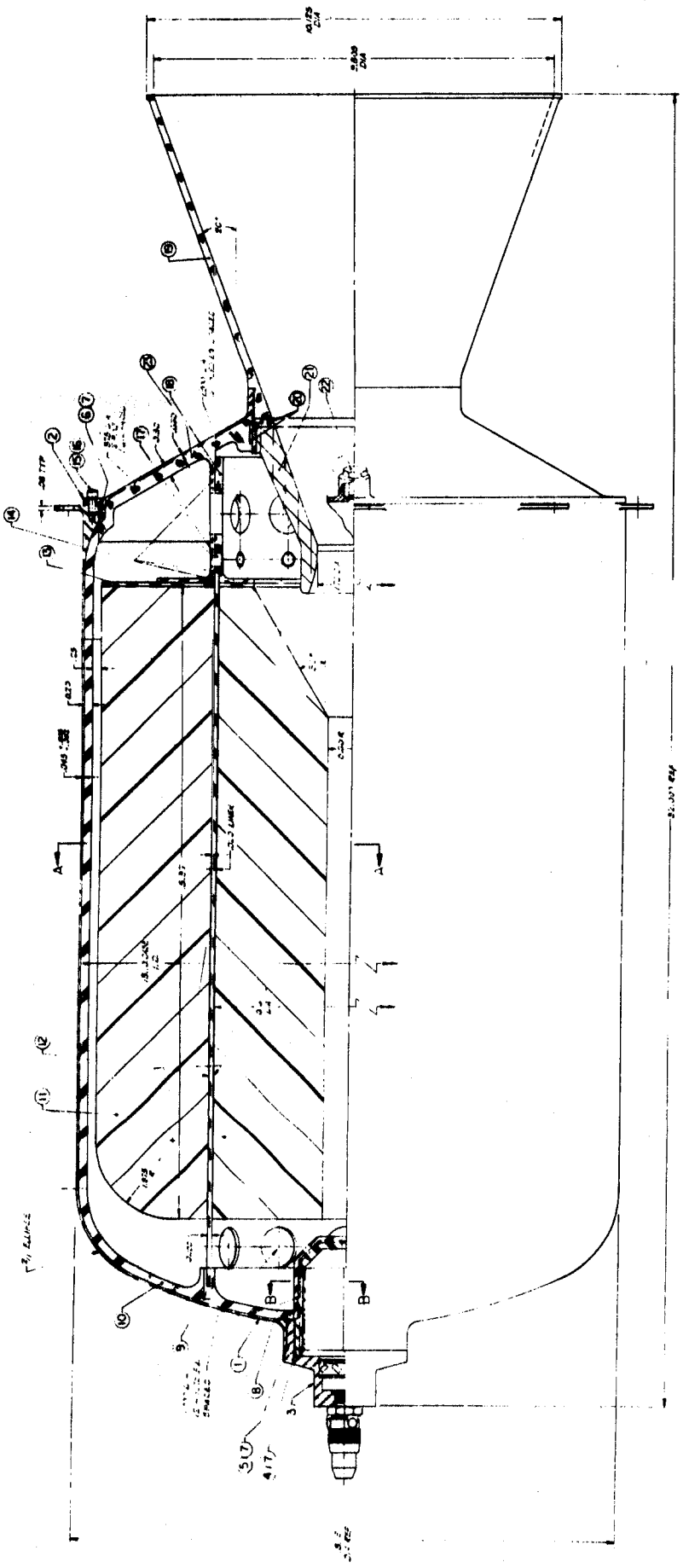

NOTES:

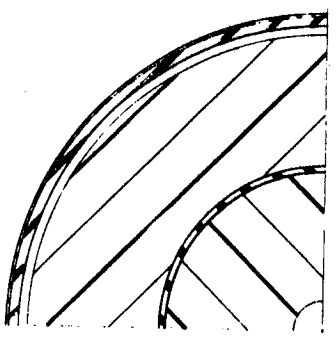

SECTION A-A

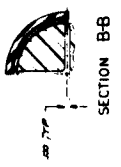

SECTION B-B

BALLISTIC PERFORMANCE AT VACUUM

	Temperature, °F		
	-40	+40	+120
Maximum Thrust, lbf	2526	2800	3104
Average Thrust, lbf	1812	2010	2230
Maximum Pressure, psia	594	659	730
Average Pressure, psia	426	473	524
Burning Time, sec	13.96	12.63	11.43
Total Impulse, lbf-sec	25,340	25,440	25,530
Propellant Specific Impulse lbf-sec/lbm	253	254	255

Thrust and chamber pressure as functions of time, at -40, +40, and +120°F, are plotted in Figures 33 and 34.

These performance values were calculated using Thiokol Computer Program No. 40243, "Internal Ballistic Performance Analysis." The following propellant and motor parameters were used. (Appendix E, Final Candidate Designs, contains a detailed listing of the motor performance parameters at -40, 0, +40, +80, and +120°F.)

PROPELLANT PARAMETERS

Burn Rate (r) at 70°F and 1,000 psi, in./sec	0.28
Burn Rate Exponent (n)	0.32
Temperature Sensitivity of Equilibrium Pressure at Constant K_n (π_k), %/°F	0.13
Characteristic Exhaust Velocity (C*) at 1,000 psi and 70°F, ft/sec	4848.0
Density (ρ), lb/in.^{3}	0.0595

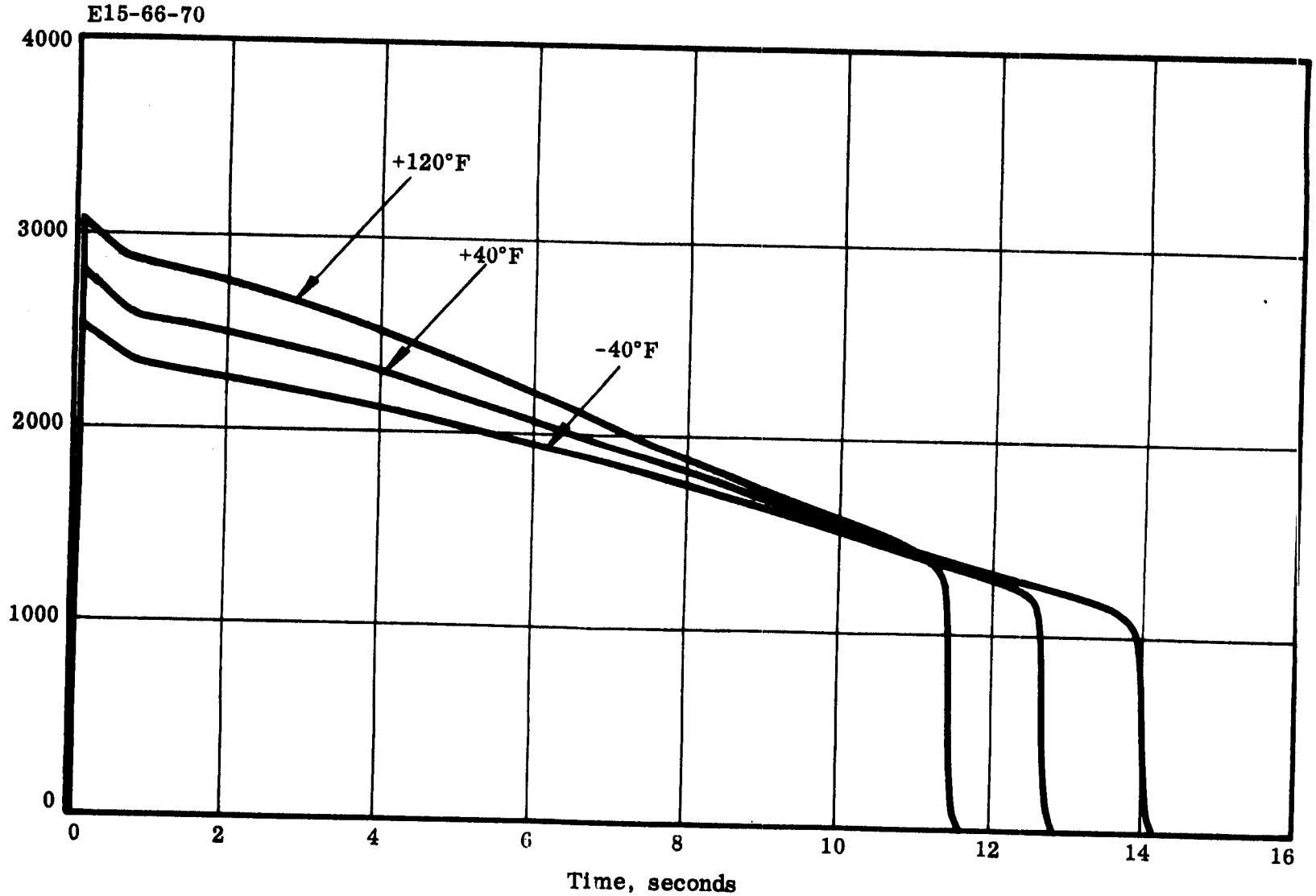

FIGURE 33. INTERNAL-EXTERNAL BURNING FREE-STANDING MOTOR DESIGN THRUST VERSUS TIME*

*Nominal Calculated at Vacuum, Expansion Ratio = 30, Discharge Coefficient = 0.96

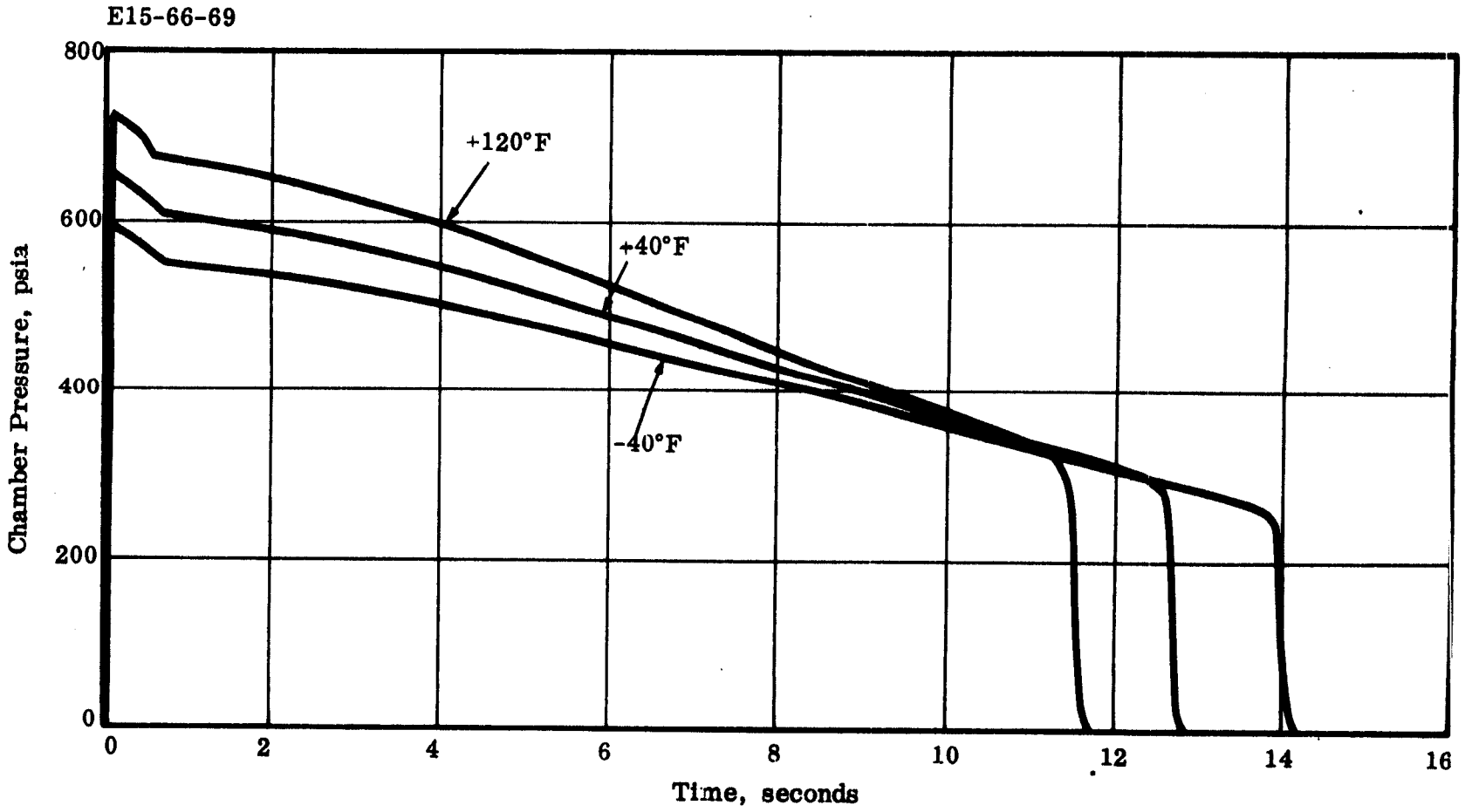

FIGURE 34. INTERNAL-EXTERNAL BURNING FREE-STANDING MOTOR DESIGN CHAMBER PRESSURE VERSUS TIME

MOTOR PARAMETERS

Nozzle Throat Area, $in.^2$	2.517
Expansion Ratio	30.0
Discharge Coefficient	0.96
Nozzle Half Angle, degrees	20

2. Heating Time

The calculated time required to heat the entire motor from 70°F to +293°F was 70 hours for the point of greatest thermal lag on the inside of the propellant charge. The analysis was performed using Thiokol Computer Program No. 40702A, "Arbitrary Node Thermal Computer Program." This analysis was performed using forced convection heat transfer coefficients. Heat flow was assumed to take place from the outside surface of the motor case only. The temperature-time histories for various nodes located along the grain cross section are shown in Figure 35. Appendix F, Heating Time Calculations, presents the complete thermal analysis.

3. Weight Breakdown

The detailed weight breakdown of the motor is shown in the following table. The calculations are given in Appendix G, Weight Analyses.

Component	Weight, lbs
Case	8.8
Insulation, Case	10.9
Liner and Adhesive	1.1
Aft Closure	2.5
Insulation, Aft Closure	2.6
Insulation, Inert	0.1
Insert	1.3
Exit Cone	2.1
Igniters	1.0
Hardware	0.1
Propellant Mounting Cylinder Support	1.3
Propellant Mounting Cylinder	1.9
Inhibitor, Propellant Aft End	0.4
Empty Motor	34.1
Propellant	100.4
Loaded Motor	134.5
Mass Fraction	0.74

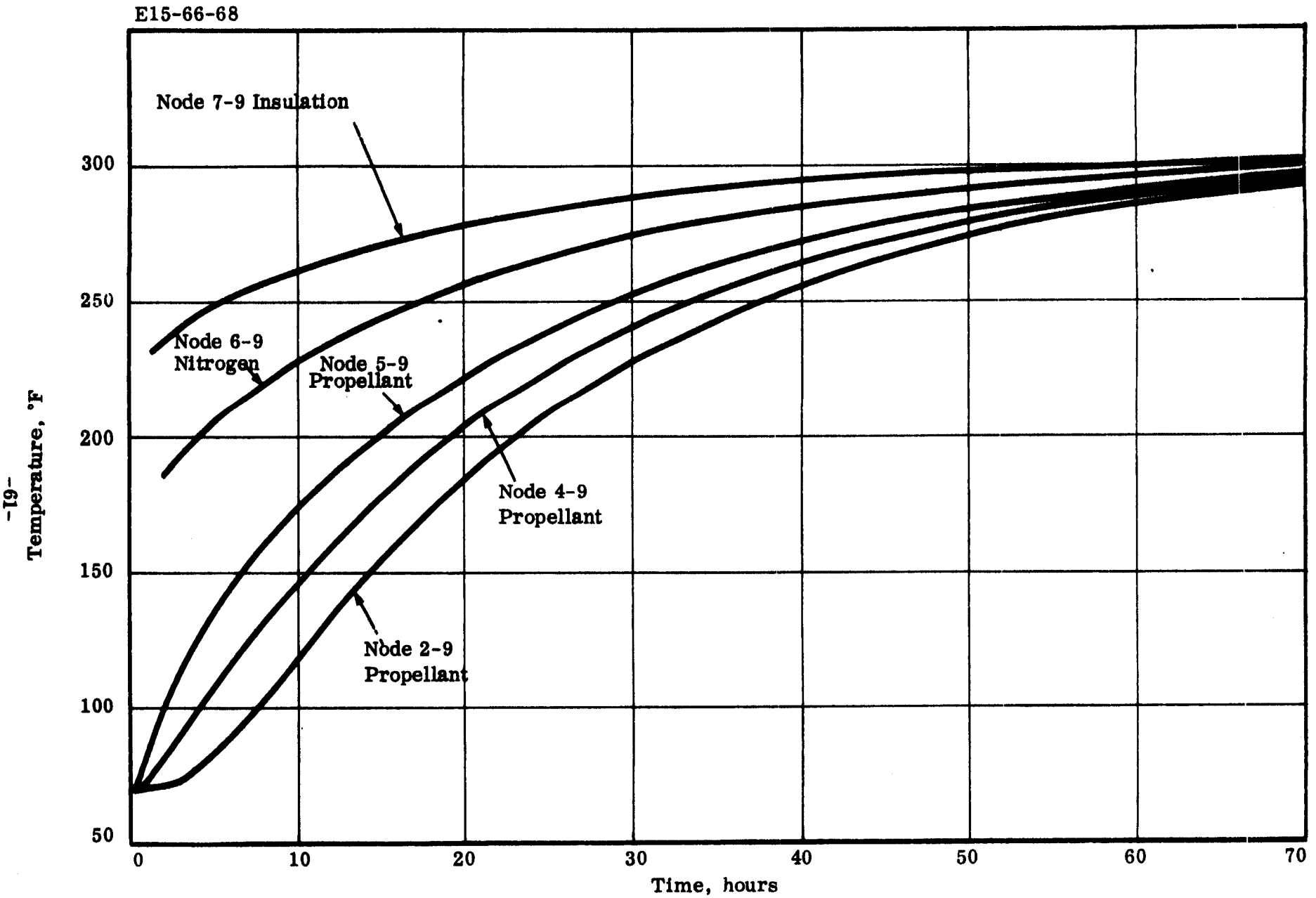

FIGURE 35. INTERNAL-EXTERNAL BURNING FREE-STANDING MOTOR DESIGN TEMPERATURE VERSUS TIME

4. Component Design

a. Case

The rocket motor chamber is a 6 Al 4V titanium cylindrical pressure vessel comprised of a 2/1 elliptical forward closure, a cylindrical center section and an aft flange incorporating a full diameter opening. The nominal membrane thickness is 0.045 inch. The case safety factor is 1.3, based on the maximum chamber pressure at 120°F, (730 psia).

Eight attachment tabs are located 45 degrees apart on the aft flange of the motor to attach it to the spacecraft and thrust to accommodate a vector control system.* The attachments shown are typical. The final design will depend upon the desired mating structure for the thrust vector control system. These attachment fittings will be integral with the aft case forging.

b. Case Internal Insulation

The motor case will be insulated on the inside surface by a high pressure molded asbestos fiber-filled phenolic insulation (RPD 150).** This insulation is needed for protection from heat and erosion.

The RPD 150 insulation extends from the aft end, full diameter case opening at a constant thickness of 0.20 inch through the cylindrical portion of the motor case and into the 2/1 head end ellipse. The head end of the motor case has a built-up section, which has a circumferential slot of the same diameter as the internal propellant grain support tube. It supports the tube radially while allowing longitudinal shrinkage or expansion. The slot has a local ramp cut in it to make it easier to locate the grain-support tube assembly.

c. Propellant Grain

(1) Design

The grain is an internal-external burning design of TP-H-3105 propellant with an internal support. It has a maximum diameter of 12.2 inches and an

*As noted earlier, the method of TVC was not specified, but JPL requested that TVC be allowed for in this manner.

**Manufactured by Raybestos-Manhattan, Inc.

overall length, including the aft end inhibitor, of 15.47 inches. It also has an internal perforation 1.2 inches in diameter. The aft end of the grain is coned out to accommodate a submerged nozzle which shortens the overall motor length. The grain is free to expand or contract in the axial direction because the support material has essentially the same expansion properties as the propellant (See discussion in Appendix A, General Design Guidelines). The design has virtually no sliver. The aft end of the grain is inhibited by a 0.10-inch layer of asbestos-filled polyisoprene insulation. This material is used to decrease the ratio of maximum to minimum burning surface area for the design.

The grain will be cast on the internal support and the resulting assembly will be loaded into the motor case. No problems are anticipated from thermal loads over the operating temperature range (-40°F to +120°F) or during sterilization. The spin rate of 100 rpm during flight should have no measurable effect upon structural or ballistic performance (based on successful performance of other Thiokol motors at higher spin rates). Acceleration and vibration loads are expected to produce no serious problems.

(2) Internal Support - Design

The internal support for the grain is a tube to be made of carbon fiber reinforced phenolic, (MX 4925).* The tube is 0.10-inch thick and extends through both ends of the grain. The forward end of this tube has twelve one-inch diameter holes to facilitate gas flow around the outside of the propellant grain. The aft end of the tube has twelve holes, 0.375-inch in diameter. Some pins, 3/8-inch in diameter, are inserted through the aft grain support and the tube to hold the tube firmly in place; the pins are bonded in place. The thermal expansion properties of the tube, in the longitudinal direction, closely match those of the propellant. The radial expansion properties of the tube closely match those of the aft support ring. Thus, the propellant-support tube assembly is essentially free of compressive and tensile stresses.

(3) Aft Closure Assembly

The aft closure assembly consists of the 6 Al 4V titanium closure, an aft closure insulation section, and the aft support ring.

The aft closure will be manufactured from a forging of 6 Al 4V titanium with a minimum yield strength of 155,000 psi. The titanium closure has

*Manufactured by the Fiberite Corporation.

a shear lip that prevents the submerged nozzle section from imparting loads to the phenolic exit cone. The closure has a threaded section into which the exit cone is screwed. The nominal thickness of the conical portion of the closure is 0.060-inch. The mating flange of the aft closure uses a piston O-ring seal and a shear lip which prevents shear load from being transmitted to the bolts. The aft closure contains two tapped bosses which permit the motor (See Drawing E18609) to be pressurized with nitrogen before sterilization.

(4) Aft Closure Insulation

The aft closure will be insulated by a high pressure molding of phenolic resin reinforced with chopped vitreous silica cloth. The minimum material thickness in this area will be 0.30-inch. The center of the aft closure insulation has a cylindrical lip onto which the aft support ring is fastened. The material for this application is covered by Thiokol Specification NE-1009. The properties of this material were treated in the discussion of the nozzle exit cone for the case-bonded spherical circular perforate design.

(5) Aft Support Ring

The aft support ring is made of vitreous silica phenolic material. This will be bonded to the aft closure using a suitable adhesive. This support has twelve machined holes one inch in diameter to allow gas flow around the outside of the grain. It has a 0.10-inch diameter slot in which the grain support tube is positioned and held by twelve 0.375-inch diameter pins. These pins are bonded in place with an adhesive. The forward portion of the aft support ring has a 0.10-inch thick flat surface which provides grain support during acceleration.

(6) Nozzle

Except for differences in size, the nozzle assembly for this design is virtually the same as the assembly used in the case-bonded design.

(7) Ignition System

The ignition system consists of a single PYROGEN igniter in the head end of the motor, partially submerged within the motor cavity. The selected design has the following features:

1) The design features a case made of 6 Al 4V titanium to minimize magnetic materials in the case design. The case is protected by asbestos-phenolic and an asbestos-filled polyisoprene internal insulation.

2) The propellant charge contains TP-H-3105 propellant in a four-point star configuration. Each star point extends the full distance to the phenolic grain cartridge. This provides a regressive burning PYROGEN igniter with the advantages already discussed under the previous design.

3) The pellet charge is boron-potassium nitrate pellets conforming to Thiokol Specification ESRM-13.

4) The PYROGEN case cap is also 6 Al 4V titanium which is screwed over the PYROGEN case and into the head end of the motor. This cap contains a single, tapped hole into which is screwed the squib cartridge. If redundancy is desired, the cap can be modified to accept two squib cartridges.

5) The PYROGEN has directed gas flow. Some of the gas is allowed to flow down through the center of the grain cavity but most of the flow is directed outward. This permits rapid ignition of the forward surface of the grain and rapid equalization of pressure and flow on the external and internal surfaces of the grain. If full flow were directed down the internal grain port, the pressure unbalance could cause failure of the grain.

6) Partially by submerging the PYROGEN within the motor cavity provides a shorter motor.

The initiator will probably be based on the existing Apollo Standard Initiator. This is a problem area and is discussed in Appendix A, Design Guidelines.

(8) Nozzle Closure

This is also a critical design problem discussed in Appendix A, Design Guidelines.

5. Grain Structural Analysis

The free-standing design was subjected to an extensive structural study. The effects of grain geometry (web thickness, cross-sectional perforation and reliefs), propellant-liner interfacing, and sterilization were considered.

The method of superposition was used to determine the stress and deformation requirements of the motor. Consideration was given to shrinkage due to cure, thermal shrinkage and expansion, pressurization, acceleration and interface bonding. Where possible, the temperature-rate dependence of TP-H-3105 was accounted for.

The results of these analyses indicate that this candidate sterilizable design is capable of withstanding the environmental and operational loadings to which it will be exposed following sterilization.

The longitudinal cross-section shown in Figure 36 performed the geometrical basis for all analyses. For purposes of optimization it was assumed that the grain was bonded over the entire sleeve section and along the full length of the aft support.

The structural response of this design was determined by means of a Thiokol digital computer program (E43113) based upon finite element stiffness theory. The cross-section of this motor, modeled for grain structural analysis, is shown in Figures 37 and 38. Figure 37 illustrates the element modeling and specifies nodal numbers. Figure 38 gives the element numbers.

The computer program calculates stresses for each element and displacements for each node corresponding to specified loads and material properties. The results of these analyses have been presented in the form of deformation profiles, interface and bore stresses.

a. Thermal Expansion Due to Sterilization

(1) Deformations

The deformation profiles due to sterilization are shown in Figures 39, 40 and 41. For this analysis it was assumed that the zero strain temperature (the temperature above cure temperature at which the internal profile of the grain corresponds to the external profile of the core) was 23°F above the cure temperature (150°F) of TP-H-3105. It was further assumed that the propellant would exhibit an equilibrium modulus of 200 psi during expansion. Deformations were obtained for a temperature rise of 122°F and for Poisson's ratios of 0.40 and 0.49. Figure 41 illustrates the effect that Poisson's ratio has on the deformed profile.

(2) Interface and Bore Stresses

The interface bond stresses and port hoop stresses corresponding to the deformations cited above are shown in Figures 42 to 46. The end boundary conditions are specified on each graph as the sleeve termination and the aft support. Note that the magnitude of the bore and bond stresses for thermal expansion is not significantly high.

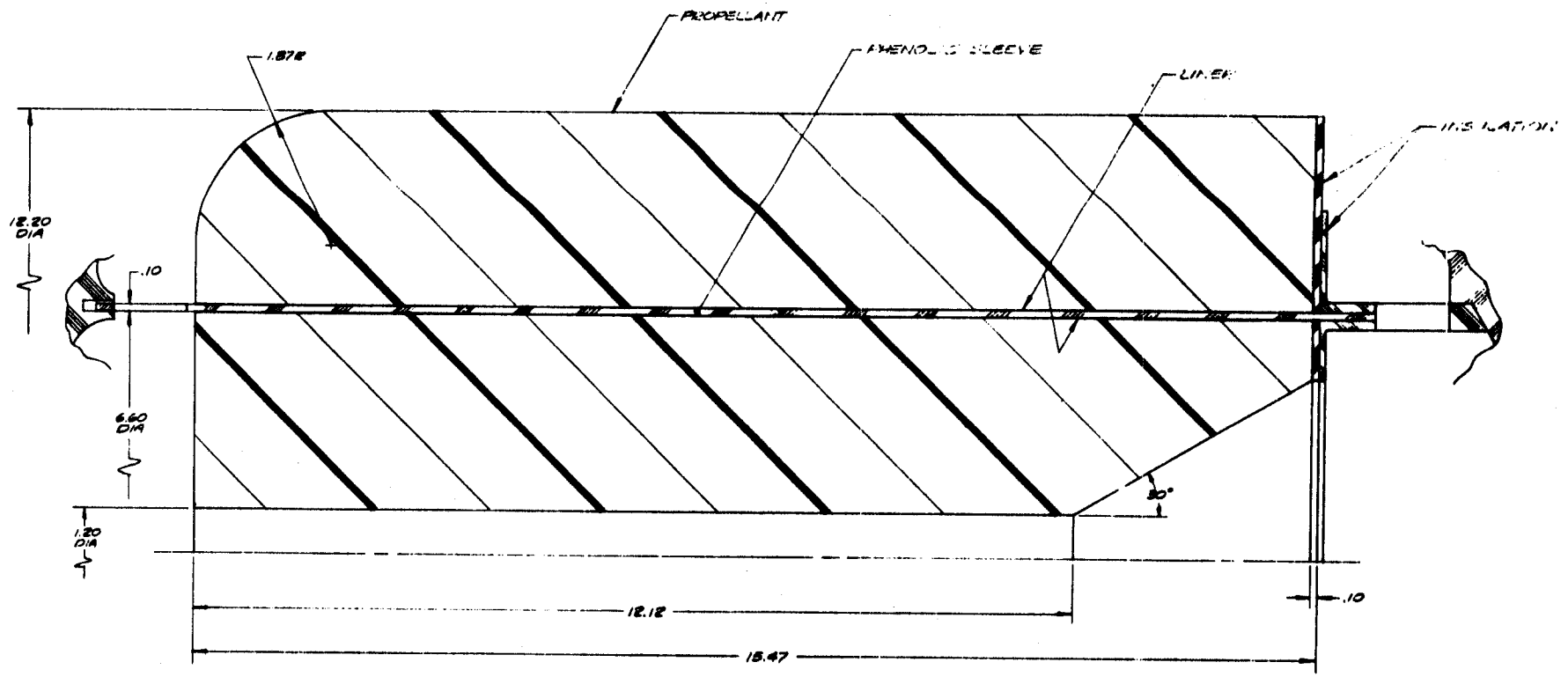

FIGURE 36. INTERNAL-EXTERNAL BURNING FREE STANDING MOTOR DESIGN

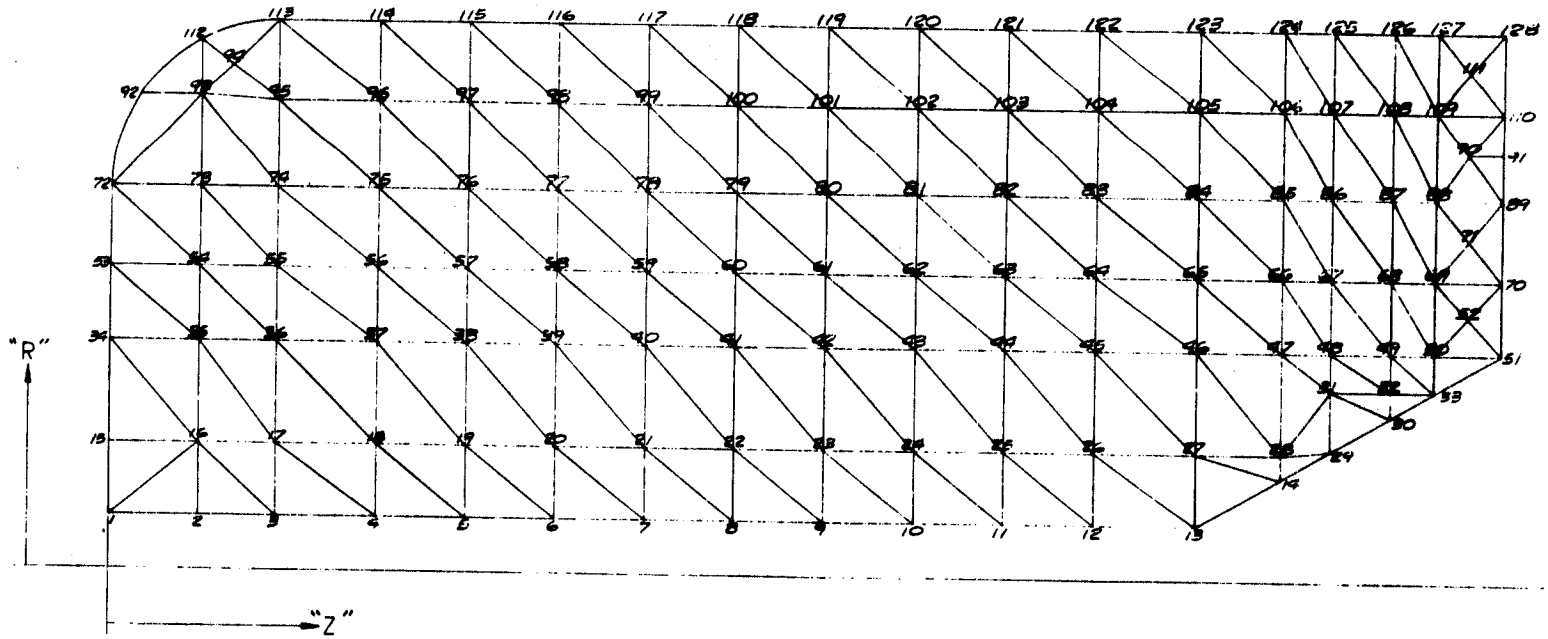

FIGURE 37. INTERNAL-EXTERNAL BURNING FREE STANDING MOTOR DESIGN. NODAL POINT NUMBERS

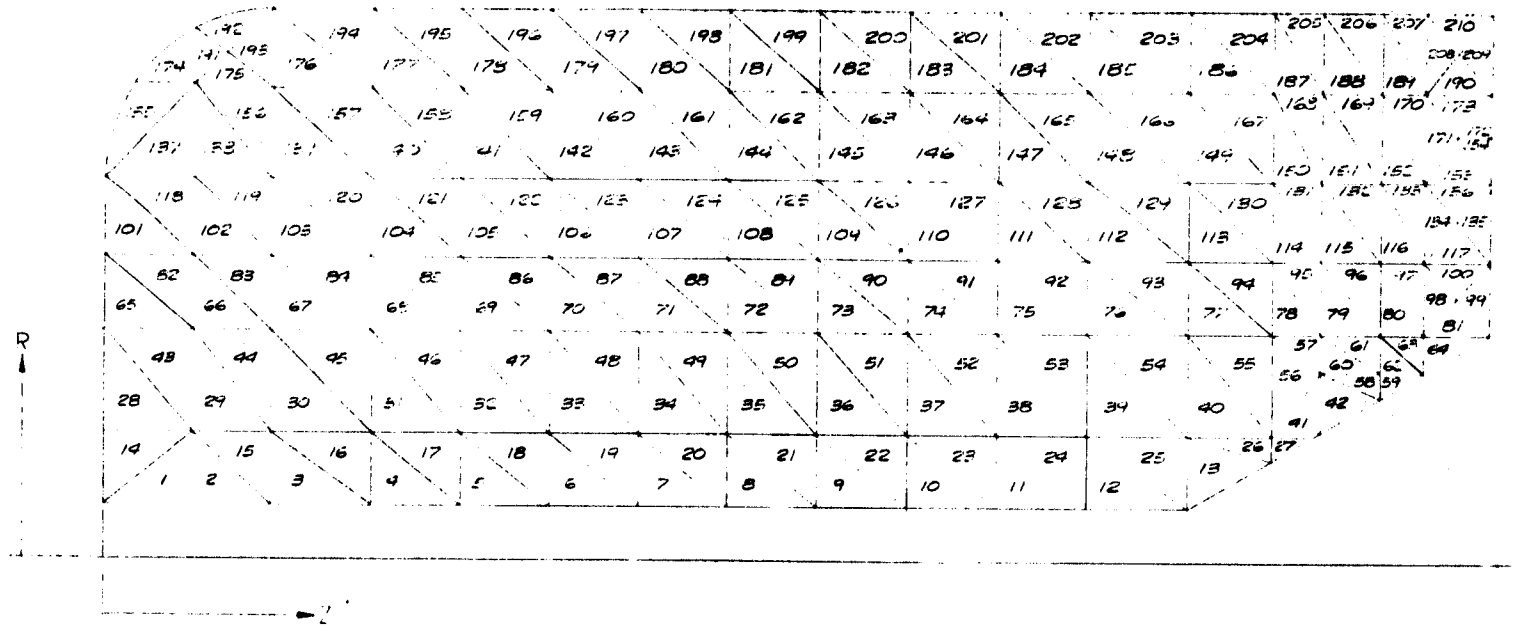

FIGURE 38. INTERNAL-EXTERNAL BURNING FREE STANDING MOTOR DESIGN. ELEMENT NUMBERS

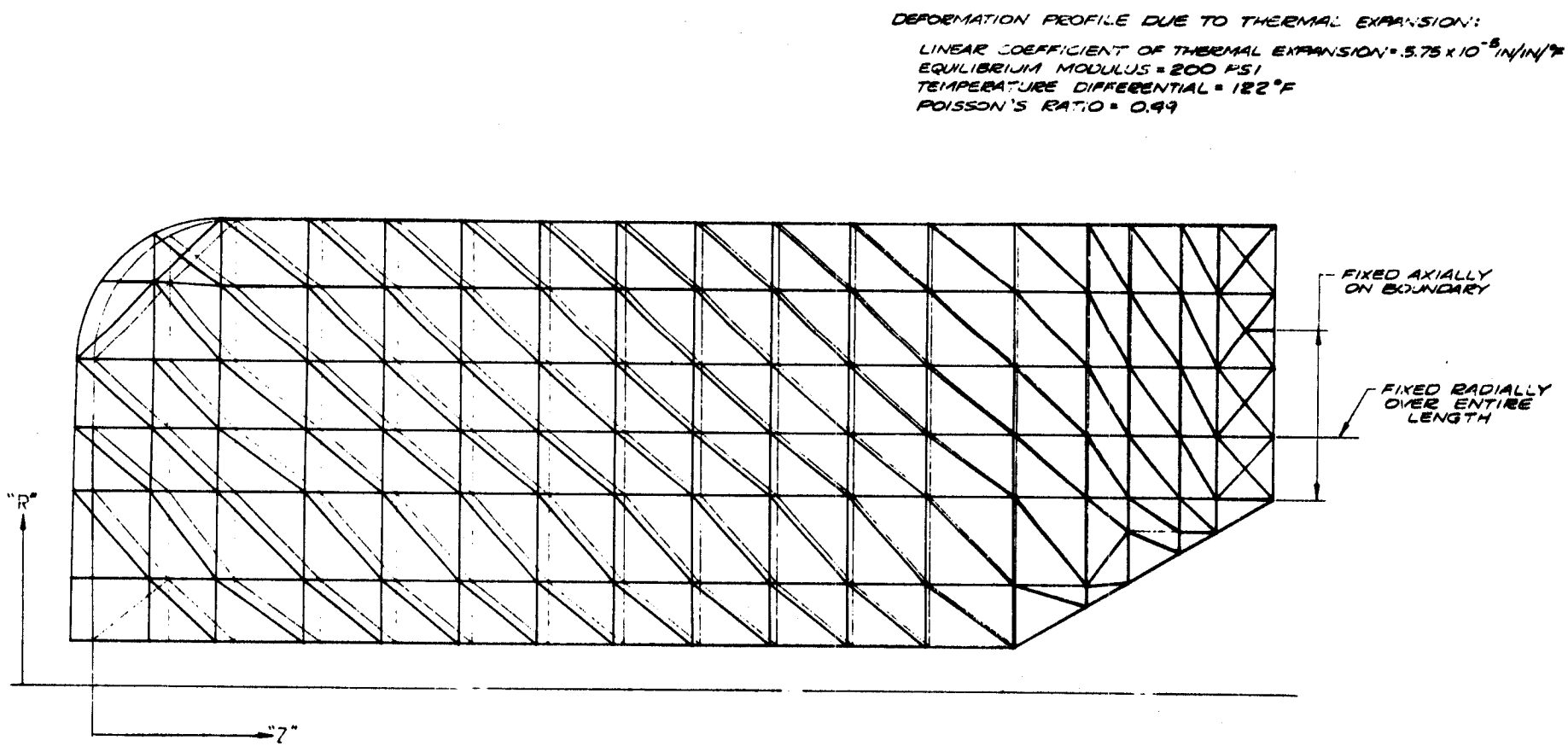

FIGURE 39. INTERNAL-EXTERNAL BURNING FREE STANDING MOTOR DESIGN

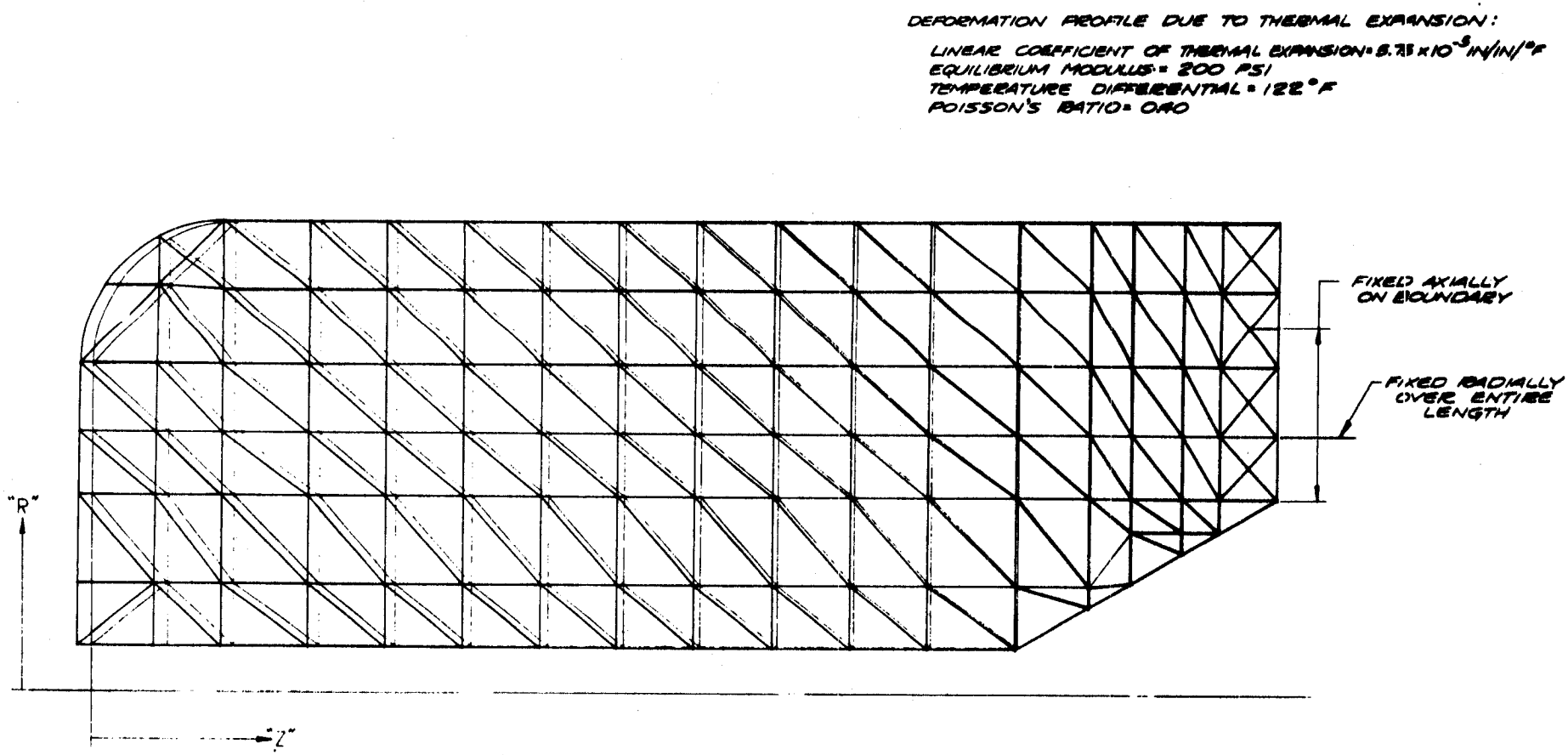

FIGURE 40. INTERNAL-EXTERNAL BURNING FREE STANDING MOTOR DESIGN

DEFORMATION PROFILES DUE TO THERMAL EXPANSION:
LINEAR COEFFICIENT OF THERMAL EXPANSION = 5.75×10^{-5} IN/IN/°F
EQUILIBRIUM MODULUS = 200 PSI
TEMPERATURE DIFFERENTIAL = 122°F
POISSON'S RATIO = 0.40 & 0.49

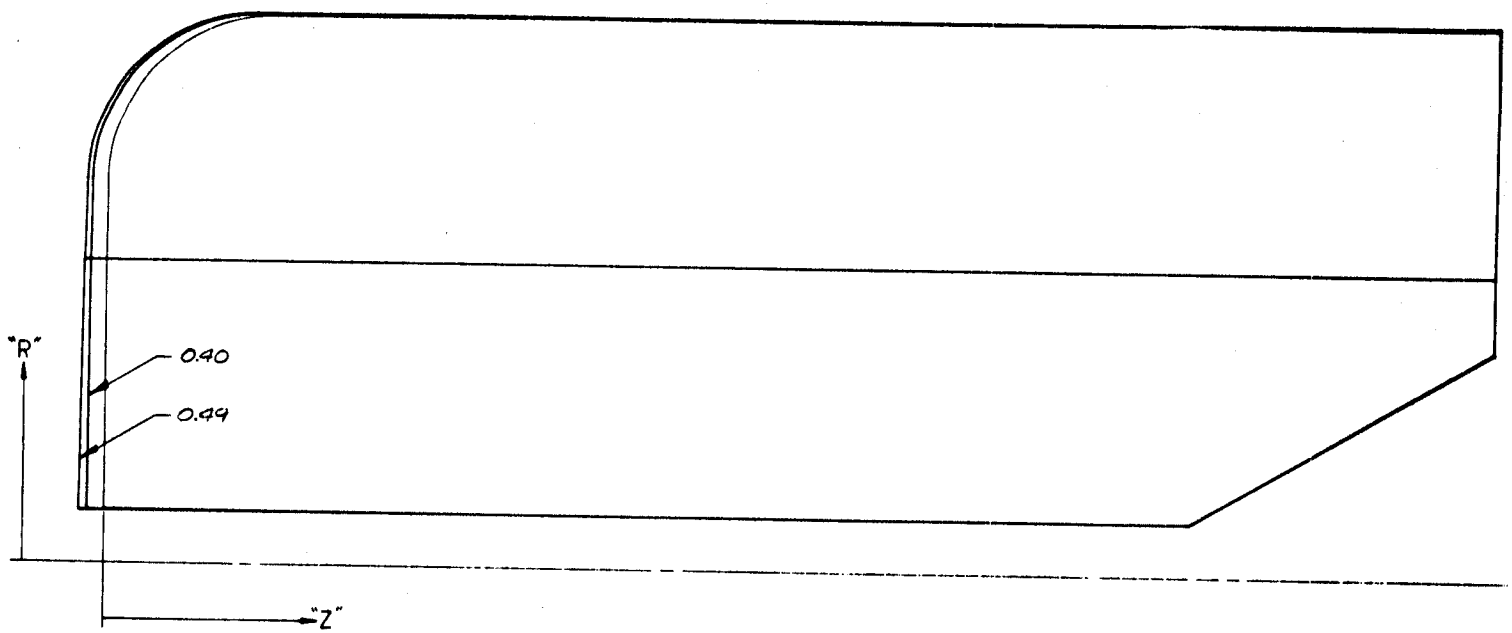

FIGURE 41. INTERNAL-EXTERNAL BURNING FREE STANDING MOTOR DESIGN

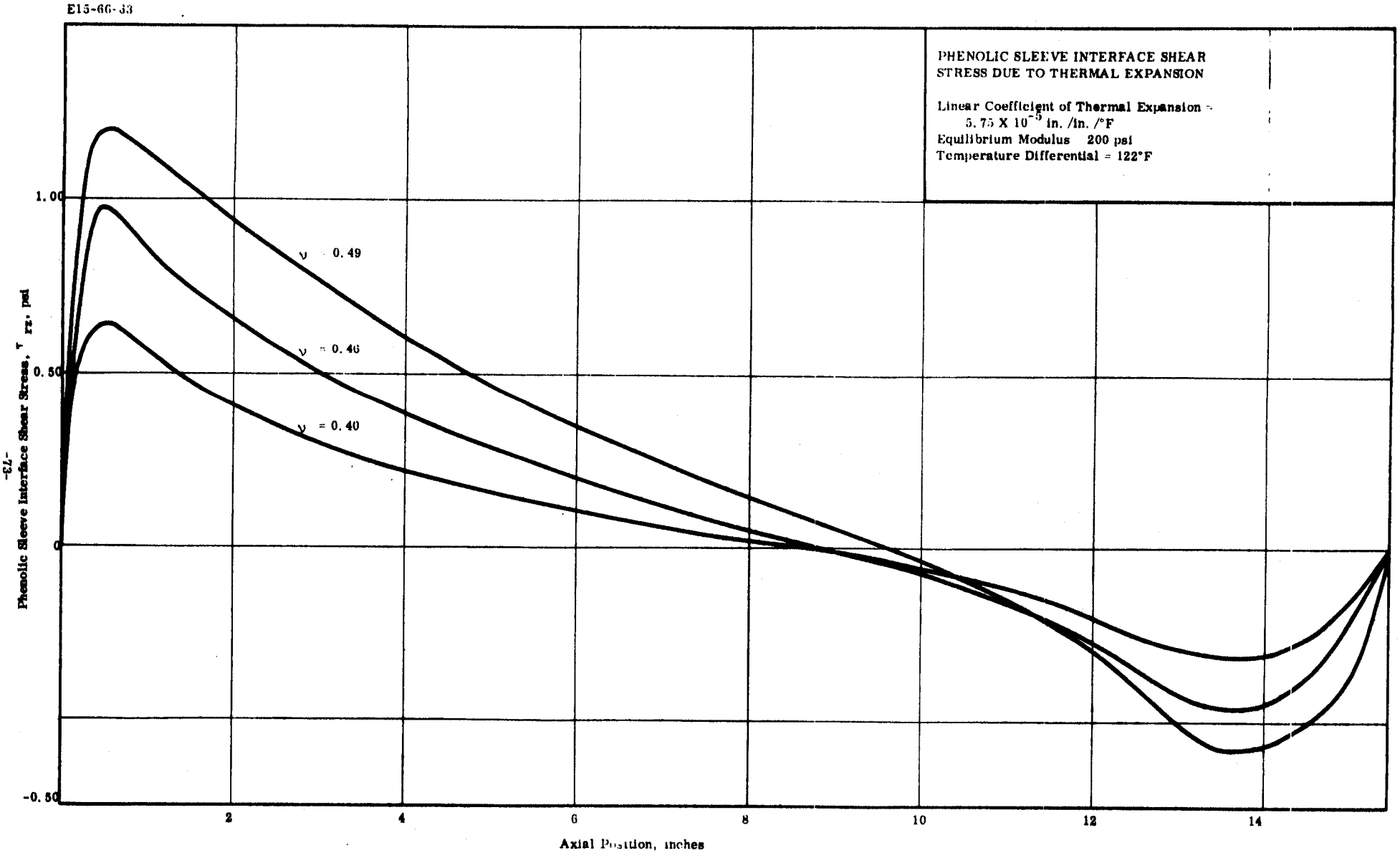

FIGURE 42. INTERNAL-EXTERNAL BURNING FREE-STANDING MOTOR DESIGN

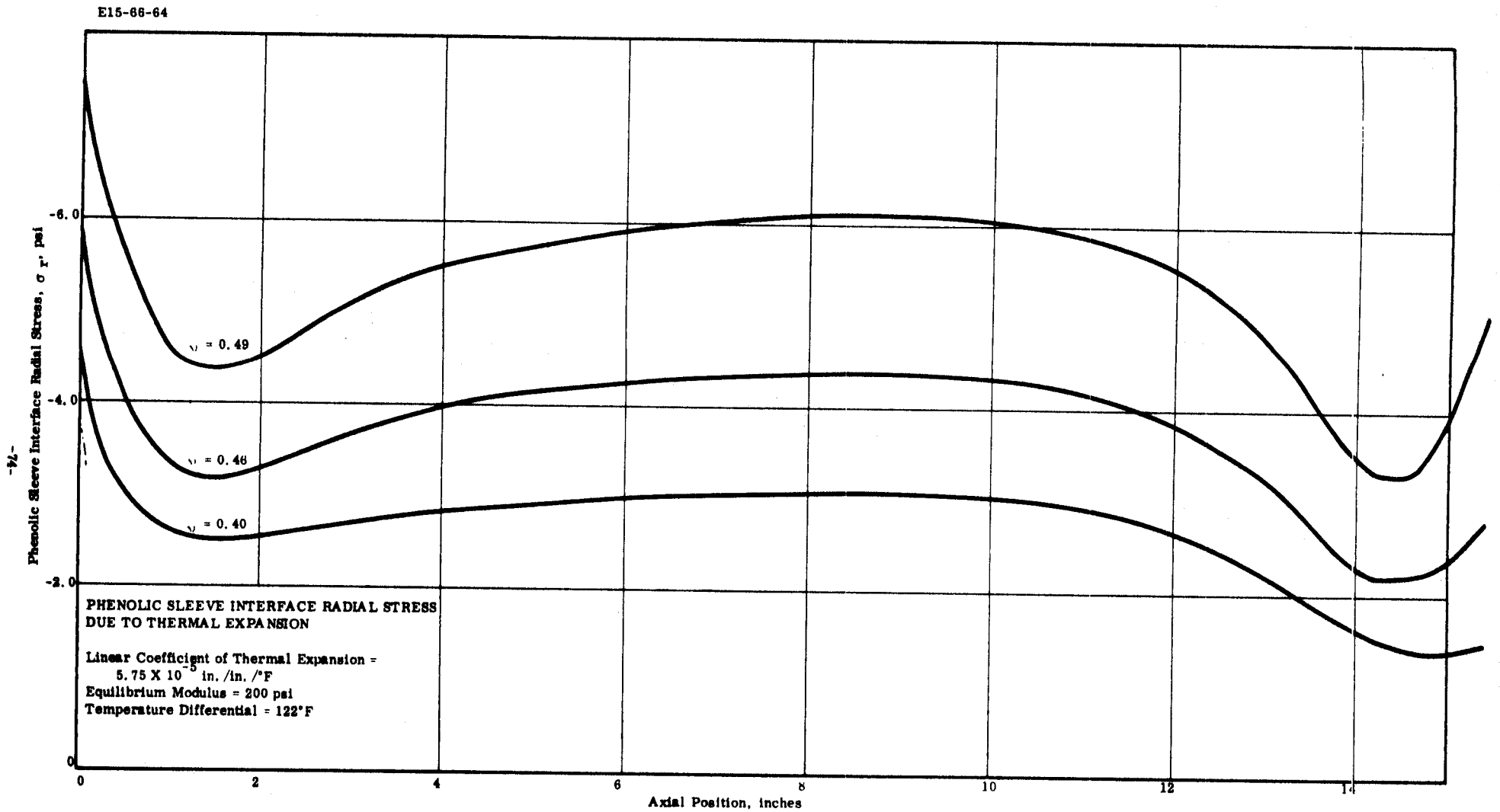

FIGURE 43. INTERNAL-EXTERNAL BURNING FREE-STANDING MOTOR DESIGN

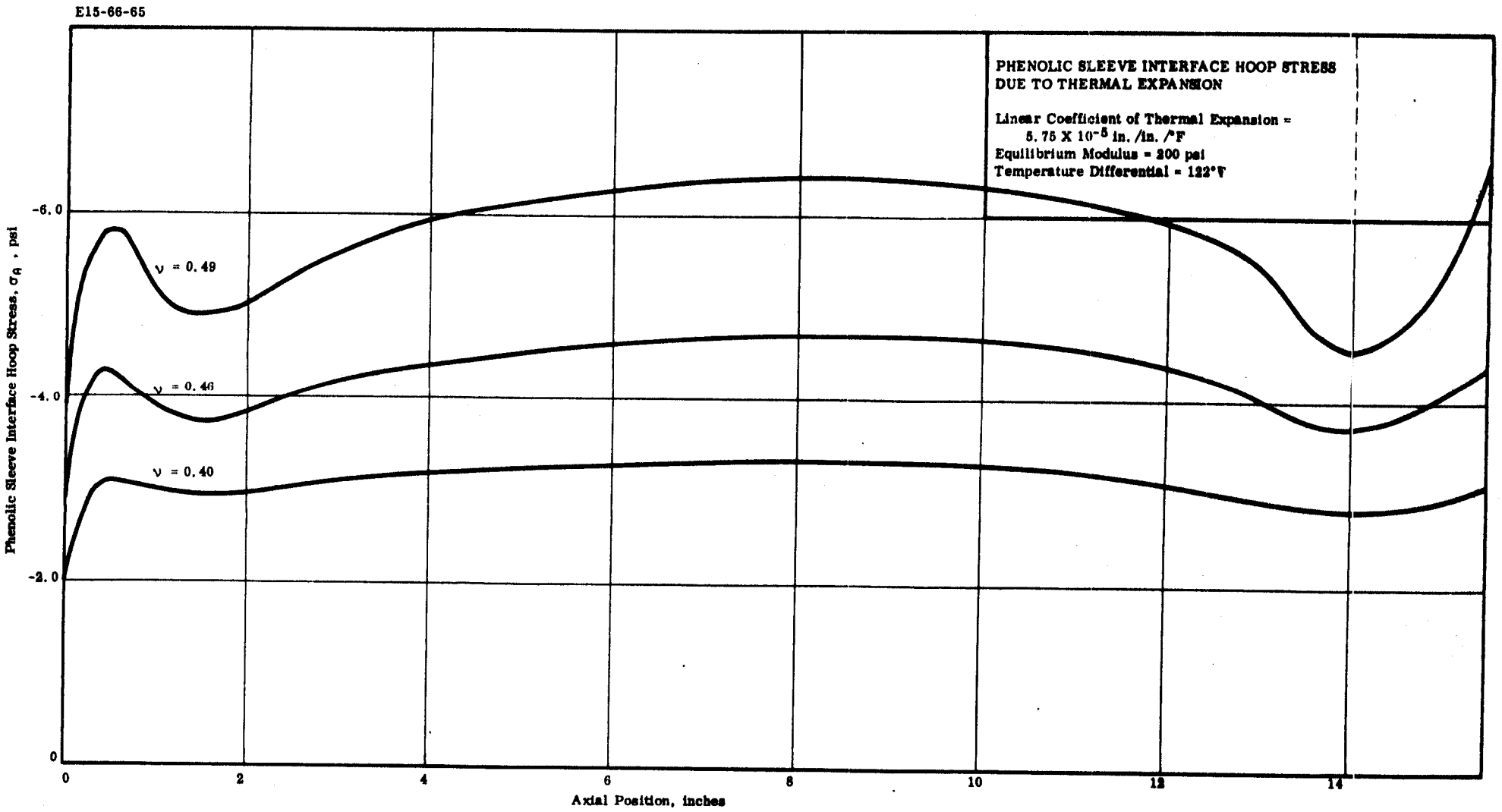

FIGURE 44. INTERNAL-EXTERNAL BURNING FREE-STANDING MOTOR DESIGN

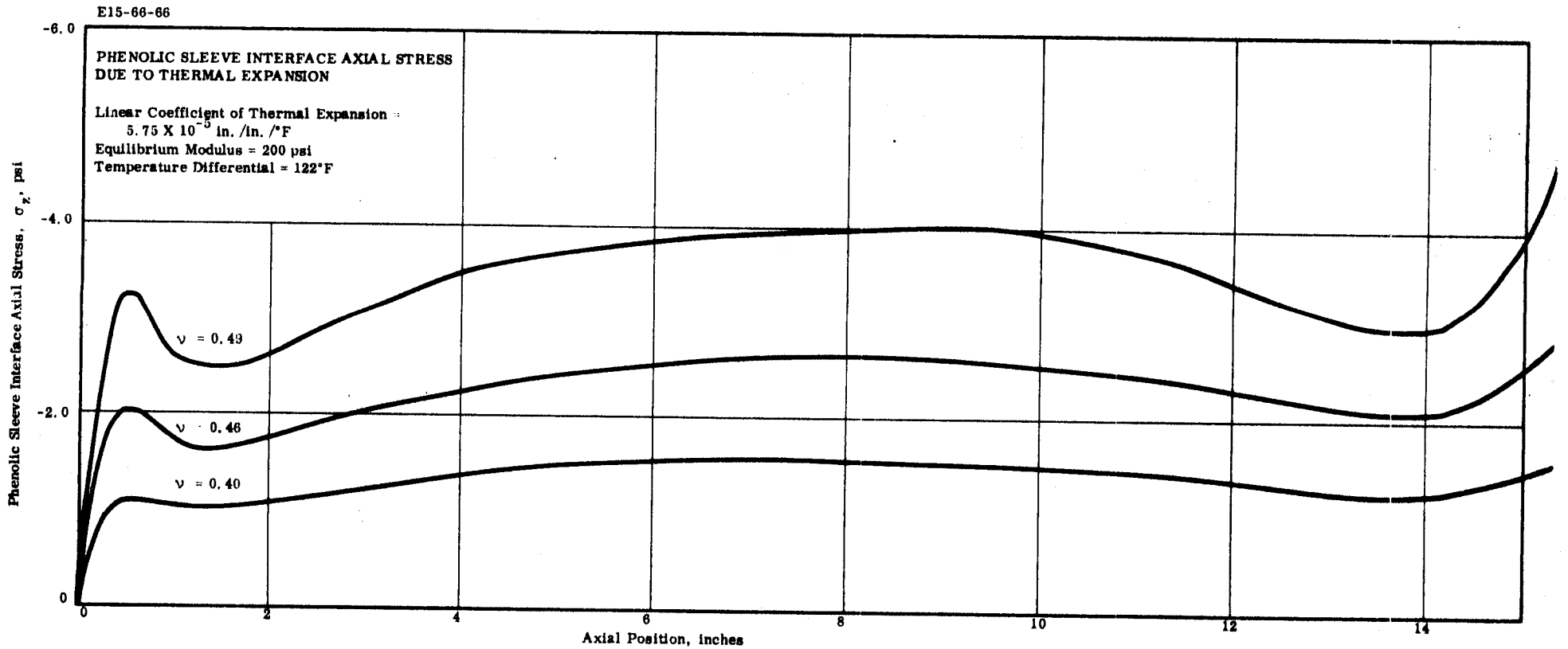

FIGURE 45. INTERNAL-EXTERNAL BURNING FREE-STANDING MOTOR DESIGN

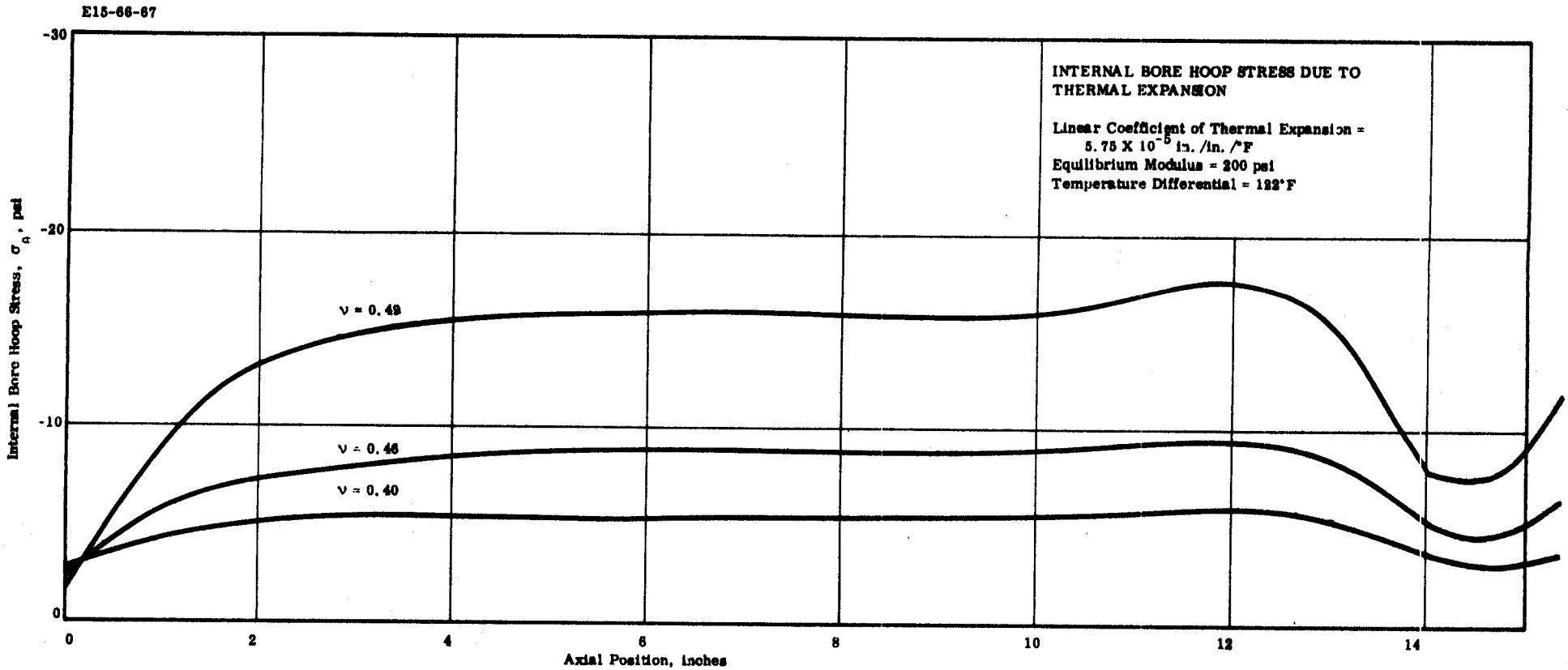

FIGURE 46. INTERNAL-EXTERNAL BURNING FREE-STANDING MOTOR DESIGN

b. Thermal Shrinkage Due to Low Temperature Space Storage

(1) Deformations

The deformation profiles resulting from a thermal drop to -40°F in space are shown in Figures 47, 48 and 49. Again, due to the low thermal conductivity of propellant, an equilibrium modulus of 200 psi was used and results were obtained from Poisson's ratio of 0.40 and 0.49. The zero strain temperature, based upon the propellant linear coefficient of thermal expansion, was assumed to be 173°F; this is a temperature differential of -213°F at -40°F.

(2) Interface and Bore Stresses

The interface bond stresses and port hoop stress corresponding to the deformations cited above are shown in Figures 50 through 54. For these problems the phenolic sleeve was allowed to deform axially but not radially. The aft support restrains the grain axially but not radially.

c. Internal Pressurization - Deformations

It was assumed that the motor would be fired at -40°F in a space environment. A maximum ignition pressure of 595 psi was used to determine the profiles in Figure 55. Due to the low temperature and the rate of loading, an elastic modulus of 10,000 psi was employed. This corresponds approximately to the glassy modulus one would expect to observe in high rate - low temperature testing of sterilized TP-H-3105. Results are shown corresponding to two values of the static bulk modulus.

d. Axial Acceleration

(1) Deformations

The response of the motor to an axial setback force corresponding to a boost launch of 15 g's is given in Figure 56. A modulus of 200 psi and Poisson's ratios of 0.40 and 0.49 were used. The sleeve and support were restrained both radially and axially in these problems.

(2) Interface Bond Stresses

Stresses at the sleeve - propellant interface due to an axial acceleration of 15 g's are presented in Figures 57 and 58.

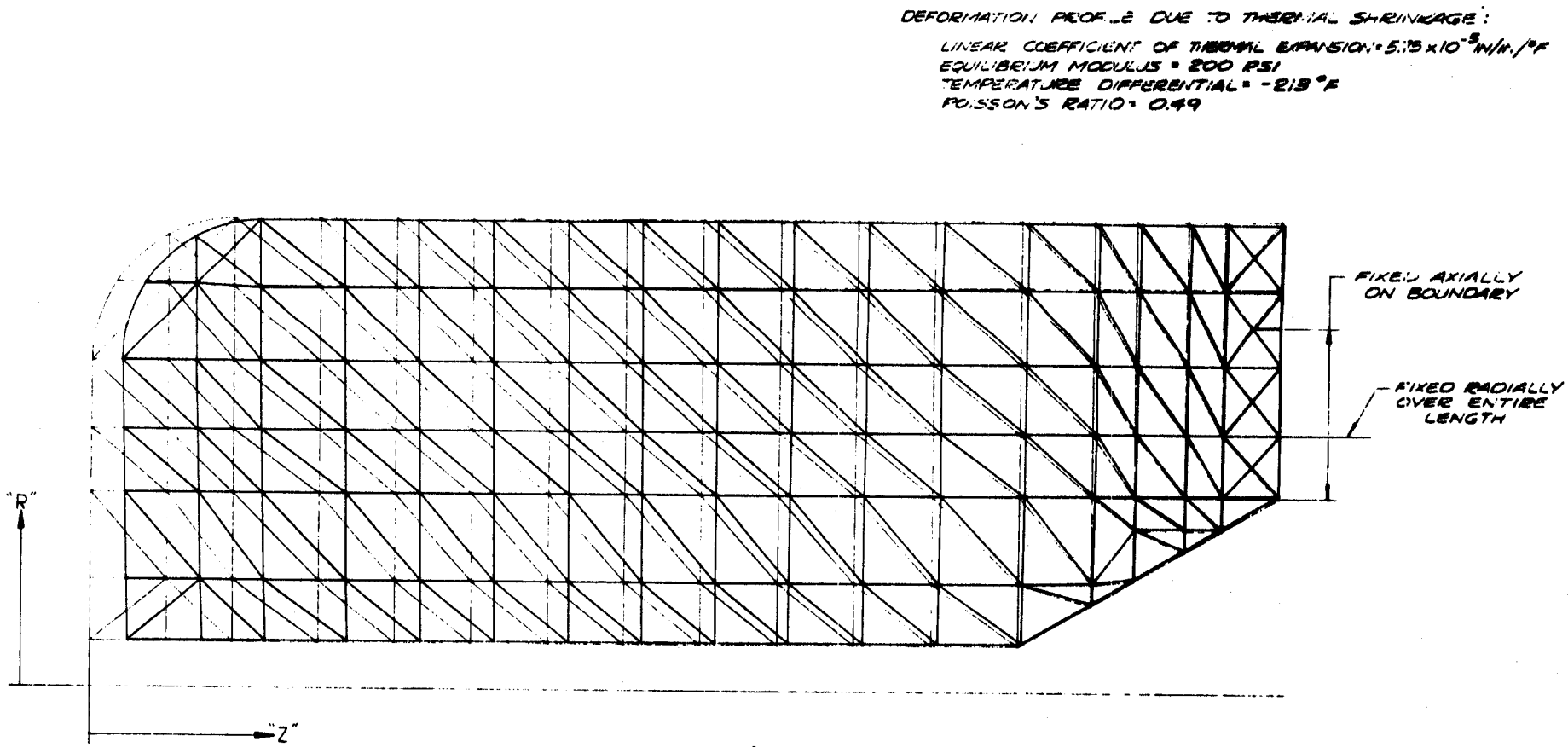

FIGURE 47. INTERNAL-EXTERNAL BURNING FREE STANDING MOTOR DESIGN

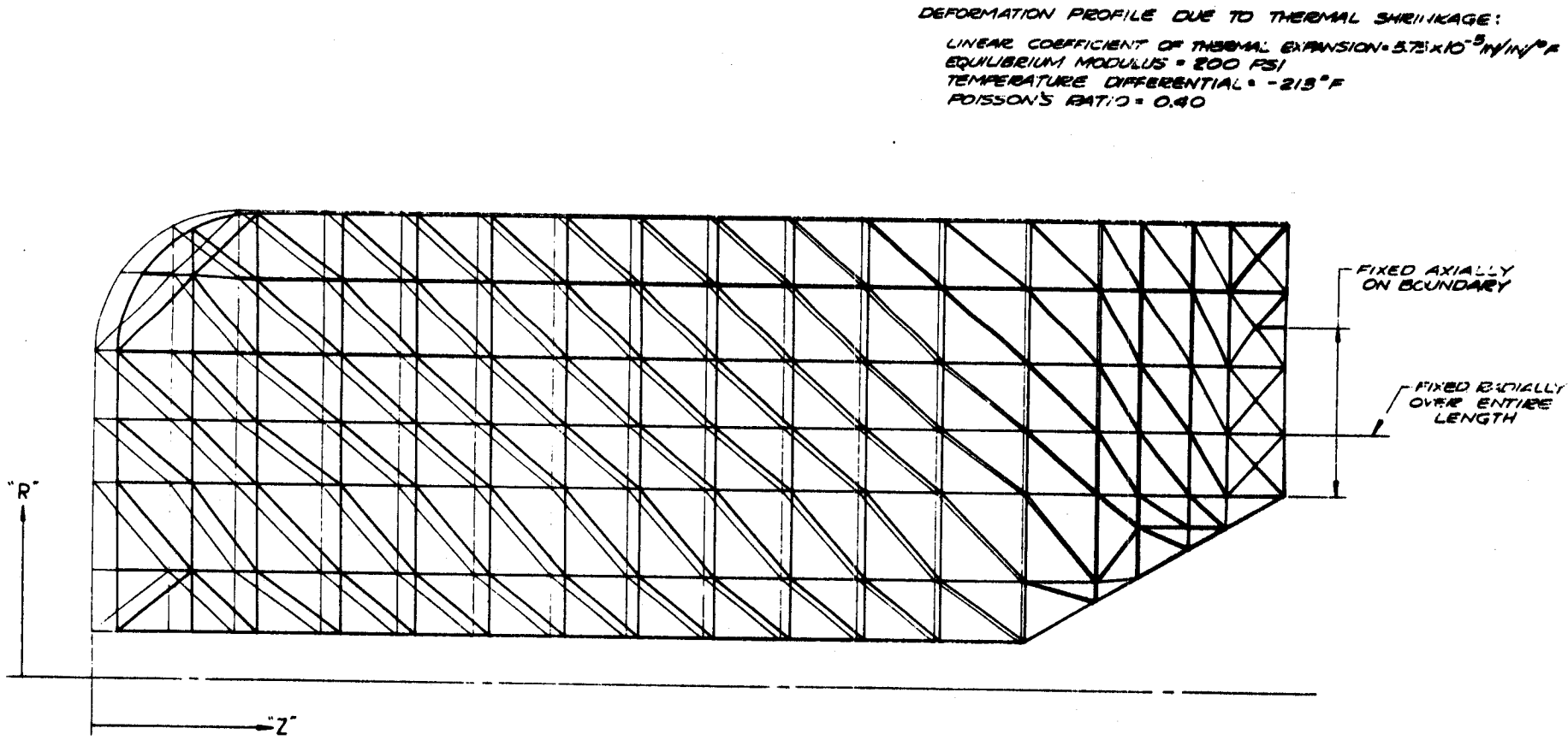

FIGURE 48. INTERNAL-EXTERNAL BURNING FREE STANDING MOTOR DESIGN

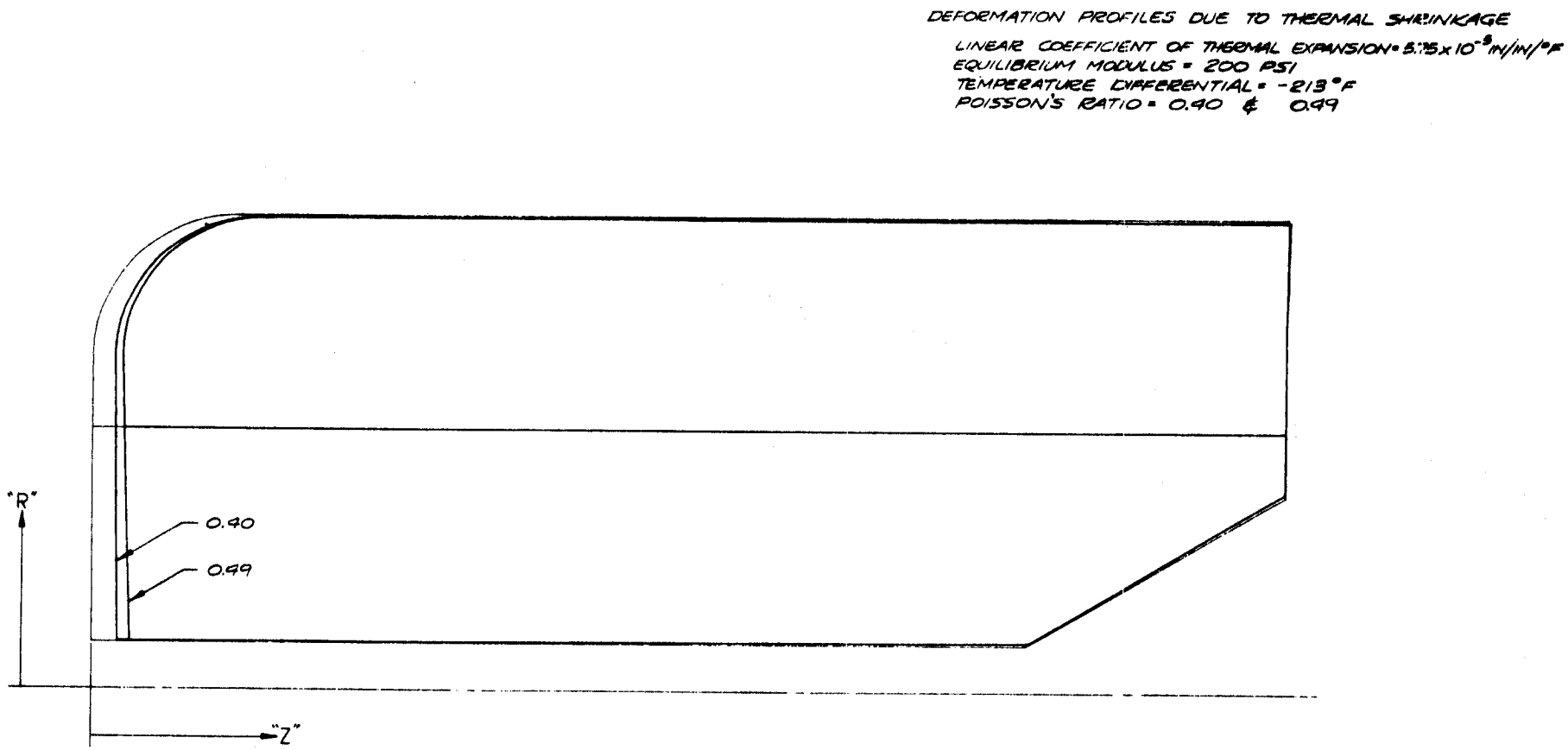

FIGURE 49. INTERNAL-EXTERNAL BURNING FREE STANDING MOTOR DESIGN

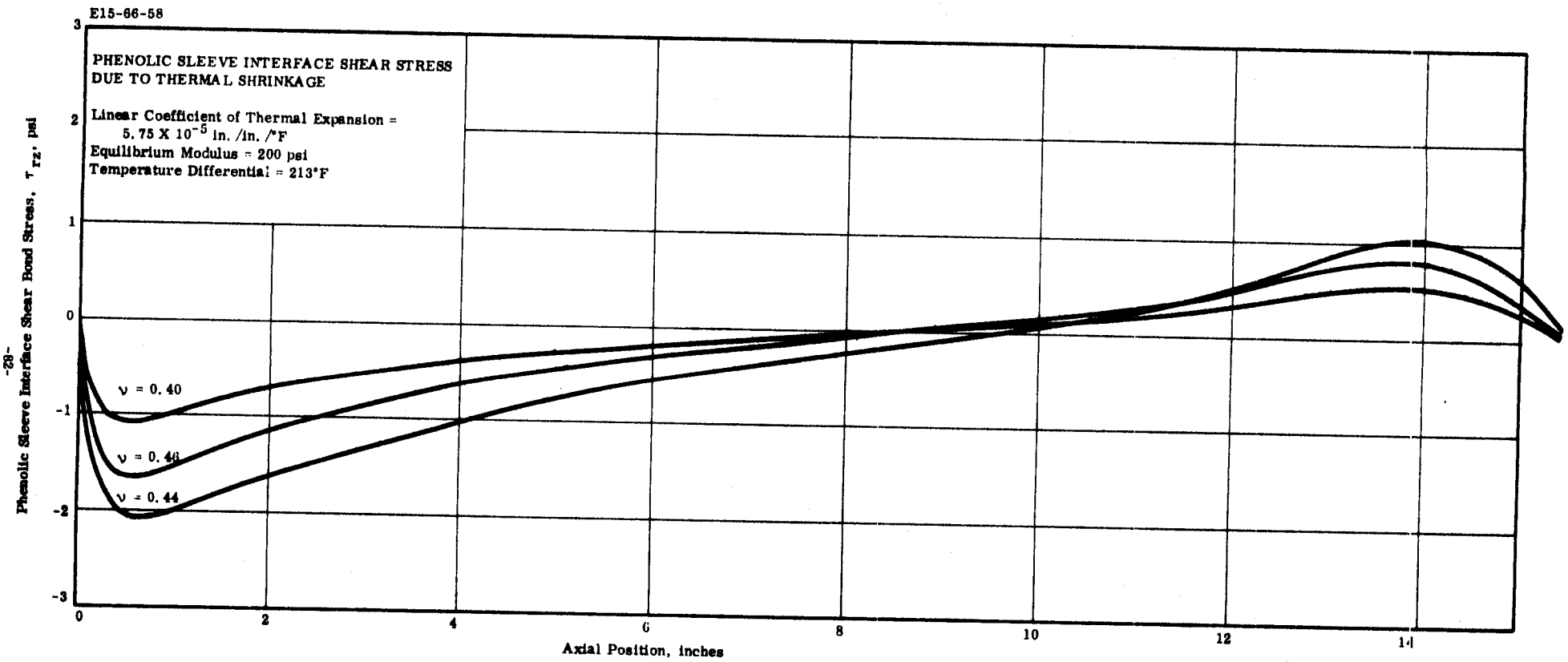

FIGURE 50. INTERNAL-EXTERNAL BURNING FREE-STANDING MOTOR DESIGN

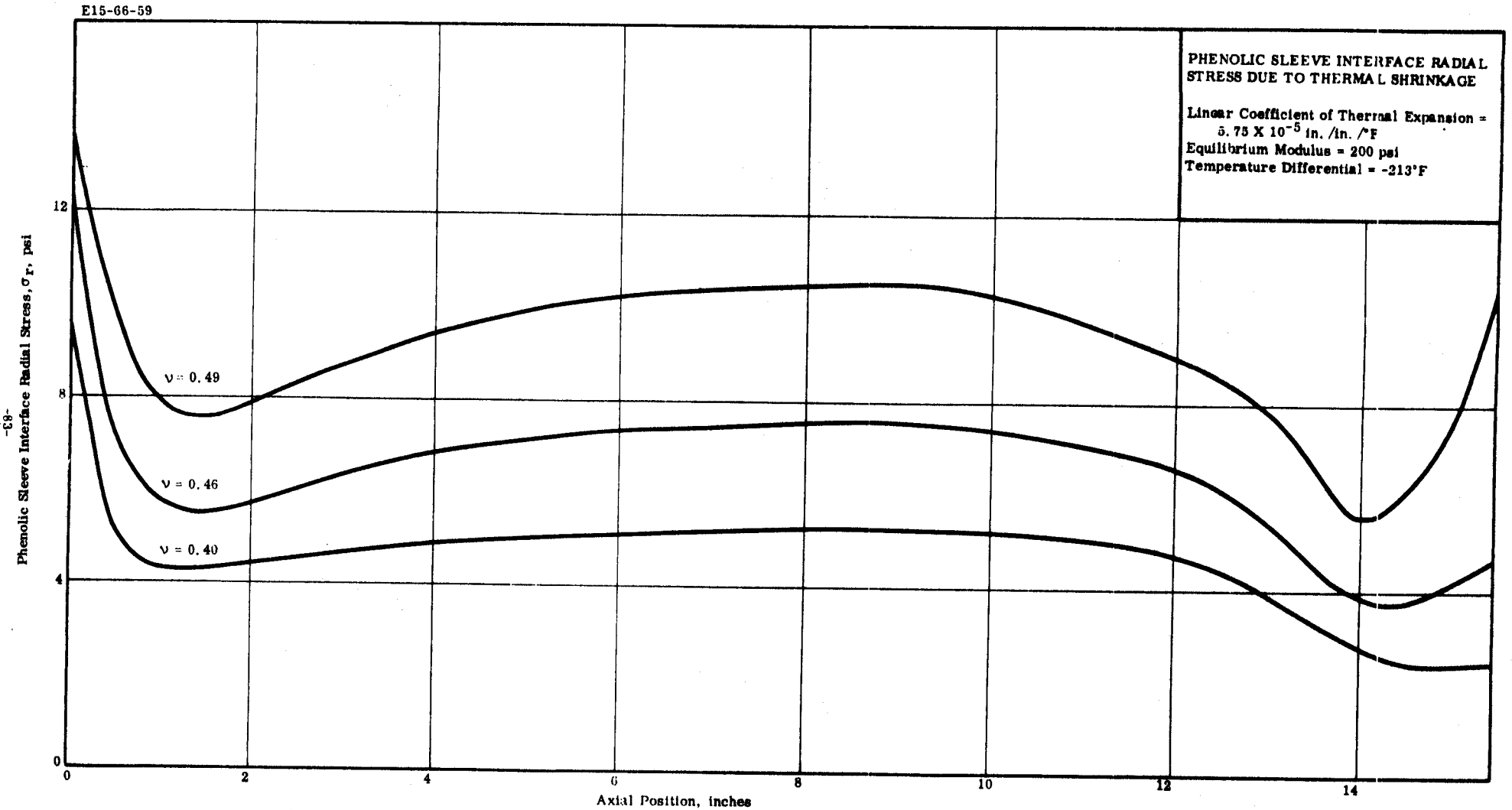

FIGURE 51. INTERNAL-EXTERNAL BURNING FREE-STANDING MOTOR DESIGN

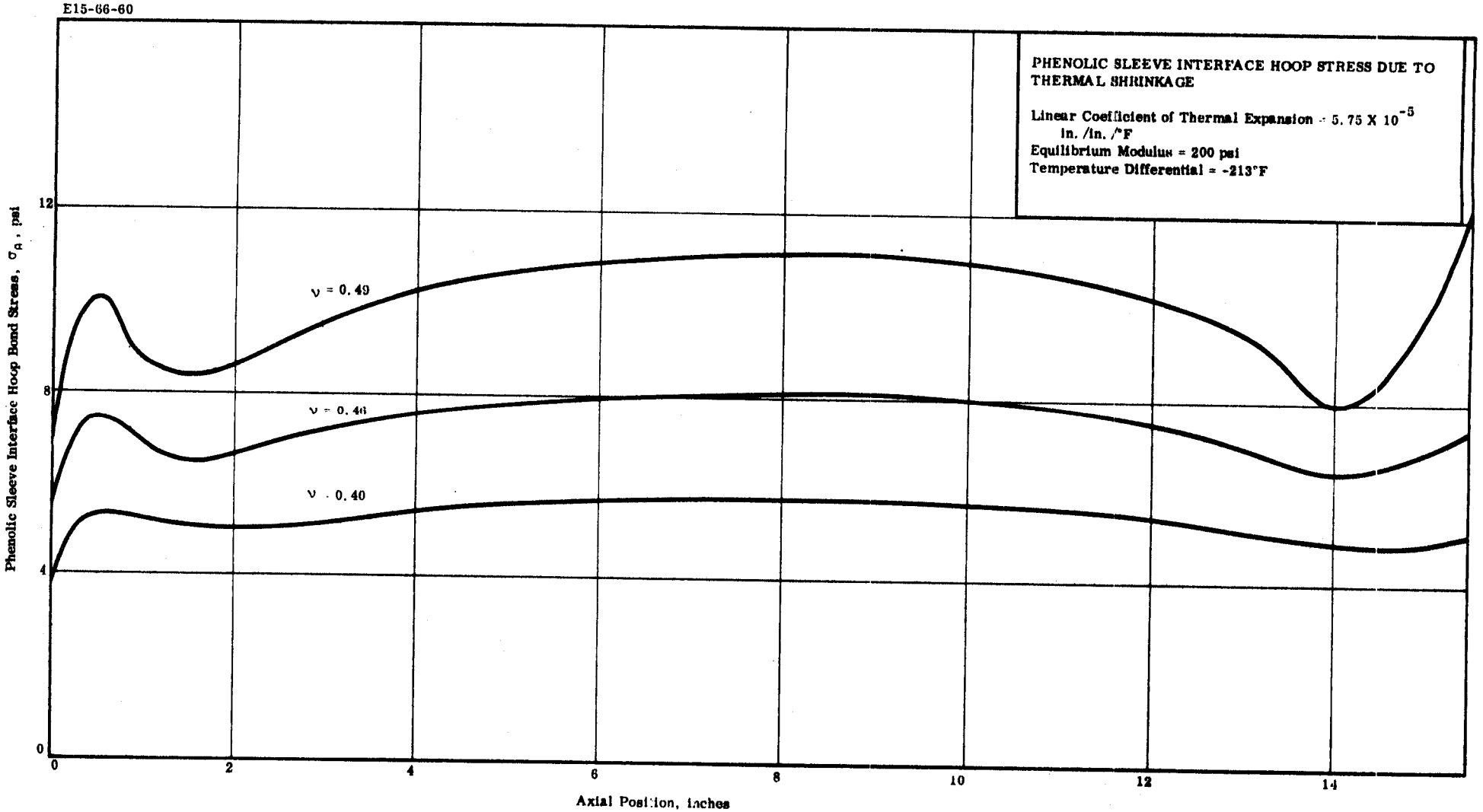

FIGURE 52. INTERNAL-EXTERNAL BURNING FREE-STANDING MOTOR DESIGN

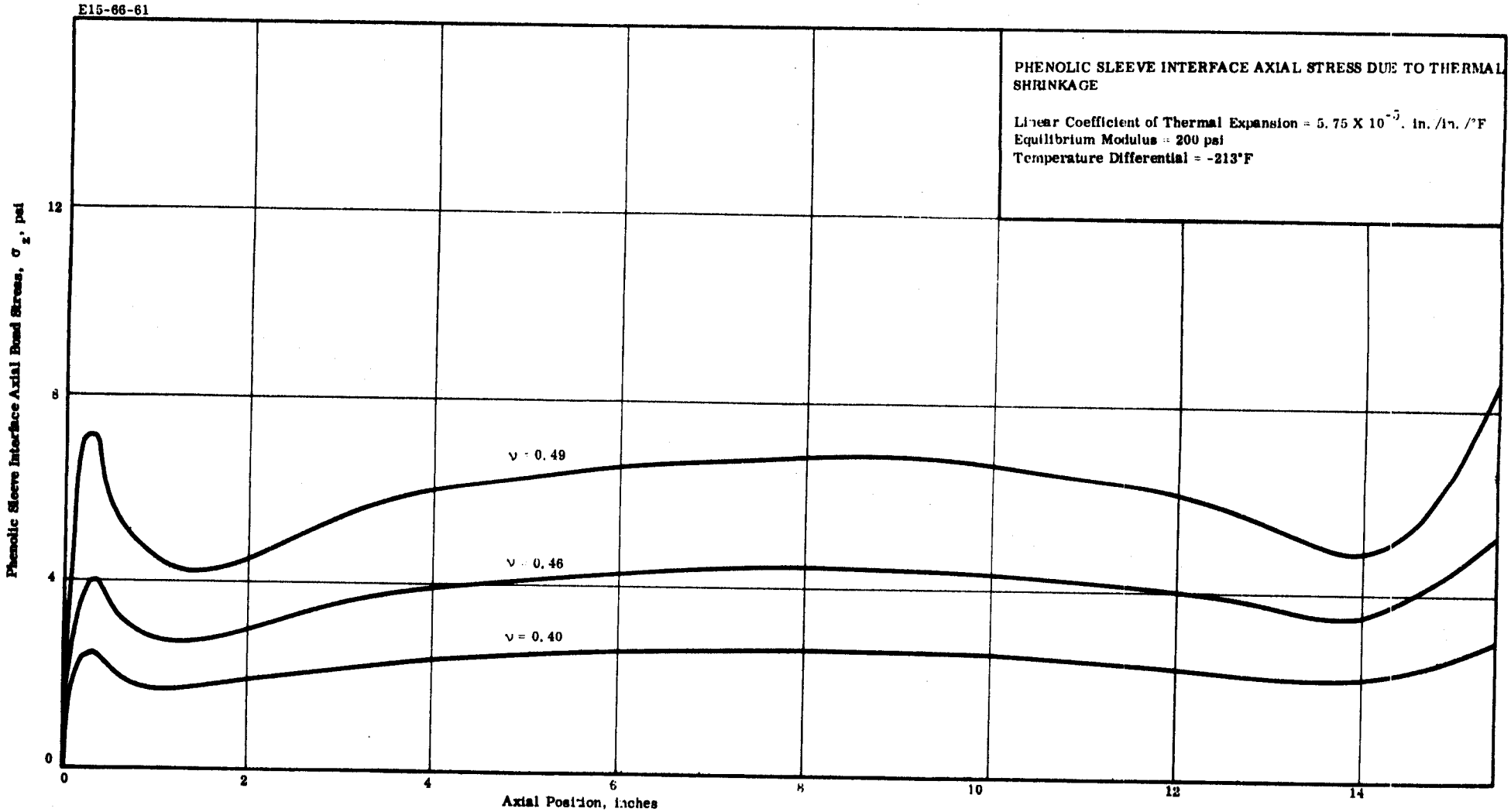

FIGURE 53. INTERNAL-EXTERNAL BURNING FREE-STANDING MOTOR DESIGN

E15-66-62

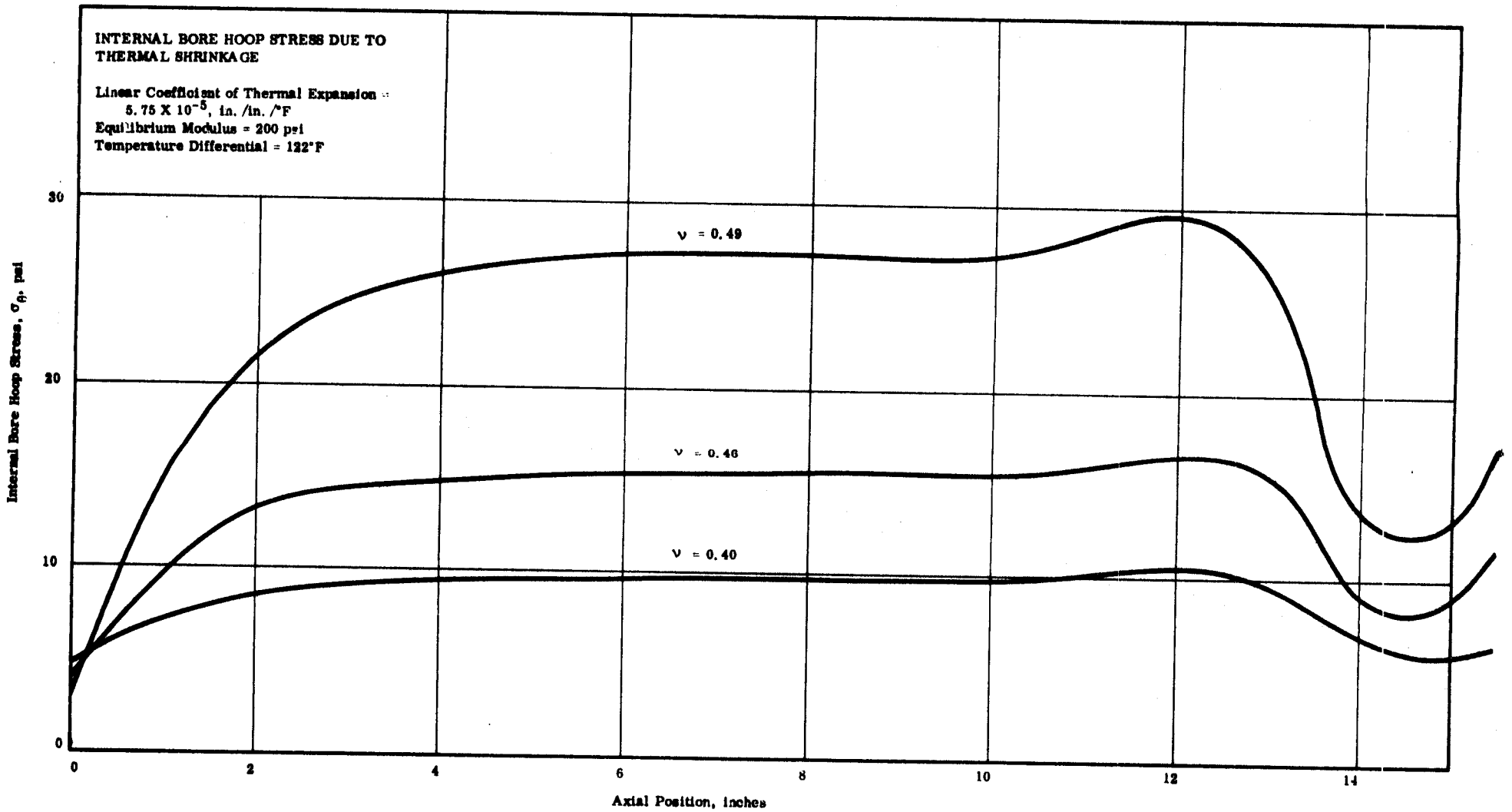

FIGURE 54. INTERNAL-EXTERNAL BURNING FREE-STANDING MOTOR DESIGN

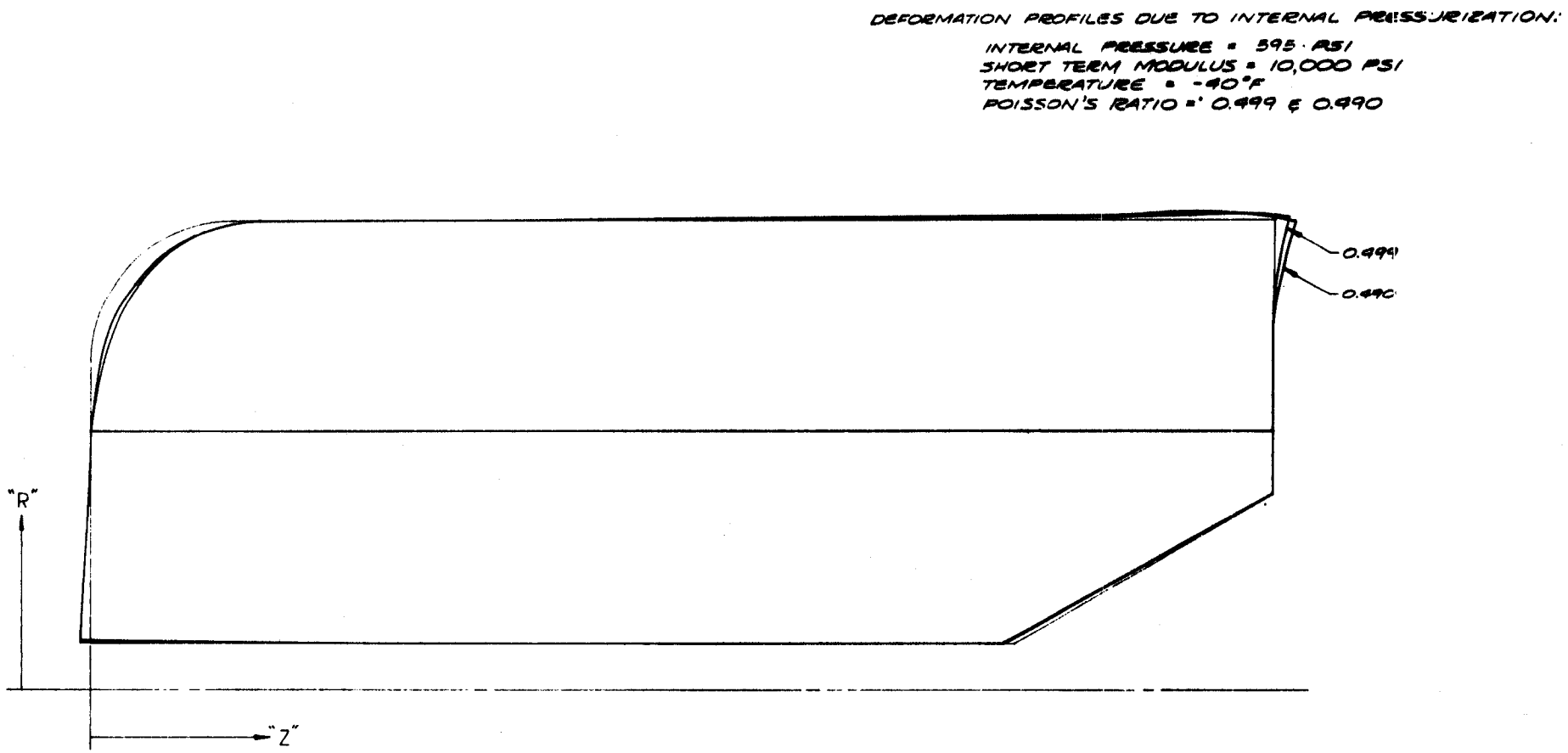

FIGURE 55. INTERNAL-EXTERNAL BURNING FREE STANDING MOTOR DESIGN

DEFORMATION PROFILES DUE AXIAL ACCELERATION:
EQUILIBRIUM MODULUS = 200 PSI
ACCELERATION = 15 G
DENSITY = 0.0595 LB/CU. IN.
POISSON'S RATION = 0.40 & 0.49

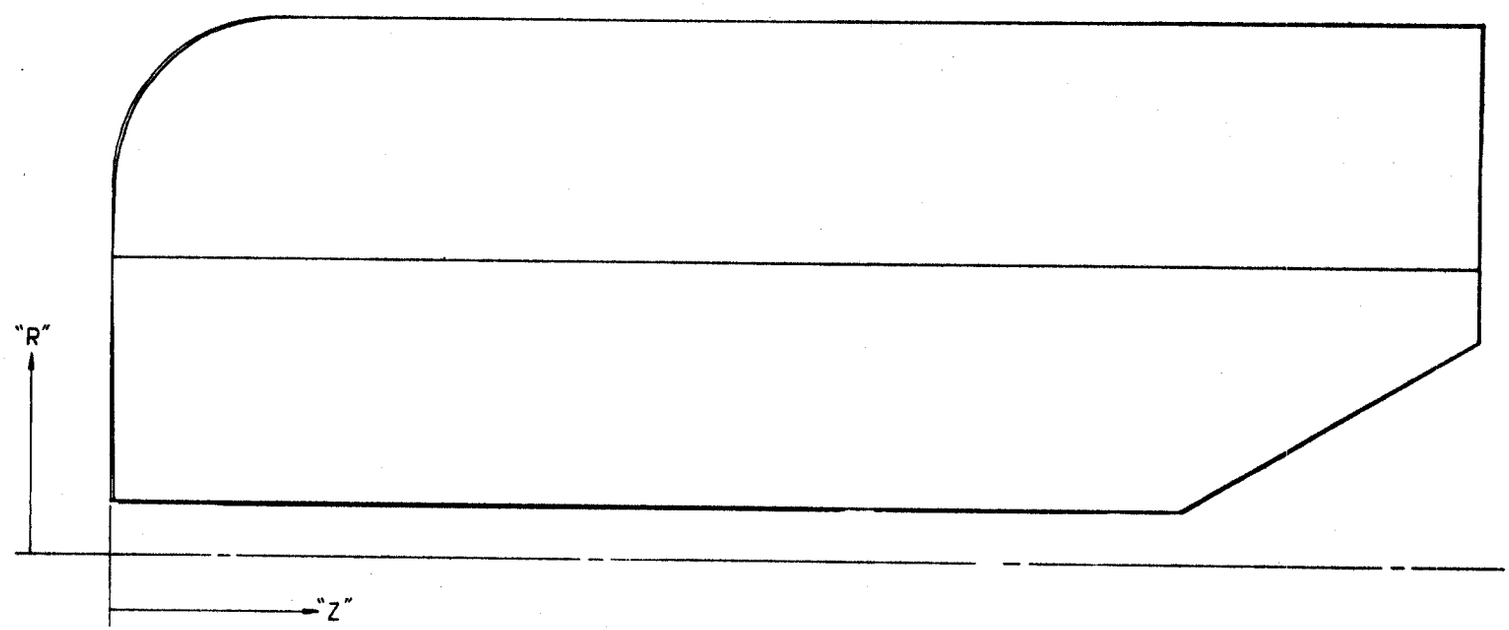

FIGURE 56. INTERNAL-EXTERNAL BURNING FREE STANDING MOTOR DESIGN

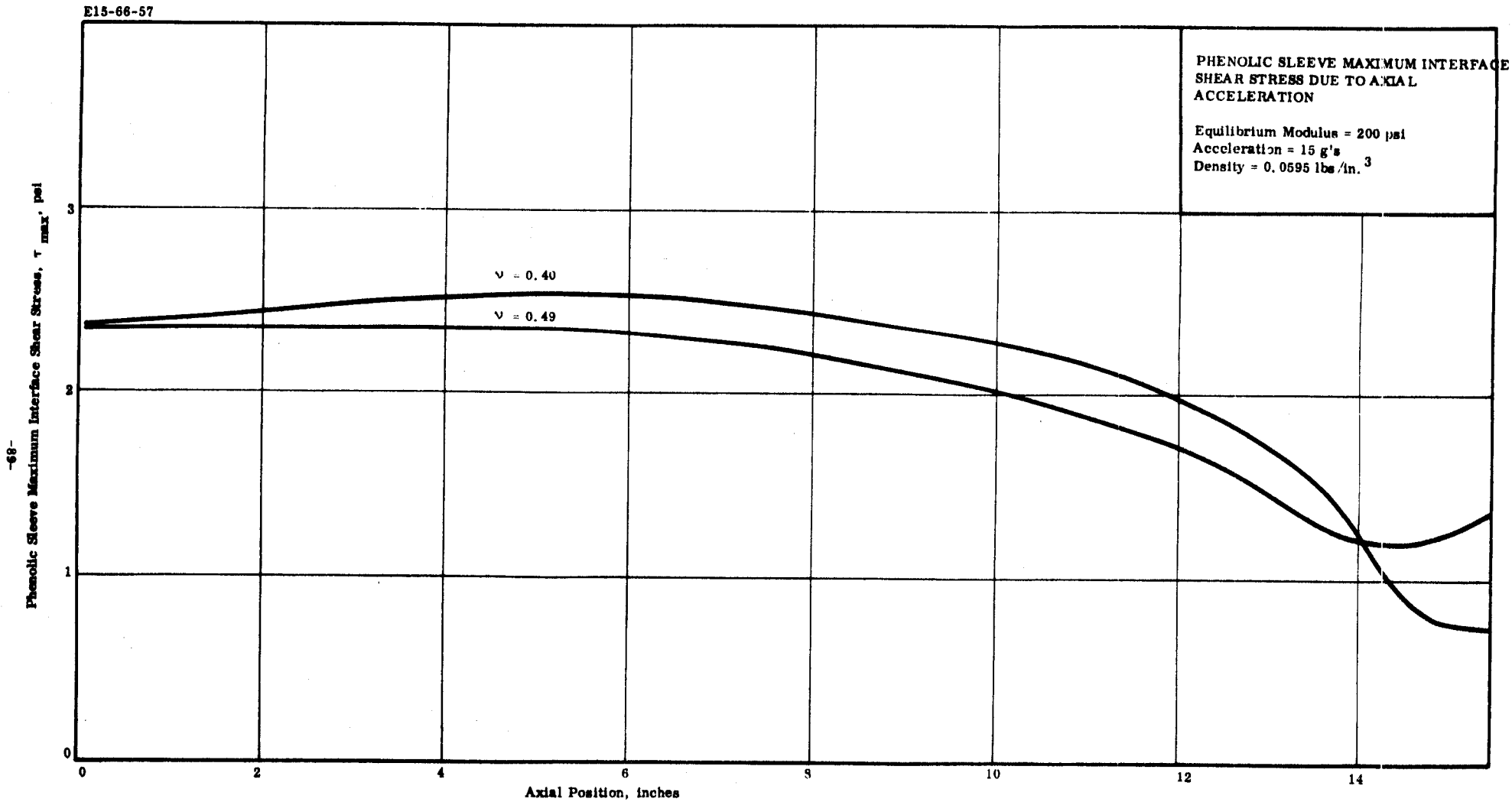

FIGURE 57. INTERNAL-EXTERNAL BURNING FREE-STANDING MOTOR DESIGN

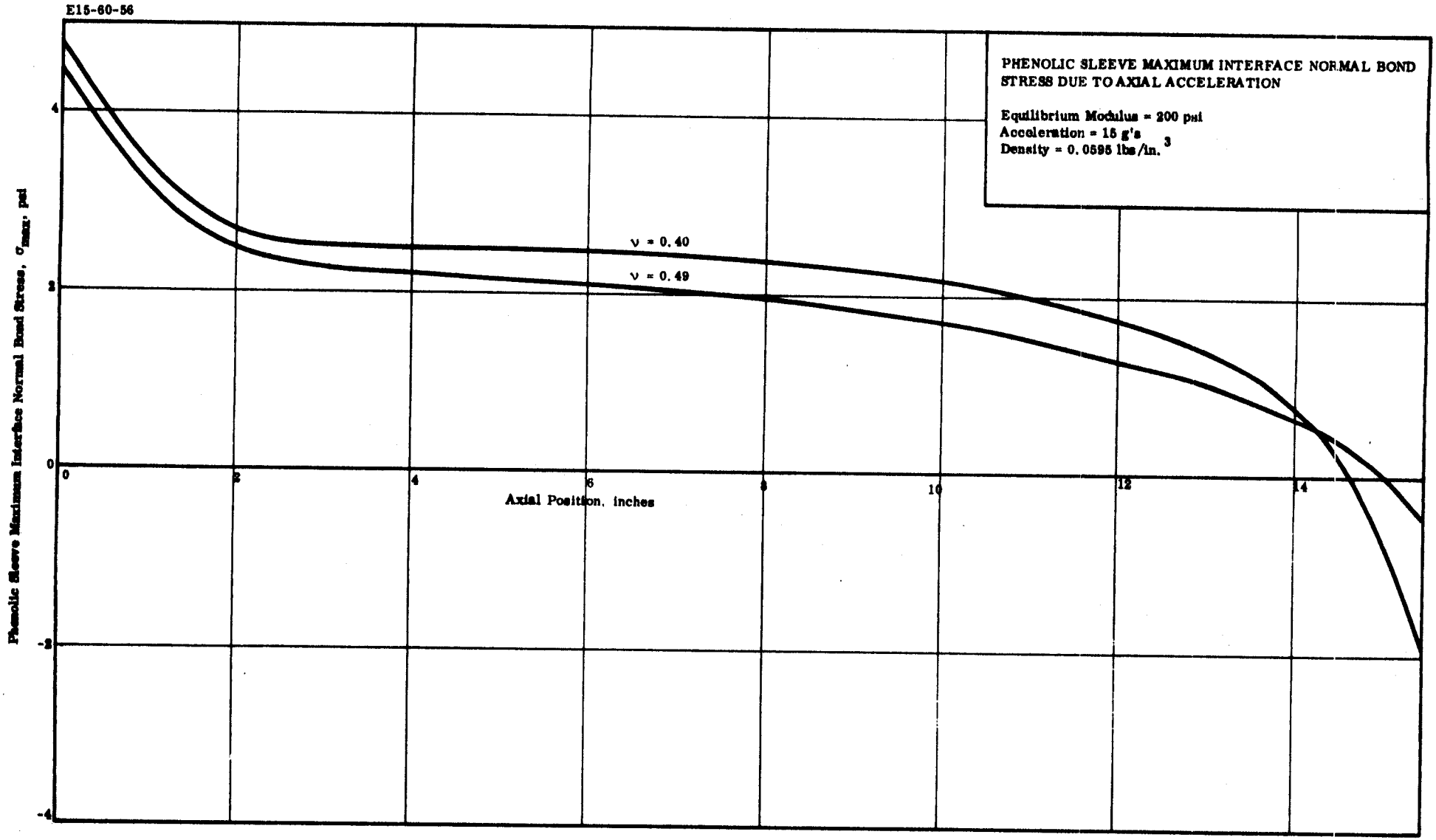

FIGURE 58. INTERNAL-EXTERNAL BURNING FREE-STANDING MOTOR DESIGN

e. Cumulative Effects

(1) Thermal Shrinkage and Internal Pressurization

The effect of superimposing the deformations due to internal pressurization on those due to thermal shrinkage can be assessed from the deformation profiles presented in Figures 49 and 55. Again, it was specified that the most stringent structural requirement for this cumulative load would be imparted by a -40°F firing in space at a maximum ignition pressure of 595 psi.

(2) Thermal Shrinkage and Axial Acceleration

The cumulative effect of deformations due to thermal loading shrinkage and axial acceleration should not affect the reliability of the propellant-liner system because

1) Booster launch will take place at moderate temperatures (50°F to 100°F) so that deformations from thermal shrinkage will be low, and

2) The axial setback force during launch is rather small (15 g's) and results in deformations which tend to cancel each other.

f. Margins of Safety

The method of superposition was used to determine determining the total induced stress and strains in the Internal-External Burning Free-Standing Motor design. Safety factors were computed based upon the theory of maximum principal strain (stress) structural failure and cumulative damage. The tensile-temperature profile of sterilized TP-H-3105, and the adhesive bond strengths of sterilized TL-H-3105 and Epon 912 were used as representative of the ultimate structural capacity of the propellant-liner system.

As shown below, accounting for variability in strength due to temperature but neglecting the effects of rate of imposed load leads to a conservative estimate of the margins of safety. The factors of safety for a particular loading may be calculated from the respective relations:

$$(S.F.)_P = \frac{\text{Structural Capacity}}{\text{Structural Requirement}} \qquad (1.1)$$

$$\frac{1}{(S.F.)_C} = \sum_{i=1}^{n} \frac{\text{Structural Requirements}}{\text{Structural Capacities}} \qquad (1.2)$$

where:

$(S.F.)_P$ = Calculated safety factor due to a particular loading.

$(S.F.)_C$ = Calculated safety factor due to n cumulative loads.

The calculated safety factors for the loadings discussed above are:

Cure and Thermal Shrinkage (-40°F)

Interface Normal Bond Stress

$$(S.F.) = \frac{70 \text{ psi}}{11 \text{ psi}} = 6.36$$

Bore Stress

$$(S.F.) = \frac{70 \text{ psi}}{30 \text{ psi}} = 2.33$$

Bore Strain

$$(S.F.) = \frac{0.15 \text{ in./in.}}{0.07} = 2.14$$

Thermal Shrinkage and Axial Acceleration (-40°F, 15 g's)

Interface Normal Bond Stress

$$\frac{1}{(S.F.)} = \frac{11 \text{ psi}}{70 \text{ psi}} + \frac{4 \text{ psi}}{70 \text{ psi}} = 4.67$$

Thermal Shrinkage and Internal Pressurization (-40°F, 325 psi)

Bore Strain

$$\frac{1}{(S.F.)} = \frac{0.03 \text{ in./in.}}{0.15 \text{ in./in.}} + \frac{0.12 \text{ in./in.}}{0.15 \text{ in./in.}} ; \quad (S.F.) = 1.67$$

These are the safety factors which are significant in the mission of the candidate design. The values as listed are conservative; the rates of loading (mean thermal and mean pressurization strain rates) were assumed to be 0.77 in./in./min. This rate is obtained directly from ultimate strength tensile tests run at a crosshead speed of 2.0 in./min. In fact, the mean thermal strain rate is of the order 1×10^{-4} in./in./min, whereas the mean pressurization strain rate is of the order, 1.0 in./in./min. Since the magnitude of the imposed stresses and strains is largely determined by those induced due to the temperature differential, the calculations are conservative.

G. POTENTIAL IMPROVEMENTS

Because a large number of motor designs were considered in this study, and because each design was examined in detail, it was not possible to completely optimize the two designs finally chosen for comprehensive study. Therefore, both of the chosen designs can be somewhat improved. These possible improvements are discussed in the following paragraphs.

1. Case Bonded Spherical - Cylindrical Perforated Motor Design

The design of the spherical motor can be improved by reducing the insulation thickness. As discussed in the Internal Insulation Section of the Case-Bonded Spherical Circular Perforate Motor design, a major portion of the aft insulation can be removed because only a short relief boot is necessary. Furthermore, complete thermal analysis should be conducted on the internal insulation of the motor case to determine the minimum amount of insulation required. It would also be desirable to study the effect of completely removing the center perforation in the head end of the motor grain. This would cause the design to be progressive and, because of the induced stresses and strains, would require re-analysis of the propellant grain; however, it would completely eliminate the need for a head end insulation section. The nozzle insert and exit cone insert could probably be reduced in weight if a more detailed analysis were performed.

The delivered total impulse could be increased significantly by using a higher nozzle expansion ratio and a contoured nozzle. The design limits of 30:1 on the nozzle expansion ratio and 100 pounds on the propellant weight seriously influence the motor design. It is probable that a lighter motor could be designed to deliver the same incremental velocity as the motor studied. If the payload is sufficiently large and the weight of the deflection motor is a very small percentage of the total weight, then the design limits mentioned above have a relatively small effect on the delivered performance. For example, by changing the nozzle expansion ratio to 60/1, the overall motor weight could be reduced by 1.9 pounds for the same total impulse. If,on the other hand, the deflection motor weight represents a large portion of the overall spacecraft weight, this reduction becomes even more significant.

The specific impulse of the propellant could be increased substantially by adding aluminum to the propellant formulation. Although the design study guidelines specified that a non-aluminized propellant should be used, it must be pointed out that this results in a severe performance penalty. TP-H-3053B, the aluminized version of TP-H-3105, has a theoretical specific impulse of 262 lbf-sec/lbm at 1000 psi.

Further analysis should be made of the web fraction and casting level to determine the effects of these parameters on grain stresses, motor neutrality and mass fraction. An effort should be made to determine whether presence of star points might offer a problem during sterilization. The advantages of the star perforate spherical

design over the circular perforate design studied are: (1) a higher volumetric loading density which would result in a more compact motor design, and (2) a more neutral pressure-time program which will result in a more efficient use of the pressure vessel.

2. Internal-External Burning - Free-Standing Design

This design can also be improved since the technology of high mass fraction, free-standing motors has lagged. Much of the work performed to date on designing free-standing motors has been for systems where high mass fraction motors are not required. These motors, therefore, tend to be over-designed and the materials selected for use are not optimized. It is very probable that the weight of insulation, nozzle and exit cone could be reduced appreciably by conducting a detailed heat transfer analysis. Another item requiring further study is the support structure. The purpose of the support structure is to join mechanically two materials (propellant and case) that have different coefficients of thermal expansion. The support structure designed in this study will accomplish this; however, there is room for improvement.

Again, as in the case-bonded design, consideration should be given to the use of a contour nozzle with a higher expansion ratio, and an aluminized propellant.

III. CONCLUSIONS

- The design study indicates that (within the guidelines established by JPL) the only major problem in the design of a heat-sterilizable solid propellant rocket motor is degradation of the physical properties of the propellant-liner system.

- The problems of differential expansion of the propellant and case materials during temperature cycling can be resolved by the judicious selection of materials and clearances in the design phase.

- The other significant conclusion resulting from this study is that the spherical case design is by far the best (within the guidelines established by JPL) of the case-bonded designs in terms of overall performance.

- Of the spherical designs, the design criteria used in this study indicated that a case-bonded circular perforate design had a higher numerical rating.

- The best of the free-standing designs is the internal-external burning grain with a central support tube.

It should be recognized other design criteria may yield better designs. Also, it is quite possible that some of the other case-bonded and free-standing designs may be sterilized and operated successfully with a slightly reduced reliability rating.

It should be noted that this study is based on a type-approval requirement of three 36-hour dry-heat cycles at 295°F. Recently, the Jet Propulsion Laboratory has considered a type-approval requirement for the Voyager Project which consists of six 53-hour dry-heat cycles at 275°F. The impact of such a requirement was not evaluated during this study; therefore, the results and conclusions reached herein must be utilized with caution.

IV. RECOMMENDATIONS FOR FUTURE WORK

Since the conclusions reached in this study have been made on a purely theoretical basis, Thiokol recommends that the spherical configuration, the better of the two Final Candidate designs, be fabricated, sterilized, and static tested. Using the hardware of the Gemini (TE-M-385) spherical motor can accelerate the schedule because it can be economically and quickly adapted to the Final Candidate Design, loaded with propellant TP-H-3105, sterilized, and tested.

We also recommend that the effect of thermal sterilization on propellant TP-H-3105 be compared with its effect on an aluminized propellant corresponding to TP-H-3105. This comparison can be made by using laboratory physical property specimens in the same manner as the work reported herein. The information generated by this comparison could introduce a good measure of flexibility into future design and analysis work on heat-sterilizable systems.

V. REFERENCES

1) Armed Forces Supply Center, Strength of Metal Aircraft Elements, MIL-HDBK-5, March 1959 (U)

2) Thiokol Chemical Corporation, Wasatch Division Mobile Mid-Range Ballistic Missile, Propulsion, Volume XI Appendix A "Materials" Brigham City, Utah 29 March 1963 (C)

3) Thiokol Chemical Corporation Computer Program "Mission Fuel Prerequisite Program", R. E. Black, Elkton, Maryland 1965 (U)

4) Lockheed Propulsion Company, Thermal Stress Investigation of Solid Propellant Grains, Volume 1, Theory and Experiment, by J. Jones, J. E. Fitzgerald and E. Francis, LPC Report No. 578-F-1, Contract AF 94(611)-8013 May, 1963 (U)

5) Thiokol Chemical Corporation, Rocket Propulsion Data, Bristol, Pennsylvania August 1964 (C)

6) Chemical Propulsion Information Agency, Rocket Motor Manual, SPIA/M1 Volume II, John Hopkins University, Applied Physics Laboratory, Contract NOw-62-0604-C, Silver Spring, Maryland (C)

7) Personal Communication with Mr. Warren Dowler (JPL).

8) California Institute of Technology, Jet Propulsion Laboratory, Effects of Space Environment Upon Plastics and Elastomers, by L. D. Jaffe, Technical Report No. 32-176, Pasadena, California, 16 November 1961 (U)

9) Reinhold Publishing Corporation, Materials in Design Engineering, Materials Selector Issue, V. 162 No. 5 Mid-October 1965 (U)

10) The General Tire and Rubber Company, Gen Gard Insulation Company Brochure, Akron 7, Ohio (U)

11) Raybestos-Manhattan, Inc. Aerospace Division, Reinforced Plastics Department, Engineering and Design Data Reinforced Plastics Products, Company Brochure, Manheim, Pennsylvania (U)

12) Titanium Metals Corporation of America, Properties of Ti-6AL-4V, Titanium Engineering Bulletin No. 1, Revised February, 1965, Company Brochure, New York, New York (U)

13) Parker Seal Company, Parker O-Ring Handbook Company Brochure, Printed July 1961 Cleveland, Ohio (U)

14) Winston Gin, "Heat Sterilization of Pyrotechnics and On-Borad Propulsion Systems" (Paper presented at the NASA National Conference on Spacecraft Sterilization Technology, Pasadena, California, 16, 17 and 18 January 1965 (U)

15) Thiokol Chemical Corporation, Elkton Division, A Proposal to the Jet Propulsion Laboratory for a Design Study of Heat Sterilizable Solid Rocket Motors, Volume 1, Technical Proposal, Elkton, Maryland, 25 June 1965 (C)

16) The Fiberite Corporation, "The Ablative Thermal Insulation Handbook", Company Brochure, Winona, Minnesota (U)

17) Southern Research Institute, The Thermophysical Properties of Plastic Materials from -50°F to over 700°F by C. D. Pears, W. T. Engelke and J. D. Thornburgh, Technical Documentary Report No. ML-TOR-64-87, Part 1, Contract No. AF 33(657)-8594, Burmingham, Alabama, August 1965

18) Appendix I (Volume II of this report) Sterilization Effect on Propellant.

APPENDIX A

GENERAL DESIGN GUIDELINES

In designing a solid propellant rocket motor, the two principal effects of the dry heat sterilization process that must be considered are:

1) Thermal degradation of the physical properties of materials used in design, and

2) thermal expansion during and after heat sterilization.

Both of these effects precipitate problems which must be resolved before manufacture. Judicious selection of materials and clearances can eliminate these problems in the design phase.

A. PROPELLANT

Propellant TP-H-3105 was selected as the propellant on the basis outlined in Appendix I, Volume II (classified).

B. LINER AND ADHESIVE

Liner TL-H-305 is a standard liner regularly used with hydrocarbon propellant. Test data on this liner and Epon 912 adhesive will be found in Appendix H, Material Selection.

C. INERT MATERIALS

Sterilization has less effect upon the inert case and nozzle materials than upon the propellant. The inert materials are generally inorganic binders, or organic binders compounded with inorganic fillers and selected for thermal resistance. Each of the inert materials is discussed below:

1. Insulation and Inhibitors

The effects of heat sterilization on insulations and inhibitors are somewhat less than the effects upon propellant. Two types of insulation are commonly used: elastomeric insulation used for relief flaps, boots and inhibitors, and rigid insulations used for insulation, supports, exit cones, and other applications where physical strength is required.

a) Elastomeric Insulations

A literature search indicated a number of possible insulations that could be used for relief flaps and inhibitors in the motor (References 8 and 9). Two of these materials have already been used as elastomeric insulations in rocket motors.

Butadiene-acrylonitrile (nitrile rubber) exhibits a 10-percent weight loss at 300 to 450°F in vacuum storage for one year (Reference 8); isoprene rubber exhibits a 10-percent weight loss at 380°F in vacuum.

These are closely related to asbestos-filled buna-N (V44, General Tire and Rubber Co.) insulation and asbestos-filled polyisoprene insulation. Both of these materials have been used as stress relief boots and insulation sections on Thiokol-manufactured motors.

A search of supplier's brochures revealed little information concerning high temperature exposure of these materials although it is reported that V-44 insulation will withstand 325°F up to 24 hours (Reference 10).

Communication with insulation specialists indicated that either V-44 or asbestos-filled polyisoprene probably would withstand exposure to 300°F for prolonged periods in the absence of oxygen. Asbestos-filled polyisoprene was probably the better choice since it does not use a plasticizer. Plasticizers can exude or evaporate during sterilization resulting in embrittlement of the insulation.

It was decided to expose samples of these materials to sterilization to determine whether substantial degradation occurred. The results of these tests indicated that sterilization had virtually no effect on the insulations. The physical properties of V-44 and asbestos-filled polyisoprene are given in Appendix H.

b) Rigid Insulation

A literature search of representative phenolic insulations indicated that relatively few problems would be experienced with phenolic materials during heat sterilization. Cure cycles of up to 5-1/2 days at 300°F have been used to improve physical properties in the postcure (Reference 11) of typical phenolic insulations such as Raybestos-Manhattan RPD 150. They also indicate that RPD 150 retains between 50% and 80% of its original physical properties when exposed for 5 hours at 700°F in 1/8-inch thick samples. Materials such as RPD 41 (a similar material) have been exposed to 300°F for 1,000 hours and show almost no change in physical properties. As a result, no appreciable degradation of phenolic-based materials is expected.

Properties of the phenolic materials selected for insulations are shown in Appendix H.

2. Case Materials

No problems are anticipated as the result of sterilization of the 6A14V titanium case materials.

3. Pressure Seals

A brief literature search indicated that buna-N O-rings were suitable for use as pressure seals for prolonged exposure at the sterilization temperature (Reference 13).

D. CRITICAL PROBLEMS

1. Squib

A brief literature search was conducted to determine the capability of existing electro-explosive devices to survive repeated exposure to sterilization. However, sterilization is not the only requirement imposed on the initiating device. JPL surveyed the existing squibs in 1964 and found none would meet all requirements (Reference 14).

In view of the widespread effort on this subject elsewhere, and because of work presently being conducted at JPL, the critical problem of heat-sterilizable squibs was not investigated fully during the course of this study.

2. Nozzle Closure

The nozzle closure is a very critical design problem which has not yet been resolved. A nozzle closure is definitely needed to exclude oxygen from the motor (preventing propellant degradation during sterilization); it also keeps volatile ingredients from the propellant and some components from being deposited on other components inside the bacteriological shroud and possibly causing failure of these components. For this reason, it is desirable to have a relatively tight pressure seal at the nozzle closure. It is also desirable to be able to pressurize the case with sterile nitrogen after assembly to a point somewhat above the ambient pressure so that, when the motor is sterilized, the internal chamber pressure will increase when the nitrogen expands. If a breathing-type closure is provided, the gases will leak out slowly; after sterilization and cool down, therefore, the pressure inside the motor could be less than ambient pressure which would allow contaminated air into the motor. Therefore, a pressure-tight nozzle closure is required.

This, in itself, is not a serious problem. However, if the thrust vector control system is a jet-vane type and if a pressure-tight non-breathing closure is used, the jet vanes could be damaged by large particles of the closure ejected when the motor is ignited.

E. THERMAL EXPANSION EFFECTS

Differential expansion of materials in the motor assembly is of some concern because interference of components can exist at the sterilization temperatures and separation of bonds can occur at the -40° F low temperature firing limit. Problems can also occur during transient temperature changes and during steady state temperature exposure.

1. Steady State Temperature Effects

When two materials with different thermal expansion characteristics are joined and subsequently heated or cooled, deflections and stresses are set up at interfaces between the materials. In certain applications this can cause failure of the adhesive bond between materials. Since propellants and plastic materials have coefficients of expansion higher than case materials, heating the motor causes compressive stresses and strains between the case and the other components; correspondingly, cooldown of the motor causes tensile stresses between the components.

Since the maximum amount of differential thermal expansion occurs between the propellant ($\alpha = 6.3 \times 10^{-5}$ Reference 15) and titanium 6 Al 4V ($\alpha = 0.55 \times 10^{-5}$ Reference 12), these were the first two items evaluated. Heating from a reference strain temperature of 170°F (zero strain temperature allowing for thermal shrinkage during cure) to 295°F will cause a differential expansion of 0.72 percent of the original length, or about 0.058 interference on the radius of a 16-inch diameter motor. The effect of cooling from +170°F to -40°F will cause a differential radial expansion of 0.097 inch between the case and the propellant charge. This effect is significant and must be allowed for in designing clearances. However, it is not large enough to cause appreciable concern as to motor integrity and functionality. A detailed discussion of the shapes of the grains at -40°F and +295°F due to thermal expansion and pressurization effects is included in Appendix F and under the detailed analysis of the case-bonded and free-standing designs in the body of this report. These same considerations apply to plastic structures bonded to propellant, but to a lesser degree, since the thermal coefficients of expansion of the plastic materials are closer to those of propellant.

Also to be considered during steady state temperature change is the differential thermal expansion between the titanium components and the plastic insulation. The thermal coefficient of expansion of RPD 41, one of the phenolic insulations, is approximately 1.4×10^{-6} in/in/°F (Reference 11). The differential expansion between the phenolic and the insulation is 0.85×10^{-6} in/in/°F. This will cause interference at high temperature, assuming that the phenolic is bonded to the inside of the metallic portion of the case. Similarly, it will tend to cause separation at the lower temperature. Assuming that the phenolic is used to insulate a spherical motor case 16 inches in

diameter, the radial interference on an 8-inch radius due to heating is 0.009 inch. Cooldown produces a separation of 0.014 inch. Assuming a phenolic thickness of 0.20 inch and a titanium case wall thickness of 0.030 inch, this deflection at -40°F would require a tensile strength between the phenolic and the wall of 209 psi at -40°F. This is a strength level and can easily be achieved by the proper selection of adhesives. If the insulation is molded in place at +300°F, the required bond strength between the insulation and case is 338 psi because of the cooldown to -40°F. This does not appear unreasonable and depends upon such things as cleanness of the case before molding and surface roughness. Actually, it is difficult to conceive of serious thermal expansion problems arising from heating the motor cast to 295°F (because the plastic parts will expand more than the case and all stresses will be compressive) or due to cooling to -40°F. Many motors using components similar to those selected are routinely handled at -75°F without failure.

2. Transient Effects

Transient effects are similar to steady state effects except that the directions of the stresses and strains introduced are opposite to those just discussed. If the case is heated rapidly, tensile stresses are set up between the cold grain and the hot case; upon cooldown, the reverse is true. The stresses set up in the motor are much lower during this phase because the expansion or contraction of the case relative to the propellant is much less. It is doubtful that there will be any appreciable effect on the propellant because the stress level set up in the propellant-liner interface, due to transient heating, will be proportional to the thermal expansion coefficient of the case material. The effect on the phenolic insulation was calculated, assuming the temperature of the motor case to be raised instantly from 70°F to 295°F. In this example, the total radial expansion of the case was 0.0105 inch which induces a stress of 154 psi between the case and the phenolic with a 16-inch diameter case and a phenolic thickness of 0.20 inch. At 295°F, the tensile strength of the adhesive used may not be this high. (The assumption used in this analysis was that the case and adhesive were immediately heated to 295°F while the phenolic insulation remained at 70°F.) This analysis was very conservative because the motor will be in a bacteriological shield or in a forced convection oven. As a result, instantaneous heating of the case relative to the phenolic insulation could not occur and the stresses would be appreciably lower.

3. Other Items Affecting the Problem of Thermal Expansion

In order to minimize the problems due to differential thermal expansion, it is desirable to select materials having the same coefficients of thermal expansion, but since the propellant has a high coefficient of expansion relative to the metallic case materials, this is not possible. An alternative approach in the case-bonded units is to select an insulating material that has a lower modulus than that of the propellant, and to use stress relief boots which allow expansion and contraction of the grain relative to the case. For the free-standing designs, especially the internal-external burning type supported by a rigid

internal support, two items are important, First, the rigid case insulation should be selected whose thermal expansion properties are relatively close to those of the case material in order to prevent failure of the insulation-case interface bond. Second, a grain support must be selected whose thermal expansion properties are close to those of the propellant.

A literature search was performed to determine if support materials of this type were available. The following materials have thermal expansion properties similar to those of propellant.

		Thermal Expansion
1)	Glass Fabric Phenolic (low pressure molding)	5.6×10^{-5} in/in/°F (Reference 9)
2)	Cast Phenolic (General Purpose)	$4.7 - 6.6 \times 10^{-5}$ in/in/°F (Reference 9)
3)	Epoxy (Filament Wound)	$2.0 - 6.0 \times 10^{-5}$ in/in/°F (Reference 9)
4)	Fiberite MX 4925	5.5×10^{-5} in/in/°F (Reference 16) Normal to wrap
		1.25×10^{-5} in/in/°F Parallel to wrap
5)	Fiberite MX 4950	7.5×10^{-5} in/in/°F (Reference 16) Normal to wrap
		0.8×10^{-5} in/in/°F Parallel to wrap
6)	Fiberite MX 4566	6.0×10^{-5} in/in/°F (Reference 16) Normal to wrap
		$.6 \times 10^{-5}$ in/in/°F Parallel to wrap
7)	30% NCR 1174/Epoxy - Eglass-Flake	5.92×10^{-5} in/in/°F (Reference 17) Normal to flake
		0.325×10^{-5} in/in/°F Parallel to flake

		Thermal Expansion
8)	23% NRD 1174/3 Epoxy - Eglass-Flake	5.0×10^{-5} in/in/°F (Reference 17) Normal to flake $.417 \times 10^{-5}$ in/in/°F Parallel to flake
9)	SC 1013 Phenyl Silicon Resin Coating	3.67×10^{-5} in/in/°F Longitudinal direction 9.37×10^{-5} in/in/°F Thickness direction
10)	DER 332 Epoxy Coating	3.41×10^{-5} in/in/°F (Reference 17)

Of these, MX 4925 was chosen because it allows freedom of expansion in the longitudional direction, like propellant, but its expansion parallel to the wrap (circumferentially in the case of a wrapped tube) is similar to that of other phenolics. This allows the tube to be joined to the support structure in the free-standing design.

Reference 16 indicated two other items of great importance. Some materials have non-uniform thermal expansion characteristics and, in addition, certain materials exhibit a hysteresis loop which causes incremental dimensional changes on thermal cycling. A material exhibiting progressive growth or shrinkage during each sterilization cycle would not be satisfactory because of the large stresses. Also, one with differential expansion properties changing rapidly with temperature may cause problems because of the dimensional difference between the propellant and the insulation, although dimensional changes from -40°F to +295°F may be the same as those of the propellant charge.

Materials 7 and 8 exhibit differential expansion properties, but not excessively. Materials 9 and 10 are relatively linear, but were eliminated because of their low expansion coefficients.

APPENDIX B

DESIGN DESCRIPTIONS—INITIAL 19 DESIGNS

A total of 19 grain designs were studied to determine which were best suited to more detailed analysis. These designs can be classified under the following four groups:

1) case-bonded or case-supported spherical;

2) case-bonded cylindrical;

3) cylindrical free-standing or partial free-standing; and

4) free-standing end burners.

A. SPHERICAL CASE BONDED DESIGNS

1. Design 1— Conventional Spherical Designs: (See Figure B-1)

This grain design is typical of spherical grain designs used for space applications. It is characterized by an eight-point star internal perforation with a web fraction of 0.61. The forward portion of the grain includes an internal cylindrical perforation which extends to the case wall. This perforation has the dual purpose of relieving some of the grain stresses and providing a more neutral burning surface. A split insulation boot is incorporated in this area to relieve grain stresses and insulate the forward portion of the case during burning. The aft section of the motor case is insulated to a point slightly forward of the case equator and has a small stress relief flap at the extreme aft end. Both insulation sections are elastomeric, fabricated usually from asbestos-filled polyisoprene insulation.

This grain can be manufactured by bonding the preformed insulation sections to the motor case, lining the case, placing the core in position and then casting and curing the propellant in the motor case. After cast and cure, the core is removed and the aft portion of the grain is cut out to accommodate a submerged nozzle.

2. Design 2— Conventional Spherical Design with Long Relief Boots (See Figure B-2)

This design is very similar to the conventional spherical design. However, in this design, an attempt has been made to minimize the stresses by employing long stress relief boots. The design is characterized by an eight-point star internal perforation with a web fraction of 0.61. It also has a circular perforation in the head end. The split boot insulation sections in the head and aft end have been increased in length.

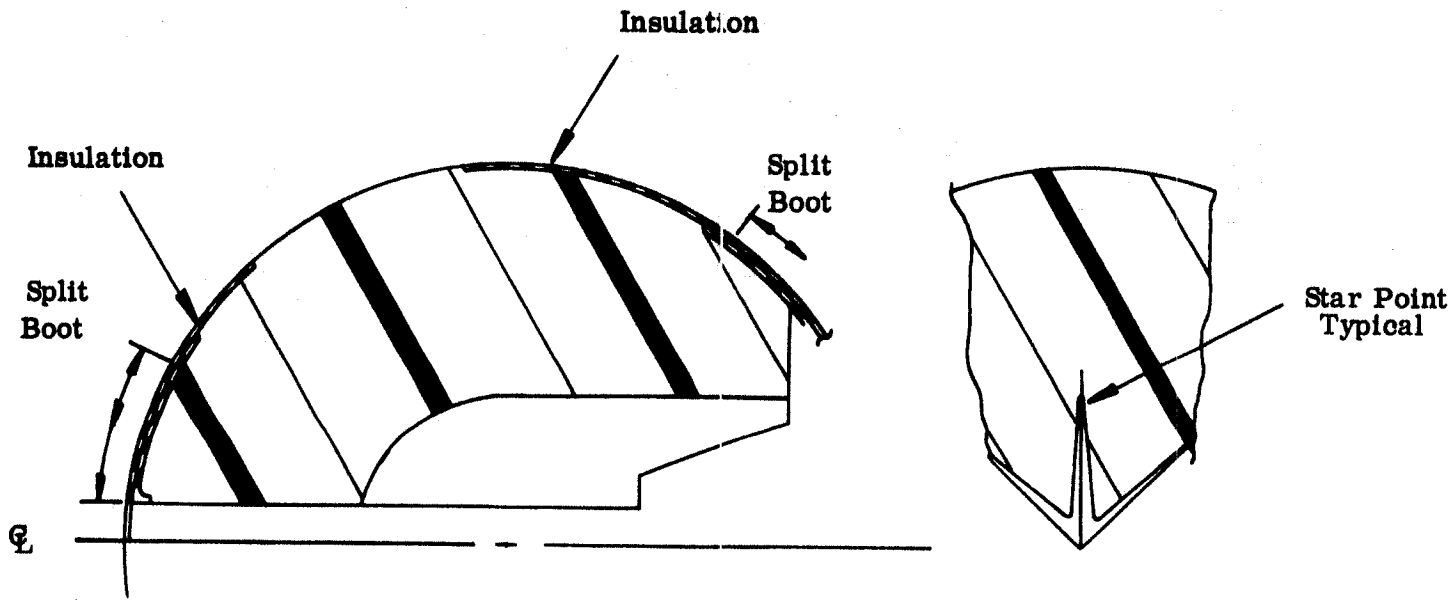

FIGURE B-1. DESIGN 1 — CONVENTIONAL SPHERICAL DESIGN

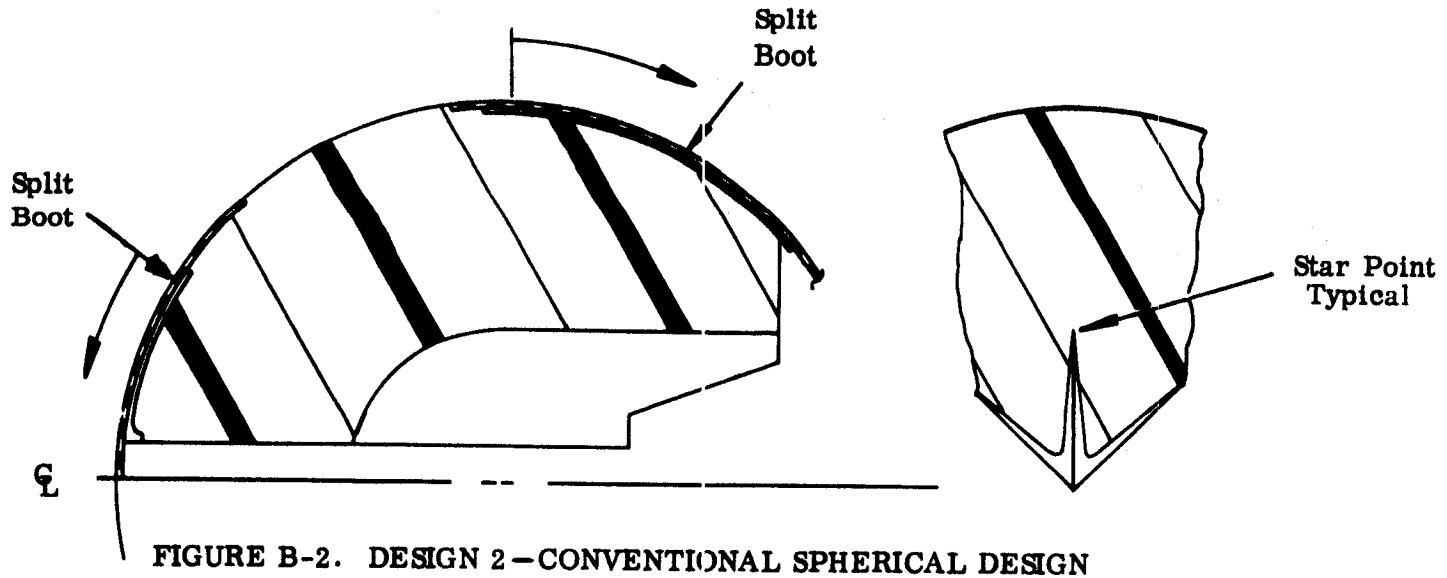

FIGURE B-2. DESIGN 2—CONVENTIONAL SPHERICAL DESIGN WITH LONG RELIEF BOOTS

The grain can be manufactured by bonding the split boots in place, lining, positioning the core, casting and curing. After the core is removed, the aft section of the grain is machined to a conical surface, allowing the use of a submerged nozzle.

3. Design 3— "Orange Slice" Design (See Figure B-3)

This design is characterized by an eight-point internal perforation that extends all the way to the motor case wall. A major portion of the sides of the star perforation is inhibited by an asbestos-filled polyisoprene. This technique provides circumferential stress relief and the same neutrality as the conventional sphere. The forward section of the motor case uses a circular perforation to relieve the stresses caused by cure and thermal shrinkage. The head and aft ends of the motor case are insulated from the combustion gases by asbestos-filled polyisoprene.

The grain can be manufactured by bonding the preformed insulation sections into place using a collapsible mandrel. The core is then removed and the motor case lined. The core is re-inserted and 8 sections resembling orange slices are cast individually and cured. After core removal, the aft end of the grain is cut into a conical shape to receive the submerged nozzle.

4. Design 4— Spherical Circular Perforate Design (See Figure B-4)

This design has no star points. It consists of a circular perforation in the aft end, a spherical cap immediately forward of the equator, and a cylindrical section in the head end of the motor case. The web fraction for this design is 0.65. Large split boots are employed in the head and aft insulation sections.

This grain is manufactured in much the same way as the conventional spherical design. The preformed asbestos-filled polyisoprene insulation boots are bonded into place, the case lined, the core inserted and the propellant cast and cured. No propellant cutback is necessary for this design.

5. Design 5— Circular Perforated Sphere with Propellant Cast around Nozzle Insert (See Figure B-5)

This design has no star points. It consists of two separate propellant sections. The first is bonded to the motor case and consists of a cylindrical aft end perforation, a spherical cap, and a cylindrical perforation in the head end. The web fraction of this section is 0.54. The design has two insulation sections. The aft section is a stress-relief boot of asbestos-filled polyisoprene insulation with the split section extending to the equator. The head-end insulation section is also formed as a split boot; however, this insulation extends the full length of the forward circular

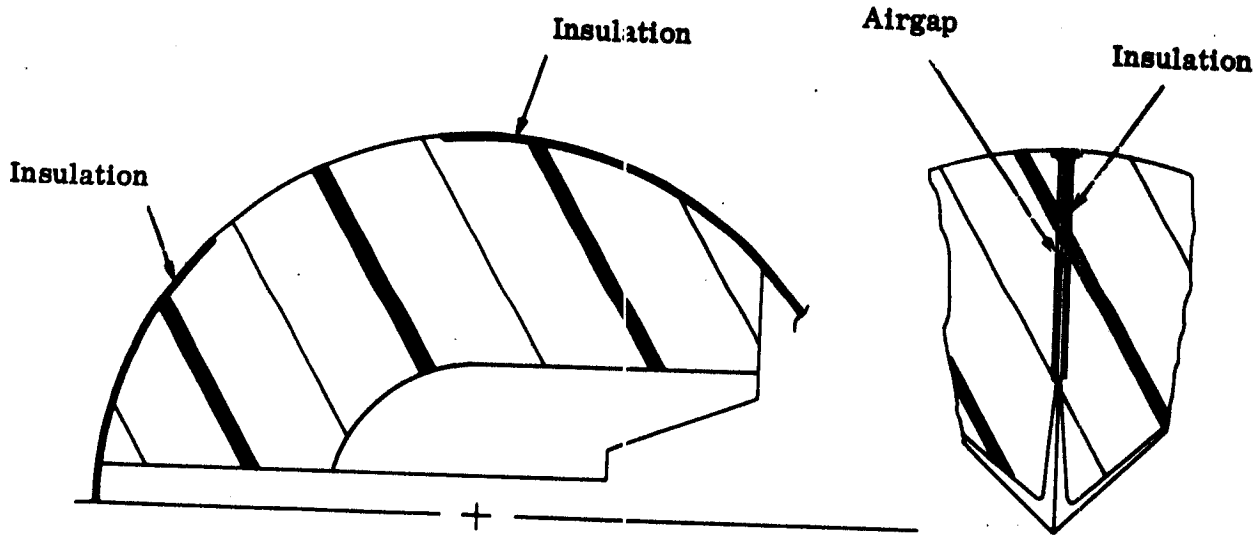

FIGURE B-3. DESIGN 3 — "ORANGE SLICE" DESIGN

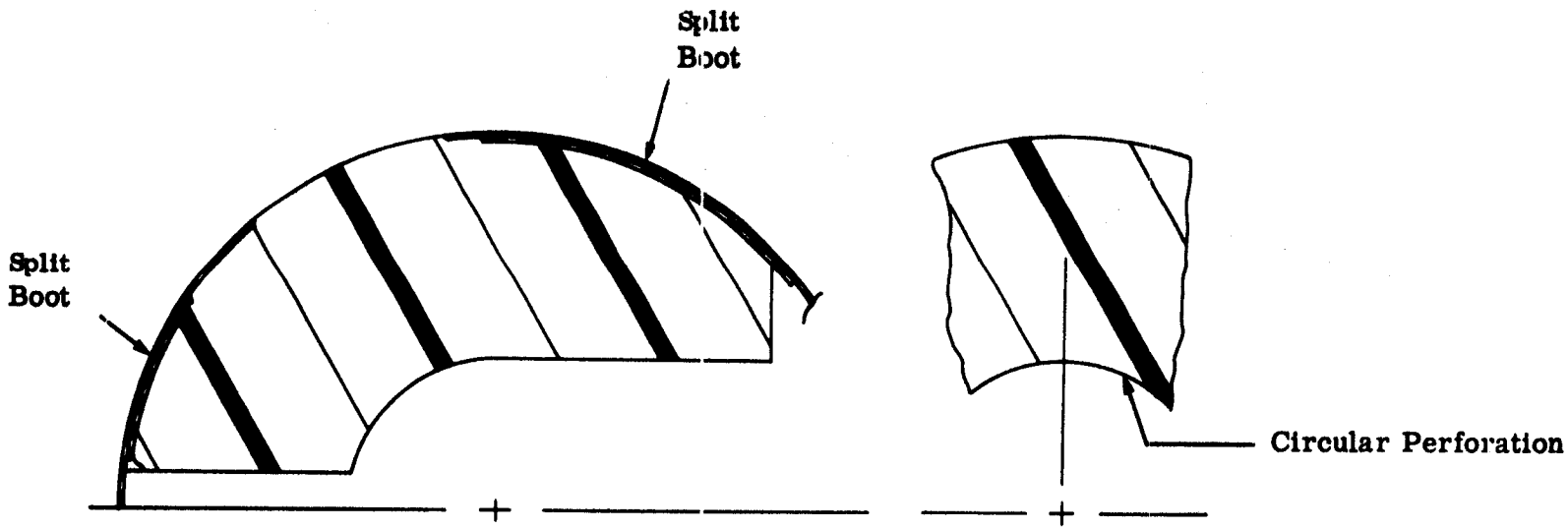

FIGURE B-4. DESIGN 4 – SPHERICAL CIRCULAR PERFORATE DESIGN

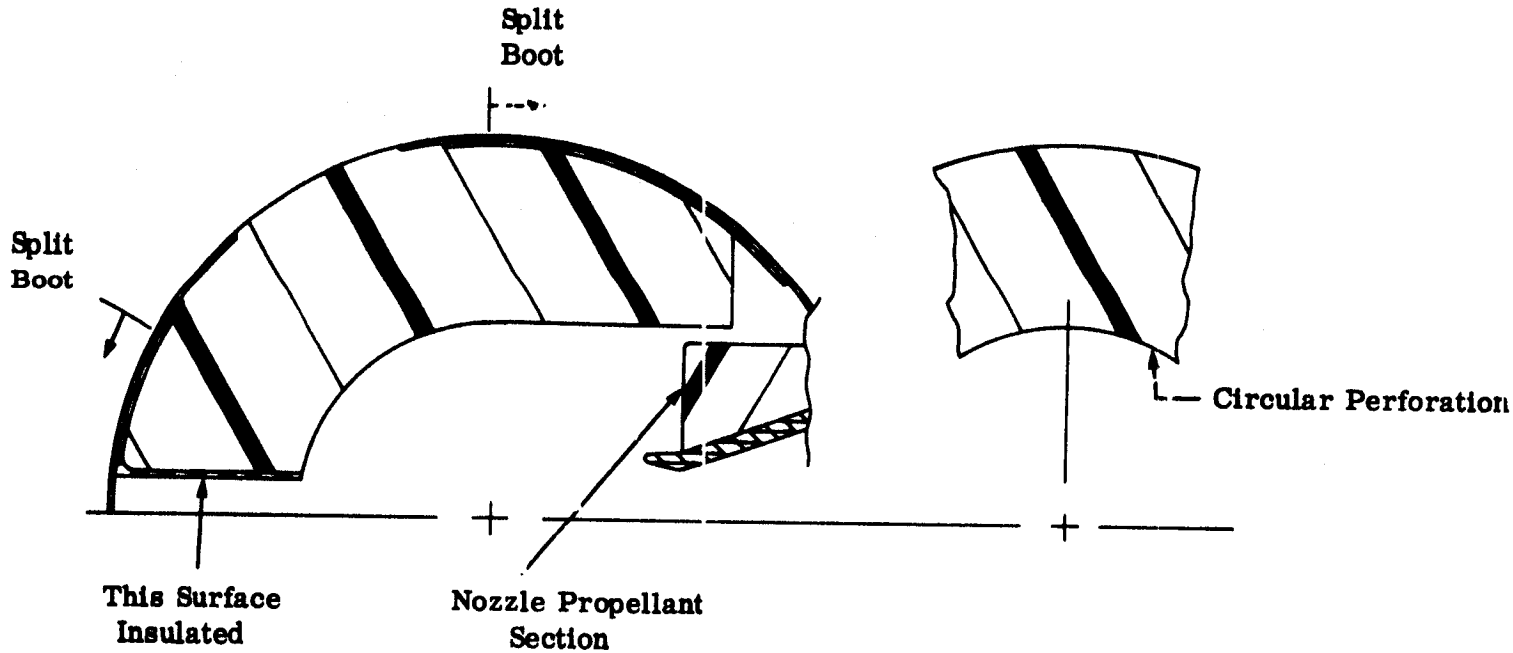

FIGURE B-5. DESIGN 5 – CIRCULAR PERFORATED SPHERE WITH PROPELLANT CAST ARCUND NOZZLE INSERT

perforate section. This decreases the ratio of maximum to minimum burning surface area. The other grain section is bonded to the nozzle insert (see Figure B-5) and burns on the outside and forward end.

The circular perforate grain section is manufactured in the conventional manner, and cast and cured inside the motor case. The other section, however, must be cast onto the nozzle insert and cured in a mold. The nozzle insert is then pressed and bonded into place in the aft closure. Following this, the aft closure is bolted into place.

6. Design 6—Conical Slotted Circular Perforated Spherical Design (See Figure B-6)

This design consists of a circular-perforated cylinder in the aft section of the grain and a spherical cap in the head end of the grain. The web fraction for this design is 0.65. The grain design incorporates a conical slot in the aft portion of the grain to improve the neutrality of the design. Asbestos-filled polyisoprene insulation extends from the aft portion of the grain approximately three-fourths of the way into the head end. A small stress-relief flap is present at the aft end of the grain.

This design is manufactured by bonding the insulation section in place, inserting the forward portion of the core, casting to the slot height, and then positioning the slot in place. The slot must be collapsible to facilitate loading and withdrawing. Following placement of the slot, casting continues and the motor is cured. The center cylindrical portion of the core is removed and the slot material either collapsed or melted out.

B. CYLINDRICAL CASE BONDED DESIGNS

1. Design 7—Conventional Star Cylinder (See Figure B-7)

This grain design has a six-point star interval perforation with a web fraction of 0.5. The internal perforation extends the full length of the motor case. The head end of the case is inhibited by asbestos-filled polyisoprene insulation on the 2/1 ellipse and through a short portion of the cylindrical section. This insulation is in the form of a split boot which extends the full length of the 2/1 ellipse. The aft end of the motor case is also insulated by a split boot assembly which extends approximately one-quarter of the distance to the forward end of the motor case.

The grain is manufactured in the conventional manner: bonding in insulation sections, lining, casting and curing with the core in place.

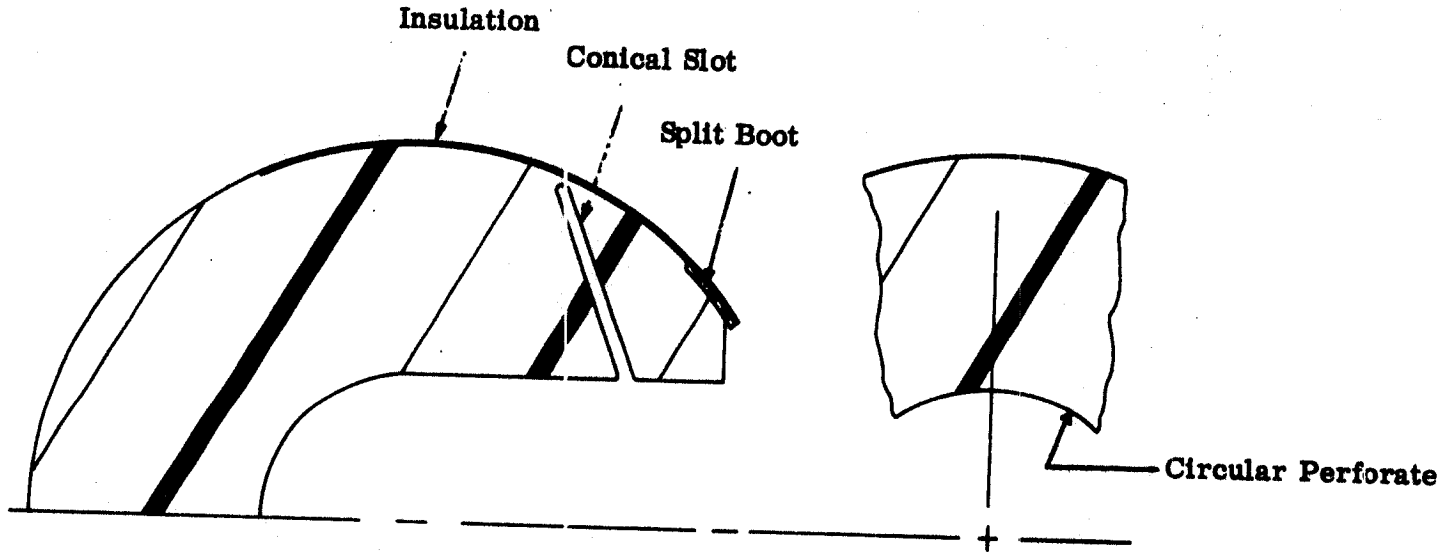

FIGURE B-6. DESIGN 6 — CONICAL SLOTTED CIRCULAR PERFORATED SPHERICAL DESIGN

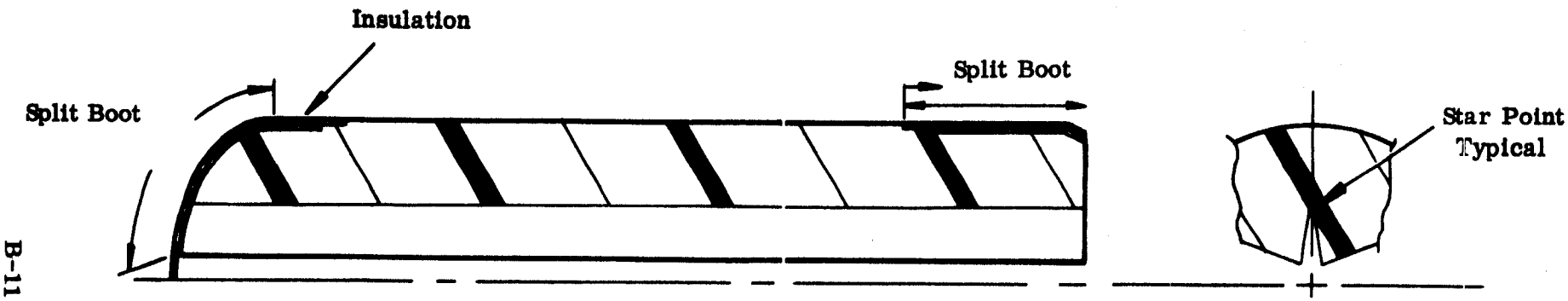

FIGURE B-7. DESIGN 7--CONVENTIONAL STAR CYLINDER

2. Design 8 — Inhibited Wedge Star (See Figure B-8)

This grain design has a six-point star internal perforation with the points extending to the motor case wall. The outside half of these star points are inhibited by asbestos-filled polyisoprene insulation. This technique provides circumferential stress relief while maintaining the same burning characteristics as the conventional star design. Insulation is provided on the 2/1 ellipse at the head end of the motor and in the aft section of the grain. No stress-relief flaps are provided.

The grain is manufactured by bonding the split insulation sections to the motor case, lining case, casting and curing the propellant.

3. Design 9 — Circular Perforate Cylinder (See Figure B-9)

This design has a circular internal perforation with a web fraction of 0.65. The forward portion of the cylindrical perforation terminates in an elliptical end. One radial slot is contained in the head end of the motor. The purpose of this slot is to reduce the grain stresses and enable the design to have a neutral burning characteristic. A short split boot of asbestos-filled polyisoprene insulation is used in the aft end of the motor to reduce grain stresses. Insulation is used in the area of the radial slot to protect the motor wall from combustion gases during motor operation.

The motor is manufactured by bonding in the insulation section, lining, casting and curing with the cylindrical core in place. The radial slots can be manufactured by using a collapsible core section or machining the grain after the core has been removed.

4. Design 10 — Double Web Star (See Figure B-10)

This design is typical of the double-web star designs although the star point is somewhat shorter than in most of these designs. The double web star gets its name from the fact that the star tip thickness is twice the thickness of the propellant web. In this design the web fraction is 0.27. The star has four points (this design is sometimes referred to as a wagon wheel design). Inside each star point is a phenolic support structure which eliminates sliver collapse at star point burnout, provides support for vibration, and eliminates slump during high temperature exposure. A short section of insulation is provided in the aft end of the case to protect the motor wall from the combustion gases during motor operation.

The motor is manufactured by bonding the phenolic supports and the motor case insulation in place, lining, casting and curing.

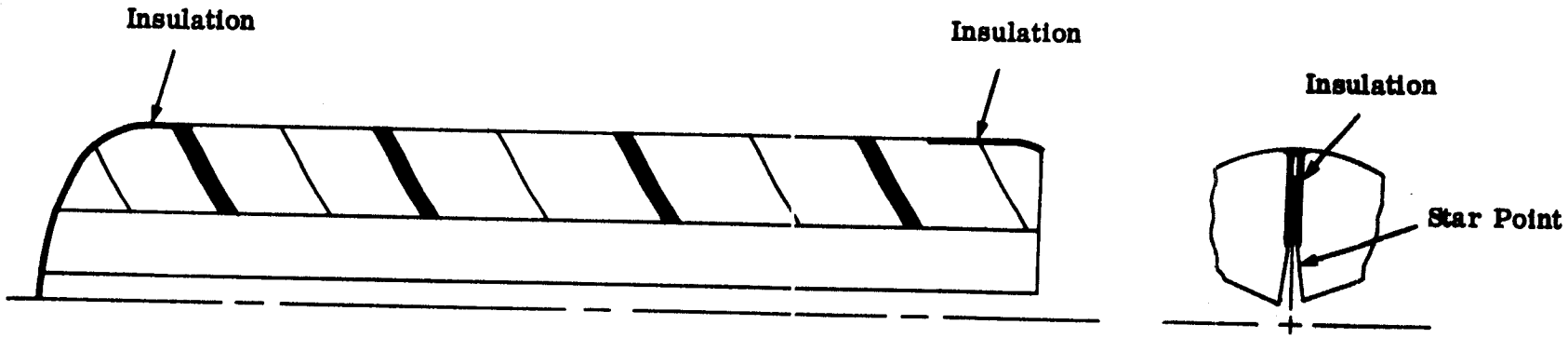

FIGURE B-8. DESIGN 8 — INHIBITED WEDGE STAR

E15-66-52

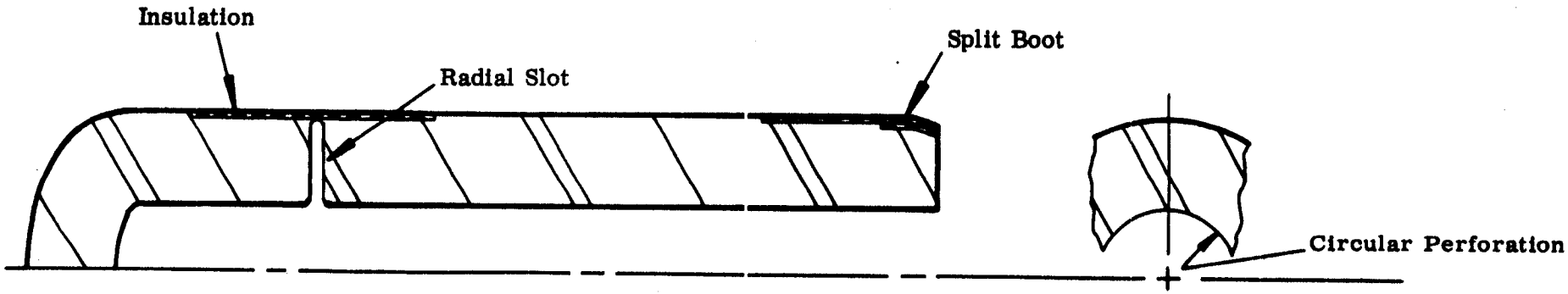

FIGURE B-9. DESIGN 9 — CIRCULAR PERFORATE CYLINDER

E15-66-53

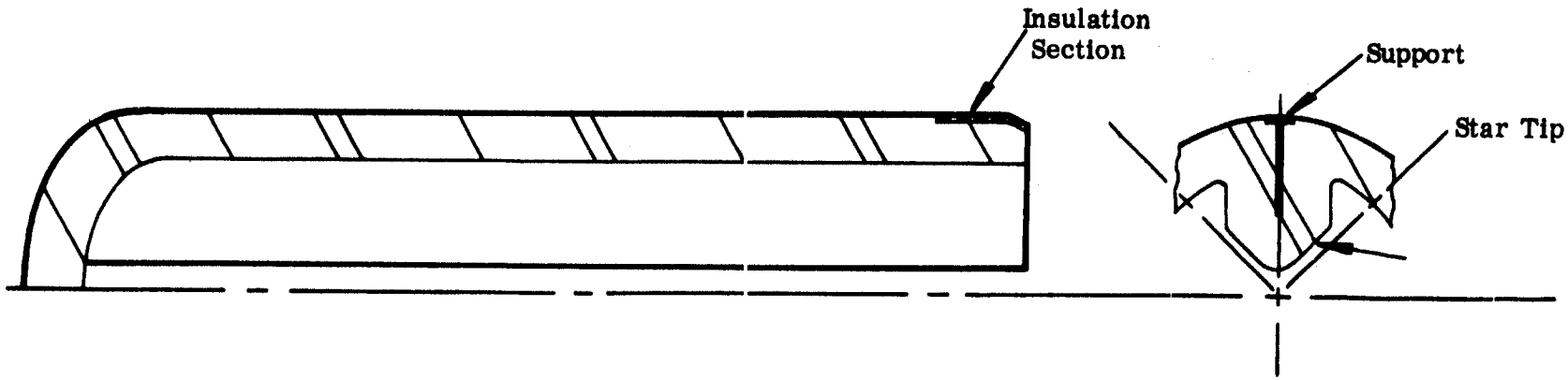

FIGURE B-10. DESIGN 10 — DOUBLE WEB STAR

5. Design 11 — Internally-Relieved End Burner (See Figure B-11)

This design unlike the other cylindrical designs discussed previously, uses a 2/1 length-to-diameter (L/D) motor case. This is because excessive burning results if a L/D of 3 is used. The design is rather unique in using an inhibited star perforation. This means that it has the stress concentration aspects of a star but burns as an end burner. The four-point star has a web fraction of only 0.18 (stress type web). The internal portion of the star is inhibited by a tapered insulation layer. This insulation is thinner at the aft end of the grain and thickest at the forward end of the grain. The motor wall insulation tapers in the reverse direction, being thickest at the aft end of the case and thinnest at the forward end; it continues through the 2/1 ellipse in the head end.

The grain is manufactured by bonding the case insulation in place and lining. The perforation insulation can be poured over the core and lined. The core can then be inserted and the motor cast and cured.

C. CYLINDRICAL FREE STANDING DESIGNS

1. Design 12— Unsupported Internal-External Burning Grain (See Figure B-12)

This grain is a free-standing cylinder of propellant. It is inhibited on the forward and aft grain surfaces to improve neutrality and to prevent burning under the supports. The unit is supported by a phenolic support at the head and aft ends. A sponge rubber spacer in the aft end of the motor provides freedom of expansion longitudinally. Radial support is obtained by using sponge rubber spacers about the grain. The spacers allow freedom of expansion in the radial direction. Since gas flow is allowed to take place on the outside of the grain, phenolic insulation is used to insulate the motor case. A rigid insulation is used here because it has superior resistance to erosion.

This grain is manufactured external to the motor case. The grain is cast and cured in a mold, final-machined,and the insulation sections bonded in place. The forward grain support is bonded into the insulated motor case and the grain and sponge rubber supports inserted in place. The sponge rubber spacer is then placed on the aft end of the grain and the aft closure with the aft phenolic support in place is bolted into position.

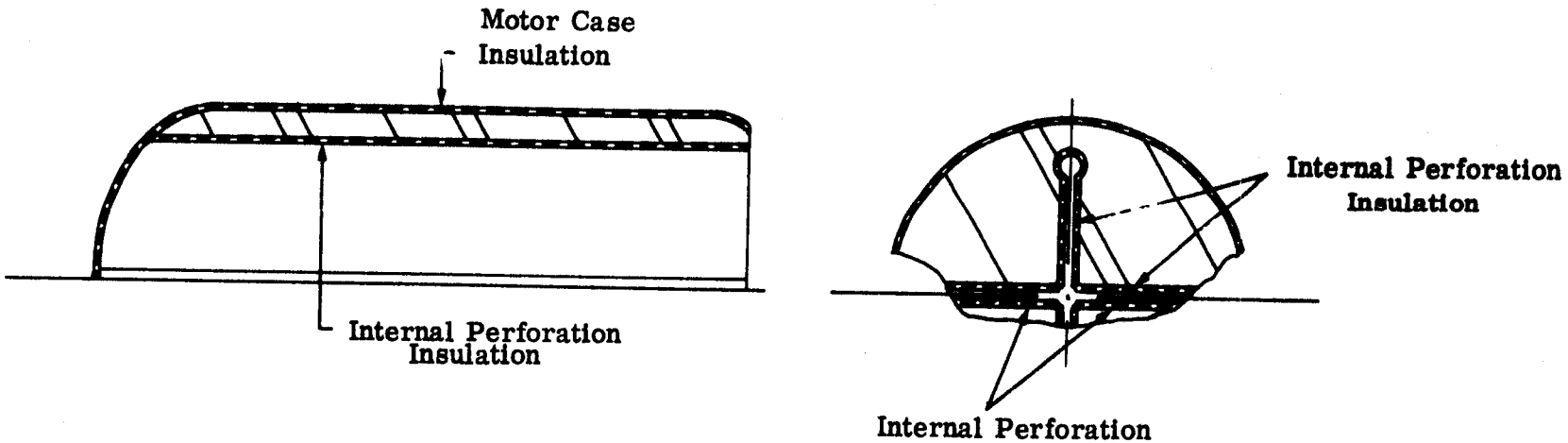

FIGURE B-11. DESIGN 11 — INTERNALLY RELIEVED END BURNER

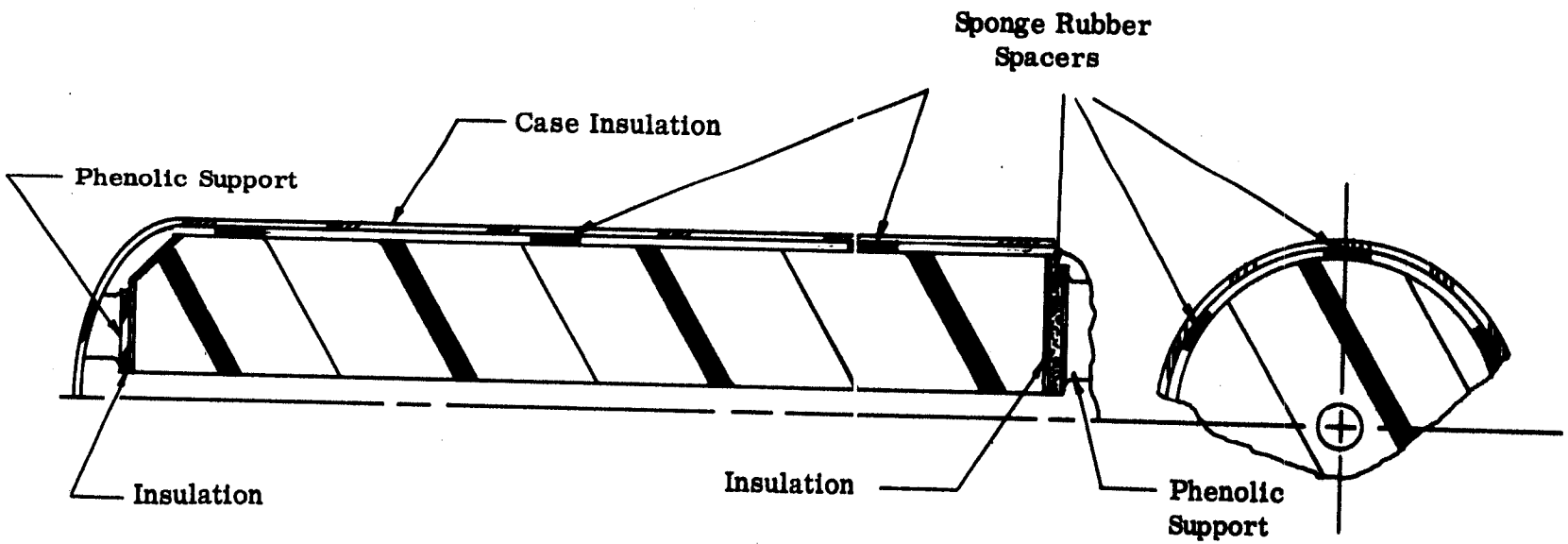

FIGURE B-12. DESIGN 12—UNSUPPORTED INTERNAL-EXTERNAL BURNING GRAIN

2. Design 13 — Supported Internal-External Burning Grain (See Figure B-13)

This design is very similar to the unsupported design discussed above; however, it has an internal phenolic support. This grain has no inhibited surfaces. Support for the grain is provided by the internal phenolic tube. Radial location and support for the grain is provided by 12 thin radial strips which extend outward from the grain support to the case insulation. The grain internal support is pinned in place to the aft closure to provide longitudinal location. Since gas flow takes place on the outside of the grain, the motor case is insulated.

This grain is also manufactured in a mold external to the motor case. The propellant is cast into the mold to the proper weight, after which the internal support is plunged and the grain cured. After cure and disassembly of the mold, the support tube is attached to the aft closure and the grain loaded into the motor case.

3. Design 14 — Multiple Tube Design (See Figure B-14)

This grain design consists of seven internal-external burning, uninhibited free-standing cylinders. They are held in place by a phenolic support in the aft end of the motor and by internal steel wires. The forward end is held in place by a phenolic support. The motor case is insulated with an appropriate phenolic insulation throughout its entire length.

These grains are cast and cured in a mold placed in position on the wires extending from the aft phenolic support and loaded into place inside the insulated motor case.

4. Design 15 — Slab Design (See Figure B-15)

This design consists of three external burning, uninhibited slabs (see Figure B-15). Each slab is supported internally by a phenolic sheet. Aft and forward structural stability is provided by phenolic supports. These supports have slots cut into them to accept the phenolic sheet supporting the grain. Since the grain is free to burn on all surfaces, the inside of the case is insulated by a phenolic insulation in much the same manner as discussed for the other free-standing designs.

This grain is manufactured by casting and curing the propellant on the phenolic sheet, trimming to the final size, and loading into the motor against the forward support. The aft closure to which the aft support is attached is then mated to the motor case.

E15-66-37

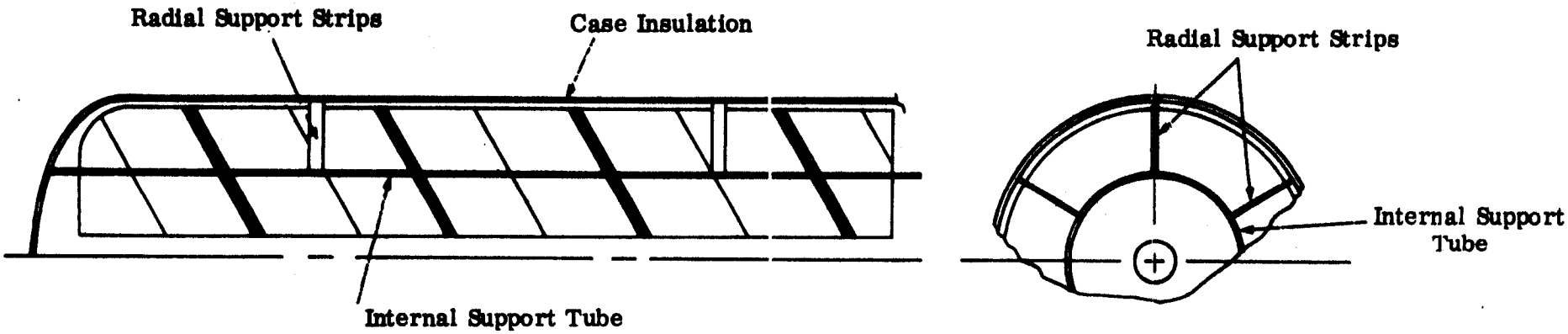

FIGURE B-13. DESIGN 13 — SUPPORTED INTERNAL-EXTERNAL BURNING GRAIN

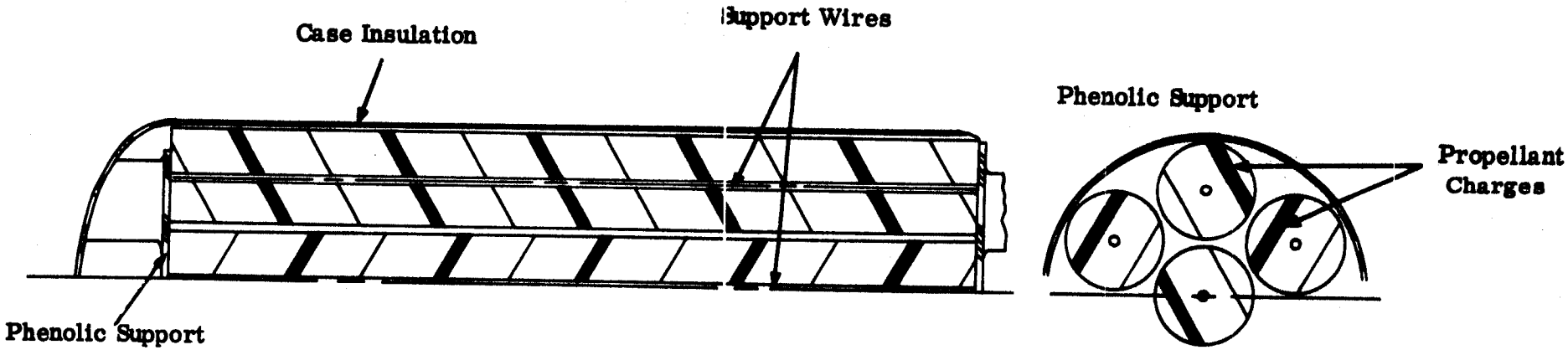

FIGURE B-14. DESIGN 14—MULTIPLE TUBE DESIGN

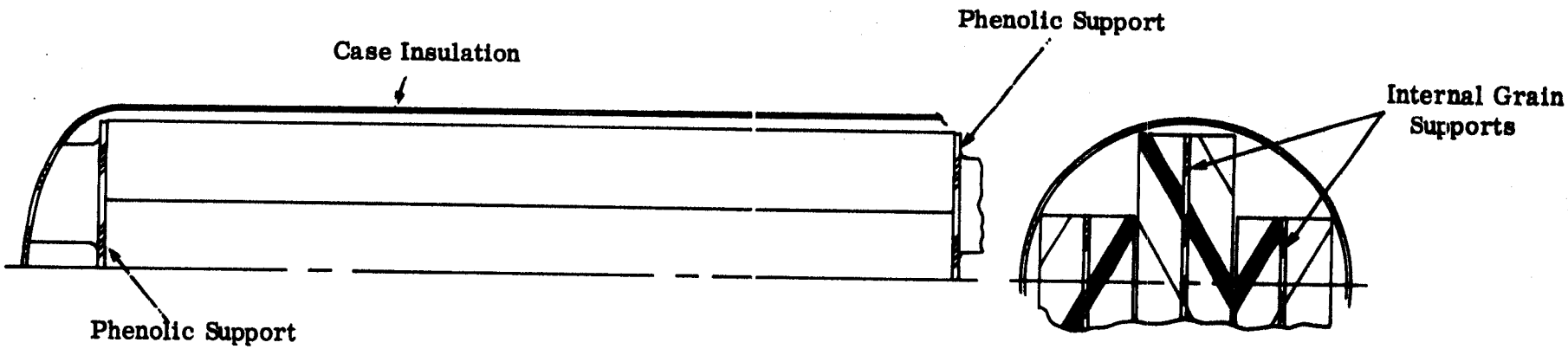

FIGURE B-15. DESIGN 15—SLAB DESIGN

5. Design 16—Cartridge Loaded Circular Perforate Grain (See Figure B-16)

This grain design is not actually free-standing. However, since it is not bonded to the motor case it is included within this group. This design consists of a circular perforated grain with a web fraction of 0.64. This grain is housed in a phenolic cartridge and held in place in the motor case by a grain support or by the motor case phenolic insulation. This design could be made free-standing by choosing a support material with the same thermal expansion properties as the propellant.

The grain is cast and cured in the phenolic cartridge tube which serves as support and inhibitor for the grain. The cartridge then is loaded into the motor case.

6. Design 17—Rod and Shell Design (See Figure B-17)

This grain design is a combination of the case-bonded or case-supported design and the free-standing design. It consists of a circular perforated shell grain with a web fraction of 0.43 and a rod grain. The shell grain is case-bonded in the motor case. The forward portion of the case, the 2/1 ellipse, and the aft section are insulated by a layer of asbestos-filled polyisoprene insulation. The rod grain has the same web thickness, but uses an internal phenolic rod as a support. This grain is essentially free-standing. The rod grain is held in place by bonding it to the head end of the motor case or by passing the forward portion of the rod through the head end case opening and using an external mechanical attachment.

This design is manufactured in two separate steps. The shell grain is manufactured by casting and curing in place. The rod grain is made by casting into a suitable mold containing the support after which it is loaded into the motor case and fixed in position.

D. FREE-STANDING END BURNING GRAINS

1. Design 18—Externally Relieved End Burner (See Figure B-18)

This design has a motor case length-to-diameter ratio of 2/1 used because of the excessive burn time that would result from a greater L/D ratio. The motor case insulation tapers from a maximum thickness at the aft end of the grain to a thin insulation section at the head end of the case. This insulation section is split the entire cylindrical length of the case. In effect, this means that the grain is free standing, being supported only at the head end.

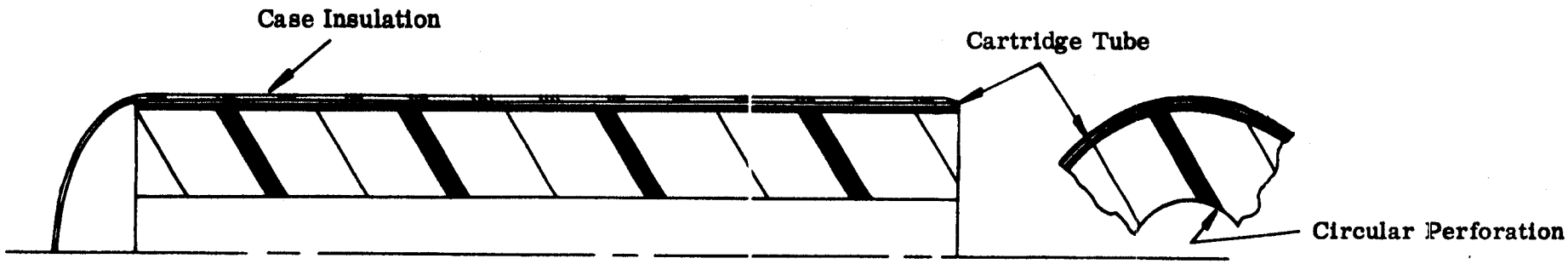

FIGURE B-16. DESIGN 16 —CARTRIDGE-LOADED CIRCULAR PERFORATE GRAIN

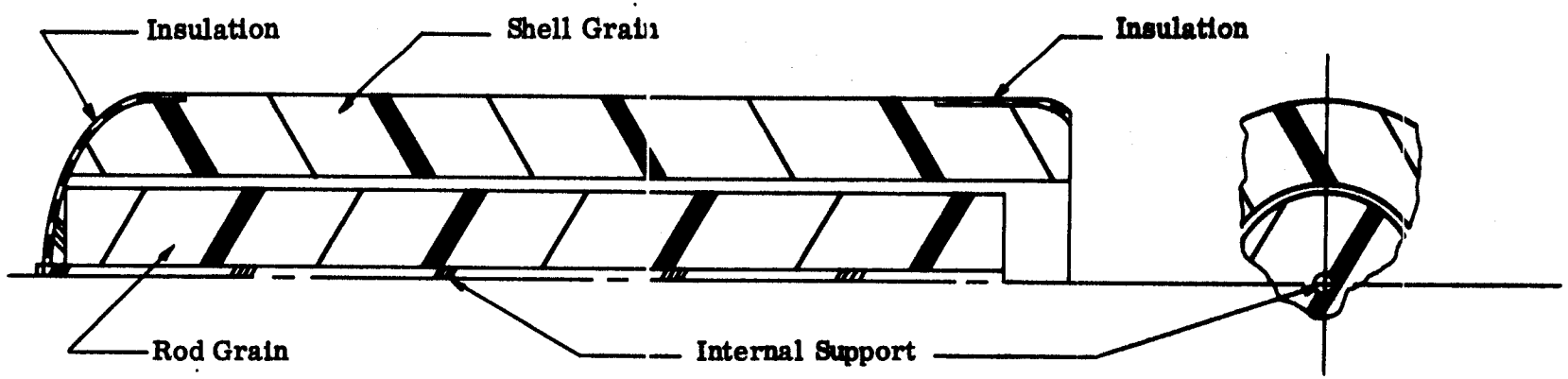

FIGURE B-17. DESIGN 17--ROD AND SHELL DESIGN

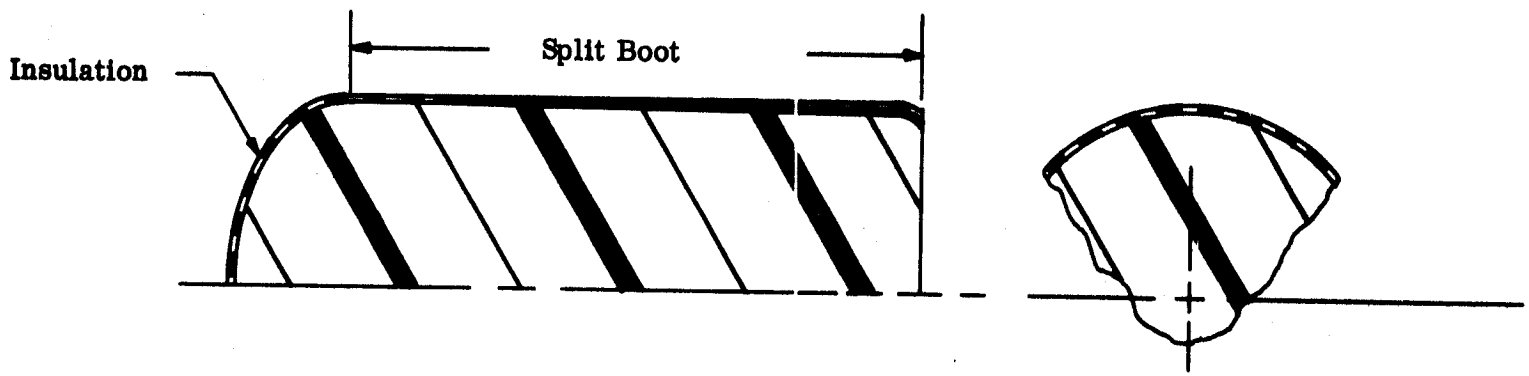

FIGURE B-18. DESIGN 18—EXTERNALLY-RELIEVED END BURNER

This grain is manufactured by bonding three split-boot insulation sections into the case, lining, casting and curing.

2. Design 19—Internally-Supported Externally-Relieved End Burners (See Figure B-19)

This design is also based on a motor case length-to-diameter ratio of 2/1. The design is characterized by a tapered, split-boot insulation section as in the design discussed above. However, this design has a phenolic internal support in the form of a cruciform. The phenolic support is mechanically attached to the head end of the motor case to carry the acceleration loads which otherwise would be transmitted to the grain structure.

This design is manufactured by bonding in the insulation section and the phenolic support, lining, casting and curing.

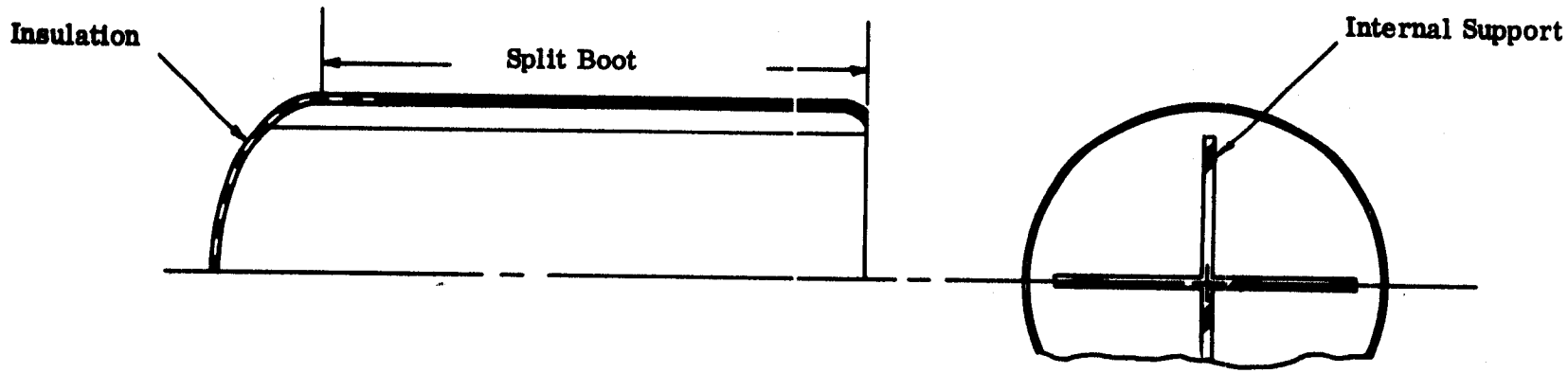

FIGURE B-19. DESIGN 19—INTERNALLY-SUPPORTED EXTERNALLY-RELIEVED END BURNER

APPENDIX C

DESIGN EVALUATION AND RATING - INITIAL 19 DESIGNS

APPENDIX C

DESIGN EVALUATION AND RATING - INITIAL 19 DESIGNS

The purpose of this phase of the program was to perform a preliminary analysis of the initial 19 grain designs to determine their capability for reliable performance after sterilization by dry heat. For the purpose of this study, heat sterilization was defined to be: bringing the temperature of the entire motor case assembly to 295 $\pm$ 2°F and holding for 36 hours. The final motor design must perform reliably after being subjected to three such cycles.

The final designs selected (one free-standing and one case-bonded) must also meet the design criteria contained in Article 1, Statement of Work, California Institute of Technology, Contract No. 951450, entitled "Design Study of Heat Sterilizable Solid Rocket Motors for Space Application."

A. BASES FOR EVALUATION

Preliminary calculations were performed on all designs to allow rapid screening of unsuitable designs. After the preliminary calculations were completed, each of the designs was rated on how well they met the following criteria. Each criterion has a numerical index of 1 to 4 and a weighting factor.

Design Criteria	Index	Weight	Possible Points
1. Maximum mass fraction	1 to 4	2	8
2. Freedom from areas which introduces stress concentrations	1 to 4	5	20
3. Freedom from differential expansion during sterilization	1 to 4	4	16
4. Time to reach sterilization temperature	1 to 4	2	8
5. Total area exposed	1 to 4	2	8
6. Design experience	1 to 4	3	12
7. Design complexity	1 to 4	5	20
8. Effects of vibration, spinning, etc.	1 to 4	2	8
9. Neutrality of motor thrust-time program	1 to 4	1	4
10. Low temperature capability (-40°F)	1 to 4	3	12
11. Effect of shortening L/D	1 to 4	2	8
		TOTAL POSSIBLE POINTS	124

These design criteria, together with the results of each individual weighting, are discussed below.

B. MASS FRACTION DETERMINATION

Mass fraction is a critical factor in rocket motor design. The higher the mass fraction, the heavier the payload weight for fixed-launch weight. When the motor is used for retrograde propulsion, or deflection of a landing vehicle in a deep space mission, any weight saving in the propulsion system can be applied almost entirely to an increase in the weight or the number of scientific experiments.

The first step in the calculation of motor mass fraction was to determine the volumetric loading density for each motor design. This was performed by laying out each grain design and calculating its volume of propellant. The spherical motors were laid out with an internal diameter of ten inches and the cylindrical motors were laid out with an internal diameter of six inches. The cylindrical motors were assumed to have 2:1 ellipses closing both ends. All the cylindrical motors, with the exception of the end-burning designs, were based on a total motor length of 18 inches (L/D = 3:1). The end-burning designs used a motor length of 12 inches (L/D = 2:1). The 3:1 L/D ratio for the cylindrical designs was used because it was determined early in the study that for a given volumetric loading density and motor operating pressure case, weight varied inversely with the L/D ratio. This can be seen in Figure C-1. The volumetric loading density is based on the total volume inside the motor case. For the spherical designs, it is based on the total volume in the motor cavity. In the cylindrical motor, it is based on the total volume inside the cylindrical case and the 2/1 elliptical ends.

C. CALCULATION OF CASE WEIGHT

The volumetric loading density was used to calculate the case diameter and weight required for 100 pounds of propellant by the following equations:

$$D_C = \left[\frac{6}{\pi} \frac{W_{prop}}{VLD\ \rho prop\ K_3} \right]^{1/3}$$

Where D_C = Case diameter, in.
W_{prop} = Propellant weight, lbs
VLD = Volumetric loading density,
$\rho prop$ = Density of propellant/lb/in.^{3}

and,

$$K_3 = 1.5 \left[L/D - .274\ K_4 \right]$$

K_4 = 1.2165 for spherical motors

and

K_4 = 1.0 for all other motors.

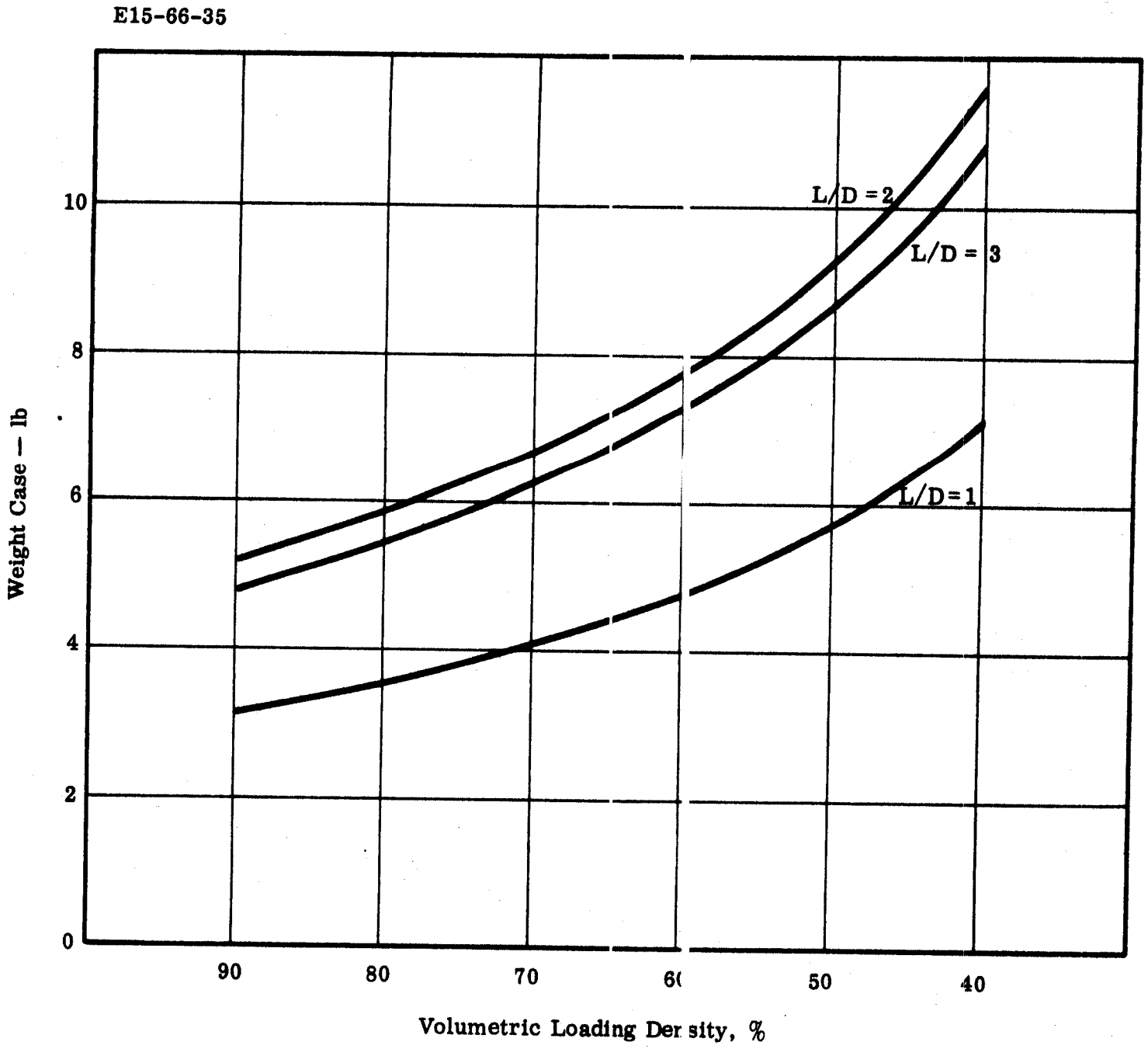

FIGURE C-1. MOTOR WEIGHT VERSUS VOLUMETRIC LOADING DENSITY
HEAT STERILIZABLE MOTOR DESIGN

The case weight is given by:

$$W_C = 1.916 \left[D_c^3 \; P_C \; SF \; \left(\frac{\rho_c}{\sigma_c}\right)\right] \left[L/D + .1095 \; K_2\right]$$

where:

W_C = weight of case, lbs
P_C = Chamber pressure, psi
SF = Safety factor
ρ_C = Density of case material, $lb/in.^3$
σ_C = Tensile yield strength of case, psi
L/D = Length to diameter ratio of case
K_2 = constant = 1 for motors of L/D of 1 and -4.566 for motors with L/D's not equal to 1.

Figures C1 and C2 show the weights and case diameters as a function of volumetric loading density for the following conditions:

W_P = 100 lbs
ρ_{Prop} = 0.0595 $lb/in.^3$
P_C = 600 psi
SF = 1.4 assumed

The case material was specified to be 6 Al 4 V titanium alloy which has the following properties:[1,2]

ρ_C = 0.16 $lb/in.^3$
σ_C = 155,000 psi

Titanium 6 Al 4V was used for purpose of design calculations because it has a high strength-to-density ratio and is a current state-of-the-art case material.

The above equations are empirical and were developed for use in Thiokol Computer Program No. 40192 entitled "Mission Fuel Prerequisite." Weights calculated with these equations and actual motor weights from detailed design calculations agree within a few percent.[3]

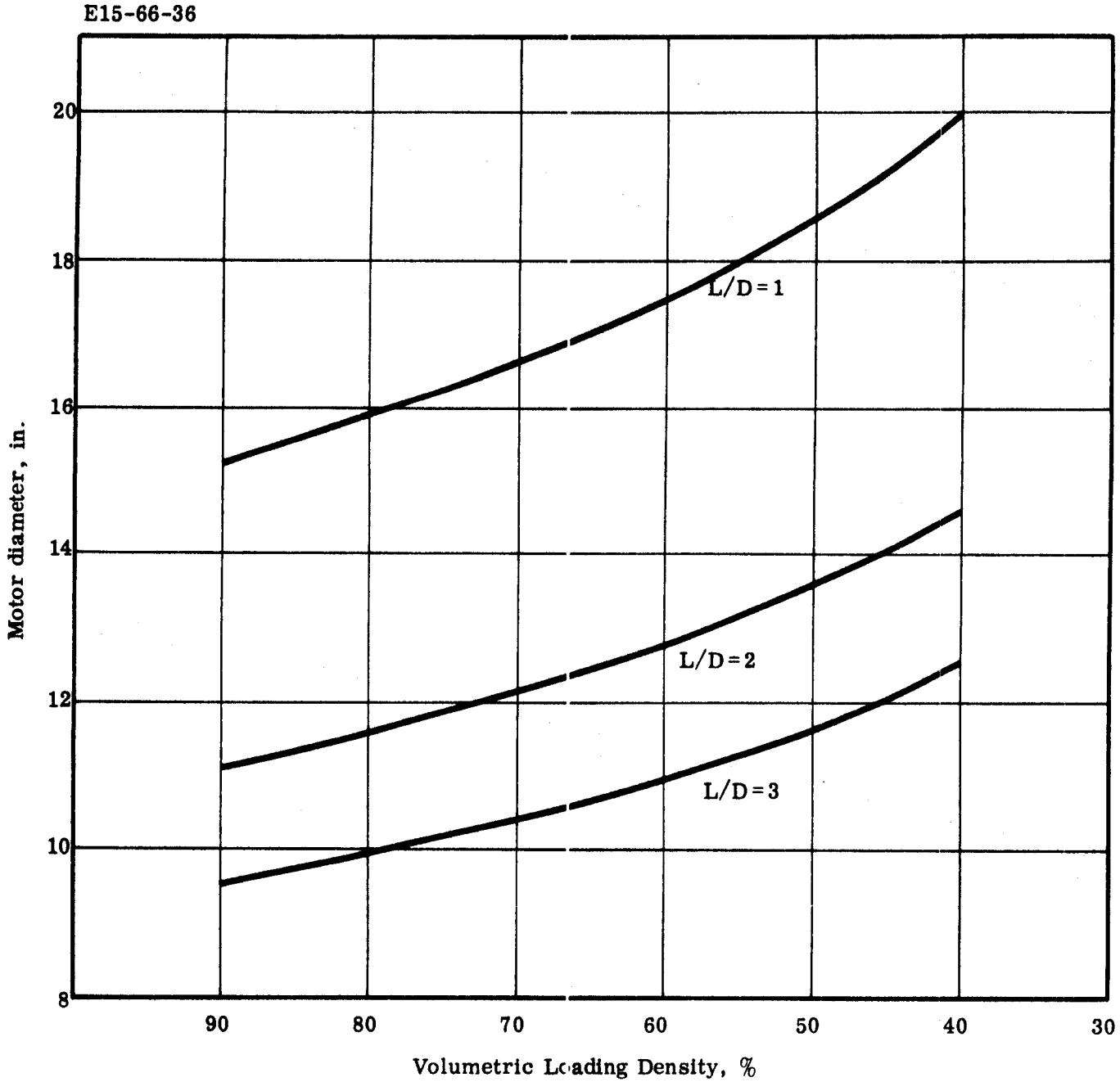

FIGURE C-2. MOTOR DIAMETER VERSUS VOLUMETRIC LOADING DENSITY
HEAT STERILIZABLE MOTOR DESIGN

D. CALCULATION OF NOZZLE WEIGHTS

The nozzle weight was also calculated from equations derived for this program. The equations used were:[3]

$$W_n = 0.469\, L_{n_{53}}\, (D_f + 0.151) -$$

$$0.0183\, (\Delta L_n) \left[0.75\, D_e + 0.75\, D_{e_{53}} + .1874\right]$$

Where:

W_n = Nozzle Weight, lbs
$W_{n_{53}}$ = Nozzle weight with an expansion ratio of 53/1, lbs
$\Delta W_n = W_{n_{53}} - W_n$, lbs
$L_{n_{53}}$ = Nozzle length for an expansion ratio of 53/1, in.
$\Delta L_n = L_{n53}$ - Actual nozzle length, in.
D_f = Throat Diameter, in.
D_e = Exit diameter, in.
$D_{e_{53}}$ = Exit Diameter for an expansion ratio of 53/1, in.

and

$$L_{n_{53}} = 1.375\, (D_{e_{53}} - D_t)$$

$$\Delta L_n = 1.375\, (D_e - D_{e_{53}})$$

E. MISCELLANEOUS WEIGHTS

The PYROGEN weight is given by the equation:[3]

$$W_{py} = 0.333\, A_t$$

W_{py} = PYROGEN wt, lbs
A_t = Throat Area, $in.^2$

The insulation weights were calculated from the original layout drawings and scaled up or down by the square of the case diameter.

The attachment brackets were assumed to weigh one pound.

F. MASS FRACTION OPTIMIZATION

Following these calculations the individual component weights were scaled up and down over the range from 300 to 1500 psi. The following approaches were used to scale these designs:

Propellant Weight - Held constant at 100 lbs
Case Weight - Directly proportional to P_c
Nozzle Weight - Directly proportional to A_t
Insulation Weight - Directly proportional to burn time
PYROGEN Weight - Directly proportional to A_t
Attachment Brackets - Constant at 1.0 lb

In addition, because of physical size, the following limitations were imposed.

Minimum PYROGEN Weight = 0.30 lb
Minimum Nozzle Weight = 1.50 lbs

G. RESULTS AND RATINGS

The results of these calculations are shown in Figures C3 and C4 which give the motor mass fractions for the case-bonded and free-standing design classes.

1. Maximum Mass Fractions

The motor mass fractions were rated on the following basis:

CASE BONDED DESIGNS

Maximum Mass Fraction Range	Index
0.81	0
0.81 & 0.83	1
0.83 & 0.85	2
0.85 & 0.87	3
0.87	4

FREE STANDING DESIGNS

Maximum Mass Fraction Range	Index
0.70	0
0.70 & 0.73	1
0.73 & 0.75	2
0.75 & 0.78	3
0.78	4

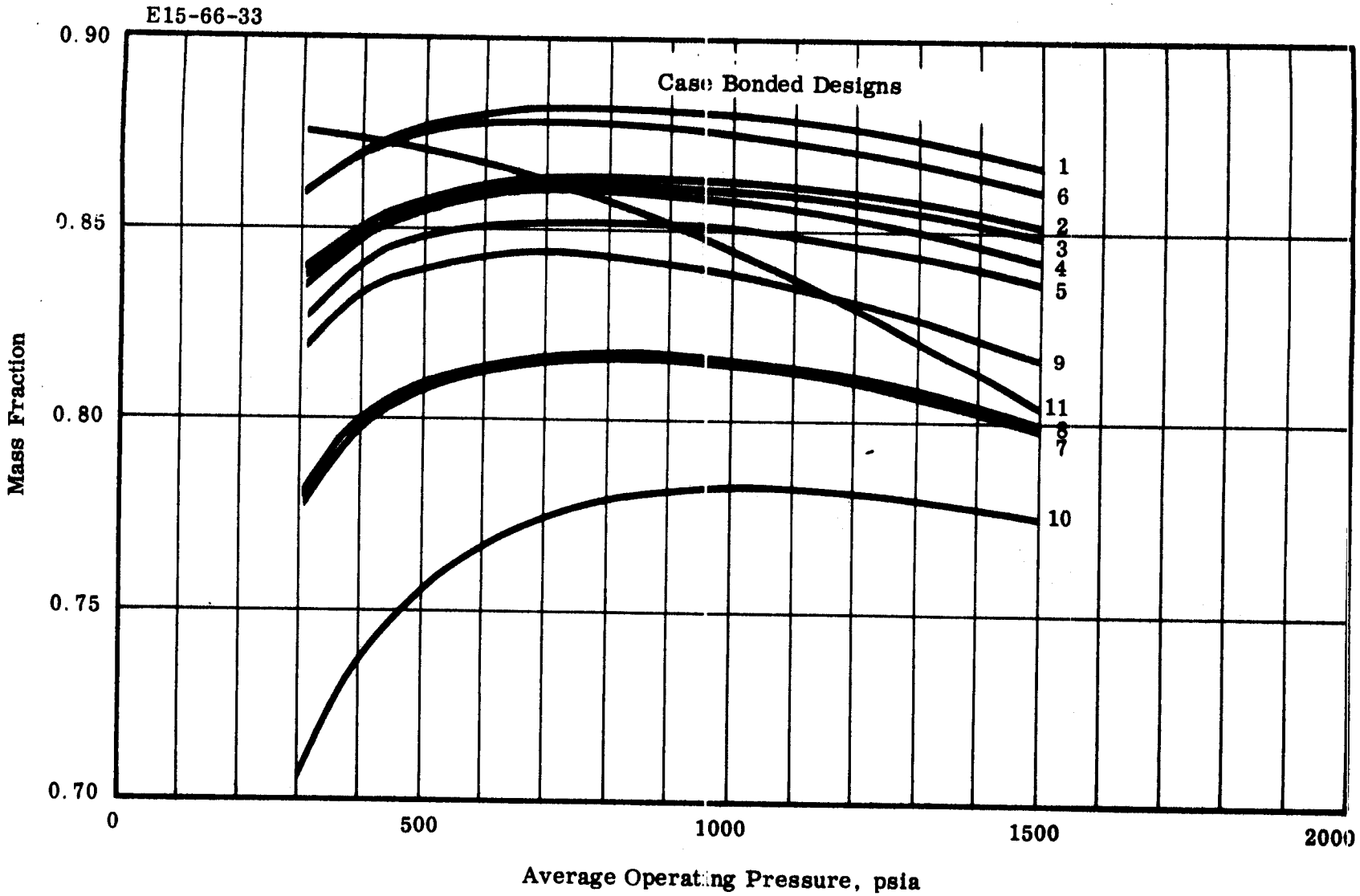

FIGURE C-3. MOTOR PRESSURE OPTIMIZATION HEAT STERILIZABLE MOTOR DESIGN

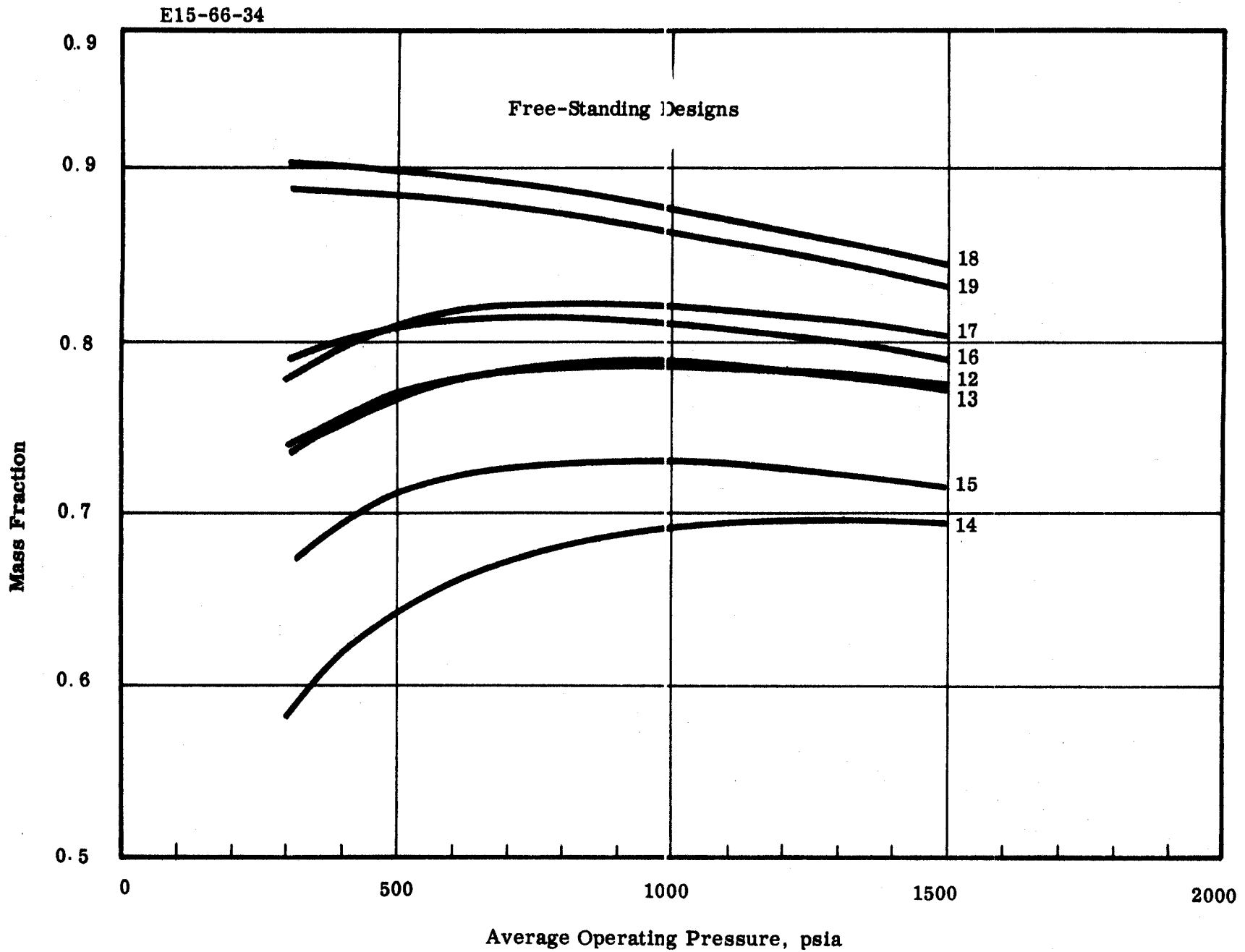

FIGURE C-4. MOTOR PRESSURE OPTIMIZATION HEAT STERILIZABLE MOTOR DESIGN

The mass fractions of the designs and their respective indices are given in figures appearing at the end of this section, (Figures C-5 through C-23).

2. Areas of Stress Concentration

Repeated exposure to sterilization temperatures is the most severe environment to which any of the candidate motor designs could be subjected. Nevertheless, in designing, one must also consider the effects of prolonged storage and operational loads due to internal pressurization and booster launch. Since, as has been discussed before (see Section II-D), propellant structural capability following sterilization is at a lower level than before exposure to high temperature, the presence of areas of stress concentration must be minimized during the preliminary design phase if reliable operation following sterilization is to be achieved. Each of the candidate designs was examined in detail for areas of stress concentration associated with star and irregular perforate geometries. During this preliminary phase, the design rating was obtained by comparing the designs in each group and evaluating them based upon engineering judgment and past experience. A summary of these ratings is given in Table C-I.

3. Freedom from Differential Expansion

The rating of each design with regard to freedom from the effects of differential expansion was based principally on engineering judgment. Differential expansion between the grain and case and between the grain and supports was a major problem. This is discussed in Appendix A. Split boots and grain support mechanisms were items considered in rating the individual designs. The number and length of split boots in each design is an important factor because the inclusion of a split boot allows both radial and longitudinal expansion of the propellant grain. The longer the split boot with regard to the grain length, the more freedom there is to expand. This is true for both the normal stress-relief boot and the split star section relief. The mechanism of support also greatly influences differential expansion. If the grain is completely unsupported or partially supported by sponge rubber blocks, the grain is free to expand in all directions. If the grain has an internal support, it is more sensitive to the effects of differential expansion.

The designs and their ratings are given below and in Table C-I.

Design	Rating	Design	Rating
1	2	10	2
2	3	11	2
3	3	12	4
4	3	13	3
5	3	14	4
6	2	15	3
7	2	16	2
8	3	17	3
9	2	18	3.5
		19	3

4. Time to Reach Sterilization Temperature

The time required to reach sterilization temperature is an important item. Because propellant is a good thermal insulator, long heating times are not uncommon. In fact, it is desirable to have the entire sterilized payload and associated equipment reach sterilization temperatures as quickly as possible in order to avoid damage to components such as electronic parts, heat shield materials, potting compounds, and insulations. Because solid propellants are good insulating materials and the motors are likely to be located within the payload (possibly even buried in the midst of the electronic components and heat shield), the rocket motor may be the item which determines the sterilization exposure time. Thus, the time required to heat the motor to sterilization temperatures is extremely important.

The time required for the inside of the propellant to reach the sterilization temperature of approximately 293°F from an initial temperature of 72°F was calculated as outlined below.

The time, t_a, for the inside surface temperature of a cylinder to begin to rise after a suddenly applied outside increase in temperature is given by the equation:[4]

$$t_a = \frac{b^2}{30K} \left(\frac{2 \rightarrow 3 \quad -3 \rightarrow 2 \quad + \quad 1}{\rightarrow 3} \right)$$

where t_a = time required for heat to reach the inner cylinder wall from a suddenly applied increase in external surface temperature, hrs.

$\lambda = \frac{b}{a}$ Where b = outside radius, ft.
a = inside radius, ft.
K = thermal diffusivity of the propellant, ft^2/hr.

defining the quantity $\eta_a^2 = \frac{1-3\lambda^2+2\lambda^3}{30\lambda^3}$ equation 2-14

Then $t_a = \frac{b^2 \eta^2}{K}$

The temperature at the inner radius as a function of time is given by the equation:

$$T_a = T_o\left[1 - e^{-\gamma(\bar{\eta}^2 - 1)}\right] \qquad \text{equation 2-16}$$

where

T_a = the difference between the initial temperature at the inner radius at time t_a and that at time t, °F

T_o = the differential driving temperature; i.e., the suddenly-applied outside temperature minus the initial temperature. °F.

$$\gamma = \frac{[3\lambda+1][2\lambda+1]}{3\lambda[5\lambda+11]}$$

and $\bar{\eta}^2 = \frac{t\,K}{\eta_a^2\, b^2}$

Rearranging

$$t = \bar{\eta}^2 \frac{\eta_a^2\, b^2}{K}$$

and the total time required to heat the motor to temperature is

$$t_{tot} = t + t_a = \frac{b^2\, \eta_a^2}{K} + \frac{\bar{\eta}^2\, \eta\, a^2\, b^2}{K}$$

The values used for the temperature T_a and T_o in this calculation are:

T_a = 293°F -72°F) = 221°F

T_o = (312°F - 72°F) = 240°F

An attempt was made to allow for the thermal lag of air gaps and insulation present by making the following adjustments to the radius a or b:

Insulation on the outside was allowed for by adding an extra thickness of propellant ΔX_p which was equal to:

$$\Delta X_p = \Delta X_{ln} \frac{K_p}{K_{in}}$$

ΔX_p = thickness of propellant ft.
ΔX_{in} = Thickness of Insulation ft.
K_p = thermal diffusivity of propellant, $ft^2/in.$
K_{in} = Thermal diffusivity of insulation, $ft^2/in.$

Where the insulation was on the inside of the grain, the value ΔX_p was subtracted from a, the inner grain radius.

When air gaps were present an extra inch was added to each radius b or a to allow for the thermal lag caused by the gap.

In the case of star points, the inner radius was taken to be roughly halfway between the star point to star valley. Note that, although this method of analysis assumes a suddenly applied increase in external surface temperature and does not consider end effects, it does determine relative heating times; in any case, with the exception of the spherical designs, end effects are probably negligible.

The results of these heat transfer calculations are shown at the end of this section.

The time to reach sterilization temperature was rated as follows:

Time to Reach Temperatures, Hrs.	Index
$\leq$ 10	4
$>$ 10 & $\leq$ 20	3
$<$ 20 & $\leq$ 30	2
$>$ 30 & $\leq$ 40	1
$>$ 40	0

5. Surface Area Exposed

This item was rated on the basis of the total surface area exposed. By rating the designs on the basis of total exposed area, an allowance can be made for the effects of surface degradation. The surface will be degraded to some effect by the sterilization of the propellant grain. By rating on the basis of exposed area, an indication of the percent of total propellant degraded is obtained. The surface area was calculated for each design and rated according to the following table.

Surface Area, $in.^2$	Index
≤ 300	4
> 300 & ≤ 600	3
> 600 & ≤ 1000	2
> 1000 & ≤ 1500	1
> 1500	0

6. Design Experience

Design experience was rated upon the experience of the solid propellant industry with the design types as well as Thiokol's experience. The design comments and ratings are summarized below:

Design	Comments	Rating
1.	Many in use; e.g. TEM-360, -364, -442	4
2.	Many in use; e.g. TEM-360, -364, -442	4
3.	Feasible, but not demonstrated in sphere	2
4.	Many similar types demonstrated TEM-364, -364, -442	3.5
5.	Similar types demonstrated, but not with propellant on nozzle TX-174, TX-175, PIA etc.	3

Design	Comments	Rating
6.	Similar types demonstrated in short L/D cylinders:	
	TX-174, TX-175, etc	3
7.	Many in use.	4
8.	Few of the inhibited slot types in use:	
	LPC MPO 532, Rocket Mtr. MK 47, Mod O	2
9.	Many demonstrated:	4
	FW, 3 TE-344, SynCom Apogee Kick, etc.	
10.	Many demonstrated,but without internal supports:	3
	TEM-380, -421, -424, etc.	
11.	Prototypes demonstrated	2
12.	Many demonstrated, but without high mass fraction.	
	Typical of JATO Units	4
13.	Demonstrated, one in use:	
	Rocket Motor MK 39, Mod O	3
14.	Many demonstrated:	
	M3 JATO, Typical of JATO Units	4
15.	Not demonstrated.	1
16.	Many demonstrated:	
	Sidewinder, Terrier, etc.	4
17.	Some demonstrated, one of high mass fraction	
	JATO type units and M-Motor	3

Design	Comments	Rating
18.	Some demonstrated, H-X Motor and Terrier Sustainer	3
19.	Not demonstrated as such but feasible	2

(References 5 and 6)

7. Design Complexity

This rating was made in order to account for manufacturing complexities which could result in reliability problems during development and qualification. Consideration was given to those problems which have resulted in schedule (development and qualification) slippages in previous high performance space motor programs. The ratings for each design are given in Table C-I.

8. Freedom from the Effects of Vibration, Spinning, etc

This rating was made by setting up a table for each design and rating it on freedom from the effects of slump, vibration, resonance, and spin, especially sliver break-up and dynamic unbalance. If a grain design was free from the effects of these items it received four points. If it was free from the effects of three of the items, but only relatively free from the fourth, it received 3.5 points. The rating table appears below:

	DESIGN FREE FROM				
DESIGN	SLUMP	VIBRATION	RESONANCE	SPIN	INDEX
1	Relatively	Yes	Yes	Yes	3.5
2	Relatively	Yes	Yes	Yes	3.5
3	Relatively	Yes	Yes	Yes	3.5
4	Relatively	Yes	No	Yes	2.5
5	Relatively	Yes	No	Yes	2.5
6	Yes	Yes	No	Yes	3
7	Relatively	Yes	Yes	Yes	3.5
8	Relatively	Yes	Yes	Yes	3.5
9	Yes	Yes	No	Yes	3
10	Yes	Yes	Yes	Yes	4
11	Yes	Yes	Relatively	Relatively	3
12	No	No	No	No	0
13	Yes	No	No	Yes	2
14	No	No	No	No	0
15	Yes	No	Relatively	No	1.5
16	Yes	Yes	No	Yes	3
17	Relatively	Relatively	No	Yes	2
18	Yes	Relatively	No	Relatively	2
19	Yes	Relatively	No	Relatively	2

9. Design Neutrality

The neutrality of a grain design directly influences its mass fraction. For a grain having a completely neutral burning surface, the maximum chamber pressure is the same as the average pressure yielding the lightest motor case. Any deviation from neutral burning means a higher maximum pressure for a fixed average pressure and, thus, a heavier motor weight. However, for this study, neutrality is not an especially important factor. Thus, the weight allowed for motor neutrality is only one.

Motor neutrality was determined by calculating the initial, final, and average surface areas for each of the designs. The maximum surface area was estimated considering the relationship between the initial and final surface areas and the average area. On this basis, each design was rated according to the following table.

Negative Deviation from Average, %	Positive Deviation from Average, %	Index
0%	0%	4
Less than 10%	Less than 10%	3
Less than 10%	Between 10 and 20%	2.5
Between 10 and 20%	Between 20 and 20%	2.0
Between 20 and 30%	Between 20 and 40%	1.0
Greater than 40%	Greater than 40%	0

10. Low Temperature (-40°F) Capability

This item is associated primarily with propellant grain capability at low temperature since other components have in the past demonstrated their reliability at low temperature. The ability of each motor design to perform reliably in a space environment of -40°F following sterilization was evaluated. The structural characteristics of TP-H-3105 following three sterilization cycles (see Section II-D), together with predicted interface bond stresses and deformations due to thermal shrinkage and internal pressurization, were the prime factors in determining the rating assigned to each candidate design. The rating of each design is given in Table C-I.

11. Effect of a L/D Change to About 1.5 to 1

In a discussion with JPL on November 5, 1966, it was indicated that because of the findings of Mariner 4 concerning the density of the Martian atmosphere and the switch to the Saturn C5 as the Voyager launch vehicle, the optimum motor length would probably be somewhat shorter than the maximum of 3/1 specified in the contract.

A motor case length-to-diameter of about 1.5 was preferred. As a result this new rating was added. It carried a weight of 2. Each motor was reviewed and rated according to the following table:

Effect of a Decrease in L/D Ratio to 1.5/1 on Overall Motor Properties	Index
Considerable Improvement	4
Slight Improvement	3
No Change	2
Slight Degradation	1
Considerable Degradation	0

H. RATING OF DESIGNS

Figures C-5 to C-23 show each design with its respective weighting according to each criterion. Table C-1 compares the totals of all ratings for the designs.

One design of each type was selected on the basis of the total weighting shown in the last column of Table C-I. The designs selected were: 1) The Case-Bonded Spherical Circular Perforate Motor Design, 2) The Circular-Perforated Cylinder, 3) The Internal-External Burning Free-Standing Motor Design, and 4) The Externally Relieved End-Burning Design. The rod and tube design was also chosen for further study; this design could not be considered either a true case-bonded or free-standing design since it incorporates design elements of each.

E15-66-32

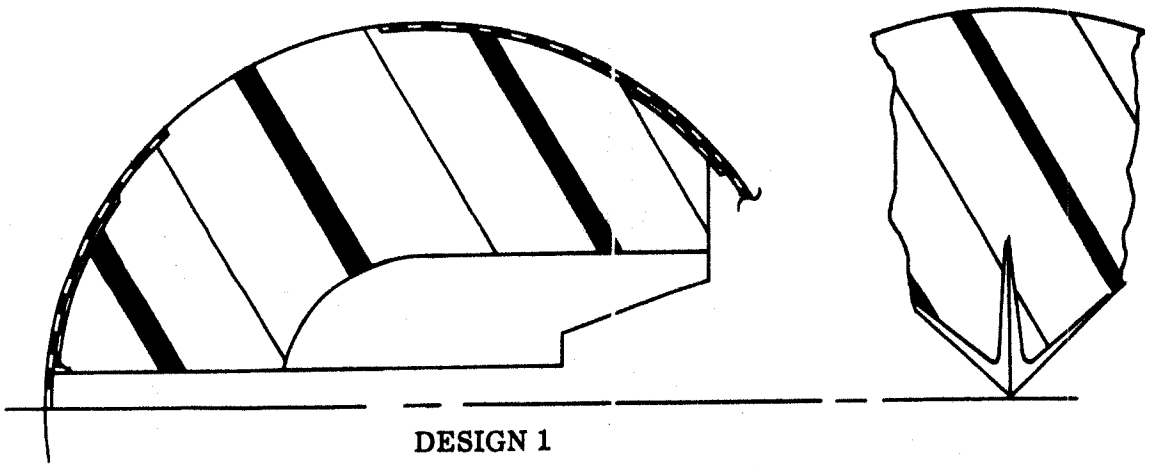

DESIGN 1
CONVENTIONAL SPHERICAL DESIGN

Criteria	Comments	Index
Volumetric Loading Density	88.7%	
Maximum Mass Fraction	0.882	4
Freedom from Stress Concentrations		3
Freedom from Differential Expansion		2
Heating Time	32 hrs.	1
Area Exposed	367 in.^{2}	3
Design Experience		4
Design Complexity		4
Effects of Vibration, spin, etc.		3.5
Neutrality	+3.6% - 15.5%	2.5
Low Temperature Capability		3
Effect of 1.5 L/D		2

FIGURE C-5.

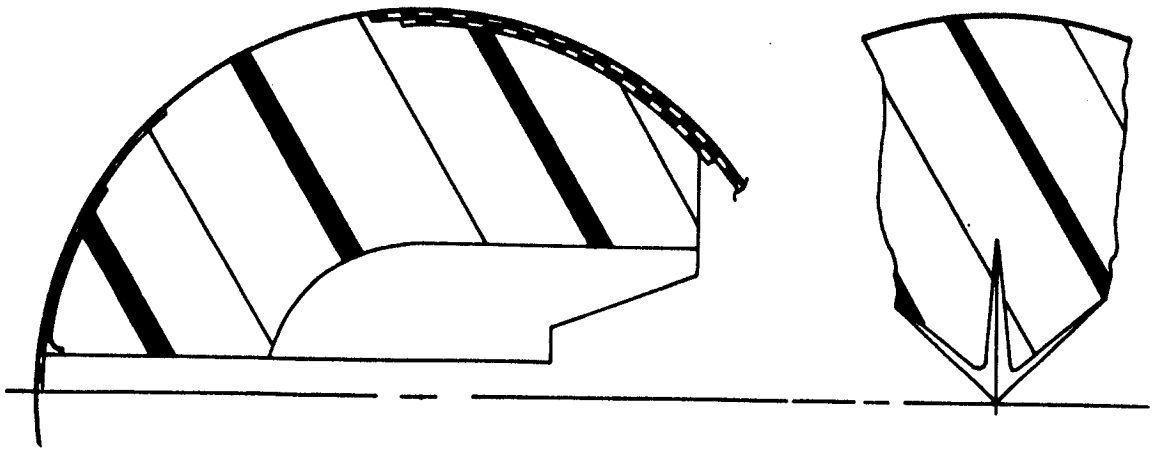

Criteria	Comments	Index
Volumetric Loading Density	84.6%	
Maximum Mass Fraction	0.863	3
Freedom From Stress Concentrations		3
Freedom From Differential Expansion		3
Heating Time	36 hrs	1
Area Exposed	381 in.^{2}	3
Design Experience		4
Design Complexity		4
Effects of Vibration, Spin, etc.		3.5
Neutrality	+3.6% -15%	2.5
Low Temperature Capability		3
Effect of 1.5 L/D		2

FIGURE C-6. DESIGN 2—CONVENTIONAL SPHERICAL DESIGN WITH LONG RELIEF BOOTS

E15-66-30

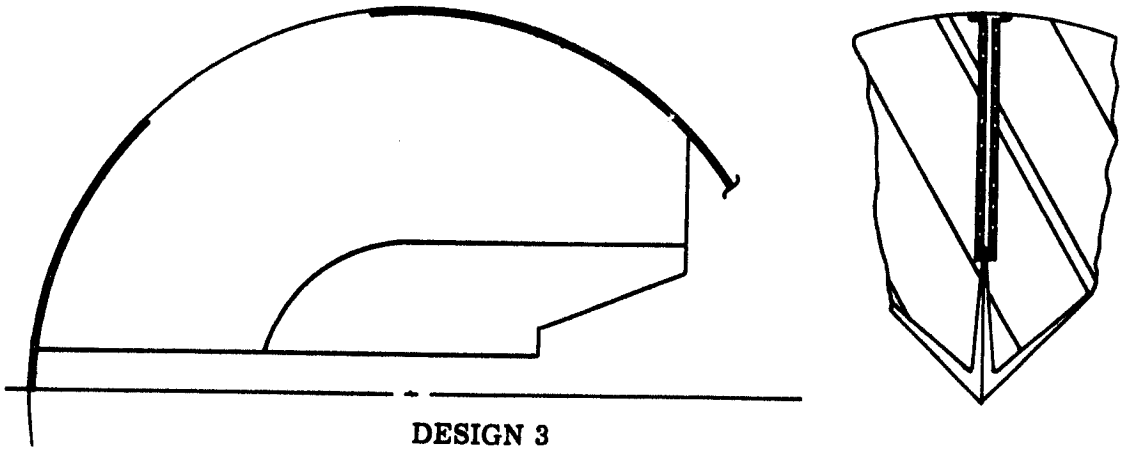

DESIGN 3
ORANGE SLICE DESIGN

Criteria	Comments	Index
Volumetric Loading Density	82.5%	
Maximum Mass Fraction	0.861	3
Freedom from Stress Concentrations		2
Freedom from Differential Expansion		3
Heating Time	32 hrs.	1
Area Exposed	387 in.^{2}	3
Design Experience		2
Design Complexity		2
Effects of Vibration, spin, etc.		3.5
Neutrality	+3.6% - 15%	2.5
Low Temperature Capability		3
Effect of 1.5 L/D		2

FIGURE C-7.

E15-66-29

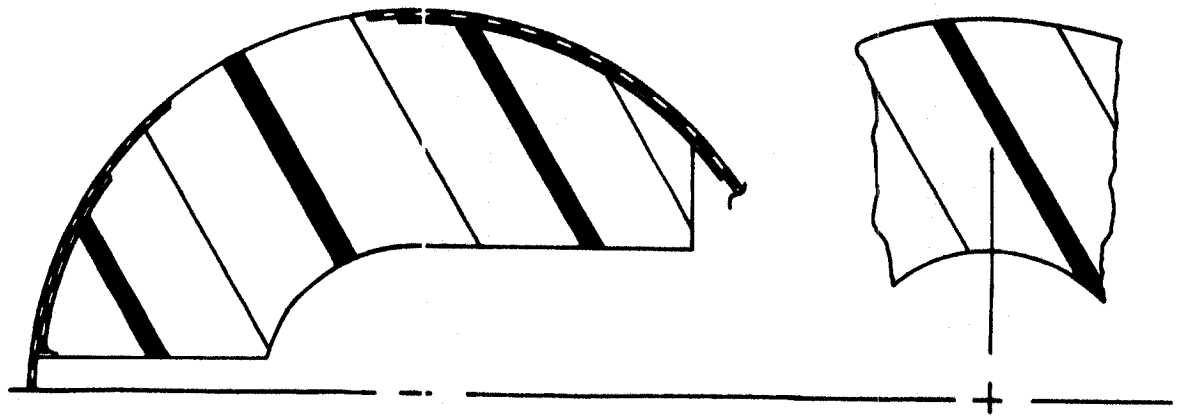

DESIGN 4
SPHERICAL CIRCULAR PERFORATE DESIGN

Criteria	Comments	Index
Volumetric Loading Density	76.1%	
Maximum Mass Fraction	0.860	3
Freedom from Stress Concentrations		4
Freedom from Differential Expansion		3
Heating Time	31 hrs.	1
Area Exposed	150 $in.^2$	4
Design Complexity		3.5
Effects of Vibration, spin, etc.		4
		2.5
Neutrality	+17% - 33%	2
Low Temperature Capability		4
Effect of 1.5 L/D		2

FIGURE C-8

E15-66-17

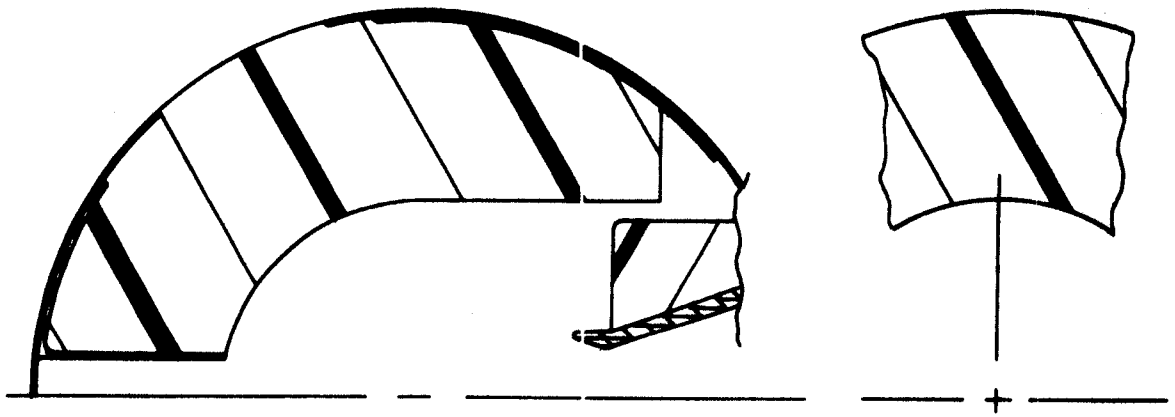

DESIGN 5
CIRCULAR PERFORATED SPHERE WITH PROPELLANT CAST AROUND MIDDLE INSERT

Criteria	Comments	Index
Volumetric Loading Density	74.1%	
Maximum Mass Fraction	0.852	3
Freedom from Stress Concentrations		4
Freedom from Differential Expansion		3
Heating Time	24.5 hrs.	2
Area Exposed	408 $in.^2$	3
Design Complexity		3, 3
Effects of Vibration, spin, etc.		2.5
Neutrality	+7%, - 5%	3
Low Temperature Capability		4
Effect of 1.5 L/D		2

FIGURE C-9.

E15-66-18

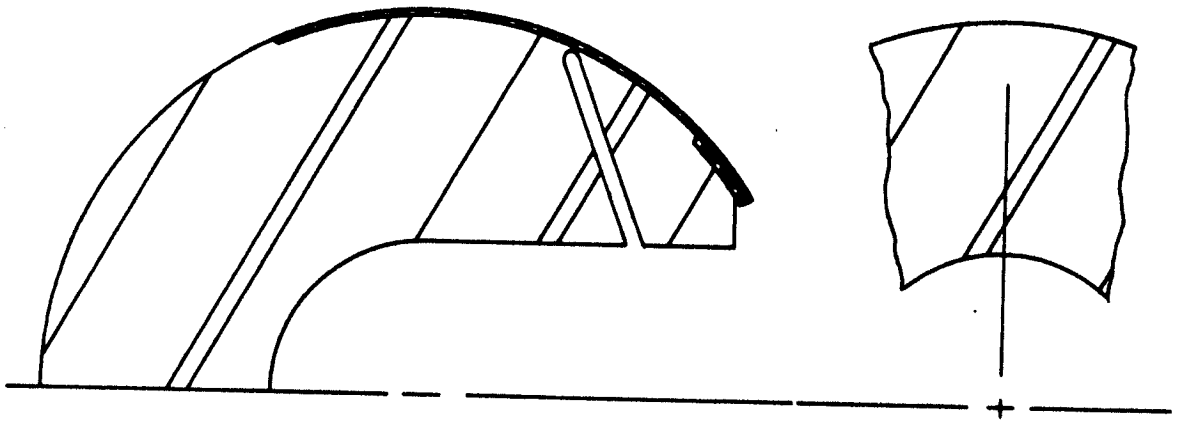

Criteria	Comments	Index
Volumetric Loading Density	81.2%	
Maximum Mass Fraction	0.878	4
Freedom from Stress Concentrations		4
Freedom from Differential Expansion		2
Heating Time	26.6 hrs.	2
Area Exposed	459 in ^{2}	3
Design Complexity		3
Effects of Vibration, Spin, etc.		3, 3
Neutrality	+40% -20%	1
Low Temperature Capability		4
Effect of 1.5 L/D		2

FIGURE C-10. DESIGN 6. CONICAL SLOTTED CIRCULAR PERFORATED SPHERICAL DESIGN

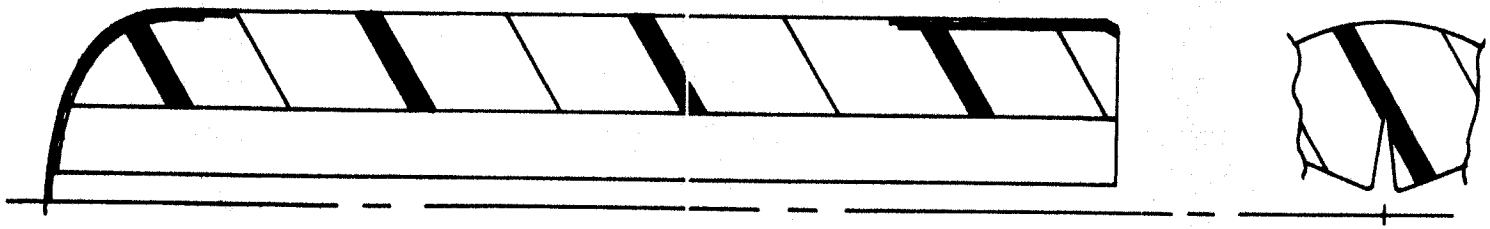

Criteria	Comments	Index
Volumetric Loading Density	80.8%	
Maximum Mass Fraction	0.816	1
Freedom from Stress Concentrations		3
Freedom from Differential Expansion		2
Heating Time	12.5 hrs.	3
Area Exposed	665 in.^{2}	2
Design Complexity		4, 4
Effects of Vibration, Spin, etc.		3.5
Neutrality	+19% -10%	2
Low Temperature Capability		3
Effect of 1.5 L/D		2

FIGURE C-11. DESIGN 7 — CONVENTIONAL STAR CYLINDER

E15-66-20

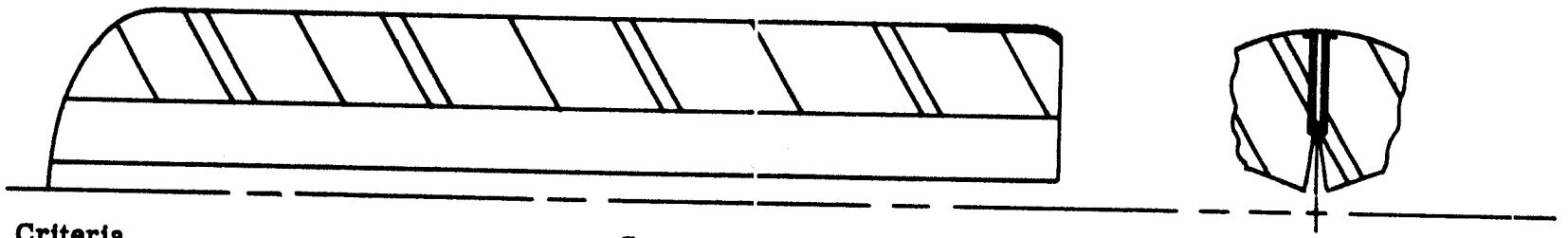

Criteria	Comments	Index
Volumetric Loading Density	78.8%	
Maximum Mass Fraction	0.817	1
Freedom from Stress Concentrations		3
Freedom from Differential Expansion		3
Heating Time	12.5 hrs	3
Area Exposed	672 in.^{2}	2
Design Complexity		2
Effects of Vibration, Spin, etc.		3, 3.5
Neutrality	+19% -10%	2
Low Temperature Capability		3
Effect of 1.5 L/D		2

FIGURE C-12. DESIGN 8 — INHIBITED WEDGE STAR

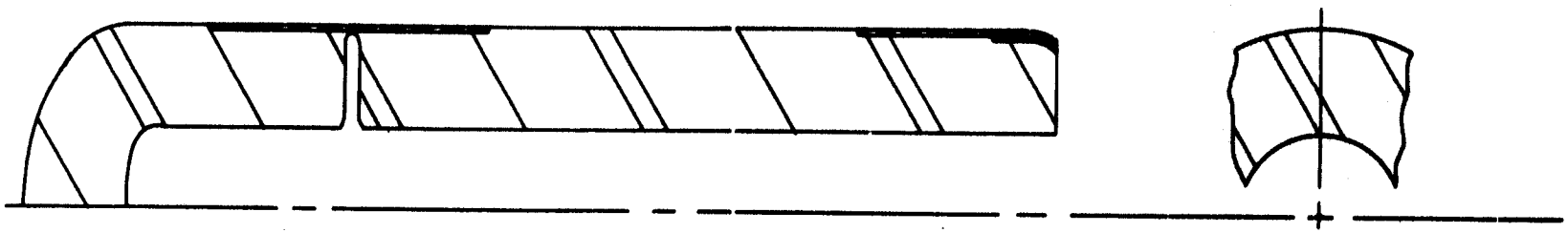

Criteria	Comments	Index
Volumetric Loading Density	80.8%	
Maximum Mass Fraction	0.843	2
Freedom from Stress Concentrations		3
Freedom from Differential Expansion		2
Heating Time	11.4 hrs	3
Area Exposed	452 $in.^2$	3
Design Complexity		4
Effects of Vibration, Spin, etc.		3, 3
Neutrality	+12% -14%	2
Low Temperature Capability		3
Effect of 1.5 L/D		4

FIGURE C-13. DESIGN 9—CIRCULAR PERFORATE CYLINDER

E15-66-22

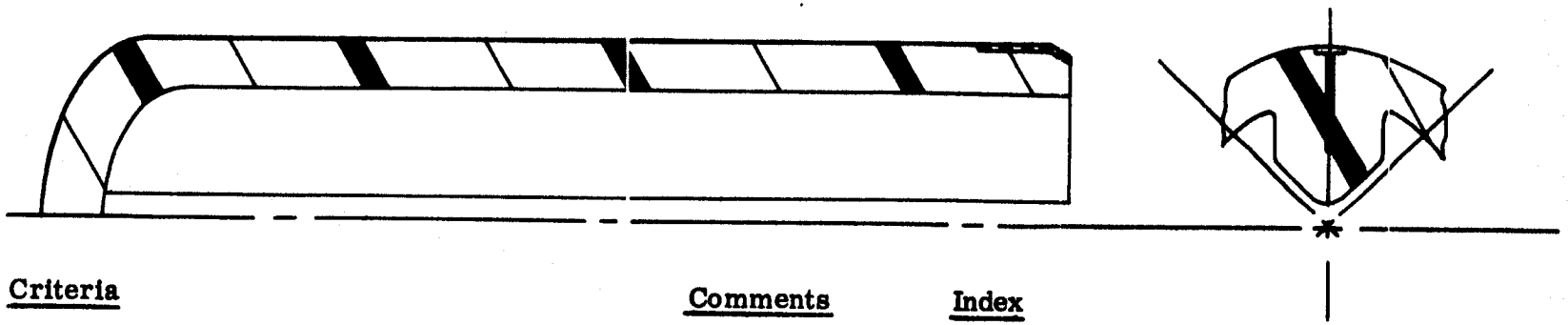

Criteria	Comments	Index
Volumetric Loading Density	78.9%	
Maximum Mass Fraction	0.783	0
Freedom from Stress Concentrations		3
Freedom from Differential Expansion		2
Heating Time	10.0 hrs	4
Area Exposed	1085 $in.^2$	1
Design Complexity		3
Effects of Vibration, Spin, etc.		3, 4
Neutrality	+8% -15%	2.5
Low Temperature Capability		2
Effect of 1.5 L/D		1

FIGURE C-14. DESIGN 10--DOUBLE WEB STAR

E15-66-23

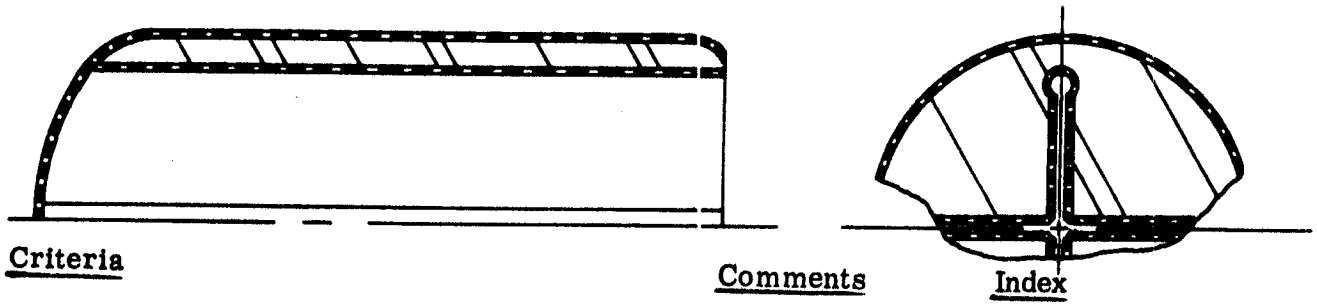

Criteria	Comments	Index
Volumetric Loading Density	80.0%	
Maximum Mass Fraction	0.873	4
Freedom from Stress Concentrations		2
Freedom from Differential Expansion		2
Heating Time	24.1 hrs	2
Area Exposed	871 in.^{2}	4
Design Complexity		2
Effects of Vibration, Spin, etc.		2, 3
Neutrality	+0% -0%	4
Low Temperature Capability		3
Effect of 1.5 L/D		4

FIGURE C-15. DESIGN 11—INTERNALLY RELIEVED END BURNER

E15-66-24

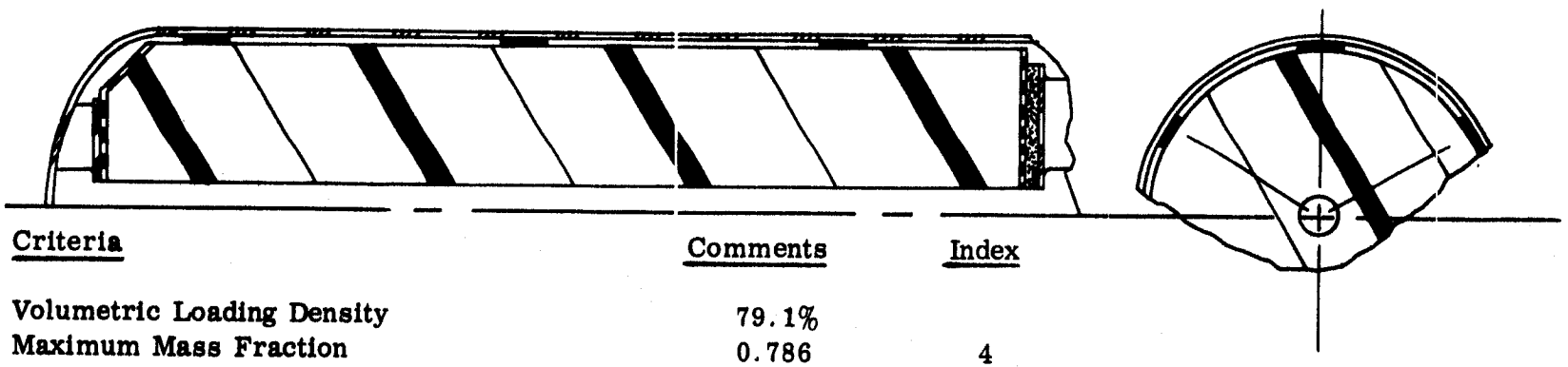

Criteria	Comments	Index
Volumetric Loading Density	79.1%	
Maximum Mass Fraction	0.786	4
Freedom from Stress Concentrations		3
Freedom from Differential Expansion		4
Heating Time	25.3 hrs	2
Area Exposed	769 $in.^2$	2
Design Complexity		4
Effects of Vibration, Spin, etc.		3, 0
Neutrality	+5% -2%	4
Low Temperature Capability		3
Effect of 1.5 L/D		1

FIGURE C-16. DESIGN 12—UNSUPPORTED INTERNAL-EXTERNAL BURNING GRAIN

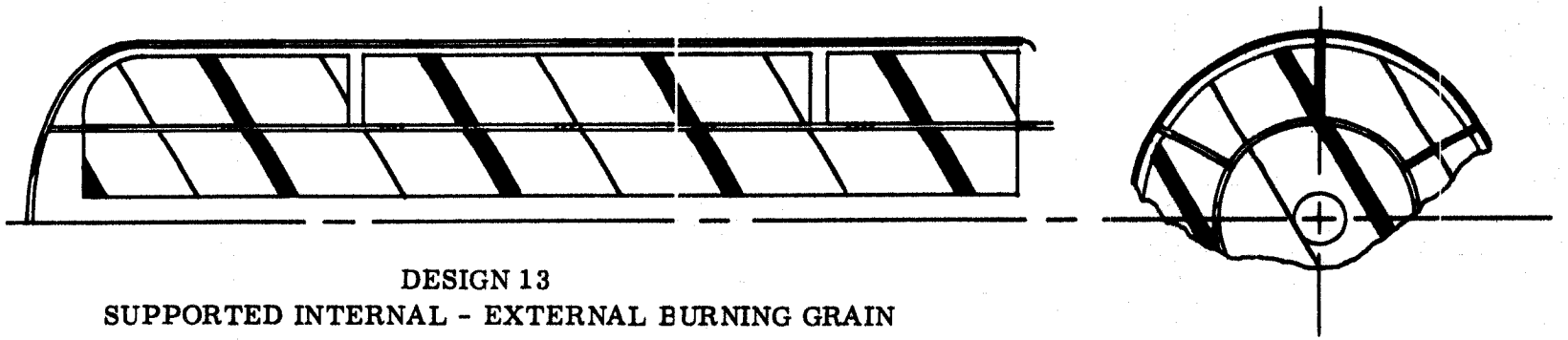

DESIGN 13
SUPPORTED INTERNAL - EXTERNAL BURNING GRAIN

Criteria	Comments	Index
Volumetric Loading Density	78.3%	
Maximum Mass Fraction	0.785	4
Freedom from Stress Concentrations		2
Freedom from Differential Expansion		3
Heating Time	25.3 hrs	2
Area Exposed	925 in ^{2}	2
Design Complexity		3, 1
Effects of Vibration, spin, etc.		2
Neutrality	+16% - 14%	2
Low Temperature Capability		2
Effect of 1.5 L/D		2

FIGURE C-17.

E15-66-26

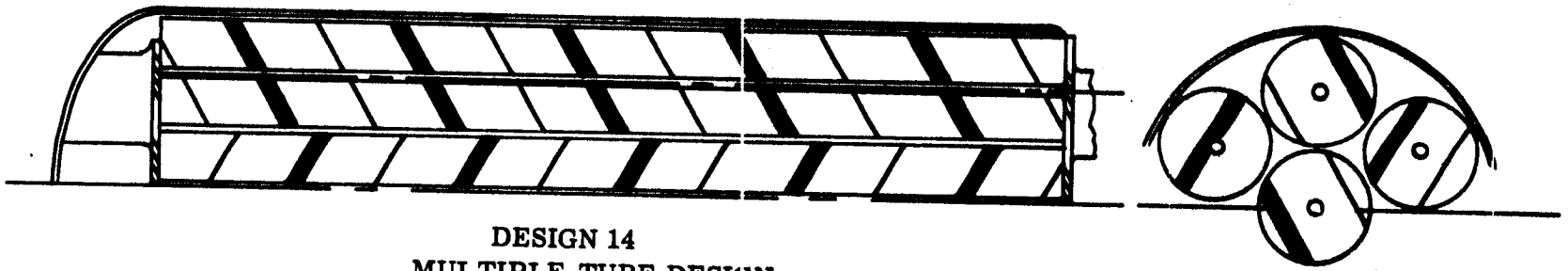

DESIGN 14
MULTIPLE TUBE DESIGN

Criteria	Comments	Index
Volumetric Loading Density	61.4%	
Maximum Mass Fraction	0.693	0
Freedom from Stress Concentrations		1
Freedom from Differential Expansion		4
Heating Time	5.2 hrs.	4
Area Exposed	2290 in.^{2}	0
Design Complexity		4
Effects of Vibration, spin, etc.		2, 0
Neutrality	+6% - 6%	4
Low Temperature Capability		3
Effect of 1.5 L/D		0

FIGURE C-18.

E15-66-27

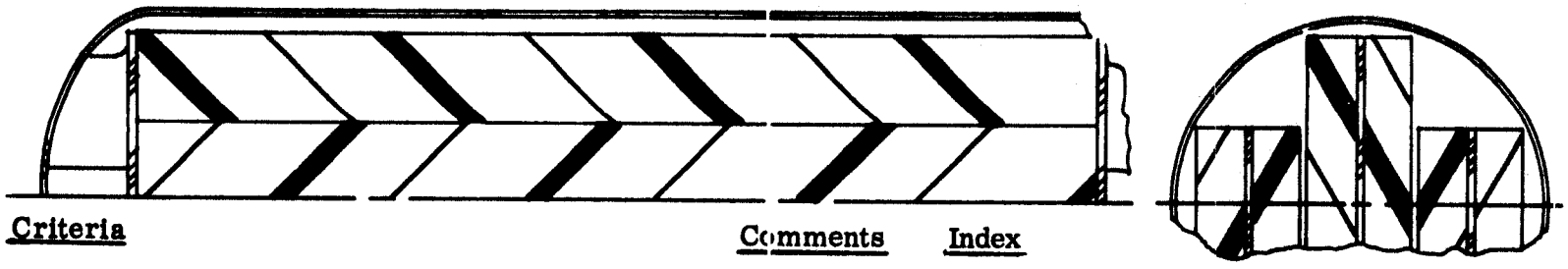

Criteria	Comments	Index
Volumetric Loading Density	52.7%	
Maximum Mass Fraction	0.729	1
Freedom from Stress Concentrations		2
Freedom from Differential Expansion		3
Heating Time	5.2 hrs.	4
Area Exposed	1720 $in.^2$	0
Design Complexity		1
Effects of Vibration, Spin, etc.		1, 1.5
Neutrality	+68% -69%	0
Low Temperature Capability		2
Effect of 1.5 L/D		0

FIGURE C-19. DESIGN 15 — SLAB DESIGN

E15-66-28

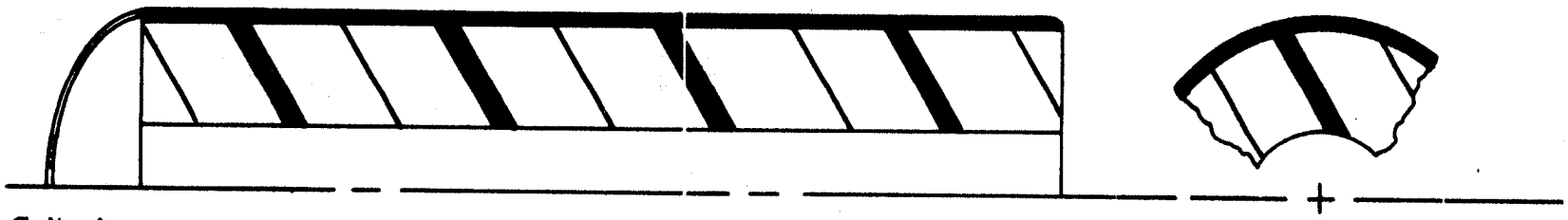

Criteria	Comments	Index
Volumetric Loading Density	71.6%	
Maximum Mass Fraction	0.814	4
Freedom from Stress Concentrations		2
Freedom from Differential Expansion		2
Heating Time	18.6 hrs	3
Area Exposed	404 $in.^2$	3
Design Complexity		4
Effects of Vibration, Spin, etc.		3, 3
Neutrality	+10% -29%	2
Low Temperature Capability		2
Effect of 1.5 L/D		2

FIGURE C-20. DESIGN 16--CARTRIDGE LOADED CIRCULAR PERFORATED GRAIN

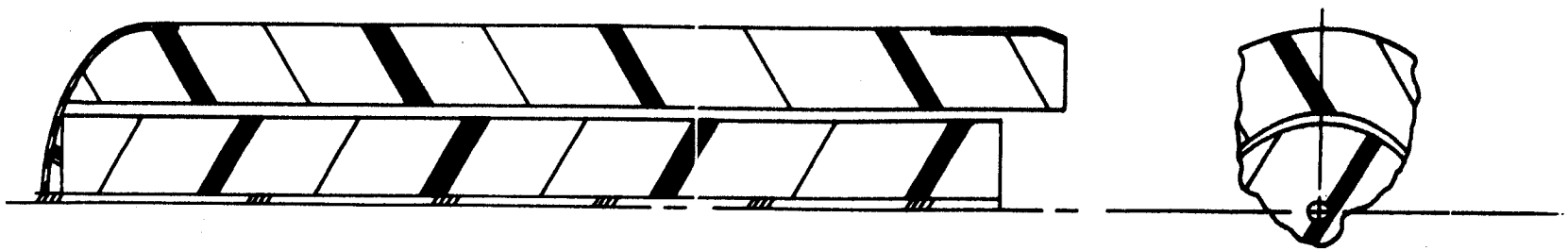

Criteria	Comments	Index
Volumetric Loading Density	82.6%	
Maximum Mass Fraction	0.821	4
Freedom from Stress Concentrations		3
Freedom from Differential Expansion		3
Heating Time	16.9 hrs.	3
Area Exposed	889 $in.^2$	2
Design Complexity		3
Effects of Vibration, Spin, etc.		3, 3, 2
Neutrality	+14% -10%	2.5
Low Temperature Capability		3
Effect of 1 5 L/D		4

FIGURE C-21. DESIGN 17— ROD AND SHELL DESIGN

E15-66-15

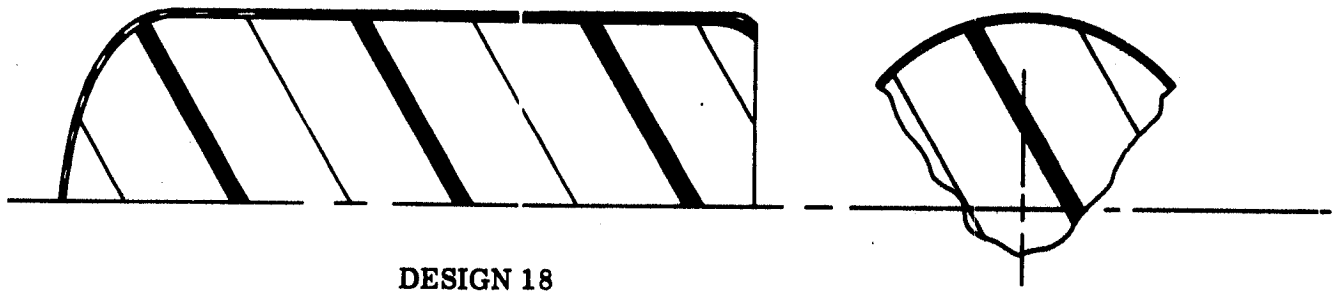

DESIGN 18
EXTERNALLY-RELIEVED END BURNER

Criteria	Comments	Index
Volumetric Loading Density	93.5%	
Maximum Mass Fraction	0.903	4
Freedom from Stress Concentrations		4
Freedom from Differential Expansion		2, 3.5
Heating Time	24.1 hrs.	2
Area Exposed	85 $in.^2$	4
Design Complexity		3,2
Effects of Vibration, spin, etc.		2
Neutrality	+0% - 0%	4
Low Temperature Capability		2
Effect of 1.5 L/D		4

FIGURE C-22.

E15-66-16

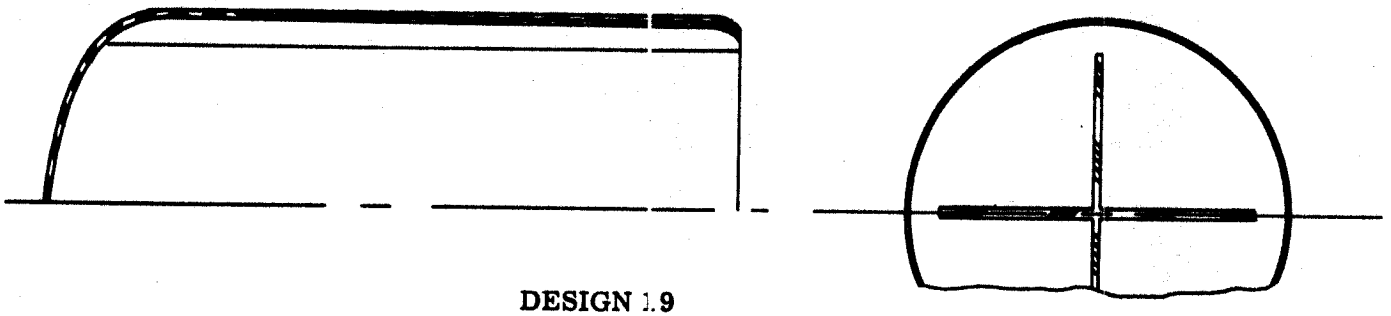

DESIGN 1.9
INTERNALLY-SUPPORTED EXTERNALLY-RELIEVED END BURNER

Criteria	Comments	Index
Volumetric Loading Density	90.7%	
Maximum Mass Fraction	0.886	4
Freedom from Stress Concentrations		2
Freedom from Differential Expansion		3
Heating Time	24.1 hrs	2
Area Exposed	87 $in.^2$	4
Design Complexity		2,2
Effects of Vibration, spin, etc.		2
Neutrality	+0% - 0%	4
Low Temperature Capability		2
Effect of 1.5 L/D		4

FIGURE C-23.

TABLE C-I

HEAT-STERILIZABLE MOTOR STUDY WEIGHTING CHART

Designs	Mass Fraction			Freedom from Stress Conc.			Freedom from Diff. Exp.			Time to Reach Temp			Total Area Exposed			Design Experience		
	Index	Weight	Points	Index	Weight	Points	Index	Weight	Points	Index	Weight	Points	Index	Weight	Points	Index	Weight	Points
1. Conventional Sphere	4	2	8	3	5	15	2	4	8	1	2	2	3	2	6	4	3	12
2. Conventional Sphere with Long Relief Boots	3	2	6	3	5	15	3	4	12	1	2	2	3	2	6	4	3	12
3. Orange Slice Design	3	2	6	2	5	10	3	4	12	1	2	2	3	2	6	2	3	6
4. Spherical Circular Perforate Design	3	2	6	4	5	20	3	4	12	1	2	2	4	2	8	3.5	3	10.5
5. Circular Perforated, Propellant on Closure	3	2	6	4	5	20	3	4	12	2	2	4	3	2	6	3	3	9
6. Conical Slotted Circular Perf Sphere	4	2	8	4	5	20	2	4	8	2	2	4	3	2	6	3	3	9
7. Conventional Star Cylinder	1	2	2	3	5	15	2	4	8	3	2	6	2	2	4	4	3	12
8. Inhibited Wedge Star	1	2	2	3	5	15	3	4	12	3	2	6	2	2	4	2	3	6
9. Circular Perforate Cylinder	2	2	4	3	5	15	2	4	8	3	2	6	3	2	6	4	3	12
10. Double Web Star	0	2	0	3	5	15	2	4	8	4	2	8	1	2	2	3	3	9
11. Internally-Relieved End Burner	4	2	8	2	5	10	2	4	8	2	2	4	4	2	8	2	3	6
12. Unsupported Internal-External Grain	4	2	8	3	5	15	4	4	16	2	2	4	2	2	4	4	3	12
13. Supported Internal-External Grain	4	2	8	2	5	10	3	4	12	2	2	4	2	2	4	3	3	9
14. Multiple Tube Design	0	2	0	1	5	5	4	4	16	4	2	8	0	2	0	4	3	12
15. Slab Design	1	2	2	2	5	10	3	4	12	4	2	8	0	2	0	1	3	3
16. Cartridge Loaded Circular Perforate	4	2	8	2	5	10	2	4	8	3	2	6	3	2	6	4	3	12
17. Rod and Shell Design	4	2	8	3	5	15	3	4	12	3	2	6	2	2	4	3	3	9
18. Externally-Relieved End Burner	4	2	8	2	5	10	3.5	4	14	2	2	4	4	2	8	3	3	9
19. Supported Externally Relieved End Burner	4	2	8	2	5	10	3	4	12	2	2	4	4	2	8	2	3	6

TABLE C-I CONTINUED
HEAT-STERILIZABLE MOTOR STUDY WEIGHTING CHART

	Design Complexity			Effects of Vibration, Spin, Etc			Neutrality of Surface			Low Temp Capability			Effect of 1.5/1 L/D			
	Index	Weight	Points	Index	Weight	Points	Index	Weight	Points	Index	Weight	Points	Index	Weight	Points	Total Points
1. Conventional Sphere	4	5	20	3.5	2	7	2.5	1	2.5	3	3	9	2	2	4	93.5
2. Conventional Sphere with Long Relief Boots	4	5	20	3.5	2	7	2.5	1	2.5	3	3	9	2	2	4	95.5
3. Orange Slice Design	2	5	10	3.5	2	7	2.5	1	2.5	3	3	9	2	2	4	74.5
4. Spherical Circular Perforate Design	4	5	20	2.5	2	5	2	1	2	4	3	12	2	2	4	101.5
5. Circular Perforated, Propellant on Closure	3	5	15	2.5	2	5	3	1	3	4	3	12	2	2	4	96.0
6. Conical Slotted Circular Perf Sphere	3	5	15	3	2	6	1	1	1	4	3	12	2	2	4	93.0
7. Conventional Star Cylinder	4	5	20	3.5	2	7	2	1	2	3	3	9	2	2	4	89.0
8. Inhibited Wedge Star	3	5	15	3.5	2	7	2	1	2	3	3	9	2	2	4	82.0
9. Circular Perforate Cylinder	3	5	15	3	2	6	2	1	2	3	3	9	4	2	8	91.0
10. Double Web Star	3	5	15	4	2	8	2.5	1	2.5	2	3	6	1	2	2	75.5
11. Internally-Relieved End Burner	2	5	10	3	2	6	4	1	4	3	3	9	4	2	8	81.0
12. Unsupported Internal-External Grain	3	5	15	0	2	0	4	1	4	3	3	9	1	2	2	89.0
13. Supported Internal-External Grain	1	5	5	2	2	4	2	1	2	2	3	6	2	2	4	66.0
14. Multiple Tube Design	2	5	10	0	2	0	4	1	4	3	3	9	0	2	0	64.0
15. Slab Design	1	5	5	1.5	2	3	0	1	0	2	3	6	0	2	0	49.0
16. Cartridge Loaded Circular Perforate	3	5	15	3	2	6	2	1	2	2	3	6	2	2	4	83.0
17. Rod and Shell Design	3	5	15	2	2	4	2.5	1	2.5	3	3	9	4	2	8	92.5
18. Externally-Relieved End Burner	2	5	10	2	2	4	4	1	4	2	3	6	4	2	8	85.0
19. Supported Externally Relieved End Burner	2	5	10	2	2	4	4	1	4	2	3	6	4	2	8	80.0

APPENDIX D

DESIGN EVALUATION AND RATING–FIVE CANDIDATE DESIGNS

The five candidate designs were examined more thoroughly in the second phase of the program. At the end of this phase the two most reliable grain designs were selected for detailed analysis.

A. BASES FOR EVALUATION

1. Weight Analysis

The first step in evaluating the five designs was to prepare detailed weight calculations for each design. Preliminary layouts were drawn to half scale. The weight of each individual motor component, except the case, aft closure, and PYROGEN, were calculated from this layout.

The case and aft closure weights were assumed to be the same as those of a spherical or cylindrical pressure vessel designed to operate at the internal pressure at which the optimum mass fraction was calculated during the preliminary design analysis. The PYROGEN weights were assumed to be constant at one pound. The liner weight was assumed to be 0.6 pound. A detailed weight breakdown is included in the discussion of each design.

2. Surface Area Calculations

The burning surface area as a function of distance burned was calculated for each of the designs at 20% increments.

3. Heating Time

The heating time for each of the designs was calculated again using the same equations as formerly used. (Appendix F) By breaking the grain design down into separate sections, we calculated the time required to heat the inside section to the sterilization temperature in an attempt to arrive at a more representative figure for that time. Some of these sections had insulation at the case wall. After calculation of separate heating times for each section the results were averaged. The heating times are discussed under each design.

4. Other Evaluations

In general, the criteria used to determine the most suitable designs were re-evaluated with the shorter L/D motors. In addition, another design criterion was included. This was called the scale-up factor. This item was added in order to assess the capability of the designs to be scaled-up or -down.

In order to avoid confusion, the designs were renamed as shown in the following table.

Design A — Case-Bonded Spherical Circular Perforate Motor Design

Design B — Circular Perforated Cylindrical Motor Design

Design C — Internal-External Burning Free-Standing Motor Design

Design D — Externally Relieved End Burning Motor Design

Design E — Rod and Tube Motor Design

These designs will now be discussed in detail.

B. INDIVIDUAL DESIGN DISCUSSION

1. Design A — Case-Bonded Spherical Circular Perforate Motor Design

The grain is a case-bonded center perforate charge of TP-H-3015 propellant. The grain is cast and cured in a 16.16-inch diameter 6 Al 4V titanium case. It is 12.45 inches in length and has a maximum outside diameter of 16.14 inches. The motor design is shown in Drawing LO 1848. The grain has a cylindrical perforate PYROGEN well 1.6 inches in diameter at the head end of the motor. A split boot of asbestos-filled polyisoprene insulation is located in the head end of the motor to insulate the case from the effects of combustion gases and to provide stress relief. The center perforation in the aft end of the motor has a radius of 2.86 inches. This blends into a spherical cap of the same radius just forward of the motor equator. A split boot of asbestos-filled polyisoprene insulation is also provided in the aft end of the motor case. This insulation section extends to a point 2.9 inches forward of the equator. The boot is split from the equator aft to provide stress relief. The insulation extends the total distance to the 6.75-inch diameter case opening.

The aft closure-nozzle assembly consists of a 6 Al 4V titanium aft closure insulated with a layer of 0.12-inch thick asbestos-filled polyisoprene insulation, a Graph-I-Tite GX nozzle insert which is submerged in the motor case, two rings of vitreous silica phenolic insulation which back up the nozzle insert, and a vitreous silica phenolic exit cone. The nozzle half angle was assumed to be 20 degrees and the expansion ratio was specified as 30:1.

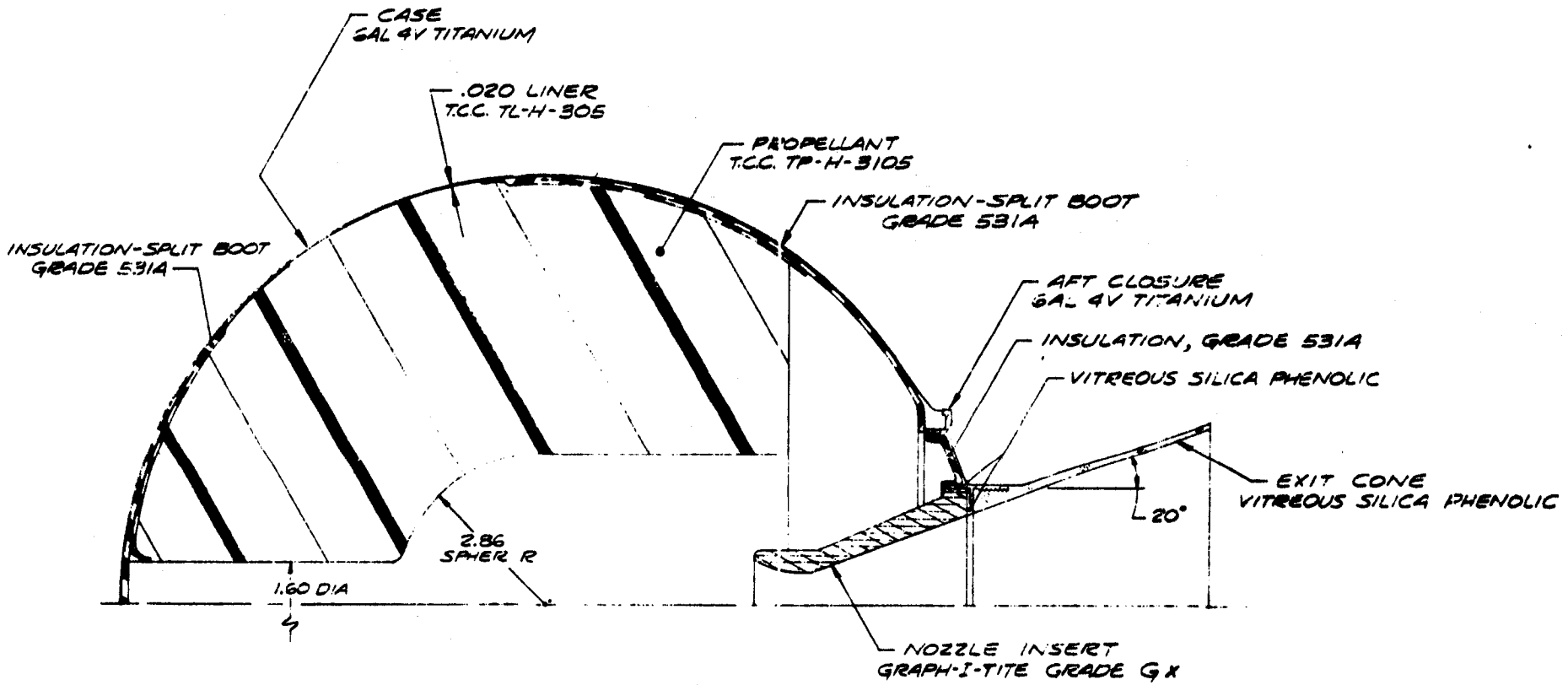

UNLESS OTHERWISE SPECIFIED: DIMENSIONS ARE IN INCHES TOLERANCES .XX ± .010 .XXX ± .005 ANGULAR ± 30' FRACTIONS ± 1/16 BREAK SHARP EDGES .005-.015 ALL SMALL FILLETS R 0-.040 R THREADS CLASS 3 PER H28 HANDBOOK AND SUPPLEMENTS DIMENSIONING PER MIL-STD-8 WELD SYMBOLS PER JAN-STD-19 SURFACE ROUGHNESS SYMBOLS PER MIL-STD-10 ALL FINISHED SURFACES 125	DRAWN	R. JOHNSON	21 JAN 66
	CHK'D		
	ENGR	[illegible]	21 JAN 66
	ENGR		
	ENGR		
	USED		
	SERIES		
	SAFETY		
	APPD		
DESIGN ACTIVITY APPROVAL John P King 25 JAN 66			

Thiokol CHEMICAL CORPORATION
ELKTON DIVISION ELKTON, MARYLAND

DESIGN "A"
CASE BONDED SPHERICAL
CIRCULAR PERFORATE MOTOR DESIGN

CODE IDENT NO.	SIZE	
07299	C	LO-1848

SCALE	WEIGHT	CALC ACTUAL	SHEET

WEIGHT BREAKDOWN AND MASS FRACTION

Component	Weight, lbs
Case	4.2
Case Insulation	3.5
Closure Insulation	0.2
Nozzle Insert	0.9
Nozzle Insulation	0.1
Exit Cone	0.8
Miscellaneous	1.0
Liner	0.6
PYROGEN	1.0
TOTAL	12.3
Propellant	100.0
TOTAL	112.3
Mass Fraction	0.89

a. Areas of Stress Concentration

The unit has no star points. The two stress relief boots should reduce stresses by allowing the grain to expand and contract over the firing temperature range of -40 to +120° F. The only areas of stress concentration are at the terminations of the split boots themselves. The boots are somewhat larger than in most spherical designs, although the unit is bonded to the head end over an area of approximately 60 degrees.

b. Differential Expansion Effects

Differential expansion of the grain during sterilization should be taken up considerably by the split boots. In the head end of the grain the split boot will allow the grain to expand inward; however, because of the relatively small PYROGEN well opening, compressive stresses are generated in this area. In the aft end, considerable relief is provided for expansion of the grain both longitudinally and radially inward. This will cause some compression of the grain,but it will be considerably less than in the area of the PYROGEN well.

c. Time to Reach Temperature

The calculated time to reach temperature based on a driving temperature of 300° F is 39 hours; however, in reality this may be somewhat conservative because of the end effect present in spherical motors.

d. Design Experience

Considerable experience exists with this design, both in booting and in the spherical configuration. Manufacture of this design consists of loading the insulation and lining, casting to weight and plunging the core over a center spike. No unproven techniques are involved.

e. Design Complexity

The design is not complex. No phenolic supports are used. The components consist of one grain plus insulation sections.

f. Effects of Vibration Spin, Etc.

The motor assembly will,to a certain extent,be affected by vibration because of the split boots. However, because of the thickness of the web relative to the split boot length, the effects of vibration should be minimal. The effects of slump should also be minimal for the same reason. This grain should be relatively free from the effects of spinning. Resonance should not be a problem because of the short L/D and the submerged nozzle cavity.

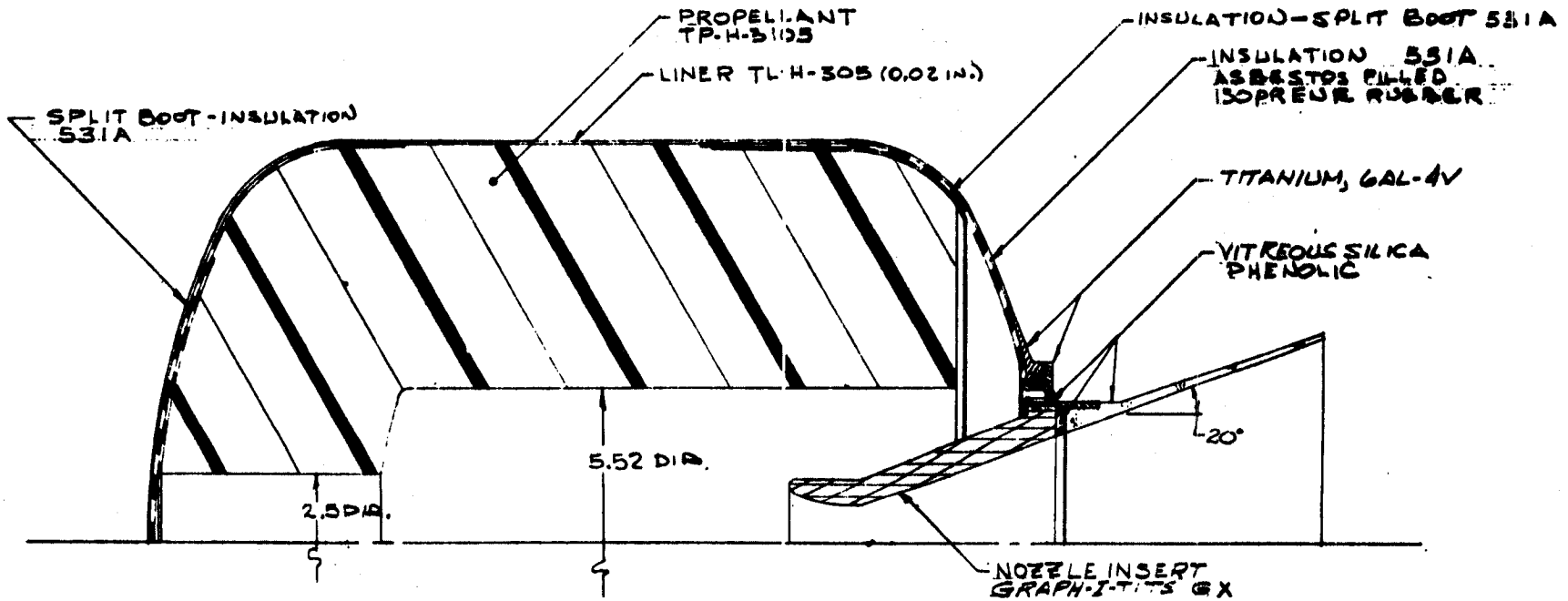

QTY REQD PER DASH NO.	ITEM NO.	CODE IDENT	PART OR IDENTIFYING NO.	NOMENCLATURE OR DESCRIPTION	MATERIAL	SPECIFICATION

LIST OF MATERIAL OR PARTS LIST

UNLESS OTHERWISE SPECIFIED:
DIMENSIONS ARE IN INCHES
TOLERANCES
.XX = ± 030: .XXX = ± .010:
ANGULAR ± 30' FRACTIONS ± 1/16
BREAK SHARP EDGES .003-.015
ALL SMALL FILLETS .020-.040 R
THREADS PER FED. HNDBK H-28 AND SUPPLEMENTS
DIMENSIONING PER MIL-STD-8
WELD SYMBOLS PER JAN-STD-19
SURFACE ROUGHNESS SYMBOLS PER MIL-STD-10
ALL FINISHED SURFACES

DRAWN	[illegible]	[illegible]
CHECKED	[illegible]	[illegible]
ENGR	[illegible]	[illegible]
ENGR		
ENGR		
USER		
STRESS		
SAFETY		
APPD		

DESIGN ACTIVITY APPROVAL
Johan P Kuy 25 Jan '66

Thiokol CHEMICAL CORPORATION
ELKTON DIVISION ELKTON, MARYLAND

DESIGN B
CIRCULAR PERFORATED CYLINDRICAL MOTOR DESIGN

CODE IDENT NO.	SIZE	
07299	C	LO-1852

SCALE	WEIGHT	CALC ACTUAL	SHEET

g. Neutrality

The ratio of maximum to minimum surface area is 1.54. This is characterized by low initial thrust, high point at approximately 50% web burn time.and low final thrust. Little improvement can be made to the trace shape unless the grain design is modified considerably.

h. Effect of Scale-up or Scale-down

The effects of scale-up or scale-down on this design are negligible and there is no reason why motors of this design can not be made up to 10,000 pounds. However, in this case, it would be necessary to increase the burning rate of the propellant for weights above the 2,000 or 3,000 pound level to keep the burn time below 60 seconds.

2. Design B – Circular Perforated Cylindrical Motor Design

This design is a case-bonded, circular perforated cylinder of TP-H-3105 propellant. The length of the charge is 14 inches with a maximum outside diameter of 14 inches. The forward end of the grain has a PYROGEN well 2.5 inches in diameter. The motor assembly is shown in Drawing LO 1852. A split boot of asbestos-filled polyisoprene insulation is incorporated in the head end of the design. The boot is split out to a nine-inch diameter. The insulation continues at reduced thickness for the full portion of the 2/1 ellipse and approximately one inch into the cylindrical section of the case. The aft end internal perforation radius is 2.76 inches. This design includes a short section of a head end web to increase the neutral burning characteristics of the grain. If a head end web were not used, the design would be excessively regressive. A split insulation boot is also included in the aft end of the motor. The insulation section of the boot extends from the 5.75-inch diameter aft case opening to a point 2.6 inches forward of the juncture of the aft case elliptical dome and the cylindrical section of the motor case. A stress relief flap provides relief from the aft end of the grain to a point 2 inches forward of the elliptical dome-cylinder juncture. The case is constructed of 6 Al 4V titanium.

The aft closure assembly consists of a 6Al 4V titanium aft closure, a Panelyte 531A aft closure insulation section, a Graph-I-Tite GX nozzle insert, two vitreous silica phenolic backup insulation sleeves and a vitreous silica phenolic exit cone. The assumed nozzle half angle is 20° F and the expansion ratio is 30:1.

WEIGHT BREAKDOWN AND MASS FRACTION

The weight breakdown for this design is shown below:

Component	Weight, lbs
Case and Closure	6.8
Case Insulation	2.6
Aft Closure Insulation	0.1
Nozzle Insert	1.5
Nozzle Backup Insulation	0.1
Exit Cone	0.6
Miscellaneous	1.0
Liner	0.6
PYROGEN	1.0
TOTAL Inert	14.3
Propellant	100.0
TOTAL	114.3
Mass Fraction	0.87

This mass fraction could be increased somewhat by either of two methods: increasing the web fraction (which would be less desirable from a stress standpoint) or increasing the grain and motor length (which would increase the L/D of the motor).

a. Areas of Stress Concentration

This design has no star points and incorporates two stress relief boots. The grain is bonded to the motor case over the forward portion of the cylindrical section of the motor and a portion of the head end. The areas of stress concentration are the splits in the stress relief boots themselves and the small radius where the head end web joins the cylindrical web. They could be reduced by increasing this radius, but this will increase the sliver in the motor.

b. Differential Expansion Effects

Differential expansion will be taken up principally by inward radial growth of the grain. However, this may cause severe compressive loading in the radius area at the juncture of the head end and cylindrical section web. The split boot will allow the propellant in the head end of the motor to deform inward at the PYROGEN well; however, compressive stresses will occur in this section of the grain. A problem exists in differential expansion of the grain in the aft split boot section of the grain because the flat 2/1 ellipse forces the grain to expand inward radially both from the radial growth and the longitudinal growth caused by the ramp effect. This can be alleviated by decreasing the flatness of the ellipse (approaching a sphere), casting only to the cylindrical section (decreasing the volumetric loading density), or casting or curing the grain with a space between the two sections of the aft split boot (this increases the complexity of the manufacturing problem). This last technique is assumed to be the one used.

c. Time to Reach Temperature

The calculated time to reach temperature for this motor is 28.3 hours—shorter than any of the motor designs calculated.

d. Design Experience

Considerable experience with this design exists. The problem cited earlier (spacing of the split boot during manufacture) can be solved by using a removable spacer.

e. Design Complexity

This design is not complex because no phenolic supports are used and the system consists of one grain and two stress relief boots.

f. Effects of Vibration, Spin, Etc.

The motor assembly will be slightly affected by normal vibrations, but because of the large web, this effect and the slump effect should be relatively minor.

This grain is subject to resonant burning to some extent. The effect could be significant because of the longer cylindrical section. Resonance in the longitudinal direction will probably not be a problem because of the submerged nozzle. The effects of spinning should not be appreciable.

g. Neutrality

The ratio of maximum to minimum surface area is 1.4. The design is characterized by a low initial surface area, which increases to a maximum at about 60 to 70 percent, and falls off slightly at 100 percent. This design has sliver in the head end which could be reduced by eliminating the head-end web to give a more regressive burning design, by decreasing the ellipse ratio which approaches a spherical design, or by using inert slivers (which increases the complexity of the design).

h. Effect of Scale-up or Scale-down

The effects of scale-up or scale-down of this design, as in the case of the spheres, are minimal.

3. Design C — Internal-External Burning Free-Standing Motor Design

Because sliver collapse at the end of burning is intolerable, this design includes an internal support. Most of the problems associated with the use of an internal support could be reduced or eliminated by selecting a support material that had thermal expansion properties close to those of the propellant. Selecting this kind of support will also make support of the grain somewhat easier. The material finally selected for the support was Fiberite MX 4925, a carbon fiber reinforced phenolic.

The grain is completely free standing except for the inclusion of a 0.10-inch web thick Fiberite MX 4925 internal support. The motor assembly is shown in Drawing LO 1850. The propellant charge is 15.37 inches long, has an external diameter of 12.2 inches and an internal diameter of 1.2 inches. The aft end of the grain is coned out to allow the use of a submerged nozzle. The outside forward edge of the grain has a 1.875-inch radius bending the outside cylinder into the front surface. The extreme aft end of the grain is insulated by a 0.10-inch thick layer of asbesto-filled polyisoprene insulation.

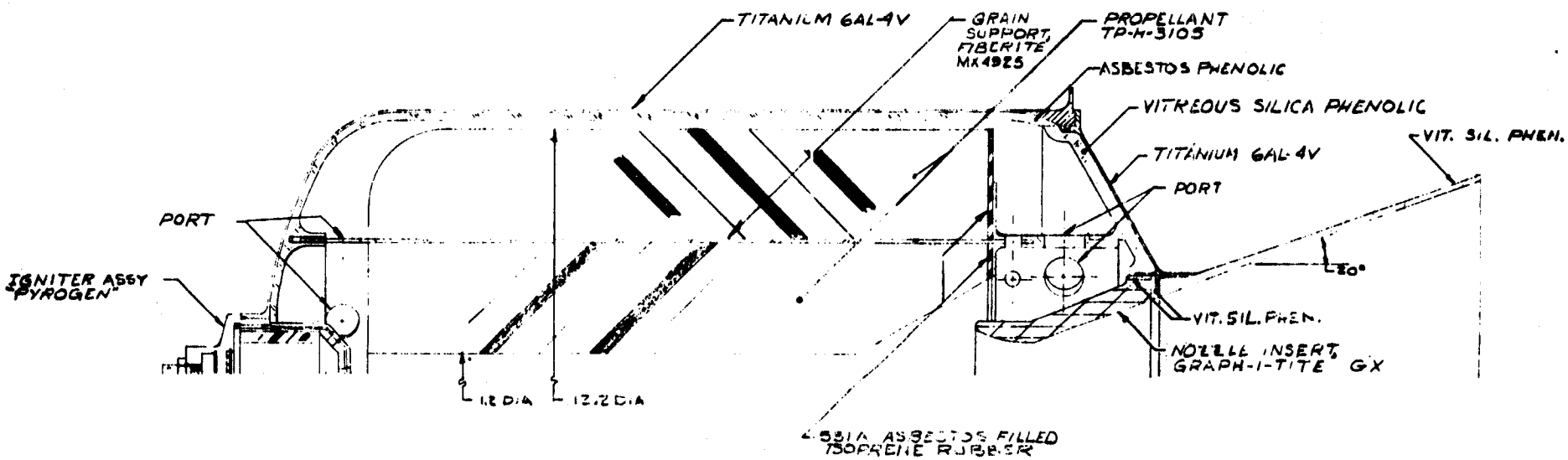

UNLESS OTHERWISE SPECIFIED: DIMENSIONS ARE IN INCHES TOLERANCES .XX = ± .030 .XXX = ± .010 ANGULAR ± 30' FRACTIONS :: 1/16 BREAK SHARP EDGES .003-.015 ALL SMALL FILLETS .020-.040 R THREADS PER FED. HNDBK H-28 AND SUPPLEMENTS DIMENSIONING PER MIL-STD-1 WELD SYMBOLS PER JAN-STD 19 SURFACE ROUGHNESS SYMBOLS PER MIL-STD-10 ALL FINISHED SURFACES ✓	DRAWN	T. J. Ryan Jr.	7/20/60
	CHECKED	J. G. Boat	7/20/60
	ENGR	T. J. Ryan Jr.	7/20/60
	ENGR		
	ENGR		
	USER		
	STRESS		
	SAFETY		
	APPD		
	DESIGN ACTIVITY APPROVAL		

Thiokol. CHEMICAL CORPORATION
ELKTON DIVISION ELKTON, MARYLAND

DESIGN C
INTERNAL-EXTERNAL BURN., FREE STANDING MOTOR DESIGN

CODE IDENT NO.	SIZE	
07299	D	LO-1850

SCALE	WEIGHT — CALC / ACTUAL	SHEET

The 0.10-inch MX 4925 grain support sleeve extends through the complete grain and insulation and is held in place by an aft support structure (see Drawing LO 1850). The internal support is held in place on the aft support structure by pins and adhesive. This allows expansion of the entire structure to take place forward. Because of vibration and spin balance it is desirable to have the tube supported on both ends rather than cantilevered. For this reason, a groove is cut into the RPD 150 case insulation to support the grain tube radially but allow it to expand longitudinally.

The case insulation is RPD 150 or similar material approximately 0.20-inch thick. A rigid insulation is used rather than elastomeric because the gas is flowing parallel to the motor walls at relatively high velocities during firing; this requires an erosion resistant rather than an ablating material.

The aft closure assembly consists of a full diameter aft closure of 6 Al 4V titanium and an aft closure insulation assembly 0.30-inch thick to which is attached the aft grain support strucutre. The nozzle insert is Graph-I-Tite GX backed up by vitreous silica phenolic insulation. The exit cone is fabricated from vitreous silica phenolic. The nozzle half angle is 20 degrees and the expansion ratio is 30:1.

WEIGHT BREAKDOWN AND MASS FRACTION

Component	Weight, lbs
Case	9.9
Case Insulation	10.3
Internal Grain Support	2.4
Grain Aft Support	1.2
Aft Grain Inhibitor	0.5
Aft Closure Insulation	2.1
Nozzle Insert	1.4
Nozzle Backup Insulation	0.1
Exit Cone	1.2
Miscellaneous	1.0

Component	Weight, lbs
Liner	0.6
PYROGEN	1.0
TOTAL, inert	31.7
Propellant	100.0
TOTAL	131.7
Mass Fraction	0.76

This design has the lowest mass fraction of any of the designs considered. The mass fraction cannot be increased substantially without introducing structural problems.

a. Areas of Stress Concentration

This design has almost no areas of stress concentrations. This is because it is free to expand in all directions both radially and longitudinally. The grain is completely supported by a phenolic or epoxy material that will have thermal expansion properties almost identical to those of the propellant. Thus, no significant areas of stress concentration should be present. (See Appendix A, page A-5.)

b. Differential Expansion Effects

Since the grain is completely free to expand in all directions and the expansion properties of the support will be very close to those of the propellant, no problems due to differential expansion of the grain are expected. However, some problems may arise due to differential expansion of the support structure relative to the case and case insulation material. This will necessitate the use of a pin-type attachment of the support structure in the aft end and the use of a slot to take up expansion in the head end.

c. Time to Reach Temperature

The time calculated for the propellant to reach the sterilization temperature is 70 hours.

d. Design Experience

Design experience in high mass fraction rocket motors of this design is seriously lacking. A number of JATO motors have been made using this design; however, the mass fraction of these motors is low. The entire grain should be made in a single casting operation. This probably requires a split casting mold. Also the grain must be installed in the motor case very carefully to ensure locating the tube in the proper manner.

e. Design Complexity

The grain for this design is very simple, consisting of a single internal-external burning grain supported by an internal phenolic support and inhibited on the aft end by an elastomeric insulation. However, the design of the motor case and support structure is quite complicated. The areas of complexity are:

1) support structure must be provided in the aft end with provisions for mechanically attaching the grain;

2) this support and the front section of the grain support must have holes cut in them to facilitate gas flow;

3) the grain support must be pinned in place to reduce the effects of g loading and vibration; and

4) a slot should be provided at the head end to take the support structure, reduce effects of lateral vibration, and locate the grain accurately.

f. Effects of Vibration, Spin, etc.

This design will be subject to some vibration because of the slot at the head end insulation. It is difficult to allow for thermal expansion in the head end of the motor (longitudinal and radial) without providing clearance that will make the grain subject to vibration. The grains are not subject to slump because of the internal support. This grain will be highly susceptible to resonant burning because of the two air gaps (toroidal and cylindrical). It is quite possible that resonant burning could occur during burning because of the organ-pipe type configuration. Resonance could be magnified to the point of failure by the vibrational characteristics of the support structure. The design is also quite sensitive to the effects of spinning. Any increase in burn rate caused by spinning will cause the internal burning portion of the grain to burn out first, resulting in an abrupt drop of burning surface and providing a two-step trace. The unit is also susceptible to g loading since all loads must be taken out by the internal support.

However, the effect of g loading should be somewhat less than in the case of the rod and tube design. G loading could be alleviated by the use of cruciform extensions of the basic circular support structure.

g. Neutrality

The ratio of maximum to minimum surface area in this design is 1.68. The design is characterized by a high initial surface area regressing gradually to the lowest value at burnout. There is virtually no sliver.

h. Effect of Scale-up or Scale-down

This design probably can not be scaled up to levels of much above 1000 pounds because of increased loading (primarily shear between the liner and the propellant and compressive loading on the support itself) plus the fact that handling problems become more difficult). Large designs approaching 1000 pounds would probably require cruciforms extending from the support structure.

4. Design D — Externally Relieved End Burning Motor Design

This motor is of a very short end burning design. The design is shown in Drawing LO 1847. External relief for the grain is provided by a long split boot which extends all the way from the aft propellant surface, through the short cylindrical portion of the motor case, and two inches into the 2/1 ellipse comprising the forward dome. This insulation sleeve is composed of asbestos-filled polyisoprene insulation and tapers from a thickness of 0.15 inch in the aft end to a thickness of 0.05 inch in the head end. The relief boot tapers from 0.05 inch in the aft end to 0.07 inch in the head end where it blends into the motor case insulation.

The solid propellant grain in this design is 11.9 inches long and approximately 14.8 inches in diameter. The grain has no internal perforation but a truncated conical depression is cast into the aft end of the grain to decrease the sliver that occurs at the end of burning. It also makes the motor burn in a more neutral manner and allows the nozzle to be submerged into the grain cavity.

The aft closure assembly consists of the 6 Al 4V titanium aft closure which is insulated by asbestos-filled polyisoprene insulation. The nozzle insert is Graph-I-Tite GX and is backed up by vitreous silica phenolic insulation sleeves. The exit cone is vitreous silica phenolic. The expansion ratio is 30/1 and the exit half angle is 20 degrees.

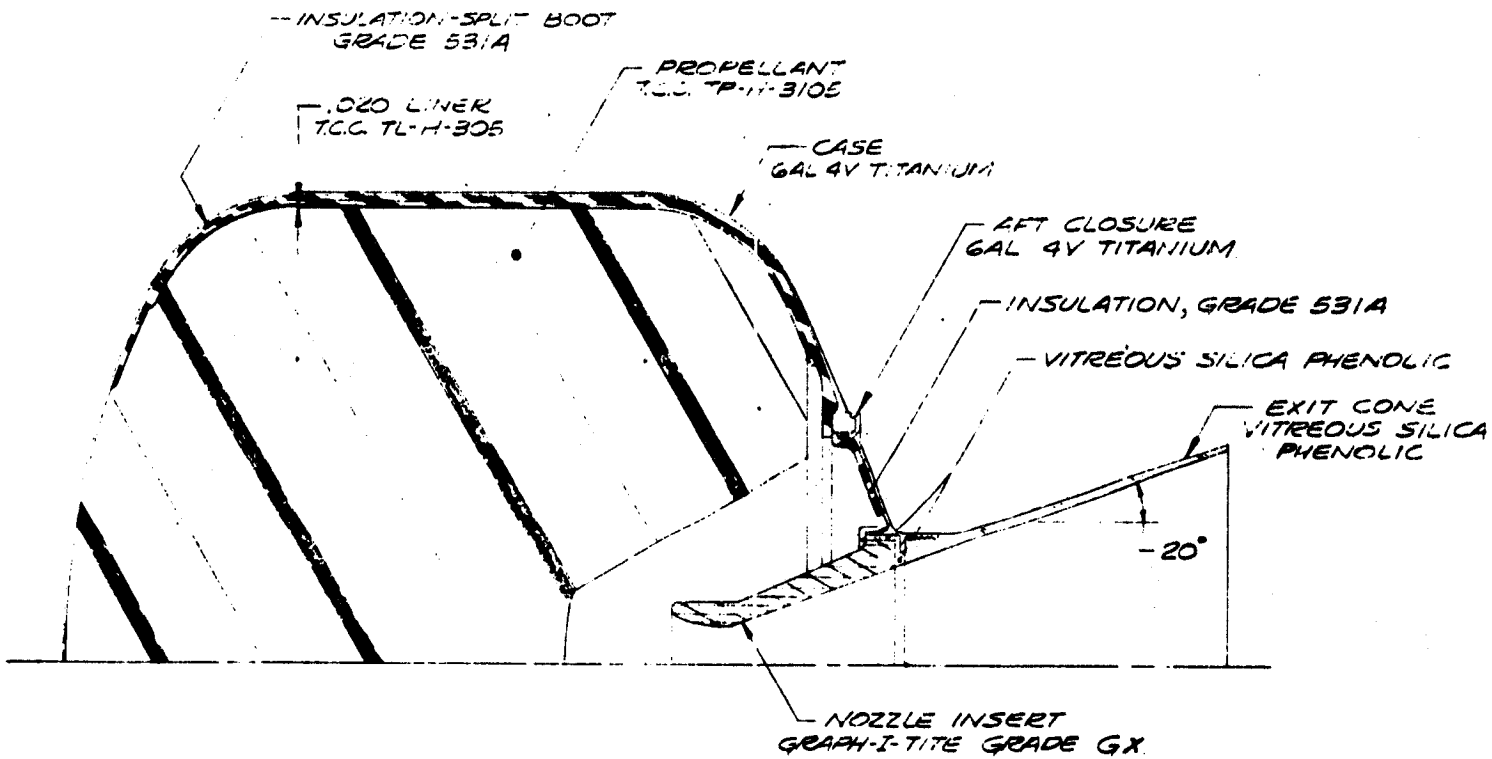

	R. JOHNSON	20 JAN 66	Thiokol CHEMICAL CORPORATION ELKTON DIVISION ELKTON, MARYLAND
	T.J. [illegible]	[illegible]	DESIGN "D" EXTERNALLY RELIEVED END BURNING MOTOR DESIGN
DESIGN ACTIVITY APPROVAL			CODE IDENT NO. 07299 / SIZE C / LO-1847
John P. King 25 Jan 66			SCALE 1/2 / WEIGHT / CALC ACTUAL / SHEET

ALL FINISHED SURFACES

WEIGHT BREAKDOWN AND MASS FRACTION

The weight of each motor component is given below:

Component	Weight, lbs
Case and Closure	3.0
Case Insulation	4.7
Aft Closure Insulation	0.2
Nozzle Insert	0.8
Nozzle Backup Insulation	0.1
Exit Cone	1.0
Miscellaneous	1.0
Line	0.6
PYROGEN	1.0
TOTAL Inert	12.4
Propellant	100.0
TOTAL	112.4
Mass Fraction	0.89

It is very doubtful that this mass fraction could be increased because the loading density of the design studied is already quite high.

a. Areas of Stress Concentration

This design consists of an end-burning grain having a truncated cone perforation on the aft end. It is cast into a split insulation sleeve which is relieved through all of the cylindrical section; the grain is bonded into place on the head end only. The split boot should allow freedom of expansion both longitudinally and radially over the firing temperature range. The areas of stress concentration are the split boot itself and possibly the truncated core portion of the aft end (due to pressurization stresses).

b. Differential Expansion Effects

Differential expansion during heat-up to sterilization can not be taken up by outward radial growth of the grain; all expansion must take place longitudinally. This might introduce serious problems because the ramp action of the aft case will force the propellant to deform inward during expansion. This problem can be alleviated by spacing the gap between the split boots during curing and removing the spaces later and also by casting only in the cylindrical section of the motor. Both of these approaches will decrease the volumetric loading density and mass fraction.

c. Time to Reach Temperature

The calculated time for this grain to reach temperature is 73 hours. This is somewhat pessimistic because no heat transfer was allowed for along the split line air gap between the insulation sections.

d. Design Experience

Some design experience exists with end-burning gas generators and rocket motor sustainers. However, there is a lack of data on such extensive relief boots, and casting the grain with a space between the sections of the split boot will be a difficult procedure.

f. Design Complexity

The design is not complex; however, stress concentrations exist where the grain is supported and there is a truncated core in the aft end of the grain.

g. Effects of Vibration, Spin, Etc.

This design, because of the unsupported nature of the grain except for head-end bonding, will be subject to vibration and slump. It will also be subject to imbalance during spin, especially at -40° F. This is because there will be clearance all the way around the motor at this temperature and any unbalance will cause the grain to deflect to one side. The grain should not be subject to resonance because of the submerged nozzle section and the absence of a long cylindrical internal cavity. It will, however, be subject to g loading because all longitudinal g loads must be taken out at the head-end extension. This could be alleviated by an internal support, but the support will increase the complexity of the grain because a strong mechanical attachment method will be necessary.

h. Neutrality

The calculated ratio of maximum to minimum surface area for this design is 1.91. The maximum surface area occurs at about 60% web. The grain could be made more neutral by increasing the depth of the truncated cone section but this would lower the volumetric loading density. This design has sliver at burnout which could be eliminated by using inert sliver to reduce the volumetric loading density or by using a flatter dome for the forward section of the grain which increases the motor weight.

i. Effect of Scale-up or Scale-down

The design probably can not be scaled up much beyond its present size because burn time would exceed 60-70 seconds, requiring more insulation. Loading due to g's, vibration, etc. will be very high requiring the use of an internal grain support. The insulation requirements for larger motors could probably be reduced somewhat if a faster burning propellant were used.

5. Design E — Rod and Tube Motor Design

This design consists of two completely separate grains. The motor assembly is shown in Drawing LO 1851. The tube grain is a cylindrically perforated, case-bonded grain of PT-H-3105 propellant. This grain is 12.3 inches in diameter and has an outside diameter of 15 inches. The perforation is 8.3 inches in diameter. At each end of this shell grain, the chamber wall is insulated by asbestos-filled polyisoprene. These insulation sections extend a distance of 0.5 inch into the cylindrical section of the motor. Each section incorporates a split boot which extends for half the web thickness.

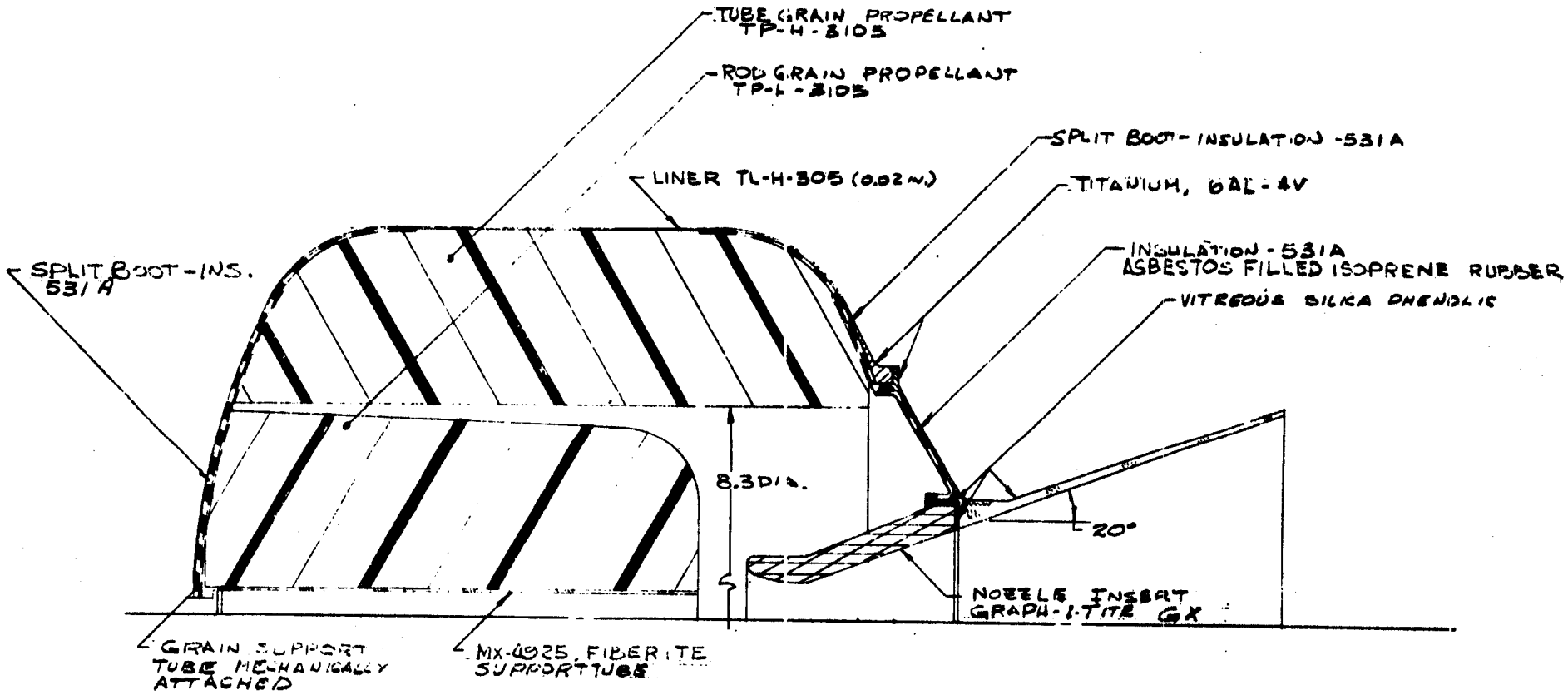

UNLESS OTHERWISE SPECIFIED: DIMENSIONS ARE IN INCHES TOLERANCES XX ± .01 XXX ± .010 ANGULAR ± 30' FRACTIONS ± 1/16 BREAK SHARP EDGES .003-.015 ALL SMALL FILLETS .020-.040 R THREADS FORMED, KNURLING AND ASSEMBLY PER MIL-STD-8 DIMENSIONING PER MIL-STD-8 WELD SYMBOLS PER JAN-STD-19 SURFACE ROUGHNESS SYMBOLS PER MIL-STD-10 ALL FINISHED SURFACES	DRAWN	T.J. Kinchen Jr.	25 Jan 66
	CHECKED	Burke	2/1/66
	ENGR	T.J. Kinchen	25 Jan 66
	ENGR		
	ENGR		
	USER		
	STRESS		
	SAFETY		
	APPD		
	DESIGN ACTIVITY APPROVAL	John P. King	25 Jan 66

Thiokol CHEMICAL CORPORATION
ELKTON DIVISION ELKTON, MARYLAND

DESIGN E
ROD & TUBE MOTOR DESIGN

CODE IDENT NO.	SIZE	
07299	C	LO-1851

SCALE	WEIGHT	CALC ACTUAL	SHEET

The rod grain is 9.6 inches long and 8 inches in diameter. It is supported internally by a 1.10-inch diameter, 0.05-inch thick, support table of MX 4925 carbon fiber reinforced phenolic. This support rod extends to the forward dome of the motor and is held in place by a mechanical attachment. The forward portion of the rod grain is inhibited by a layer of asbestos-filled polyisoprene insulation.

The aft closure assembly consists of the 6Al 4V titanium aft closure which is insulated by a 0.10-inch thick layer of asbestos-filled polyisoprene insulation. The nozzle insert is Graph-I-Tite GX backed up by two vitreous silica phenolic insulation sleeves. The exit cone is vitreous silica 30/1 with a 20-degree half angle.

WEIGHT BREAKDOWN AND MASS FRACTION

The weight breakdown for the motor is shown below:

Component	Weight, lbs
Case and Closure	7.0
Case Insulation	1.8
Aft Closure Insulation	0.3
Rod Grain Support	0.1
Nozzle Insert	1.3
Nozzle Backup Insulation	0.1
Exit Cone	1.3
Miscellaneous	1.0
Liner	0.6
PYROGEN	1.0
TOTAL Inert	14.5
Propellant	100.0
TOTAL	114.5
Mass Fraction	0.87

This mass fraction can be increased by casting some propellant on the aft closure of the motor (i.e., around the nozzle section). This increases the complexity of the design.

a. Areas of Stress Concentration

This design has no star points; however, it is made up of two grains. The shell grain has two stress relief boots which will allow some expansion in the radial direction over the firing range required. The rod grain is completely supported by an internal support structure which probably can be designed to have the same expansion properties as the propellant. This rod is completely supported by the internal support. The areas of possible stress concentration are the two split boots in the shell section and the support and split insulation section in the rod portion of the grain.

b. Differential Expansion Effects

Some differential expansion will be taken up by the short relief boots at the ends of the shell grain; however, as in the case of the cylindrical design, compressive stresses will probably be set up because of the ramp effect discussed previously. Expansion of the shell grain must take place in a radial direction. This could be alleviated somewhat by casting the grain with spacers between the split parts of the boot. However, the boot would have to be moved out to the cylindrical section of the case.

Differential expansion of the rod grain will be a problem if a support material is used which has a coefficient of linear expansion much different from that of propellant. It appears that a cast phenolic or epoxy material could serve the purpose of the support; this will allow the grain to expand radially and longitudinally.

c. Time to Reach Temperature

The time calculated for this grain to reach sterilization temperature is 76 hours. This may be somewhat less since there was no heat transfer by convection assumed between the shell and rod grains.

d. Design Experience

Design experience is somewhat lacking. The shell portion of the grains can probably be manufactured by existing techniques except for the somewhat more complex use of spacers between the sections of the split boot. The rod grain must be manufactured separately, loaded into the motor and mechanically supported from the head end.

e. Design Complexity

This design is much more complex than any of the designs previously discussed. The design consists of two grains. The shell grain uses two split boots and is cast into the case. The rod grain consists of an internal support of rigid material and an insulation section on the forward end of the grain. The support must be mechanically held in the motor.

f. Effects of Vibration, Spin, Etc.

Vibration will certainly have an effect on this motor because of the cantilevered nature of the rod grain. The effects of slump, however, should be negligible because of the internal grain support. Resonance can occur because of the toroidal nature of the air space. If resonance occurs it can coupled with the vibrational characteristics of the rod and amplify the vibration to the point of failure. Spinning will also have a pronounced effect on this design. Differences in the inward or outward radial burn rate will cause the rod or tube to burn out rapidly and cause "psuedo-sliver" (i.e., the rod portion of the grain will still be burning). If the spin rate is very high, this difference in burn rate is magnified considerably. G-loading may also be severe since all the load must be taken out by the support structure. Cruciform sections extended outward from the internal support can alleviate the problem.

g. Neutrality

The ratio of maximum to minimum surface area for this design is 1.86. This can be reduced considerably by changing the angle on the rod grain outside surface or by increasing the web thickness on the rod grain; however, this would introduce sliver. The support sleeve could also be tapered to reduce this ratio. The maximum surface area occurs at 0% web and regresses gradually until, at the 100% point, the surface area drops off suddenly.

h. Effect of Scale-up or Scale-down

This design probably can not be scaled up above 1000 pounds because of the nature of the support for the rod grain. It would have to be changed to a cruicform design requiring a stronger support member.

C. RATING AND SELECTION OF TWO CANDIDATES

The designs were re-weighted in the same manner as before, with these exceptions:

1) the effort of scale-up criteria was substituted for the effort of a shorter L/D and

2) the rating for neutrality was modified to include the effects of sliver. If sliver was present,the neutrality rating decreased one point.

The rating numbers were changed slightly during this phase to reflect the use of the shorter L/D designs. The changes in these ratings are summarized below:

MASS FRACTION RATING

	Quality Points
> 0.88	4
> 0.84 to ≤ 0.88	3
> 0.80 to ≤ 0.84	2
> 0.76 to ≤ 0.80	1
≤ 0.76 and below	0

FREEDOM FROM DIFFERENTIAL EXPANSION

	Quality Points
Grain free to move in all directions	4
Grain free to move radially on outside surface and longitudinally	3
Grain free to move radially inside and longitudinally	2
Grain free to move longitudinally	1

TIME TO TEMPERATURE

	Quality Points
< 20 hrs	4
> 20 and ≤ 40 hrs	3
> 40 and ≤ 60 hrs	2
> 60 and ≤ 80 hrs	1
> 80 hrs	0

EXPOSED SURFACE AREA

< 200 MS	4
> 200 and ≤ 300	3
> 300 and ≤ 400	2
> 400 and ≤ 500	1
> 500	0

NEUTRALITY OF SURFACE AREA
RATIO MAXIMUM TO MINIMUM SURFACE AREA

< 1.25	4
> 1.25 ≤ 1.5	3
> 1.5 ≤ 1.75	2
> 1.75 ≤ 2.0	1
> 2.0	0

(In addition, the presence of sliver reduces the rating index by 1 point.)

All other parameters used to weight the designs were the same as those previously discussed.

Based on the Final Weighting Chart, Table D-I, the Case-Bonded design selected was a Circular Perforated Spherical Design. From the Free-Standing designs, the Internal-External Burning Grain was selected.

TABLE D-I

FINAL WEIGHTING CHART
HEAT STERILIZABLE MOTOR DESIGN STUDY

	Mass Fraction Weight 2		Freedom from Stress Concentrations Weight 5		Freedom from Differential Expansion Weight 4		Time to Sterilization Temperature Weight 2		Surface Area Exposed Weight 2		Design Experience Weight 3		Design Complexity Weight 5		Effects of Vibration, Spin, etc. Weight 2		Neutrality of Surface Area and Freedom from Sliver Weight 1		Low Temperature Capability Weight 3		Effect of Scale-up or Scale-down Weight 2		Total Points
	Quality Points	Total	Quality Points	Total	Quality Points	Total	Quality Points	Total	Quality Points	Total	Quality Points	Total	Quality Points	Total	Quality Points	Total	Quality Points	Total	Quality Points	Total	Quality Points	Total	
CASE BONDED DESIGNS																							
A. Circular Spherical Perforate Design	4	8	4	20	3	12	3	6	2	4	3.5	10.5	4	20	2.5	5	3	3	4	12	4	8	108.5
B. Circular Perforated Cylindrical Design	3	6	3	15	2.5	10	3	6	1	2	4	12	3	15	3	6	2	2	3	9	4	8	91.0
Free Standing Designs																							
C. Internal-External Burning Free-Standing Grain	0	0	3	15	3.5	14	1	2	0	0	4	12	3	15	2	4	2	2	3	9	2	4	77.0
D. Externally Relieved End Burner	4	8	2	10	1	4	1	2	3	6	3	9	2	10	2	4	0	0	2	6	1	2	61.0
E. Rod and Shell Design	3	6	3	15	2	8	1	2	0	0	3	9	3	15	2	4	1	1	3	9	2.5	5	74.0

APPENDIX E

FINAL CANDIDATE DESIGNS

PRELIMINARY DESIGN

CASE-BONDED SPHERICAL CIRCULAR PERFORATE MOTOR DESIGN
REF: DRAWING E-18605

PROPELLANT	TP-H-3105
GRAIN DESIGN	
Type	Case-bonded, cylindrical perforate sphere
Outside Diameter, in.	16.14
Length, in.	12.45
NOZZLE DESIGN	
Throat Area, $in.^2$	1.306
Expansion Ratio	30.0
Exit Area, $in.^2$	39.18
Nozzle Half Angle, degrees	20
CASE DESIGN	
Material	6 Al 4V Titanium
Yield Strength at 120° F, psi	147,000
Outside Diameter, in.	16.23
Minimum Wall Thickness, in.	0.023
Yield Pressure, psia	835
Hydrostatic Test Pressure, psia	695
Hydrostatic Test Pressure/Maximum Pressure at 120° F	1.10
Yield Pressure/Hydrostatic Test Pressure	1.20

MOTOR PERFORMANCE: Nominal Calculated at Vacuum Expansion Ratio = 30.0, Discharge Coefficient = 0.96

Temperature, °F	-40	+0	+40	±80	+120
Thrust, Maximum, lbf	1134	1195	1258	1325	1395
Thrust, Average, lbf	943	993	1043	1101	1160
Thrust, Minimum, lbf	644	678	715	754	794
Pressure, Maximum, psia	514	541	570	600	632
Pressure, Average, psia	427	450	474	499	525
Pressure, Minimum, psia	292	307	324	342	360
Burning Time, sec.	26.85	25.54	24.30	23.11	21.98
Propellant Specific Impulse lbf-sec/lbm	253	254	254	255	255
Total Impulse, lbf-sec	25,340	25,390	25,440	25,490	25,530

PRELIMINARY DESIGN

INTERNAL-EXTERNAL BURNING FREE-STANDING MOTOR DESIGN
REF: DRAWING E-18609

PROPELLANT	TP-H-3105
GRAIN DESIGN	
Type	Free-Standing, Internal-External Burning
Outside Diameter, in.	12.2
Length, in.	15.47
NOZZLE DESIGN	
Throat Area, $in.^2$	2.517
Expansion Ratio	30.0
Exit Area, $in.^2$	75.51
Nozzle Half Angle, Degrees	20.
CASE DESIGN	
Material	6 Al 4V Titanium
Yield Strength at 120°F, psi	147,000
Outside Diameter, in.	13.19
Minimum Wall Thickness, in.	0.043
Yield Pressure, psia	962
Hydrostatic Test Pressure, psia	805
Hydrostatic Test Pressure/Maximum Pressure at 120°F	1.10
Yield Pressure/Hydrostatic Test Pressure	1.20

MOTOR PERFORMANCE: Nominal Calculated at Vacuum, Expansion Ratio = 30.0
Discharge Coefficient = 0.96

Temperature, °F	-40	+0	+40	+80	+120
Thrust, Maximum, lbf	2526	2660	2800	2949	3104
Thrust, Average, lbf	1812	1909	2010	2117	2230
Thrust, Minimum, lbf	1119	1178	1241	1307	1378
Pressure, Maximum, psia	594	625	659	693	730
Pressure, Average, psia	426	449	473	498	524
Pressure, Minimum, psia	263	277	292	307	324
Burning Time, sec	13.96	13.28	12.63	12.02	11.43
Propellant Specific Impulse lbf-sec/lbm	253	254	254	255	255
Total Impulse, lbf-sec	25,340	25,390	25,440	25,480	25,530

E15-66-12

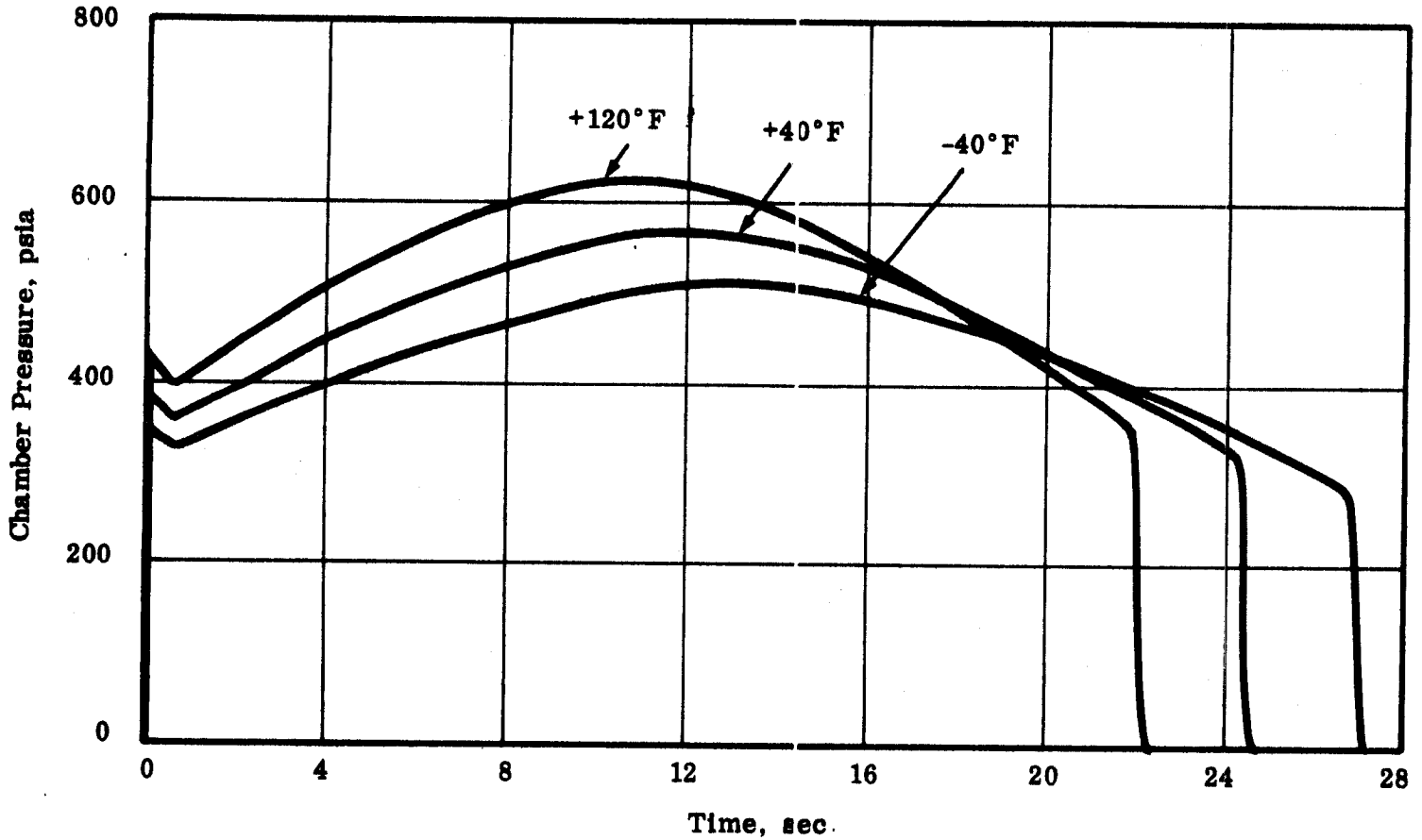

FIGURE E-1. CASE-BONDED SPHERICAL CIRCULAR PERFORATE MOTOR DESIGN CHAMBER PRESSURE VS TIME

E15-66-13

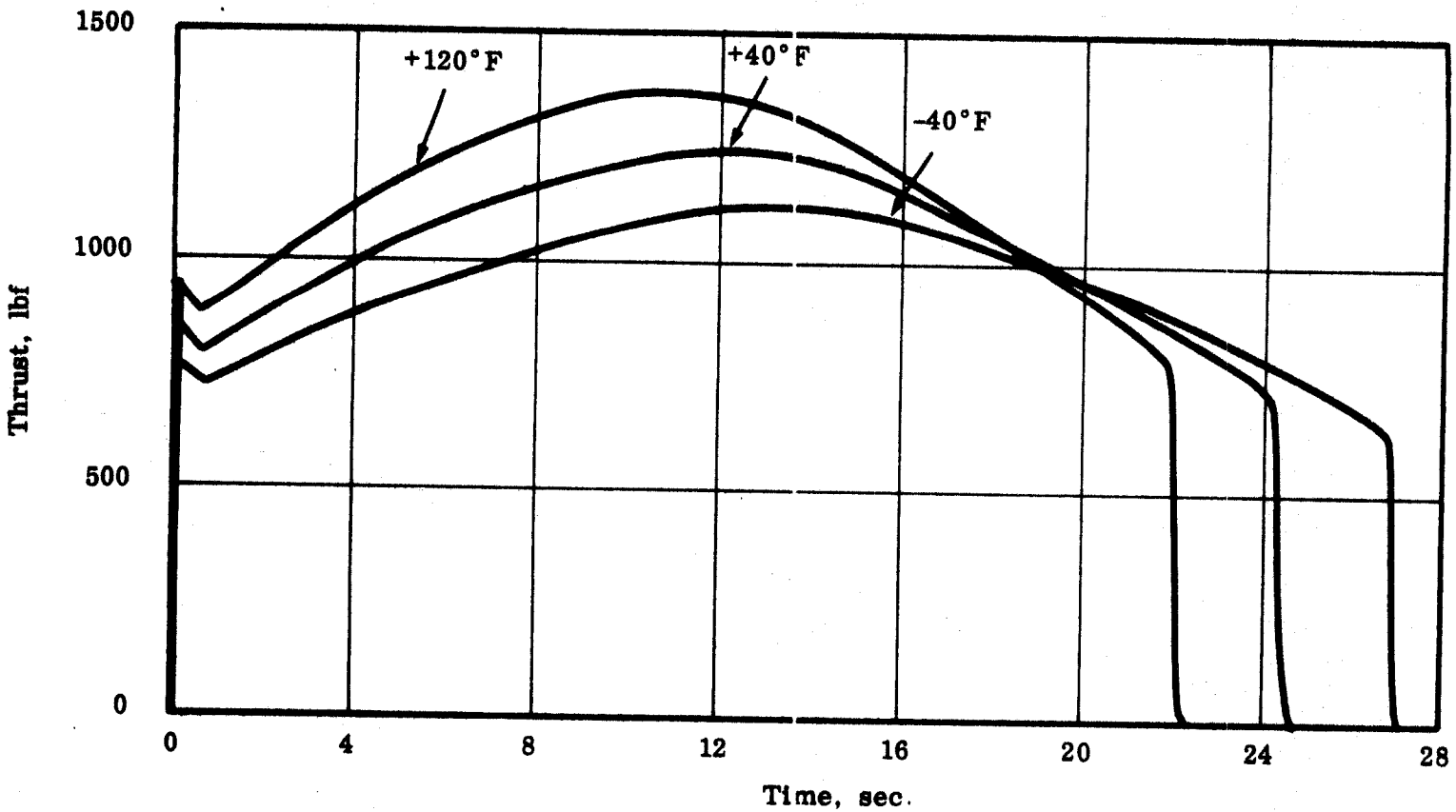

FIGURE E-2. CASE-BONDED SPHERICAL CIRCULAR PERFORATE MOTOR DESIGN THRUST VS TIME*

*Nominal Calculated at Vacuum, Expansion Ratio = 30, Discharge Coefficient = 0.96

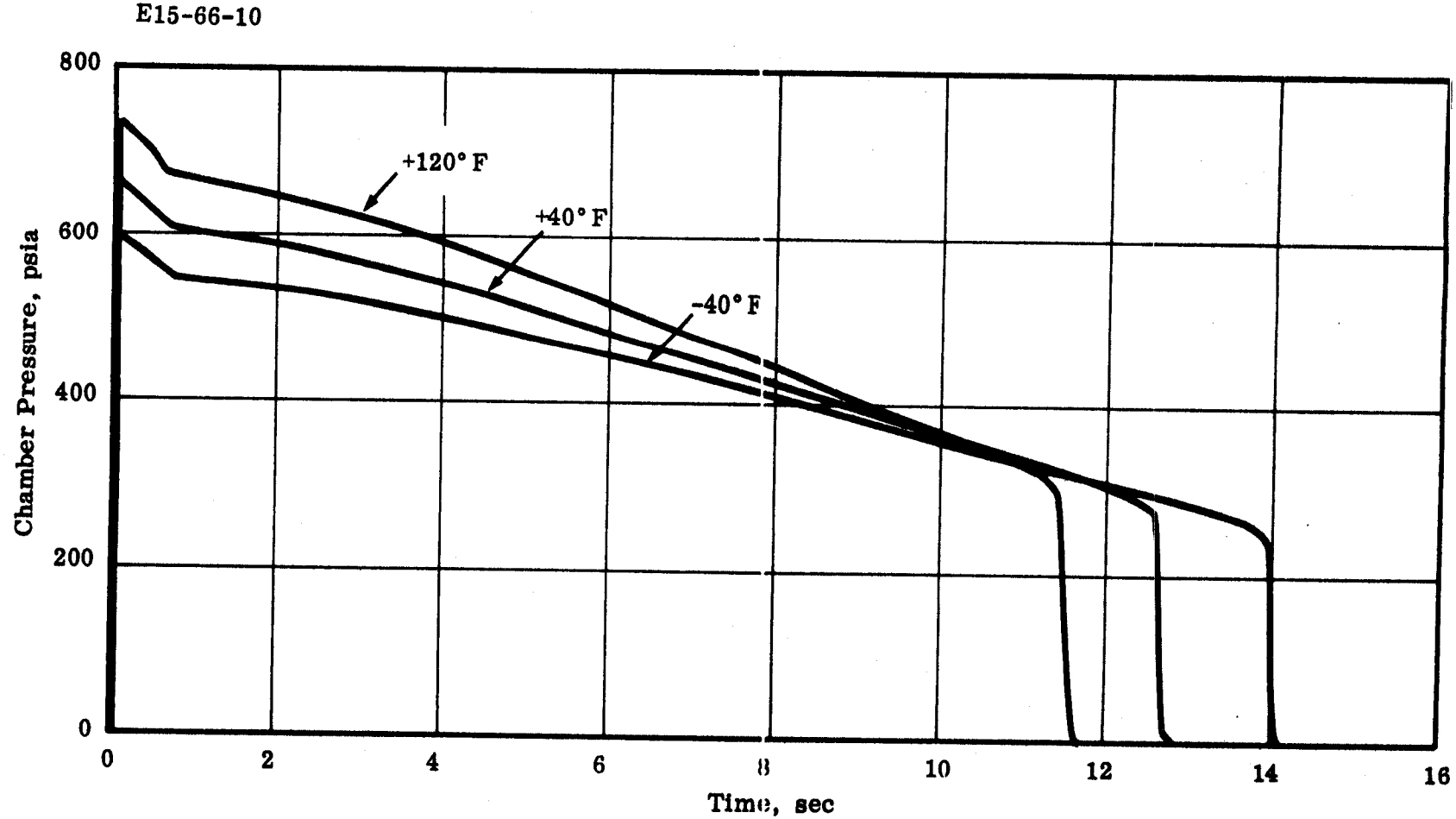

FIGURE E-3. INTERNAL-EXTERNAL BURNING FREE-STANDING MOTOR DESIGN CHAMBER PRESSURE VERSUS TIME

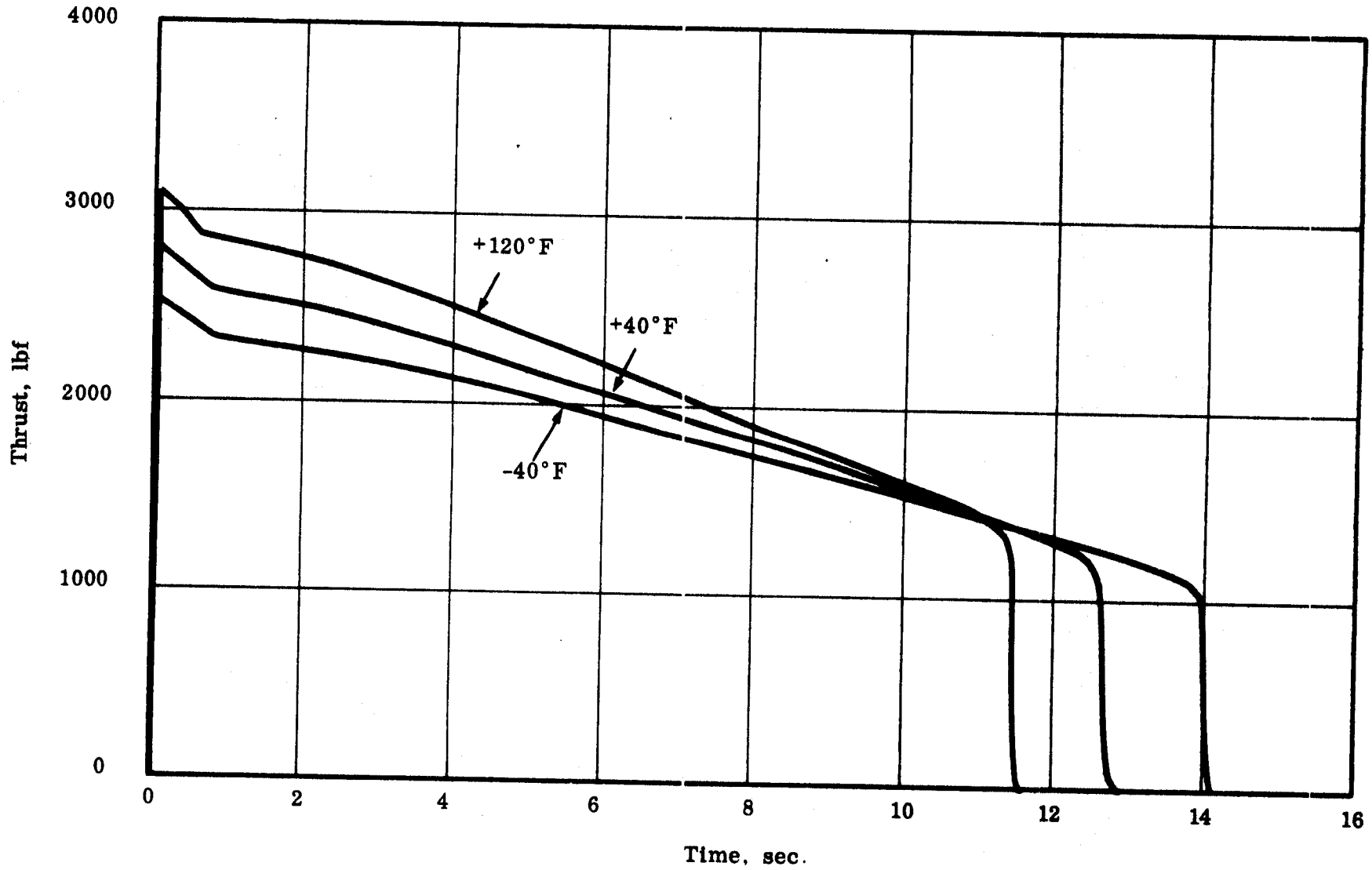

FIGURE E-4. INTERNAL-EXTERNAL BURNING FREE-STANDING MOTOR DESIGN THRUST VS TIME*

*Nominal Calculated at Vacuum, Expansion Ratio = 30, Discharge Coefficient = 0.96

APPENDIX F

HEATING TIME CALCULATIONS — FINAL CANDIDATES

An analysis was made to determine the time required to heat the grain from 70° F to the sterilization temperature of 295 ±2° F. This analysis assumed that heat flow occured through the external boundary only and the external film coefficient was based on forced convection. The heating time was 40 hours for the case-bonded motor and 70 hours for the free-standing design.

THERMAL MODEL AND THEORETICAL ANALYSIS

The results for determining the heating time of the motor were calculated by using a two-dimensional axisymmetrical transient heat transfer analysis. This was performed using Thiokol Program No. 40702 Entitled "Arbitrary Node Thermal Computer Program." This program performs a two-dimensional axisymmetrical heat transfer analysis and can consider as many as 12 different materials. Material properties can be varied with respect to temperature and almost any variation in boundary conditions can be analyzed with respect to time and location. The program can also simulate air gaps by using zero capacity nodes and contact resistances between adjacent nodes.

The thermal model for the case-bonded spherical design is shown in Figure F-1, a two-dimensional nodal array that closely approximates the longitudinal grain section. Figure F-2 shows the locations and numbers of nodes. For this analysis, the case material was neglected. This simplifying assumption has little effect on the results of the calculations since the thermal diffusivity of the case material is high compared to that of the propellant and case insulation. Heat flow is allowed to take place through the external spherical surface only. The internal portion of the grain and the end of the grain are assumed to be adiabatic surfaces. This makes the analysis somewhat conservative since, in actuality, case heating of the motor on all surfaces (especially the nozzle structure) would reduce the time required to heat to 295 ±2° F.

The properties of the propellant and insulation used are as follows:

Material	Density	Specific Heat	Thermal Conductivity
Asbestos-filled polyisoprene Insulation	0.043 lb/m^3	0.392 btu/lb/° F	2.638×10^{-6} btu/M sec ° F
TP-H-3105 Propellant	0.0595 lb/m^3	0.272 btu/lb/° F	3.528×10^{-6} btu/in. sec ° F

The external film coefficient was based on forced convection on the outside of the motor case. A heat transfer coefficient of 2.0×10^{-6} btu/° F sec $in.^2$ at 50° F increasing to 2.199×10^{-6} btu/° F sec $in.^2$ + 305° F was used. The driving temperature for this analysis was 305° F.

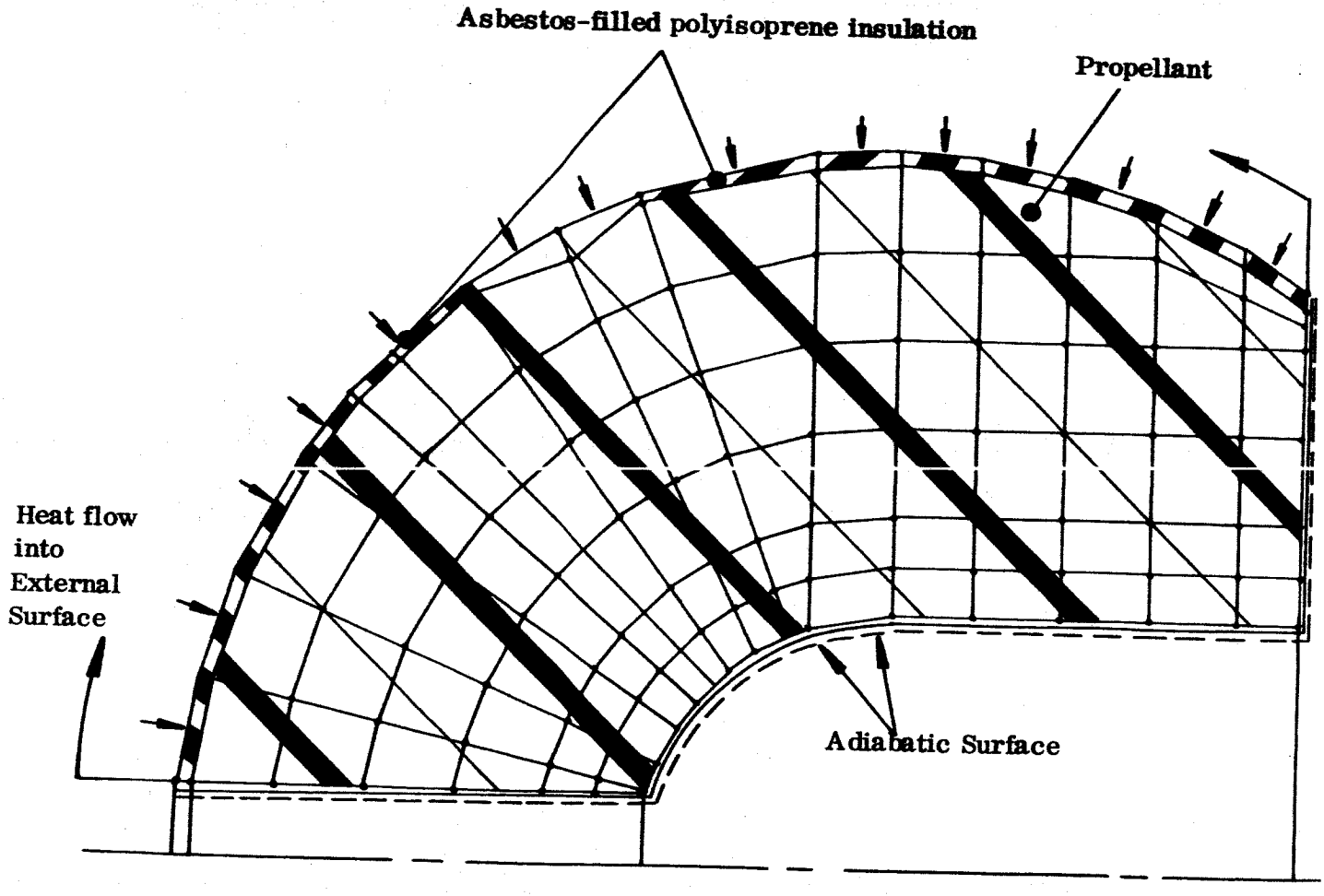

FIGURE F-1. THERMAL MODEL CASE-BONDED SPHERICAL CIRCULAR PERFORATE MOTOR DESIGN

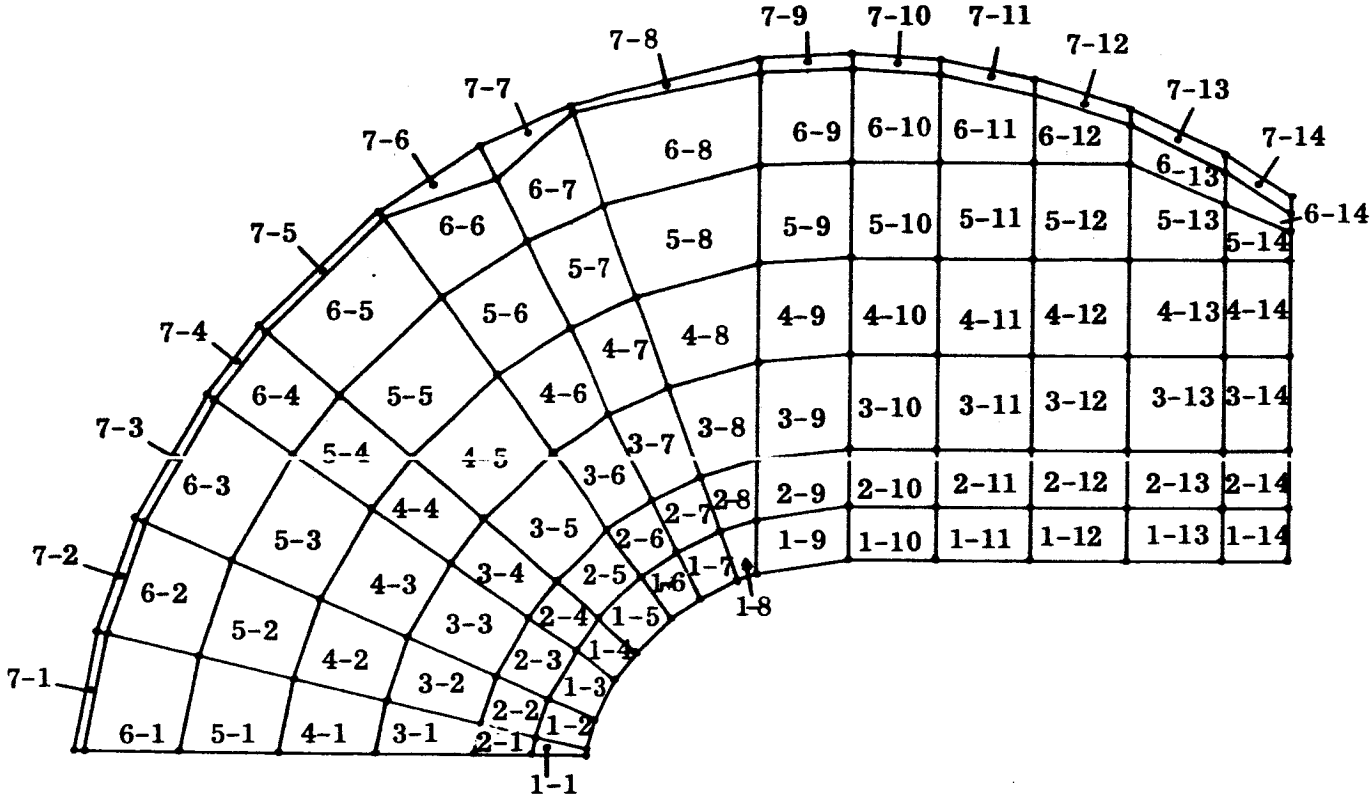

FIGURE F-2. NODAL LOCATIONS AND NOTATION
CASE-BONDED SPHERICAL CIRCULAR PERFORATE MOTOR DESIGN

Figure F-3 presents the temperature-time history of various nodes through the grain, and Figure F-4 shows the temperature distribution throughout the grain at the end of 40 hours.

The thermal model used for the Internal-External Burning Free-Standing Motor is shown in Figure F-5. The numbers and locations of the nodes are given in Figure F-6.

In this case, there is an 0.25-inch wide nitrogen gap between the propellant and case insulation. This is simulated by the use of a zero capacity thermal node. Heat flow in this design also takes place through the external surface of the motor only. Note that the phenolic support cartridge has been removed. This was done in order to reduce the computation time to acceptable levels because the initiation time for the computer is based on the smallest dimension. However, since the thermal conductivity of phenolic materials is very similar to that of propellant, this assumption does not seriously affect the analyses. This calculation is somewhat conservative for the same reasons that were discussed previously.

The material properties used for this calculation were:

Material	Density	Specific Heat	Thermal Conductivity
RPD 150 Insulation	0.0642 lb/in.^{3}	0.308 btu/lb °F	3.843×10^{-6} btu/in. sec °F
TP-H-3105 Propellant	0.0595 lb/in.^{3}	0.272 btu/lb °F	3.528×10^{-6} btu/in. sec °F
Nitrogen Gas	4.209×10^{-5} lb/in.^{3}	0.0	3.517×10^{-7} btu/in. sec °F

The external film coefficients and driving temperatures were identical to those used for the case-bonded design.

The results of this analysis are shown in Figure F-7 which presents a temperature-time history for various nodes. Figure F-8 gives the temperature through the grain at the end of 70 hours.

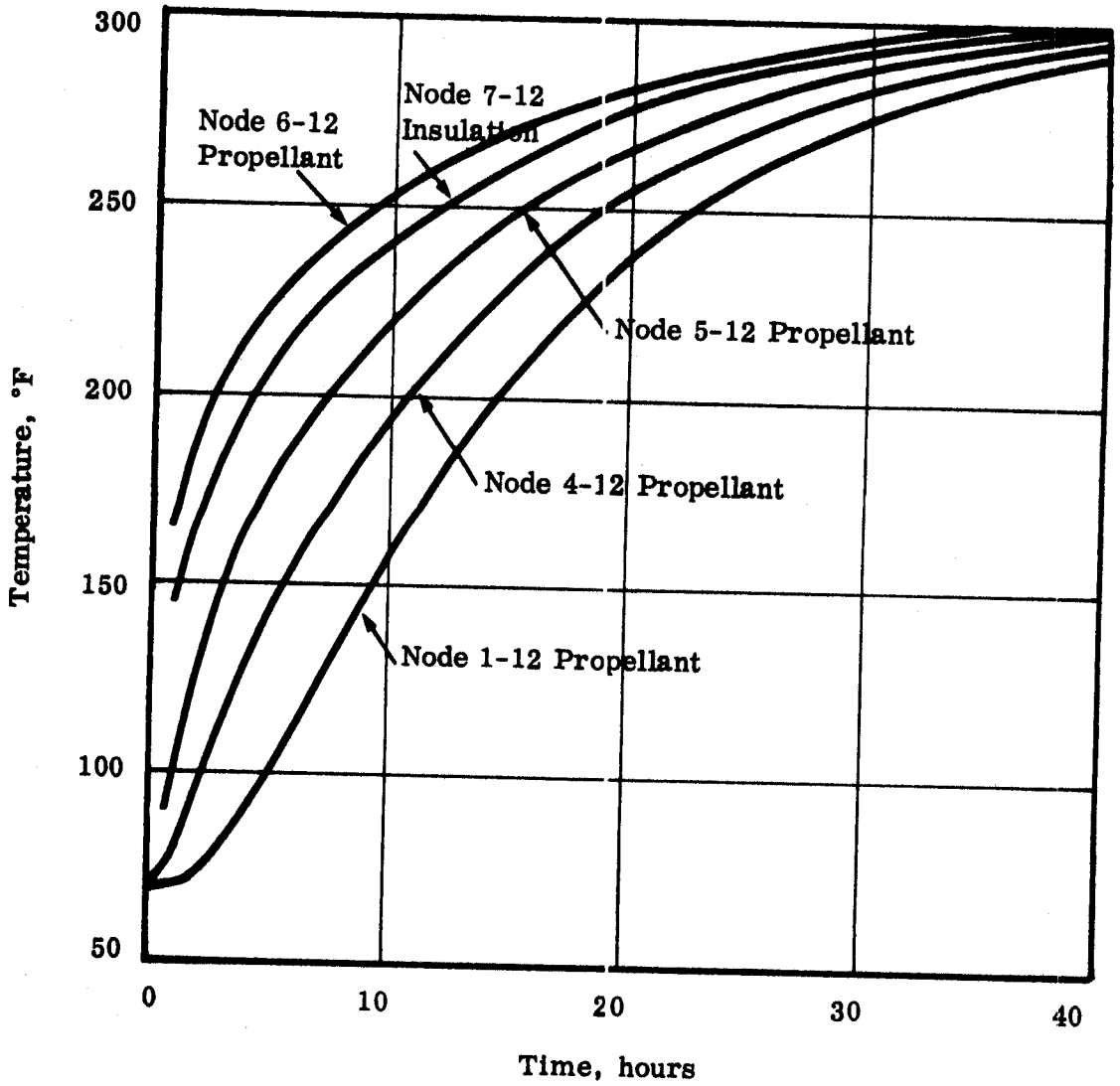

FIGURE F-3. CASE-BONDED SPHERICAL CIRCULAR PERFORATE MOTOR DESIGN TEMPERATURE VERSUS TIME FOR HEATING BY FORCED CONVECTION

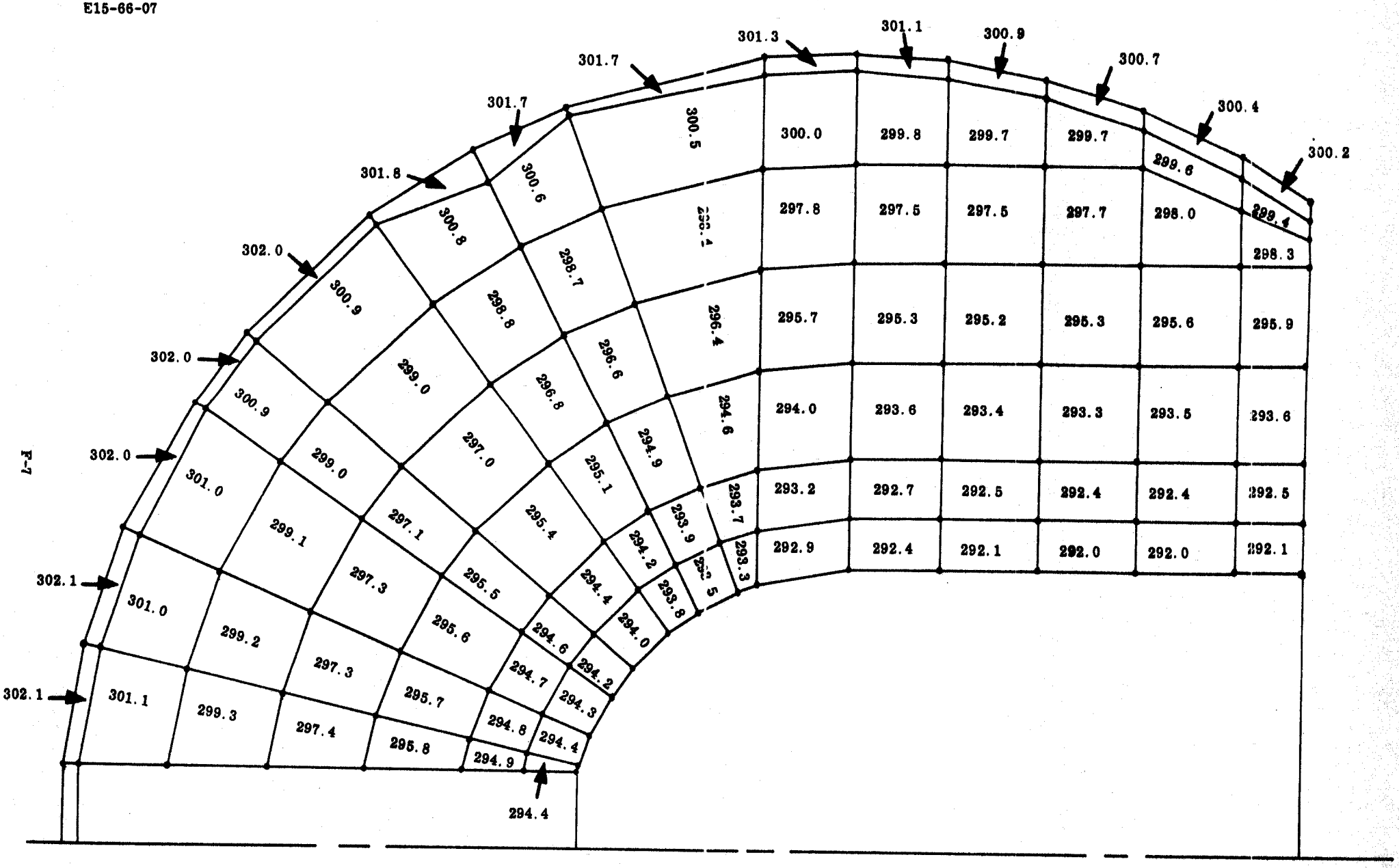

F-7

Nodal Temperatures After 40 Hours

FIGURE F-4. CASE-BONDED SPHERICAL CIRCULAR PERFORATE MOTOR DESIGN

E15-66-05

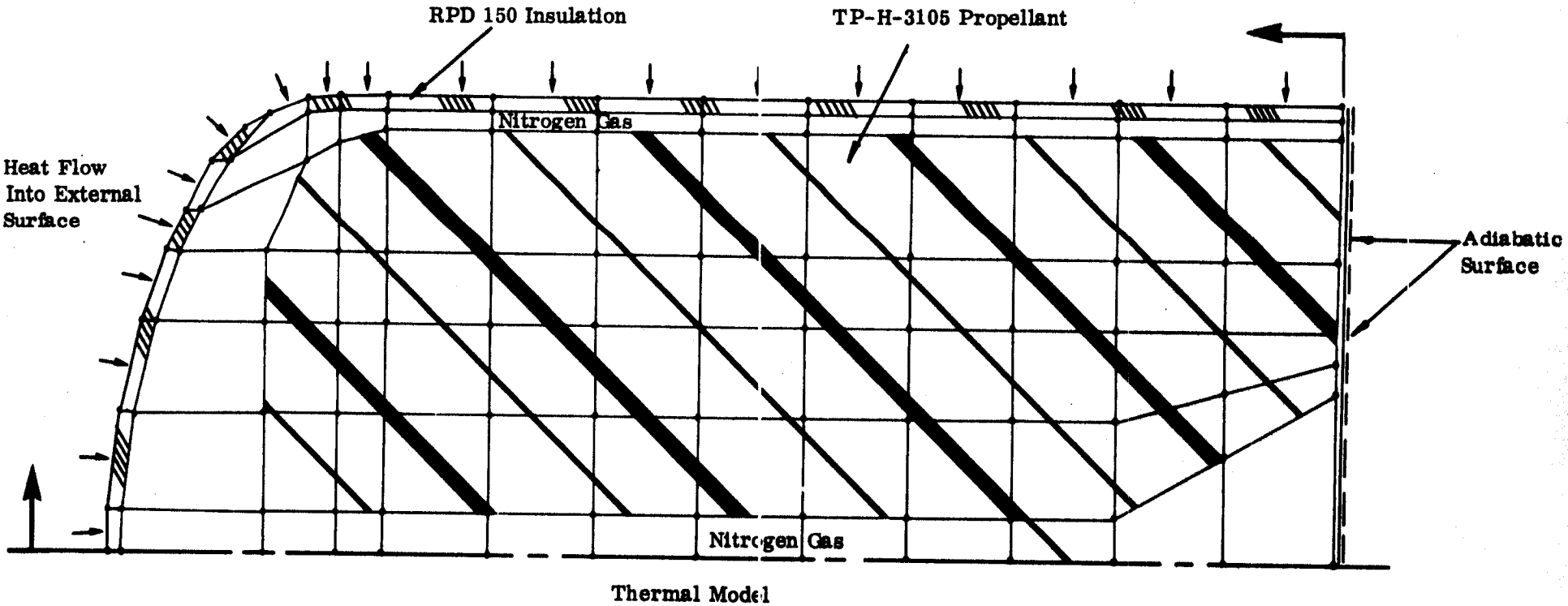

FIGURE F-5. INTERNAL-EXTERNAL BURNING FREE-STANDING MOTOR DESIGN

E15-66-04

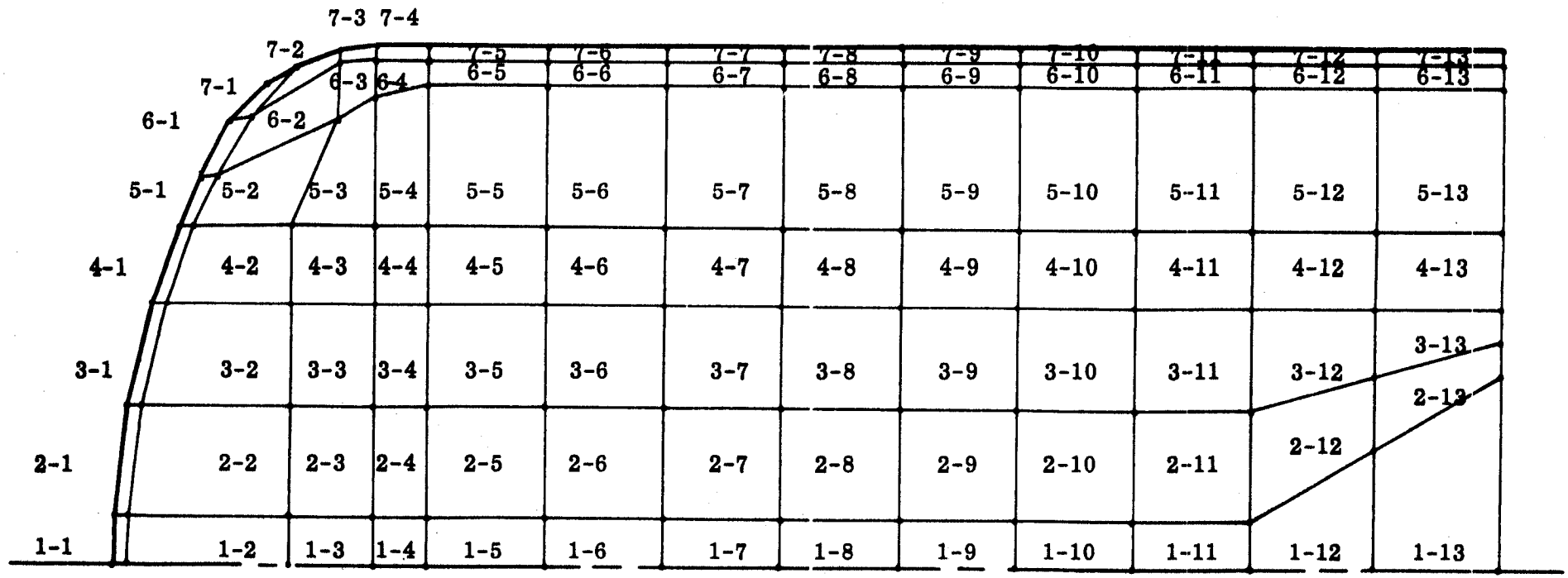

Nodal Locations and Notation

FIGURE F-6. INTERNAL-EXTERNAL BURNING FREE-STANDING MOTOR DESIGN

E15-66-03

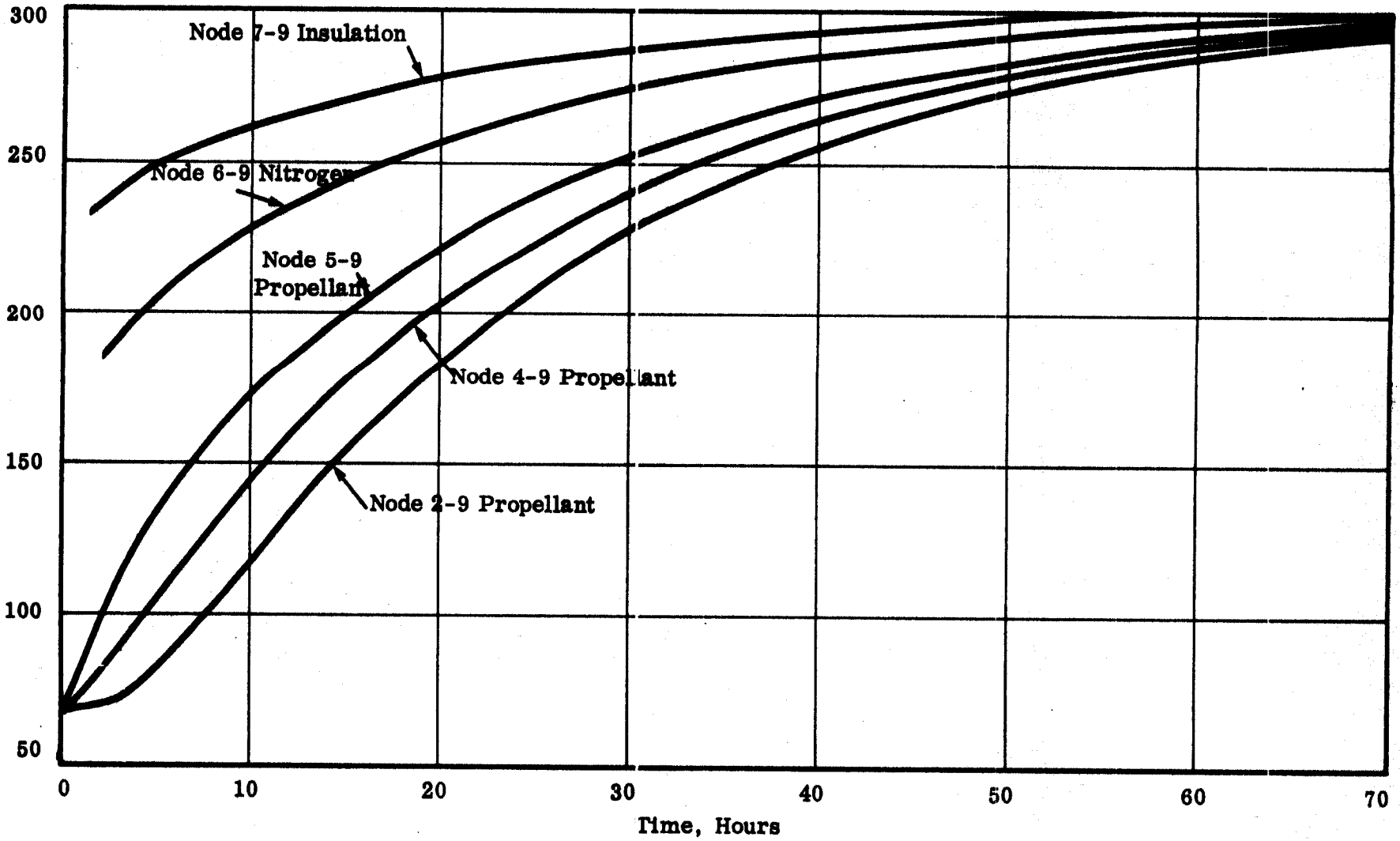

FIGURE F-7. INTERNAL-EXTERNAL BURNING FREE-STANDING MOTOR DESIGN
TEMPERATURE VERSUS TIME
FOR HEATING BY FORCED CONVECTION

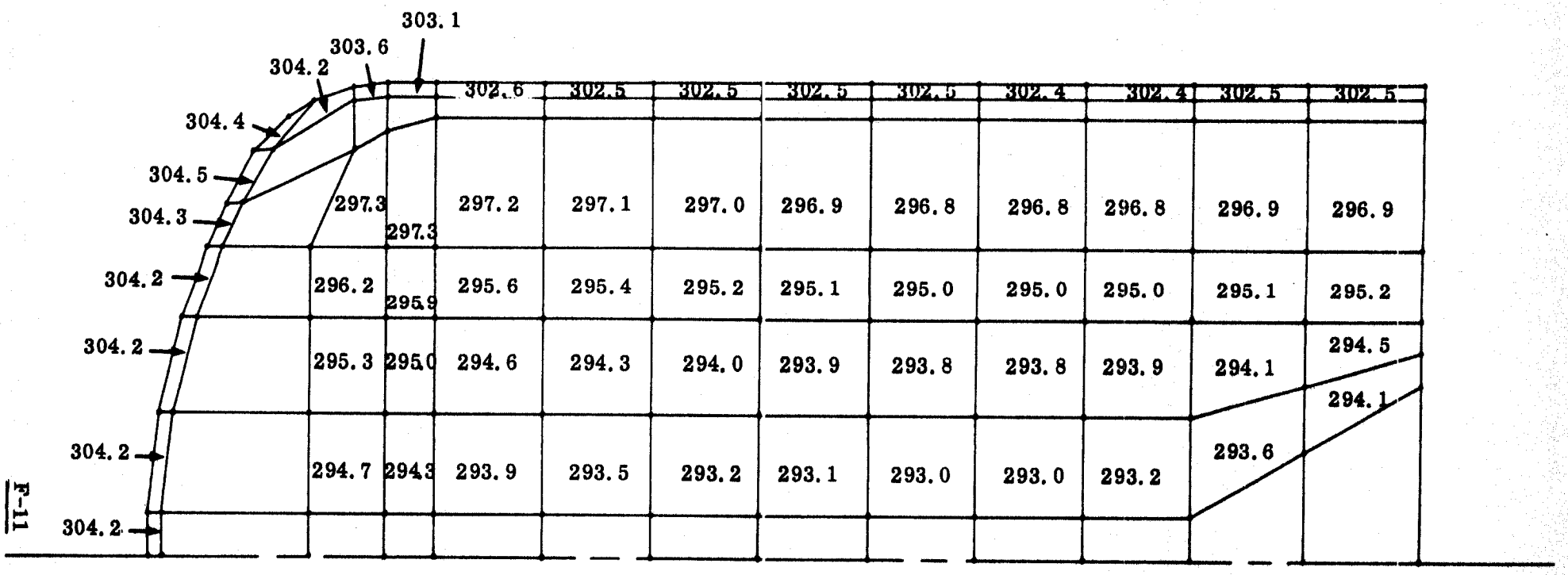

FIGURE F-8. NODAL TEMPERATURES AFTER 70 HOURS
INTERNAL-EXTERNAL BURNING FREE-STANDING MOTOR DESIGN

APPENDIX G

WEIGHT ANALYSIS — FINAL CANDIDATES

A. CASE-BONDED SPHERICAL — CYLINDRICAL PERFORATED MOTOR DESIGN
REF: DRAWING E-18605

Case

Sphere Shell $(.025)(15.23)(16.205)(\pi)(.162)$ =	3.14
Trans only at Aft Clos. $1/2(.100)(1.4)(8.25)(\pi)(.162)$	.29
Aft Clos. Boss $(.343)(.40)(7.1)(\pi)(.162)$	.50
Mounting Lugs $16(.050)(.75)(.60)(.162)$	.06
Trans. only $(.050)(2.5)(16.3)(\pi)(.162)$ =	1.04
	5.03 lbs

Insulation, Fwd Case

$(.14)(\pi)(.8)^2$ =	.28
$(.15)(2.15)(3.7)(\pi)$	3.75
$(.13)(2.95)(8.3)(\pi)$	10.00
$(.072)(1.5)(11.8)(\pi)$	4.00
$(.1)(.35)(1.7)(\pi)$	.19
$(.25)^2(.215)(1.9)(\pi)$ =	.08
	(18.30 cu in.)
	(.043) = .79

Insulation, Aft Case (ASB, Filled Polyisoprene)

$(.07)(2.1)(15.6)(\pi)$ =	7.21
Displaces Prop. 54.08 cu in. $(.12)(5.9)(15.3)(\pi)$	34.04
$(1/2)(.09)(14.4)(6.3)(\pi)$	12.83
$(.12)(4.3)(10.2)(\pi)$	16.54
	(70.62 cu in.)
	(.043) = 3.04

Liner & Adhesive $(.025)(15.23)(16.2)(\pi)(.05)$ = .97 lb

Exit Cone (Vitreous Silica Phenolic)

$(1/2)(.2 + .125)(3.84)(5.6)(\pi)(.065) =$ .71

$(.19)(.22)(4.3)(\pi)(.065)$ .04

$(1/2)(.38 + .12)(.72)(4.0)(\pi)(.065)$ .15

.87

Igniters (Gemini Type with Titanium Case)

$2\left[(.5)(.33 \text{ lb}) + (.5)(.33 \text{ lb})\left(\frac{.160}{.283}\right) + .08 \text{ lb}\right] =$ .68 lb

Closure Bolts

$(30)\left[(.138^2)(.375)+(.226^2-138^2)(.138)\right](.785)(.283) =$ .1

Propellant (.0595 lb/in.^{3})

Sphere $(4/3)(\pi)(8.09)^3(.0595) =$ 131.98

(-)Segment-$(1/3)(\pi)(3.48)^2\left[3(8.09)-348\right](.0595)$ 15.67

(-)Ign. Hole-$(1.6)^2(.785)(5.07)(.0595)$ .61

(-)Core H. Sphere-$(2/3)(\pi)(2.86)^3(.0595)$ 2.92

(-)Core, Cyl-$(\pi)(2.86)^2(4.61)(.0595)$ 7.05

(-)Fwd Insul. Vol (18.30 cu in.)(.0595) 1.09

(-)Aft Insul. Vol (54.08 cu in.)(.0595) 3.22

(-)Vol Liner & Adh-$(.97 \text{ lb})\left(\frac{.0595}{.05}\right)$ 1.15

100.27

Aft Closure

$(.14)(.29)(6.7)(\pi)(.162)$ =	.14
$(.53)(.15)(7.0)(\pi)(.162)$	.28
$(.070)(1.02)(5.5)(\pi)(.162)$	.20
$(.06)(.45)(4.5)(\pi)(.162)$	.06
$(.06)(.30)(4.2)(\pi)(.162)$	.04
$(.10)(.70)(4.4)(\pi)(.162)$	.16
$4(.75^2 - .43^2)(.785)(.57)(.162)$ =	.11
	.99 lb

Insulation, Aft Closure

$(.10)(1.7)(5.5)(\pi)(.043)$ =	.13 lb

Insert Insulation

$(.10)(.37)(4.3)(\pi)$ =	.50
$(.46)(.20)(3.9)(\pi)$	1.13
$-(.24)(.06)(4.15)(\pi)$ =	- .18
	(1.45 cu in.)
	(.065) = .09 lb

Insert, Graph-I-Tite G

$(.31)(1.0)(1.7)(\pi)(.069)$ =	.11
$(.42)(2.89)(2.8)(\pi)(.169)$ =	.74
	.85 lb

B. INTERNAL-EXTERNAL-BURN FREE-STANDING MOTOR DESIGN
REF: DRAWING E-18609

Case

Ign. Boss (.07)(.78)(2.93)(π)(.162) =	.08
Elip. Dome (.048)(4.16)(7.0)(π)(.162)	.71
Elip. Dome (.048)(2.43)(12.4)(π)(.162)	.74
Cyl (.048)(16.8)(13.2)(π)(.162)	5.42
Aft Boss(.33)(.44)(12.8)(π)(.162)	.95
Trans only 1/3(.33)(1.1)(12.9(π)(.162)	.79
Lugs 8(.10)(.7)(.8)(.162) =	.07
	8.76 lb

Insulation, Case (RPD 150)

(.20)(4.33)(6.7)(π)(.064) =	1.17
(.20)(2.29)(12.2)(π)(.064)	1.12
(.20)(16.1)(12.9)(π)(.064)	8.35
(.20)(.65)(6.7)(π)(.064)	.18
$(.312)^2$(.38)(7.3)(π)(.064)	.05
$(.5)^2$(.13)(6.3)(π)(.064) =	.04
	10.91 lb

Adhesive (Insul to Case & Closure)

(.010)(22.0)(13.08)(π)(.050) -	.45 lb

Aft Closure

$(.16)(.44)(12.3)(\pi)(.162) =$	.44
$(.53)(.14)(12.7)(\pi)(.162)$	.48
$(.060)(4.0)(8.7)(\pi)(.162)$	1.06
$(.062)(.56)(5.1)(\pi)(.162)$	.09
$(.25)(.10)(4.8)(\pi)(.162)$	.06
$(.15)(.80)(5.1)(\pi)(.162)$	.31
$2(.75^2)(.785)(.57)(.162) =$	.08
	2.51

Insulation, Aft Closure (Vit. Sil. Phen.)

$(.16)(.30)(12.3)(\pi)(.065) =$	.12
$(.20)(.56)(11.3)(\pi)(.065)$	.27
$(.30)(3.8)(8.5)(\pi)(.065)$	1.98
$(1/2)(.54)(.3)(5.3)(\pi)(.065)$	.09
$(.36)(.20)(5.4)(\pi)(.065) =$	.08
	2.54

Insulation, Insert (Vit. Sil. Phen.)

$(.10)(.64)(4.9)(\pi)(.065) =$	.06
$(.10)(.54)(4.5)(\pi)(.065)$	.05
$(.10)(.24)(4.3)(\pi)(.065) =$	.02
	.13

Insert (Graph-I-Tite G)

$(1/2)(.22 + .42)(1.23)(2.3)(\pi)(.069) =$ .20

$(1/2)(.42 + .67)(2.8)(3.4)(\pi)(.069) =$ 1.12

1.32 lb

Exit Cone (Vit. Sil. Phen.)

$(1/2)(.45 + .17)(.75)(4.7)(\pi)(.065) =$ .20

$(.27)(.29)(5.0)(\pi)(.065)$ .08

$(1/2)(.200 + .125)(7.33)(7.35)(\pi)(.065) =$ 1.79

2.07 lb

Support, Prop Mtg Cyl (Vit. Sil. Phen)

$(4.8^2-2.5^2)(\pi)(.10)(.065) =$ .34

$(.30)(3.03)(6.7)(\pi)(.065)$ 1.24

$-(.10)(.6)(6.9)(\pi)(.065)$ - .08

$-(12)(.785)(.3)(.065)$ - .18

1.32 lb

Prop. Mtg. Cyl. (Carbon Fiber Phenolic MX 4925)

$(.10)(18.12)(6.7)(\pi)(.051) =$ 1.95

$-(12)(.785)(.10)(.051) =$ - .05

1.90 lb

Close. Bolts

$(52)\left[(.138)^2(.375)+(.226^2-.138^2)(.138)\right](.785)(.283) =$ .13

Igniter Assembly

Cap Assy. $(1.5^2)(.785)(1.2)(.162)$ =	.34
$-(1.1^2)(.785)(.82)(.162)$	- .13
$(3^2-1.5^2)(.785)(.23)(.162)$	.20
$(2.8^2-2.5^2)(.785)(.9)(.162)$	.18
Case $(.04)(2.8)(2.3)(\pi)(.162)$	.13
Phenolic $(.06)(2.2)(2.15)(\pi)(.047)$	.04
$(.15)(1.2)(1.15)(\pi)(.047)$	.03
Prop $(2.1^2-1.6^2)(.785)(2.0)(.0595)$	.17
Outer Insul $(.10)(2.0)(2.4)(\pi)(.043)$ =	.06
	1.02 lb

Inhibitor Aft End of Prop (Panelyte 531)

$(6.1^2-2.5^2)(\pi)(.10)(.043)$ = .42 lb

Prop

$(6.1^2-.6^2)(\pi)(15.37)(.0595)$ =	105.87
Corner Rad. $-(1.875)^2(.2146)(11.362)(\pi)(.0595)$	-1.06
Aft Bevel $-(1/2)(1.84)(2.87)(2.426)(\pi)(.0595)$	-1.20
Liner & Mtg Cyl $-(.14)(15.37)(6.7)(\pi)(.0595)$ =	-2.70
	100.37 lb

Liner

$2(.020)(15.4)(6.7)(\pi)(.05)$ = .65 lb

APPENDIX H

MATERIAL SELECTION

A. CASE MATERIAL SELECTION

Reliable, high performance rocket motor cases are fabricated from hotwork die steel like Ladish D6AC, 18 Ni maraging steel, and titanium alloys, primarily Ti-6Al-4V. For the studied motor chamber designs Thiokol selected the titanium 6Al-4V alloy. When a material was selected for the 37-inch-diameter spherical case of the Surveyor Main Retro in 1960, the reliability of neither maraging steel nor titanium alloys had been adequately demonstrated, so Ladish D6AC was chosen. Today, both 18 Ni maraging steel and the Ti-6Al-4V titanium alloy are proven materials. Both metals have strength-to-density ratios significantly greater than Ladish D6AC. For rocket motors that must meet stringent weight budgets, these two alloys are well-proven metals that provide an economical approach to minimizing total motor weight.

The reliability of the Ti-6Al-4V alloy, which was developed under Government sponsorship by the Armour Research Foundation, has been thoroughly demonstrated both by TE-M-385, the 12.7-inch-diameter spherical motor that was qualified for the Gemini Retro-Abort mission and by the Minuteman second stage motor. The following characteristics qualify this alloy for use as a rocket motor case material.

1) Low density, 0.161 lbs/in.^{3}
2) Excellent elevated temperature properties
3) Readily forged and machined
4) Metallurgically stable in annealed and heat-treated condition under stress to 950° F
5) Weldable
6) Consistently reproducible characteristics
7) Paramagnetic, nonferromagnetic
8) Excellent corrosion resistance
9) Well known to case manufacturers
10) Proven reliability in spherical rocket motors

The effect of temperature on ultimate tensile and tensile yield strength for 6 Al 4V titanium is illustrated in Figures H-1 and H-2, respectively.

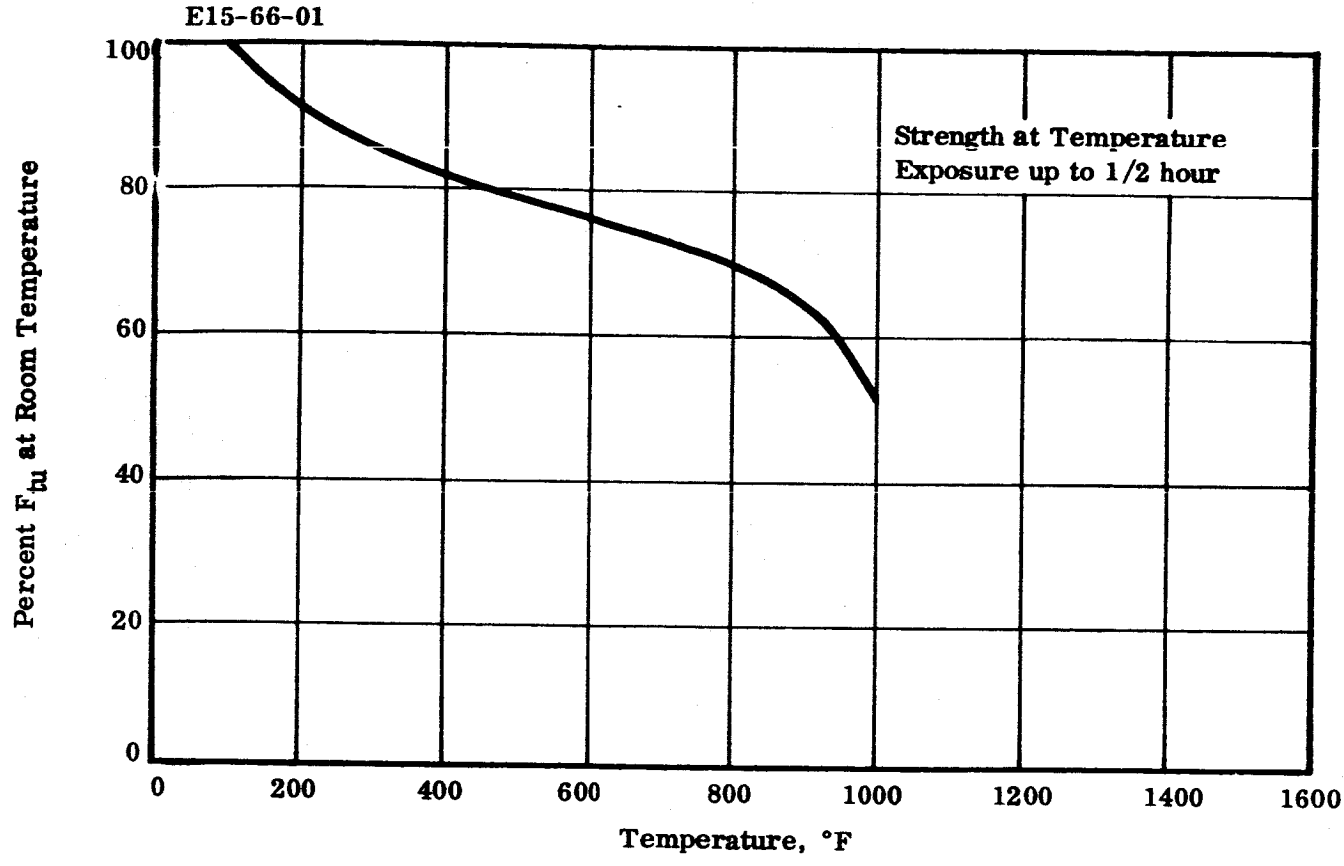

FIGURE H-1. EFFECT OF TEMPERATURE ON THE ULTIMATE TENSILE STRENGTH (F_{tu}) OF SOLUTION-TREATED AND AGED Ti-6Al-4V ALLOY

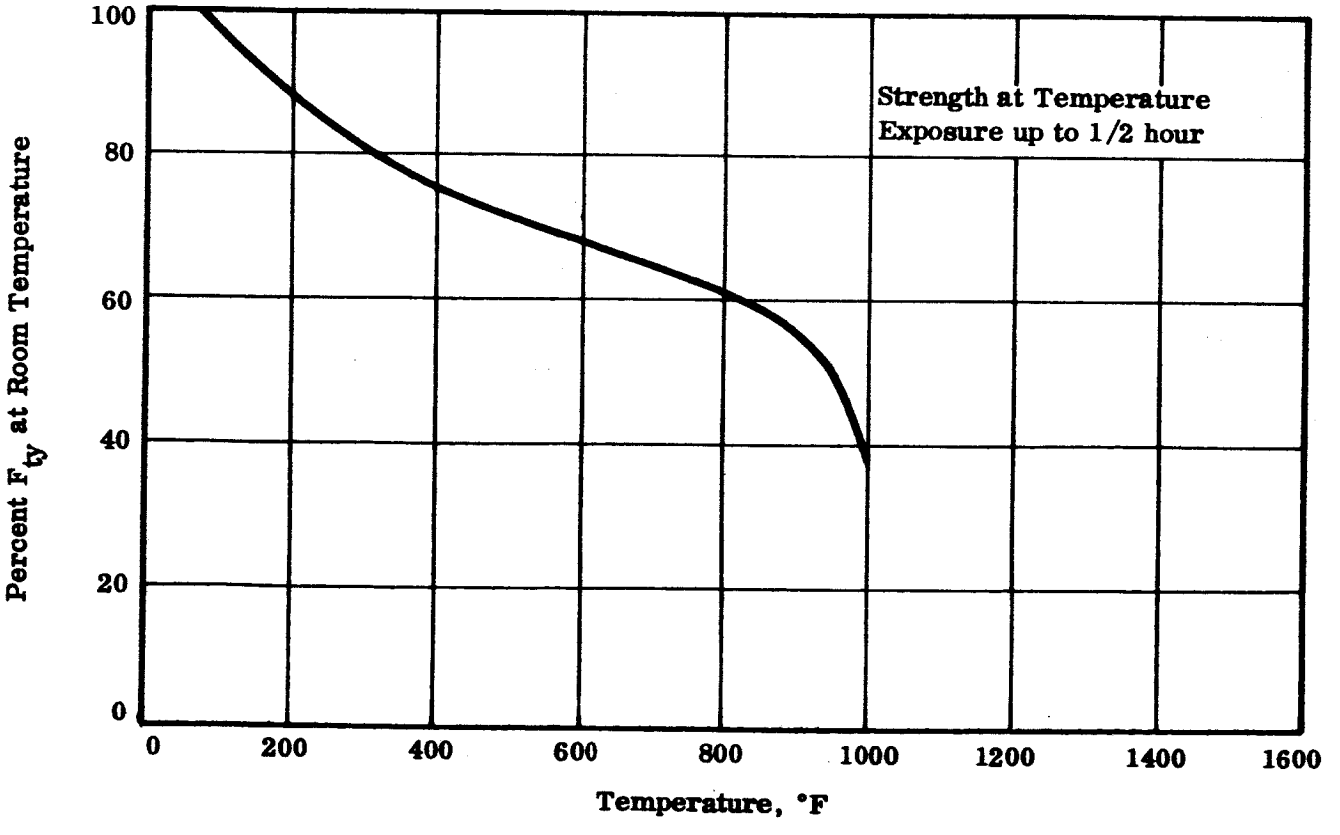

FIGURE H-2. EFFECT OF TEMPERATURE ON THE TENSILE YIELD STRENGTH

The important minimum guaranteed mechanical properties for this alloy, as outlined in Thiokol Specification ME2003 and P14001, are:

Ultimate tensile strength, psi	165,000 — 180,000
Yield strength, 0.2% offset, psi	155,000 minimum
Elongation, % 4D	8% minimum

The uniaxial tensile properties of 6 Al 4V titanium determined,for example, from control specimens tested per specification P14001 under the Gemini Retro motor program were:

	0.2% Yield Strength	Ultimate Strength
Mean, $\bar{X}$	166,344 psi	177,281 psi

All samples met the 155,000 psi minimum yield and 165,000 psi minimum ultimate strength requirements of specification P14001.

The lowest burst pressure of two TE-M-385 Gemini Retro motor cases hydrotested to failure was 2300 psig, which represents a 168,000 psi ultimate strength in the case wall.

B. CASE

Fabrication

The Gemini program permitted full evaluation and characterization of Ti-6Al-4V alloy processing methods for spherical shapes, as well as material characterization and development of acceptance test methods and hydrotest procedures.

Thiokol has found that it is good practice to use two different closed die forgings to produce spherical rocket motor hemispheres of titanium alloy. With this technique, the grain flow can be controlled and optimized, and the material can be effectively placed to give best utilization of forging stock. This technique, in conjunction with proper heat treating, also develops optimum material properties throughout the entire spherical structure.

This material has a hardness of Rc 36, which allows machining, drilling, and tapping to be performed using conventional tools and techniques. Only speeds, feeds, and depth of cut are unique to the titanium alloy.

The case can best be fabricated by using standard forging techniques. It is necessary, however, to use rigid production methods to maintain control on physical dimensions. During forging, the billet stock temperature is maintained below Beta Transus temperature (1820° F). Forging is the standard method for fabricating hemispheres since, in addition to the controlled optimizing of grain structure, forgings provide approximately a 10-percent improvement in strength-to-weight ratio and better reproducibility than hemispheres formed by spinning or deep drawing.

The 6 A1 4V alloy of titanium, unlike the all-beta alloy and many of the other alpha-beta alloys, can be successfully fusion welded by either the tungsten electrode inert gas (TIG), or the Electron Beam technique. Although either technique was acceptable, straight fusion welding, without filler material additions, is recommended since it yields weld efficiences of greater than 85 percent.

The heat-treating technique for this alloy is specified in Thiokol Process Specification P14001. This specification requires forgings to be solution treated at 1750° F for 1 to 1-1/2 hours and quenched in water at 50° to 90° F. The forgings may or may not be rough machined before the solution treatment, depending on the maximum section thickness of the forgings. To obtain maximum properties, the maximum section thickness of the forging should not be greater than 1/2 inch. After solution treatment, the hemispheres are final machined, welded together, and then aged at 900° to 1100° F. The aging process serves as a stress relief treatment for the weld. This technique yields the properties discussed in previous paragraphs. An acceptable alternative sequence is to partially or fully age the hemispheres before final machining, and then machine, weld, and stress relieve. The latter sequence permits better machining characteristics for details and for dimensional stability in the overall processing.

The main operations during the case fabrication are outlined below:

1) Make forging for:

   a) Head-end hemisphere

   b) Aft-end hemisphere

2) Machine head-end hemisphere to configuration

3) Machine aft-end hemisphere to configuration

4) Machine and fabricate the attachment brackets to configuration.

5) Heat treat components as outlined in Thiokol specification P14001, paragraphs 3.3.1, 3.3.2, and 3.3.3.

6) Weld components together per Thiokol specification P14001.

7) Stress relieve and age per Thiokol specification P14001.

8) Final-machine critical surfaces, such as O-ring mating surfaces and critical tolerance areas. No drawing requirements.

9) Hydrostatic test the case to 1110 psi for one minute per Thiokol specification SE-1000

Forgings and welds will be radiographically inspected in accordance with specification MIL-I-6865. Cases will be dye penetrant-inspected in accordance with MIL-I-6866, Type I. When necessary (welding, heat treating, and aging), the case will be fabricated in an inert atmosphere, either argon, helium, an argon-helium mixture, or in vacuum. These atmospheres are required because of titanium's affinity for gases commonly found in air, particularly nitrogen, oxygen, carbon, and hydrogen.

The cylindrical case for the free-standing grain design will be made in a very similar manner using a ring forging for the aft end, a rolled and welded tube for the center section, and a forging for the head-end dome. Machining, welding, and inspection techniques are the same as discussed previously.

The aft closure ring fabrication steps are similar:

1) Forge and radiographically inspect

2) Rough-machine to eliminate thickness over one-half inch.

3) Solution treat per Thiokol specification P14001.

4) Stress relieve and age per the same specification.

5) Final-machine surfaces

6) Drill and countersink holes

C. SELECTION OF ELASTOMERIC INSULATION

The motor performance specification requires an insulation material capable of withstanding high temperature (340° F), low temperatures (-40° F), and erosion, and able to withstand the sterilization temperatures. For this reason, a polyisoprene-base, elastomeric insulation was selected. Thiokol Specification No. NE 1018.*

The insulation is comprised of a polyisoprene rubber base and an asbestos fiber fill. The unvulcanized material may be stored for as long as six months.

The low temperature properties are excellent for the proposed application. The low temperature elongation at -40° F is 87% and the low temperature brittleness point is -65° F.

Chemlok 203 primer and Caram 216 cement are used to improve the adhesion between the insulation and the chamber. These materials were used successfully on the TE-449 demonstration motors and are the recommended materials for use in conjunction with asbestos-filled polyisoprene insulation. The results of shear-strength tests performed on asbestos-filled polyisoprene insulation bonded to steel are shown in Table H-1. These data indicate fully satisfactory strength levels before and after aging for six weeks at temperatures between -75° F and +170° F.

The diffusivity value** of 0.0038 $ft^{2/hr}$ indicates an insulation capability comparable to the well-known Gen Gard V-44. A comparative listing of properties of asbestos-filled polyisoprene and Gen Gard V-44 materials is shown in Table H-2.

Other materials were considered, such as asbestos or silica-loaded buna-N and buna-S materials that were plasticized to obtain satisfactory low temperature flexibility while retaining their excellent insulating capability. We have found none that equals the non-plasticized polyisoprene material. A test was performed on samples of asbestos-filled polyisoprene insulation to determine the effect of sterilization on these materials. The results of these tests indicated virtually no effect after three sterilization cycles.

---

*Formerly marketed as Panelyte 531A. This material is now supplied to Thiokol Specification NE-1018.

**Diffusivity α, a measure of insulating capability, is defined by the equation $\alpha = K/C_p\rho$, where conductivity (K) is in BTU ft/hr-° F-ft^2, specific heat (c_p) is in BTU/lb-° F, density (ρ) in lb/cu ft, and, therefore, the resultant diffusivity, α, in ft^2/hr. The lower the diffusivity, the better the thermal insulating quality.

TABLE H-1

SHEAR STRENGTH BETWEEN STEEL AND ASBESTOS-FILLED POLYISOPRENE INSULATION (WITH CHEMLOK 203 PRIMER AND CARAM 216 CEMENT)

Aging Temperature, °F	Property Test	0	1	2	3	4	5	6
170	Shear (psi)	38	-	-	-	-	-	133
135	Shear (psi)	255	-	504	-	100	-	234
70	Shear (psi)	617	-	-	442	-	-	318
-10	Shear (psi)	812	-	-	-	-	-	768
-75	Shear (psi)	838	-	604	-	690	-	853

TABLE H-2

INSULATION PROPERTIES

	Asbestos-Filled Polyisoprene	Gen-gard V-44 Asbestos-Filled buna-N
Conductivity, $\frac{\text{BTU-ft}}{\text{hr-°F}}$	0.114	0.127
Specific Heat, $\frac{\text{BTU}}{\text{lb-°F}}$	0.392	0.45
Density, $\frac{\text{lb}}{\text{cu ft}}$	74.3	80.35
Diffusivity, $\frac{\text{ft}^2}{\text{hr}}$	0.0039	0.0035
Ultimate Tensile, psi	1600	1700
Ultimate Elongation, %	700	600
Low Temperature		
Torsional Modulus[1]		
G = 5,000	-60°F	9°F
G = 10,000	-64°F	1°F
Brittleness Temperature[2]	-65°F	-6°F

[1]Torsional modulus per ASTM D1043-51 measures resistance of material to angular deflection when subjected to an applied torque.

[2]Brittleness per ASTM D746-577 measures the temperature at which the majority of test specimens will fail when held rigidly at one end (cantilever beam) and struck by a swinging arm traveling at a specified speed.

D. MATERIAL PROPERTIES OF GRAPH-I-TITE-GX

Graph-I-Tite GX was selected for use as the throat material in the studied design. This material was selected on the basis of its superior mechanical properties which are superior to other graphites and its successful performance in the TE-M-364, (Surveyor Main Retro Motor), the TE-M-442 (26-inch diameter Spherical Motor), and the TE-M-449 (Sparrow Prototype Motor). The material properties of Graph-I-Tite GX are compared to other available graphite insert materials in the following table, H-3.

E. SELECTION OF MOTOR CASE INSULATION.

The motor specification requires an insulation capable of withstanding three heat sterilization cycles, low temperatures (-40° F), and erosion for the duration of firing. RPD-150 insulation, an asbestos-filled phenolic resin system was selected to meet these requirements. A series of tests was conducted using RPD-150 insulation for a portion of a composite tensile shear specimen (see Appendix H, Section G). These samples were exposed to three sterilization cycles. The RPD-150 insulation suffered no apparent physical degradation.

The RPD-150 phenolic case insulation will be molded directly into the case, or molded external to the case and bonded in place. If the latter technique is employed, the aft flange of the motor case would be flared out, rather than in, as shown in the case design. The properties of RPD-150 insulation are shown in the following tabulation.

Specific Gravity, average, g/cc	1.77
Compressive Strength, psi	25,000
Tensile Strength, psi	8,800
Flexural Strength, psi	21,900
Shear Strength, psi	20,800
Thermal Conductivity, $\frac{\text{btu-ft}}{\text{hr-ft}^2\text{-}^\circ\text{F}}$	0.166
Specific Heat $\frac{\text{btu}}{\text{lb-}^\circ\text{F}}$	0.308

TABLE H-3

MATERIAL PROPERTIES

Properties	Graph-I-Tite GX	ATJ	CGW
Grain Size, in.	0.004	0.006	-
Bulk Density, g/cc	1.88	1.73	1.82
Tensile Strength, psi			
With grain	2,900	1,790	2,000
Across grain	2,170	1,420	1,800
Compressive Strength, psi			
With grain	10,500	8,270	10,500
Across grain	11,000	8,540	11,000
Flexural Strength, psi			
With grain	5,000	4,010	4,500
Across grain	5,000	3,580	4,100
Young's Modulus of Elasticity, 10^6 psi			
With grain	1.8	1.45	1.75
Across grain	1.3	1.15	1.20
Coefficient of Thermal Expansion, $10^{-6}/°F$			
With grain	0.90	1.22	1.22
Across grain	1.125	1.90	1.89
Thermal Conductivity, $\frac{BTU\text{-}ft}{hr\text{-}ft^2\text{-}°F}$			
With grain	92	55	65
Across grain	69	42	50
Gangler Number, $\frac{10^3\ BTU}{ft\text{-}hr}$			
Across grain	103	27	40
Erosion Rate in Test Motor, mil/sec	1.1	1.9	1.8

F. SELECTION OF INTERNAL SUPPORT MATERIAL

The internal support material selected was Fiberite Corporation MX 4925. This material is a carbon fiber-filled modified phenolic. The main reason for selection of this material was its thermal expansion properties. These have been discussed in some detail in Appendix A.

The physical properties of the molded material are listed below:

Specific Gravity, g/cc		1.41
Compressive Strength, psi		30,000
Tensile Strength, psi		9,500
Flexural Strength, psi		19,000
Shear Strength, psi		10,000
Thermal Conductivity at 300° F $\frac{\text{btu-in}}{\text{ft}^2\text{hr °F}}$		3.79
Specific Heat, btu/lb °F		0.29
Linear Thermal Expansion:	norm to fiber in./in. °F	5.5×10^{-5}
	Parallel to fiber	1.25×10^{-5}

G. BONDING MATERIALS (LINER AND ADHESIVE)

Satisfactory bonding must be developed at various interfaces in the candidate motor designs, and bond strength must be maintained after three sterilization cycles if the motor is to operate as intended. Where one of the components of the interface is propellant (e.g., where propellant must be bonded to the case or to insulation) a liner formulation is employed.

The liner specified for this study is TL-H-305. This liner is routinely employed for bonding propellant like TP-H-3105. The liner is compounded from the same polymer used in TP-H-3105; for this reason it is completely compatible with, and adheres well to, the propellant. The liner also contains an epoxide which provides good adhesion to relatively inert surfaces such as metal and insulation.

At non-propellant interfaces (e.g., where insulation is to be bonded to the case wall) an epoxide adhesive, Epon-912, has been specified. Epoxides are particularly attractive as adhesives in an application requiring heat sterilization since they perform well at elevated temperatures.

Composite shear test specimens were used to determine location and level of failure in various bonding situations. The samples were prepared as follows, depending on the components to be tested:

> Two one-inch by three-inch strips of steel were coated over one square inch with a 0.030-inch film of liner. The strips were pre-cured to a slight tack.

Following pre-cure the lined strips were placed in a jig and aligned in parallel, one-half inch apart. Uncured TP-H-3105 propellant was packed into the volume between the plates, and the assembly was cured for 64 hours at 135° F.

or

> Two one-inch by three-inch strips of steel were coated over one square inch with Epon-912 adhesive. One square inch segments of insulation (either asbestos-filled polyisoprene or RPD-150) were then bonded into the Epon-912.

The insulation segments were then lined and the liner was precured. Propellant was packed between the plates as above, and the assembly was cured for 64 hours at 135° F.

The attached table presents the results of shear tests of the assemblies at three test temperatures. Where sterilization is specified, it was three 40-hour cycles at 295° F under nitrogen. It is significant to note the location of failures as shown in the table. These composite assemblies undergo failure at the weakest point; thus, the next-weakest component or interface is not tested.

In addition to the above tests, pieces of RPD-150, asbestos-filled polyisoprene, and Gen-Gard V-44 insulation were subjected to three sterilization cycles. There was no apparent change in the physical properties of the insulation materials after sterilization.

The following conclusions are drawn from this work:

1) When tested in shear at 78°F, after sterilization, the weakest component of the assembly was the propellant. This was as expected. It is noteworthy that propellant shear strength still exceeded 70% of its magnitude in the unsterilized condition.

2) When tested at 295°F after sterilization, the weakest component again was propellant.

3) When tested at -40°F after sterilization, failure occurred in the liner or epoxy adhesive. But, in any case, shear strength was at least 70 psi. Failure at this point was probably due to low-temperature embrittlement of the epoxy adhesive.

The test results are summarized in Table H-4 as follows.

TABLE H-4

SHEAR ADHESION ASSEMBLY TESTS

Test	Assembly	Sterilized	Test Temperature, °F	Shear Strength, psi	Failure Type and Location
1AB	Liner, Propellant	No	78	110	Cohesive, propellant
1CD	Liner, Propellant	Yes	78	80	Cohesive, propellant
1EF	Liner, Propellant	Yes	295	28	Cohesive, propellant*
1GH	Liner, Propellant	Yes	-40	255	Adhesive, L/M
2AB	Liner, Propellant, Asbestos-Filled Polyisoprene	No	78	90	Cohesive, propellant
2CD	Liner, Propellant, Asbestos-Filled Polyisoprene	Yes	78	126	Cohesive, propellant
2EF	Liner, Propellant, Asbestos-Filled Polyisoprene	Yes	295	27	Cohesive, propellant
2GH	Liner, Propellant, Asbestos-Filled Polyisoprene	Yes	-40	190	Epon Failure
3AB	Liner, Propellant, RPD-150	No	78	85	Cohesive, propellant
3CD	Liner, Propellant, RPD-150	Yes	78	80	Cohesive, propellant
3EF	Liner, Propellant, RPD-150	Yes	295	15	Cohesive, propellant
3GH	Liner, Propellant, RPD-150	Yes	-40	70	Epon Failure

* L/M = separation at liner/metal interface